Revista de Ciencia y Tecnología

ARGENTINE JOURNAL OF SCIENCE AND TECHNOLOGY

Engineering, Technology and Informatics, Health, Biology and Genetics, Biochemistry and Pharmacy, and Technical Note

YEAR 27 / Nº 44 / 2025

INDEX

Engineering, Technology and Informatics

10 **Strengthening statistical tests in low-frequency and fuzzy number contingency tables through linear scaling**
Fortaleciendo pruebas estadísticas en tabla de contingencia con baja frecuencia y números borrosos a través del escalado lineal
Matilde I., Césari; Santiago, Pérez

21 **Diagnosis of the circular economy in municipalities of Misiones, Argentina**
Diagnóstico de Economía circular en municipios de Misiones, Argentina
Sonia R., Niezwida; María F., Kaczynski; Fernando A., Santacruz; Juan C., Michalus; Chiara M., Villalba Auras

Health

31 **Physicochemical characterization, viability and *in vitro* gastrointestinal resistance of probiotic *Bacillus* spp. in cheese bread**
Caracterización fisicoquímica, viabilidad y resistencia gastrointestinal *in vitro* de *Bacillus* spp. probióticos en pan de queso
Mariana, Silva de Souza Malaquias; Sara, Pereira Leandro; Nataly, de Almeida Costa; Isabela, Campelo Queiroz; Wellingta Cristina A., do Nascimento Benevenuto; Maurílio, Lopes Martins; Eliane Mauricio, Furtado Martins

Biology and Genetics

39 **Gastrointestinal nematodes in small ruminants: genus identification and evaluation of anthelmintic resistance in Misiones, Argentina**
Nematodos gastrointestinales en pequeños rumiantes: identificación de géneros y evaluación de resistencia antihelmíntica en Misiones, Argentina

Samuel O., Miño; Aylén R., Díaz; Cristian, Miño; Ricardo, Díaz Alarcón; Domingo J., Liotta; Miguel, Da Luz

50 **Functional microsatellites in cassava (*Manihot esculenta Crantz*): genomic mapping and genetic characterization in cultivars from Misiones**

Microsatélites funcionales en mandioca (*Manihot esculenta Crantz*): mapeo genómico y caracterización genética en cultivares de Misiones

César Adrián, Preussler; Patricia Mabel, Aguilera; María Isabel, Fonseca

58 ***In vitro* and *ex vitro* germination of *Jatropha gossypiifolia* and initiation of *in vitro* cultivation**

Germinación *in vitro* y *ex vitro* de *Jatropha gossypiifolia* e inicio del cultivo *in vitro*

Jack B. S., Rojas; Maria da P. F., Silva; Adriano. P., Guilherme; Milena. G., Malosso

65 **Mycoinsecticide capacity of five strains of *Beauveria bassiana* isolated from Misiones (Argentina)**

Capacidad micoinsecticida de cinco cepas de *Beauveria bassiana* aisladas de Misiones (Argentina)

Marilyn R. V., Silva; Gustavo A., Bich; Marcela A., Sadañoski; María L., Castrillo; Pedro D., Zapata; Laura L., Villalba; María I., Fonseca

Biochemistry and Pharmacy

76 ***In vitro* evaluations of warfarin tablets available in the brazilian market**

Evaluación *in vitro* de tabletas de warfarina disponible en el mercado brasileño

Isabela C. F., Barbosa; Vitoria C., Crestani; Nathalia S., Rodrigues; Tatiana, Staudt; Ana L. S., Alves; Charise D., Bertol

Technical Note

85 **Study on the need for a new Technology Acceptance Model**

Estudio sobre la necesidad de un nuevo Modelo de Aceptación de Tecnología

Fábio, Corrêa; Dárlinton Barbosa Feres, Carvalho; Vinícius, Figueiredo de Faria; João Victor, Boechat Gomide

97 **Accessibility in Pure Data for visually impaired musicians: a real-time soundscape strategy**

Accesibilidad en Pure Data para músicos con discapacidad visual: una estrategia de paisaje sonoro en tiempo real

Evandro J., Grisolio; Antonio C., Penteado; Vilson, Zattera; Guilherme N. N., Nogueira; Percy, Nohama

105 **Simulation of a phthalic anhydride production process through gaseous catalytic oxidation of o-xylene in ChemCAD® simulator**

Simulación de un proceso de producción de anhídrido ftálico mediante la oxidación catalítica gaseosa del o-xileno en el simulador ChemCAD®

Amaury, Pérez Sánchez; Elizabeth, Ranero González; Eddy J., Pérez Sánchez; Lizthalía, Jiménez Guerra

118 **Fuel interchangeability: a comparative study of propane and methane in an industrial furnace burner**

Intercambiabilidad de combustible: un estudio comparativo de propano y metano en un quemador de horno industrial

Alexandre Tiago, Martins; Aldo, Ramos Santos

Argentine Journal of Science and Technology on line: www.fceqyn.unam.edu.ar/recyt. Made the deposit of Law 11723. Printed in Argentina. ISSN of the printed journal: 0329-8922. ISSN of the electronic journal: 1851-7587.

All correspondence related to the Journal should be addressed to Argentine Journal of Science and Technology. Félix de Azara 1552, 3300, Posadas, Misiones, Argentina. E-mail: recyt@fceqyn.unam.edu.ar.
Biannual journal.

Argentine Journal of Science and Technology on line: www.fceqyn.unam.edu.ar/recyt. Made the deposit of Law 11723. Printed in Argentina. ISSN of the printed journal: 0329-8922. ISSN of the electronic journal: 1851-7587.

All correspondence related to the Journal should be addressed to Argentine Journal of Science and Technology. Félix de Azara 1552, 3300, Posadas, Misiones, Argentina. E-mail: recyt@fceqyn.unam.edu.ar.
Biannual journal.

Argentine Journal of Science and Technology on line: www.fceqyn.unam.edu.ar/recyt. Made the deposit of Law 11723. Printed in Argentina. ISSN of the printed journal: 0329-8922. ISSN of the electronic journal: 1851-7587.

All correspondence related to the Journal should be addressed to Argentine Journal of Science and Technology. Félix de Azara 1552, 3300, Posadas, Misiones, Argentina. E-mail: recyt@fceqyn.unam.edu.ar.
Biannual journal.

PhD. María Laura Vera. Facultad de Ciencias Exactas, Químicas y Naturales. Universidad Nacional de Misiones. Argentina.
PhD. Nancy Lovera. Facultad de Ciencias Exactas, Químicas y Naturales. Universidad Nacional de Misiones. Argentina.
MSc. Amada Beatriz Pucciarelli Román. Facultad de Ciencias Exactas Químicas y Naturales. Universidad Nacional de Misiones. Argentina.

Argentine Journal of Science and Technology on line: www.fceqyn.unam.edu.ar/recyt. Made the deposit of Law 11723. Printed in Argentina. ISSN of the printed journal: 0329-8922. ISSN of the electronic journal: 1851-7587.

All correspondence related to the Journal should be addressed to Argentine Journal of Science and Technology. Félix de Azara 1552, 3300, Posadas, Misiones, Argentina. E-mail: recyt@fceqyn.unam.edu.ar.
Biannual journal.

Revista de Ciencia y Tecnología
Argentine Journal of Science and Technology

Presentation Note Nº 44

The Editorial Board presents in this opportunity the second issue of the year 2025 of the Argentine Journal of Science and Technology (Facultad de Ciencias Exactas, Químicas y Naturales, Universidad Nacional de Misiones).

It is available on the web page http://www.fceqyn.unam.edu.ar/recyt/.

This issue corresponds to number 44 and the following thematic areas are involved: Engineering, Technology and Informatics, Health, Biology and Genetics, Biochemistry and Pharmacy, and Technical Note.

The institutions where the papers published in this issue were developed are the following:

- Federal Institute of Education, Science and Technology of Southeast Minas Gerais. Minas Gerais, Brazil.
- Instituto de Saúde e Biotecnologia de Coari. Universidade Federal do Amazonas (ISB/UFAM). Brazil.
- University of Passo Fundo. Passo Fundo, Brasil.
- Universidade FUMEC (Fundação Mineira de Educação e Cultura, FUMEC University. Minas Gerais, Belo Horizonte, Brasil.
- Universidade Federal de São João del-Rei (UFSJ). Minas Gerais, Brasil.
- Programa de Pós-Graduação em Música. Instituto de Artes. Universidad Estadual de Campinas (UNICAMP). Brazil.
- Programa de Pós-Graduação em Tecnologia em Saúde (PPGTS). Pontifícia Universidade Católica do Paraná. Curitiba, Brazil.
- Universidade Santa Cecília (UNISANTA). Santos, Brasil.
- Facultad de Ciencias Aplicadas. Universidad de Camagüey “Ignacio Agramonte Loynaz”. Camagüey, Cuba.
- Empresa de Servicios Automotores SA. Ciego de Ávila, Cuba.
- Consejo Nacional de Investigaciones Científicas y Técnicas (CONICET). Buenos Aires, Argentina.
- Grupo Regional de Investigación y Desarrollo en Ecosistemas de Conocimiento (GiDeCo). Universidad Tecnológica Nacional. Mendoza, Argentina.
- Subsecretaría de Economía Circular de Misiones. Ministerio de Cambio Climático. Posadas, Misiones, Argentina.
- Instituto Nacional de Tecnología Agropecuaria (INTA). Centro Regional Misiones, EEA Cerro Azul. Misiones, Argentina.
- Estación Experimental Agropecuaria Montecarlo (INTA). Montecarlo, Misiones, Argentina.
- Instituto de Macroeconomía Circular (IMAC). Posadas, Misiones.
- Instituto Nacional de Medicina Tropical (INMeT) - ANLIS “Dr. Carlos Malbrán”. Puerto Iguazú, Misiones, Argentina.

- Laboratorio de Biotecnología Molecular. Instituto de Biotecnología Misiones "Dra. María Ebe Reca" (INBIOMIS). Facultad de Ciencias Exactas, Químicas y Naturales. Universidad Nacional de Misiones. Misiones, Argentina.
- Facultad de Ingeniería. Universidad Nacional de Misiones (FI-UNaM). Oberá, Misiones, Argentina.
- Laboratorio de Biología Molecular Aplicada (LaBiMAp). Facultad de Ciencias Exactas, Químicas y Naturales. Universidad Nacional de Misiones. Posadas, Misiones.
- Instituto de Biología Subtropical (IBS). Facultad de Ciencias Exactas Químicas y Naturales. Universidad Nacional de Misiones. Misiones, Argentina.

Special thanks are given to the guest editors of this issue: PhD. Nancy Lovera (Guest), PhD. Nancy B. Ganz (Guest).

Likewise, we want to thank the Science and Technique General Secretariat of the Universidad Nacional de Misiones, the Administrative Secretariat and the Research, Development and Innovation Secretariat of the Facultad de Ciencias Exactas, Químicas y Naturales for their financial support, as well as, the Editorial Team for their constant work (Agustina Gaona Duarte, Marcos Oliva, Lara Granada Lanús, Ana Paula Maier, José Roa, Fernanda Villamil, Lara Granada Lanús, PhD. Nancy Ganz, and ASC. Víctor Narváez).

PhD. Alicia E. ARES
Editor-in-Chief
Revista de Ciencia y Tecnología (RECyT)
Argentine Journal of Science and Technology
Facultad de Ciencias Exactas, Químicas y Naturales
Universidad Nacional de Misiones
recyt@fceqyn.unam.edu.ar
www.fceqyn.unam.edu.ar/recyt

RECyT
Year 27 / Nº 44 / 2025 /
DOI: https://doi.org/10.36995/j.recyt.2025.44.001

Strengthening statistical tests in low-frequency and fuzzy number contingency tables through linear scaling

Fortaleciendo pruebas estadísticas en tabla de contingencia con baja frecuencia y números borrosos a través del escalado lineal

Matilde I., Césari[1, *]; Santiago, Pérez[1]

1- Grupo Regional de Investigación y Desarrollo en Ecosistemas de Conocimiento (GiDeCo). Universidad Tecnológica Nacional. Mendoza, Argentina.
* E-mail: matilde.cesari@frm.utn.edu.ar

Received: 12/11/2024; Accepted: 18/09/2025

Abstract
This study introduces an innovative methodology aimed at enhancing the application of statistical tests in contingency tables with low expected cell frequencies. By means of a linear scaling technique, we address the limitations of traditional tests—such as the Chi-Square and Fisher's Exact Test—when dealing with small values and fuzzy data, thereby facilitating a robust statistical analysis adapted to conditions of uncertainty. Classical contingency table analysis presents constraints when cell values are extremely small, particularly when decimal values fall below one. In such contexts, methods that rely on these tables, including the Chi-Square Test and Fisher's Exact Test (FET), may prove inadequate for appropriately managing the associated uncertainty, especially when the degree of imprecision within the data is non-negligible. This study develops: (1) an innovative adaptation of contingency tables that enhances the robustness of statistical tests under suboptimal sampling conditions, and (2) a computational tool that automates its implementation. Moreover, examples of scalability are discussed as a resource applicable to any contingency table facing the challenge of small values, as well as the effective use of information embedded in fuzzy or imprecise data across diverse research domains.

Keywords: Contingency table, Linear scaling, Statistical tests**.**

Resumen
Este trabajo presenta una metodología innovadora para fortalecer la aplicación de pruebas estadísticas en tablas de contingencia con baja frecuencia esperada en las celdas. Con esta técnica de escalado lineal, abordamos las limitaciones de pruebas tradicionales, como Chi-Cuadrado y Fisher, al enfrentar valores pequeños y datos borrosos, facilitando un análisis estadístico robusto y adaptado a condiciones de incertidumbre. El análisis clásico de Tabla de Contingencias presenta una limitante para valores muy pequeños, en las celdas de las tablas, con valores decimales menores a uno. En este contexto, métodos que involucran su utilización, como la Prueba de Chi-Cuadrado y Prueba Exacta de Fisher (FET) pueden no ser apropiados para manejar adecuadamente la incertidumbre asociada, y en especial, cuando el grado de la misma que poseen los datos no es despreciable.
En este trabajo se desarrolló: 1) una adaptación innovadora de las Tablas de contingencia, que mejora la robustez de las pruebas estadísticas bajo condiciones de muestra subóptima y 2) una herramienta informática que automatiza su aplicación. Asimismo, se discuten ejemplos de la escalabilidad como herramienta para cualquier Tabla de contingencia que enfrente el desafío de valores pequeños, así como también el aprovechamiento eficaz de la información contenida en datos borrosos o imprecisos en una variedad de campos de investigación.

Palabras clave: Escalado lineal, Pruebas estadísticas, Tabla de contingencia**.**

1 INTRODUCTION

In numerous engineering disciplines, contingency tables employed in research are not exclusively based on integer frequencies; rather, they often incorporate very small decimal values, and even values expressed in scientific notation, due to the precision of measurement instruments and the nature of the phenomena under study. These measurements, although minimal, are highly valuable given the richness of the information they provide and the considerable time and cost associated with their collection. Nevertheless, conventional statistical analysis of such tables presents challenges, as methods like the Chi-Square Test [1–4] require higher frequencies to validate their assumptions of independence. This issue is exacerbated in situations where the small magnitude and precision of the data are critical for

accurate interpretation of results. In this context, the linear scaling proposed herein offers an innovative solution, enabling these small decimal values to be transformed into an expanded and more manageable scale without compromising the integrity of the original data. This transformation facilitates the application of robust statistical tests capable of effectively handling measurement precision, thereby allowing engineers and scientists to fully leverage the potential of their data to understand and explain complex phenomena.

The Fisher's Exact Test (FET) [5–8] is a widely used non-parametric alternative to the Chi-Square Test for small datasets, particularly useful when one or more cells in a contingency table have expected frequencies below five. Its primary objective is to test the null hypothesis that the observed dichotomous frequency distributions are associated, against the alternative hypothesis that they are independent. FET is especially effective in analyzing small datasets, notably when at least one cell in the contingency table has an expected frequency under five.

Small datasets and sparse cells may compromise the validity of the Chi-Square Test, which relies on asymptotic normality. Since FET is a non-parametric test, this assumption does not apply. FET calculates the exact probability (p-value) of observing the given table or a more extreme distribution of the data. This probability is determined by evaluating all possible rearrangements of the table (in the direction of the alternative hypothesis).

Despite their utility, both the FET and Chi-Square tests [9] exhibit limitations in adequately addressing the uncertainty inherent in low-frequency data, which may lead to erroneous statistical conclusions or diminished test power. Specifically, when comparing proportions of a categorical outcome across different independent groups, various statistical tests are considered, including the Chi-Square Test, FET, and the Mann–Whitney Test [10–12].

The Chi-Square Test and FET are suitable for evaluating the independence between two variables when the comparison groups are independent and uncorrelated. The Chi-Square Test applies an approximation assuming a large sample size, whereas the Fisher's Exact Test performs an exact procedure, particularly for small samples.

This issue is magnified in research settings, where data often contain a degree of uncertainty or vagueness that cannot be disregarded. One example of these challenges is fuzzy data analysis [13–15], where values are not classified into discrete categories but are instead assigned degrees of membership, reflecting their uncertainty.

Transforming original data into fuzzy sets introduces a deliberate level of imprecision to capture the uncertainty inherent in certain measurements or subjective perceptions. This approach, which employs fuzzy logic and fuzzy variables, enables a more nuanced and realistic analysis of data, especially in contexts where absolute precision is unattainable or does not accurately reflect the nature of the observed phenomena. However, when working with possibility values derived from this fuzzy transformation, traditional statistical analysis faces additional complications.

Contingency tables based on these possibility values tend to contain inherently small numbers, posing a challenge to conventional association tests. The solution proposed in this article is to linearly scale these possibility values from the 0–1 range to a broader 0–100 range. This adjustment, although conceptually simple, is novel in its capacity to adapt contingency tables derived from fuzzy data for analysis using traditional statistical tests.

This study proposes an innovative adaptation of contingency tables that enhances the robustness of statistical tests under suboptimal sampling conditions. The central technique of this approach is the linear scaling of possibility values from the 0–1 range to an expanded 0–100 range.

This adjustment not only facilitates compliance with the statistical assumptions required for tests such as Chi-Square and Fisher's Exact Test, but also optimizes the interpretation and detection of significant patterns that might otherwise remain undetected due to the high variability and small magnitude of the original values.

In light of the above, and with the aim of contributing to a clearer understanding of the definition and scope of this pioneering methodology, Section 2 presents the Methodology, detailing contextual examples; Section 3 explores a more complex case study applying the methodology; Section 4 addresses the use of the methodology in tables with fuzzy numbers; Section 5 provides a detailed analysis of results and the advantages of using simple correspondence in scaled contingency tables; and finally, Section 6 summarizes the conclusions derived from this proposal and experimental study.

2 METHODOLOGY

2.1 Overview

The software developed in this study enables automated linear scaling, adapting to various data formats and providing an accessible interface for researchers across different fields. Its capacity to accurately scale low values in contingency tables enhances the compatibility of these data with tests

such as Chi-Square and Fisher's Exact Test, without compromising the integrity of the original proportions.

The software developed in this study, available at GitHub [21], enables automated linear scaling, adapting to various data formats and providing an accessible interface for researchers across different fields. Its capacity to accurately scale low values in contingency tables enhances the compatibility of these data with tests such as Chi-Square and Fisher's Exact Test, without compromising the integrity of the original proportions. A live version of the application can be accessed on the server at DaFu App [22].

In the present study, a computer tool has been developed that automates the linear scaling process, transforming this approach into a practical and efficient solution for researchers.

The software is designed to accept data inputs in various formats, automatically analyze the distribution of values, and apply linear scaling from 0 to 100 to each value in the contingency table.

This automation includes determining the minimum and maximum values within the dataset, as well as calculating the slope (M) and the intercept (B) required for the linear transformation, according to the formulas presented in the study.

Once scaled, the data are restructured into new contingency tables that preserve the original proportionality while amplifying the values, thereby facilitating the application of statistical tests that require specific assumptions regarding frequency size.

This tool accelerates data preparation and ensures precision and consistency in the application of linear scaling, which is crucial for the validity of subsequent statistical analyses.

Detailed analyses and illustrative examples are proposed to demonstrate the usefulness of the linear scaling of values as a methodological resource to improve the interpretation of contingency tables and provide a solid basis for decision-making. The proposal consists of scaling the values of the original contingency table, which range from 0 to 1, obtaining an equivalent table through the linear normalization method for values from 0 to 100 and subsequently deriving results from it by applying statistical tests such as Chi-Square or Fisher's Exact Test. Formally, this process involves selecting the optimal maximum and minimum; in this case, the maximum is represented by a value of one (a) and the minimum by a value of zero (b). The remaining values are then adjusted using the linear equation:

$$y = M \cdot x + B \quad (Equation\ 1)$$

Where M = slope and B = intercept.

The parameters M and B are calculated according to the maximum and minimum values of the attribute to be normalized (Equation 2). Finally, the standardized values are obtained from MMM and BBB using Equation (3).

$$M = \frac{a - b}{maximum - minimum} * B = (y - M \cdot x) = (a - M * maximum) \quad (Equation 2)$$

The parameters a and b correspond to the maximum and minimum, respectively, of the new value scale to which the data are to be standardized.

$$NormalizedValue = M * ObservedValue + B \quad (Equation\ 3)$$

2.2 Simple Example

Let us consider a simple example involving a binary contingency table with 0/1 values. In Table 1, on the left, we observe the original data, and on the right, the table linearly scaled to values ranging from 0 to 100. A simple correspondence analysis enables the examination of both tables and confirms their equivalence (Tables 1 to 3, Fig. 1).

A Simple Correspondence Analysis is conducted on both the original contingency table, with values ranging from 0 to 1, and the scaled table, which adjusts these values to a 0–100 range. It is expected that, although the numerical values in the scaled table cells are larger, the relative proportions among the cells remain unchanged.

To implement the factor analysis strategy for correspondences and association tests, the factor analysis module of the commercial software XLSTAT is employed [16]. The resulting maps from each analysis—both for the original and the scaled tables—should exhibit similar clustering patterns among the corresponding categories. This indicates that the transformations applied (i.e., linear scaling) have not altered the underlying relationships between the variable categories.

Table 1: On the left, original example table; on the right, table scaled from 0 to 100.

Values of 0 to 1

Ori	C1	C2	C3	C4
F1	0	0	0	1
F2	0	0	0	1
F3	0	1	0	0
F4	0	1	0	0
F5	0	0	1	0
F6	0	0	0	1
F7	1	0	0	0

Scalation of 0 to 100

Scale	C1	C2	C3	C4
F1	0	0	0	100
F2	0	0	0	100
F3	0	100	0	0
F4	0	100	0	0
F5	0	0	100	0
F6	0	0	0	100
F7	100	0	0	0

Table 2: Inertia per cell.

ORIGINAL

Inertia per cell:

	C1	C2	C3	C4
F1	0,02041	0,04082	0,02041	0,10884
F2	0,02041	0,04082	0,02041	0,10884
F3	0,02041	0,25510	0,02041	0,06122
F4	0,02041	0,25510	0,02041	0,06122
F5	0,02041	0,04082	0,73469	0,06122
F6	0,02041	0,04082	0,02041	0,10884
F7	0,73469	0,04082	0,02041	0,06122

Eigen values and percentages of inertia:

	F1	F2	F3
Eigen value	1,000	1,000	1,000
Inertia (%)	33,333	33,333	33,333
% accumulated	33,333	66,667	100,000

Table 3: Inertia per cell.

ESCALATION 0 to 100

Inertia per cell:

	C1	C2	C3	C4
F1	0,02041	0,04082	0,02041	0,10884
F2	0,02041	0,04082	0,02041	0,10884
F3	0,02041	0,25510	0,02041	0,06122
F4	0,02041	0,25510	0,02041	0,06122
F5	0,02041	0,04082	0,73469	0,06122
F6	0,02041	0,04082	0,02041	0,10884
F7	0,73469	0,04082	0,02041	0,06122

Eigen values and percentages of inertia:

	F1	F2	F3
Eigen value	1,000	1,000	1,000
Inertia (%)	33,333	33,333	33,333
% accumulated	33,333	66,667	100,000

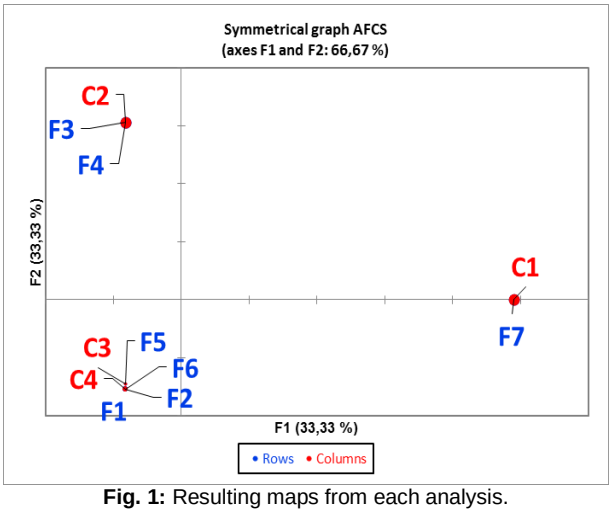

Fig. 1: Resulting maps from each analysis.

A key element is the total inertia explained by the first two axes. If the structure of the information remains consistent, the inertia (which reflects the variance explained by these axes) should be equivalent between the two tables, adjusted for the effect of scaling. It is important to note that the significant dimensions (axes) emerging from the correspondence analysis, as well as the contributions of the categories to these axes, are consistent between the original and the scaled tables. The relative positions of the categories within the correspondence space should remain stable, indicating that the structural relationships are preserved despite the scaling (Tables 4 to 7 and Tables 8 to 11).

Table 4: Test of independence using Chi-Square.

ORIGINAL

Test of independence between rows and columns (Chi-square):

Chi-square (Observed value)	21
Chi-square (Critical value)	28,869
GL	18
p-value	0,279
alfa	0,05

Test interpretation:

H0: The rows and columns of the table are independent.

Ha: There is a dependency between the rows and columns of the table.

Since the calculated p-value is greater than the significance level alpha=0.05, the null hypothesis H0 cannot be rejected.

Theoretical frequencies less than 5 have been detected. To safely use the Chi-square test based on the approximation by the Chi-square distribution, the theoretical frequencies should not be less than 5.

Table 5: Test of independence using Wilks' G^2.

Test for independence between rows and columns (Wilks' G^2):

Wilks G^2 (Observed Value)	17,878
Wilks G^2 (Critical Value)	28,869
GL	18
p-value	0,464
alfa	0,05

Test interpretation:

H0: The rows and columns of the table are independent.

Ha: There is a dependency between the rows and columns of the table.

Since the calculated p-value is greater than the significance level alpha=0.05, the null hypothesis H0 cannot be rejected.

Table 6: Association coefficients.

Association coefficients:

Coefficient	Value
Pearson Phi	1,732
Contingency coefficient	0,866
Cramer's V	1,000
T for Tschuprow	0,841
Tau by Goodman and Kruskal (F/C)	0,500
Goodman and Kruskal Tau (C/F)	1,000

Table 7: Significance per cell using Fisher's Exact Test.

Significance per cell (Fisher's exact test):

	C1	C2	C3	C4
F1	<	<	<	>
F2	<	<	<	>
F3	<	>	<	<
F4	<	>	<	<
F5	<	<	>	<
F6	<	<	<	>
F7	>	<	<	<

Values in red are significant at the alpha=0.05 level.

Table 8: Test of independence using Chi-Square.

SCALATION 0 a 100

Test of independence between rows and columns (Chi-square):

Chi-square (Observed value)	2100
Chi-square (Critical value)	28,869
GL	18
p-value	< 0,0001
alfa	0,05

Test interpretation:
H0: The rows and columns of the table are independent.
Ha: There is a dependency between the rows and columns of the table.
Since the computed p-value is less than the significance level alpha=0.05, the null hypothesis H0 should be rejected, and the alternative hypothesis Ha should be accepted.

Table 9: Test of independence using Wilks' G^2.

Test for independence between rows and columns (Wilks' G^2):

Wilks G^2 (Observed Value)	1787,848
Wilks G^2 (Critical Value)	28,869
GL	18
valor-p	< 0,0001
alfa	0,05

Test interpretation:
H0: The rows and columns of the table are independent.
Ha: There is a dependency between the rows and columns of the table.
Since the computed p-value is less than the significance level alpha=0.05, the null hypothesis H0 should be rejected, and the alternative hypothesis Ha should be accepted.

Table 10: Association coefficients.

Association coefficients:

Coeficiente	Value
Pearson Phi	1,732
Contingency coefficient	0,866
Cramer's V	1,000
T for Tschuprow	0,841
Tau by Goodman and Kruskal (F/C	0,500
Goodman and Kruskal Tau (C/F)	1,000

Table 11: Significance per cell using Fisher's Exact Test.

Significance per cell (Fisher's exact test):

	C1	C2	C3	C4
F1	<	<	<	>
F2	<	<	<	>
F3	<	>	<	<
F4	<	>	<	<
F5	<	<	>	<
F6	<	<	<	>
F7	>	<	<	<

Values in red are significant at the alpha=0.05 level.

The application of the proposed methodology preserves the proportions of the original table while scaling the values to enable statistical testing.

- It allows for the analysis of tables with small values, where standard statistical tests may not be valid.
- Scaling to a broader range increases the statistical power to detect associations.
- The linear transformation preserves the original relationships among cells, ensuring that the results of tests such as Chi-Square remain unchanged.
- It facilitates the interpretation of table values expressed on a percentile scale.
- It enables simple correspondence analysis with greater statistical validity.

It is inferred that the proposed linear scaling allows for the full utilization of information in tables with small values, rendering the analysis more robust and powerful without altering the original relationships. Its application in the analysis of fuzzy data and scenarios with low expected frequencies is highly promising.

3 A MORE COMPLEX EXAMPLE

In [17], Bolboaca and co-authors employed Fisher's Exact Test to illustrate the analysis of independence in the experimental data reported by Fisher [18] (Table 12). In this study, Fisher's table is used to provide a more complex exemplification of the proposed methodology. These experimental values correspond to the response to manure fertilization across different potato varieties. The comparison is made between Treatment and Variety; UD, KK, KP, TP, ID, GS, AJ, BQ, ND, EP, AC, DY: potato varieties (UD = Up to Date; KK = King of K; KP = Kerr's Pink; TP = Tinwald Perfection; ID = Iron Duke; GS = Great Scott; AJ = Ajax; DY = Duke of York); DS, DC, US, UC, UB: treatment types (D* – manure; U* – no manure; S – sulfate; C – chloride; B – basal). Based on this Fisher table, established methods were applied to compare the original table and the scaled version (Tables 12 to 16 and Tables 17 to 21, respectively).

Table 12: Experimental values: response to manure fertilization across different potato varieties (original Fisher table).

ORIGINAL

TV	UD	KK	KP	TP	ID	GS	AJ	BQ	ND	EP	AC	DY
DS	25	28	23	20	23	21	22	22	18	15	14	10
DC	26	27	24	19	21	24	17	21	20	16	11	12
DB	27	24	14	20	20	22	22	21	16	14	11	13
US	23	20	18	20	16	16	13	13	12	13	13	8,2
UC	19	17	21	18	18	14	20	14	13	12	13	8,3
UB	9,5	6,5	4,9	7,7	4,4	2,3	4,2	6,6	1,6	2,2	2,2	1,6

Table 13: Test of independence using Chi-Square.

ORIGINAL

Test of independence between rows and columns (Chi-square):

Chi-square (Observed value)	22,022
Chi-square (Critical value)	73,311
GL	55
p-value	1,000
alfa	0,05

Test interpretation:
H0: The rows and columns of the table are independent.
Ha: There is a dependency between the rows and columns of the table.

Since the calculated p-value is greater than the significance level alpha=0.05, the null hypothesis H0 cannot be rejected.

Theoretical frequencies less than 5 have been detected. To safely use the Chi-square test based on the approximation by the Chi-square distribution, the theoretical frequencies should not be less than 5.

Table 14: Test of independence using Wilks' G^2.

Test for independence between rows and columns (Wilks' G^2):

Wilks G^2 (Observed Value)	22,505
Wilks G^2 (Critical Value)	73,311
GL	55
p-value	1,000
alfa	0,05

Test interpretation:
H0: The rows and columns of the table are independent.
Ha: There is a dependency between the rows and columns of the table.

Since the calculated p-value is greater than the significance level alpha=0.05, the null hypothesis H0 cannot be rejected.

Table 15: Association coefficients.

Association coefficients:

Coefficient	Value
Pearson Phi	0,14
Cramer's V	0,06

Table 16: Significance per cell using Fisher's Exact Test.

Significance per cell (Fisher's exact test):

	UD	KK	KP	TP	ID	GS	AJ	BQ	ND	EP	AC	DY
DS	<	>	>	<	>	<	>	>	>	<	>	<
DC	<	>	>	<	<	>	<	>	>	>	<	>
DB	>	<	<	<	<	>	>	>	<	>	<	>
US	>	>	>	>	<	<	<	<	<	>	>	<
UC	<	<	>	>	>	<	>	<	<	>	>	<
UB	>	>	<	>	<	<	<	>	<	<	<	<

Values in red are significant at the alpha=0.05 level.

Table 17: Original Fisher table scaled from 1 to 100.

SCALATION 0 to 100

TV	UD	KK	KP	TP	ID	GS	AJ	BQ	ND	EP	AC	DY
DS	90	100	82	70	81	73	78	77	63	50	46	32
DC	92	96	86	66	72	86	58	73	71	53	36	39
DB	94	84	48	70	70	77	76	72	55	48	36	44
US	81	71	63	70	54	54	42	42	39	41	41	25
UC	64	58	73	63	60	48	68	46	43	39	42	25
UB	30	19	13	23	11	3	10	19	0	2	2	0

Table 18: Test of independence using Chi-Square.

SCALATION 0 to 100

Test of independence between rows and columns (Chi-square):

Chi-square (Observed value)	118,334
Chi-square (Critical value)	73,311
GL	55
p-value	< 0,0001
alfa	0,05

Test interpretation:
H0: The rows and columns of the table are independent.

Ha: There is a dependency between the rows and columns of the table.

Since the computed p-value is less than the significance level alpha=0.05, the null hypothesis H0 should be rejected, and the alternative hypothesis Ha should be accepted.

Table 19: Test of independence using Wilks' G^2.

Test for independence between rows and columns (Wilks' G^2):

Wilks G^2 (Observed Value)	134,224
Wilks G^2 (Critical Value)	73,311
GL	55
p-value	< 0,0001
alfa	0,05

Test interpretation:
H0: The rows and columns of the table are independent.
Ha: There is a dependency between the rows and columns of the table.

Since the computed p-value is less than the significance level alpha=0.05, the null hypothesis H0 should be rejected, and the alternative hypothesis Ha should be accepted.

Table 20: Association coefficients.

Association coefficients:

Coefficient	Value
Pearson Phi	0,18
Cramer's V	0,08

Table 21: Significance per cell using Fisher's Exact Test.

Significance per cell (Fisher's exact test):

	UD	KK	KP	TP	ID	GS	AJ	BQ	ND	EP	AC	DY
DS	<	>	>	<	>	<	>	>	>	<	>	<
DC	<	>	>	<	<	>	<	>	>	>	<	>
DB	>	<	<	<	<	>	>	>	<	>	<	>
US	>	>	>	>	<	<	<	<	<	>	>	<
UC	<	<	>	>	>	<	>	<	<	>	>	<
UB	>	>	>	>	<	<	<	>	<	<	<	<

Values in red are significant at the alpha=0.05 level.

The benefits of applying linear scaling to adjust the values in contingency tables for statistical analysis are as follows:

- Homogenization of the value scale: Transforming all data to a common scale from 0 to 100 minimizes the impact of the wide variability in original ranges. This normalization not only facilitates direct comparisons between groups but also ensures a more uniform and equitable application of statistical tests.
- Increased statistical power: Expanded scaling significantly enhances the ability to detect associations in cells containing small values and to identify subtle yet statistically significant patterns. This modification is essential for revealing trends that might otherwise remain undetected under more restrictive scales.
- Compliance with statistical assumptions: Adjusting the values increases those that are small, thereby facilitating compliance with critical assumptions for tests such as the Chi-Square, which require expected frequencies greater than five in each cell.
- Ease of interpretation: Employing a common metric from 0 to 100 simplifies the visual interpretation of data, making trends and patterns more evident—patterns that might be difficult to discern on the original scale.
- Applicability of multiple statistical tests: Standardization through scaling enables the application of a broader range of statistical tests that require specific conditions in the data, thereby maximizing the utility of the contingency table.
- Preservation of association structure: Despite the transformation of values, the row/column association structure of the original table remains intact, ensuring that the conclusions drawn are consistent with the underlying data structure.
- Comprehensive view of relationships: By complementing traditional tests with scaling, a more robust and comprehensive perspective of the relationships between variables is achieved, enhancing the overall interpretation of the data.
- Although scaling may introduce variations in the inertia of contingency tables, it does not compromise the original data structure. In fact, this adjustment allows for a more detailed evaluation of underlying associations, offering a richer and more nuanced view that may be critical in research contexts where small values predominate.

In conclusion, the application of linear scaling balances analytical conditions and enhances analytical capacity without distorting the intrinsic relationships within the data. As a result, this technique facilitates the identification of findings that might otherwise remain invisible without such adjustment, thereby improving the quality and precision of statistical analysis.

4 CASE OF TABLES WITH FUZZY NUMBERS

In the case of tables containing fuzzy numbers or possibility values, once equivalence is established through linear scaling, a simple correspondence analysis may be performed. By preserving the original proportions of the table, linear scaling maintains the fuzzy relationships between cells. For instance, if cell A has twice the possibility value of cell B in the original table, this ratio is preserved in the scaled version.

This aspect is essential when working with fuzzy logic, as the relative distribution of possibility values conveys critical information regarding the fuzzy nature of the categories. Scaling the table does not distort these relationships, thereby allowing the same interpretative conclusions to be drawn from the fuzzy data. Moreover, expanding the values to a broader range through scaling enhances the resolution of intermediate possibilities. For example, a probability of 0.2 may be expanded to 20, offering clearer differentiation from a value of 0.3, which would be scaled to 30.

This provides greater degrees of freedom for statistical tests, rendering them more robust and precise in detecting diffuse relationships and associations within the data. Tests such as Chi-Square or Fisher's Exact Test tend to be less reliable when expected frequencies are very low.

Finally, in fuzzy tables, possibility values are typically low, often concentrated between 0 and 0.5. By scaling them to a broader range, the statistical power of the tests is increased, enabling the identification of diffuse relationships that might otherwise go unnoticed due to the small magnitude of the values.

5 COMPARATIVE ADVANTAGES USING SCALED CONTINGENCY TABLES

The linear scaling of contingency tables—particularly those incorporating fuzzy numbers or possibility values—is performed to adapt the data structure to the requirements of more robust

statistical analyses, such as Simple Correspondence Analysis (SCA). This transformation process is crucial when the original tables contain minimum values that do not correspond to zero, which could distort data interpretation if not properly adjusted.

5.1 Effects of Linear Scaling

Preservation of proportional structure: When applying a linear scale, the original proportional structure of the table is maintained. For example, if cell A in the original table contains a possibility value twice that of cell B, this ratio is preserved after scaling (e.g., 0.2 to 20 and 0.1 to 10). This consistency is essential to ensure that the interpretations derived from the analysis are not affected by the transformation of the data.

Increased resolution of intermediate possibilities: By expanding values to a broader numerical range, scaling improves the resolution of the data. Subtle differences between possibility values become more distinguishable, increasing the sensitivity of subsequent statistical tests.

This is particularly valuable in contexts where small differences may carry significant practical implications.

5.2 Impact on Simple Correspondence Analysis

Variability in inertias: Although scaling preserves the proportional structure, the inertias calculated in SCA may vary. This is because inertia depends on the absolute distribution of frequencies within the table, and scaling modifies these absolute values. However, since the relative pattern among cells remains constant, the qualitative interpretation of the correspondence maps should not change significantly.

Robustness in detecting fuzzy relationships: Given that possibility values are typically low—often concentrated between 0 and 0.5—scaling broadens the analytical spectrum by converting them into a wider range, such as 0 to 100. This adjustment not only enhances the ability to detect subtle and diffuse relationships among categories, but also increases the statistical power of tests like Chi-Square and Fisher's Exact Test, which are less effective when expected frequencies are low.

6 VAGUE CONTINGENCY DATA

Aslam and Alamri [19] describe a method that modifies Fisher's Exact Test using neutrosophic statistics, focusing on the analysis of contingency data that are not precisely defined. This approach enables the use of neutrosophic numbers, which represent data with inherent uncertainty through a format that incorporates degrees of truth, falsehood, and indeterminacy for each data element.

This method differs from the traditional Fisher's Exact Test, which employs precise and well-defined values to calculate the probability of observing a data distribution at least as extreme as the one observed, under the null hypothesis that no differences exist between groups. In contrast, the neutrosophic modification allows uncertainty and indeterminacy to be incorporated directly into the data, which is particularly useful in contexts such as social surveys or perception studies, where responses are not always clear or direct. In practice, the principles of neutrosophic theory are applied to expand the contingency matrices used in Fisher's test with additional dimensions that capture these degrees of indeterminacy, thereby enabling a richer and more realistic interpretation of the data under analysis.

The approach proposed in this study addresses uncertainty in the data by applying a one-time preprocessing step prior to conducting classical statistical tests such as Fisher's Exact Test.

The data are transformed into fuzzy sets before statistical analysis, maintaining the use of traditional statistical tests, albeit adapted to the new data structure.

- Identification of Imprecision: Imprecision in the data is identified as a consequence of various factors, including missing values, measurement error, subjectivity, and the complexity of the phenomenon under study. The uncertainty inherent in this context requires specialized handling, for which the use of fuzzy logic tools is essential.
- Use of fuzzy variables: The original variables are transformed into fuzzy sets, representing imprecision through degrees of membership rather than binary or discrete values. This allows for a more flexible and adaptive interpretation of the data, avoiding the rigidity of strict and potentially inaccurate categorizations.
- Construction of Contingency Tables with Possibility Values: Contingency tables are constructed incorporating these degrees of membership, with values scaled to a range from 0 to 100. This is a fundamental step in adapting Fisher's Exact Test and other association tests to the diffuse nature of the data.
- Application of Statistical Tests: Despite the transformation of the data into fuzzy form, conventional statistical methods such as Fisher's Exact Test are used to evaluate

independence or association between variables, with these tests adapted to work effectively with the new data structures.

6.1 Comparison of Both Methods

Both methods aim to address the challenge of working with data that contain uncertainty or vagueness, albeit through distinct theoretical frameworks and data transformation strategies. While our approach in [18] employs fuzzy set theory to modify the data prior to applying established statistical tests, the neutrosophic method adapts the statistical test itself to directly accommodate uncertain data without prior transformation at the data value level.

- Regarding the use of fuzzy sets: The proposed method involves transforming the original variables into fuzzy sets, which entails defining degrees of membership of the data to specific sets, based on the membership function that best characterizes the uncertainty or vagueness of the data. For instance, rather than relying on classical binary data, an element may belong to a set with a degree of 0.7, indicating a level of membership rather than a strict binary classification. In contrast, the neutrosophic method utilizes neutrosophic numbers that incorporate degrees of truth, falsehood, and indeterminacy. Each element in the analysis provides information about its potential truthfulness, falsity, and a degree of uncertainty that is typically not considered in conventional statistical approaches.
- Regarding the construction of contingency tables: The proposed method constructs contingency tables using possibility values derived from fuzzy sets, which reflect the uncertainty in the classification of each entry. These values are scaled to a range of 0 to 100 to standardize and facilitate the application of association tests. This scaling helps to manage small values that could compromise the validity of traditional statistical tests. In the neutrosophic method, contingency tables are modified to incorporate indeterminacy alongside truth and falsehood, thereby expanding the classical contingency matrix into a more complex structure that better captures the uncertainty inherent in the data.
- Regarding the application of statistical tests: Once the contingency table has been adjusted to reflect uncertainty through fuzzy sets and appropriately scaled, Fisher's Exact Test is applied to assess independence or association between variables. This step maintains a robust statistical approach, adapted to the new data structure. In the neutrosophic method, the application of neutrosophic statistics may require modifying the calculation of Fisher's Exact Test to incorporate degrees of indeterminacy, potentially by adjusting the computation of the exact probability of the observed tables under the null hypothesis.

The methodology proposed in this study offers interpretative flexibility and is compatible with existing theories that utilize multiple ranges or categories, thereby enabling a more nuanced understanding. Both approaches provide valuable frameworks for managing uncertainty in statistical analysis, each pursuing different theoretical and practical paths to integrate or accommodate imprecision in data. The approach presented herein is distinguished by its adaptability and its capacity to incorporate fuzzy logic in a manner that is more intuitive and closely aligned with the way humans interpret imprecise information.

7 DATA WITH SMALL SAMPLE SIZES

In [20], the authors present an independent contingency testing approach using the bootstrap method to enhance precision in contingency tables, particularly in cases involving small sample sizes where Chi-Square and Fisher's Exact Test may be less effective. The Chi-Square and Fisher tests are discussed and critiqued for being asymptotic and conservative, respectively, which can lead to errors, especially in tables with low cell frequencies. To address this issue, bootstrap versions of the Chi-Square tests (both Pearson and likelihood ratio) are proposed. These simulate the distribution of the test statistic under the null hypothesis through resampling, resulting in more accurate tests that are less dependent on sample size. Simulation studies are used to demonstrate that bootstrap tests maintain the nominal level more accurately than traditional asymptotic approximations and Fisher's Exact Test.

Both methods aim to improve the validity of independence tests in contingency tables under conditions of uncertainty or small sample sizes, but they do so from different operational philosophies: modifying the data versus modifying the testing process.

The method presented in this study stands out for its ability to integrate fuzzy logic in a way that is more accessible and relevant to those directly involved in

the collection or interpretation of ambiguous data.

- Theoretical foundation: This study proposes the application of fuzzy logic transformations to the variables prior to analysis, creating contingency tables based on degrees of membership, which can better reflect the uncertainty present in the data. The bootstrap method seeks to improve the precision of standard tests through resampling, without altering the nature of the data, but rather adjusting the evaluation of the test statistic.
- Data transformation: A data structure is proposed that results from converting values into fuzzy degrees of membership prior to any statistical analysis. The bootstrap method does not require modification of the data; instead, it adapts the statistical evaluation process to be more robust in the context of small samples and low frequencies.
- Evaluation and comparison: An intuitive approach is offered, directly aligned with human interpretations of imprecise data, adapting existing tests for use with new data formats. It is proposed to scale contingency tables incorporating these degrees of membership from a 0–1 range to a 0–100 range. This scaling allows for the adaptation of traditional statistical tests such as Fisher's Exact Test to conditions where small or near-zero values could negatively affect the test's validity. The bootstrap method provides a robust and flexible approach that can be applied without prior modifications to the data, which may be advantageous in applications requiring the preservation of the original data integrity or when the optimal way to parameterize uncertainty is unknown.
- Adaptation of the testing process: Similar to the bootstrap method, the approach presented in this thesis also adapts the testing process to better handle suboptimal sampling conditions. However, this is achieved by modifying the data structure to reflect uncertainty, unlike bootstrapping, which adjusts the statistical evaluation procedure.

8 CONCLUSIONS

The linear scaling approach is ideal for fully leveraging the information contained in fuzzy tables, rendering the analysis more robust and sensitive to uncovering complex underlying fuzzy relationships. Although the scaling process modifies the absolute values of the entries in the contingency table, it does not affect the conclusions that can be drawn from Simple Correspondence Analysis. This validates the use of scaling as a technique that facilitates the application of statistical tests without compromising the analytical integrity of the data.

Correspondence analysis applied to scaled tables demonstrates that, while the relative proportions and relationships between cells are preserved, the analysis benefits from higher resolution and an expanded range, allowing for a deeper exploration of fuzzy associations. These findings confirm the effectiveness of linear scaling as a technique for preparing fuzzy data for complex statistical analyses, while ensuring that the fundamental interpretation of the data remains intact.

Linear scaling not only enables the robust application of tests such as Chi-Square and Fisher's Exact Test to tables with very low frequencies, but also provides a practical tool for researchers in diverse fields such as agronomy, medicine, engineering, and sensor analytics. The methodology developed, along with its associated software, allows for the automatic transformation of data from a 0–1 scale to a 0–100 scale, preserving cell relationships and enhancing the detection of patterns that might otherwise remain hidden.

This opens new avenues for the analysis of imprecise data—such as membership matrices in recommender systems or ultrafine measurements in geoscience and biometrics. It is recommended to integrate this approach with other rescaling techniques and to extend its application to multidimensional tables, time series, and machine learning algorithms. Likewise, the development of software packages in various programming languages and the comparison of this method's performance with alternative approaches will contribute to its consolidation within the scientific community.

This study represents a significant advancement in the management of imprecise data and offers new pathways for exploring categorized data across various scientific disciplines and industrial applications. For future research, it would be beneficial to explore the application of linear scaling to other types of statistical data that face similar challenges, such as biometric or geostatistical data, where measurements are often extremely precise but small in magnitude.

REFERENCES

[1] Y. Zhai, W. Song, X. Liu, L. Liu, and X. Zhao, "A Chi-Square Statistics Based Feature Selection Method in Text Classification," in *IEEE 9th International Conference on Software Engineering*

and Service Science (ICSESS), Beijing, China, 1918.
[2] S. Rosidin, G. Fajar Shidik, and A. Zainul Fanani, "Improvement with Chi Square Selection Feature using Supervised Machine Learning Approach on Covid-19 Data," *International Seminar on Application for Technology of Information and Communication*, Semarangin, Indonesia, 2021.
[3] J. Angulo-Paniagua, and J. Quirós-Tortós, "Comparing Chi-square-Based Bad Data Detection Algorithms for Distribution System State Estimation," *IEEE PES Transmission & Distribution Conference and Exhibition - Latin America (T&D LA)*, Montevideo, Uruguay, 2020.
[4] Z Wang, Z. Huang, Y. Xu, Y. Zhang, and X. Li, "Image Noise Level Estimation by Employing Chi-Square Distribution," *21st International Conference on Communication Tech*, Tianjin, China, 2021.
[5] I. Chen, "A Novel and Fast Distributed Computation Method for Fisher's Exact Test and Its Application in Gene Expression Profiling Studies," *IEEE MIT Undergraduate Research Technology Conference (URTC)*, Cambridge, MA, USA, 2022.
[6] A. Poon, S. Jankly, and T. Chen, "Privacy Preserving Fisher's Exact Test on Genomic Data," *IEEE International Conference on Big Data (Big Data)*, Seattle, WA, USA, 2018.
[7] P. Campos, I. Cantador, F. Díez, and I. Fernández-Tobías, "A Criterion Based on Fisher's Exact Test for Item Splitting in Context-Aware Recommender Systems," *33rd International Conference of the Chilean Computer Science Society (SCCC)*, Talca, Chile, 2014.
[8] R. Yano, H. Tanioka, K. Matsuura, M. Sano, and T. Ueta, "Quantitative Measurement and Analysis to Thinking as a Way of Programming for Elementary School in Japan," *9th International Congress on Advanced Applied Informatics (IIAI-AAI)*, Kitakyushu, Japan, 2020.
[9] H. Kim, "Statistical notes for clinical researchers: Chi-squared test and Fisher's exact test," *Restorative Dentistry & Endodontics*, vol. 42, pp. 152-155, 2017.
[10] K.T. Jafseer, S. Shailesh, and A.Sreekumar, "Feature Drift Detection using Overlapping Window and Mann-Whitney U Test," *4th International Conference on Innovative Trends in Information Technology (ICITIIT)*, Kottayam, India, 2023.
[11] M. Fetaji, L. Morina, and B. Fetaji, "Devising and evaluating B2B conceptual model for B2B portal for mobile interactive devices using Mann-Whitney U test," *6th Mediterranean Conference on Embedded Computing (MECO)*, Bar, Montenegro, 2017.
[12] K. Jafseer, S. Shailesh, and A. Sreekumar, "Feature Drift Detection using Overlapping Window and Mann-Whitney U Test," *4th International Conference on Innovative Trends in Information Technology (ICITIIT)*, Kottayam, India, 2023.
[13] M. Césari, N. Ventrera, and A. Gámbaro, "Análisis de datos sensoriales de tomate triturado con lógica difusa y técnicas multivariadas.", *Revista de la Facultad de Ciencias Agrarias, Universidad Nacional de Cuyo*, vol. 50(1), pp. 233-248, 2028.
[14] M. Césari, N. Ventrera, and A. Gámbaro, "Análisis de datos sensoriales de tomate triturado con lógica difusa y técnicas multivariadas," *Revista de la Facultad de Ciencias Agrarias, Universidad Nacional de Cuyo*, vol. 50(1), pp. 233-248, 2018.
[15] M. Césari, and R. Césari, "La lógica difusa aplicada para valorar rúbricas de evaluación," *X Congreso Nacional de Ingeniería Informática / Sistemas de Información - CoNaIISI 2022*, Facultad
[16] Addinsoft Xlstat versión 2018, licencia para investigación. Análisis estadístico para Microsoft Excel desarrollada por Addinsoft 1996-2018, Available in www.xlstat.com/es/products/xlstat-pro/.
[17] S. Bolboacă, L. Jäntschi, A. Sestraş, R. Sestraş, and D. Pamfil, "Fisher chi-square statistic revisited. Information," *Pearson*, vol. 2(3), pp. 528-545, 2011.
[18] R. Fisher, "The conditions under which χ 2 measures the discrepancy between observation and hypothesis," *Journal of the Royal Statistical Society,* pp. 442-450, 1924.
[19] M. Aslam, and F. Alamri, "Data analysis for vague contingency data.", *Journal of Big Data*, vol. 10(1), pp. 131, 2023.
[20] J. Lin, C. Chang, and N. Pal, "A Revisit to Contingency Table and Tests of Independence: Bootstrap is Preferred to Chi-Square Approximations as Well as Fisher's Exact Test," *Journal of Biopharmaceutical Statistics*, vol. 25(3), pp. 438-458, 2015, DOI: 10.1080/10543406.2014.920851.
[21] Césari, M. (2024). *DaFu: Automated Linear Scaling for Statistical Analysis in Contingency Tables* [Computer software]. GitHub. https://github.com/matucesari/DaFu
[22] Césari, M. (2024). *DaFu03: Fuzzy Associations Web Application* http://micesari.servehttp.com:3838/DaFu03_AsociacionesDifusas/

RECyT
Year 27 / Nº 44 / 2025 /
DOI: https://doi.org/10.36995/j.recyt.2025.44.002

Diagnosis of the circular economy in municipalities of Misiones, Argentina

Diagnóstico de Economía circular en municipios de Misiones, Argentina

Sonia R., Niezwida [1, *]; María F., Kaczynski [1]; Fernando A., Santacruz [2]; Juan C., Michalus [1]; Chiara M., Villalba Auras [1]

1- School of Engineering. National University of Misiones (FI-UNaM). Oberá, Misiones, Argentina.
2- Undersecretary of Circular Economy of Misiones. Ministry of Climate Change. Posadas, Misiones, Argentina.
* E-mail: sonia.niezwida@fio.unam.edu.ar

Received: 20/10/2024; Accepted: 24/09/2025

Abstract
This article outlines the methodology and summarizes the main results of the 2023 circular economy assessment carried out in Misiones Province, Argentina. The research was held through a collaborative agreement between the academy and the government, aiming to provide inputs for the preparation of the first provincial report on circular economy. The stratified sampling method was used to obtain selection of a representative sample of 21 localities out of 78 municipalities. In addition to surveying these municipalities, information was collected from private companies involved in household waste recycling. The analysis made it possible to estimate the circularity index, identify circular practices, quantify recycled and composted fractions, assess the available infrastructure, and recognize challenges according to municipality size. The results indicate that only 15.36% of the generated waste returns to productive or biological cycles, with higher circularity levels in more populated municipalities. The findings suggest that waste management should be reinforced and circular strategies broadened through collaborative work, policymaking, and further research.

Keywords: circular economy, management, municipalities, household waste, surveys.

Resumen
Este artículo presenta la metodología y los principales resultados sobre el diagnóstico de economía circular en la provincia de Misiones, Argentina para el período 2023. La investigación se desarrolló mediante un convenio de colaboración entre la Academia y el Estado, con el objetivo principal de generar insumos para la elaboración del primer informe provincial sobre economía circular. Se aplicó el muestreo estratificado, el cual permitió seleccionar una muestra representativa de 21 localidades a partir de la población constituida por 78 municipios. Además de encuestar a dichos municipios, se recolectó información de las empresas privadas vinculadas al reciclaje de residuos domiciliarios. El análisis permitió estimar el índice de circularidad, identificar prácticas circulares, cuantificar las fracciones recicladas y compostadas, evaluar la infraestructura disponible y reconocer desafíos según el tamaño municipal. Los resultados indican que solo el 15,36 % de los residuos generados vuelve a ciclos productivos o biológicos, con mayores niveles de circularidad en municipios más poblados. Se concluye que es necesario fortalecer la gestión de residuos y ampliar las estrategias circulares, mediante el trabajo colaborativo, políticas públicas y futuras investigaciones.

Palabras clave: economía circular; gestión; municipios; residuos domiciliarios, encuestas.

1 Introduction

Globalization and urban growth have contributed to significantly increased solid waste production, challenging the capacity of municipalities to manage them in a proper way. In this context, Circular Economy (CE) arises as a new paradigm that redefines the concept of waste, allowing it to be a resource through strategies by reusing, recycling, repairing, and reducing consumption of unspoiled resources. According to the Ellen MacArthur Foundation [1], CE is a proposal for closing productive cycles, minimizing natural resources extraction by reducing the environmental impact of waste generated along consumption stages or industrial processes.

CE has also been catalogued as a transversal strategy that promotes sustainability and innovation in waste management. Geissdoerfer et al. [2] describe it as a convergence among environmental sustainability, economic efficiency, and social responsibility.

In Latin America and the Caribbean, recent studies reveal that the CE approach continues to emphasize recycling, whereas strategies like reuse and prevention remain underused because of institutional and governmental barriers, insufficient incentives, and inadequate municipal infrastructure, among other issues [3,4,5].

In Argentina, the adoption of the circular model at the municipality level is still incipient in most

localities. Some cities have developed circular strategies based on the Comprehensive Urban Solid Waste Management Plan (from Spanish, GIRSU Plan), while others still reveal structural deficits and limited coordination among public, private, and social actors, which constrain municipalities' ability to adequately address management needs.

In Misiones Province, municipalities have a higher-level entity for the province, the Undersecretary of Circular Economy, which has been promoting these initiatives since 2022. In this context, several municipalities in the province have begun exploring initiatives related to the circular economy through the installation of "eco-points" and "clean points" (recycling stalls or stands). These are community spaces for daily use where residents can separately dispose of recyclable and bulky waste. In addition, public programs were implemented, such as "My school recycles" and organic waste composting [8].

In 2024, the School of Engineering of the National University of Misiones, in Oberá, and the Ministry of Climate Change agreed to work collaboratively on fields related to Circular Economy (CE), producing the first provincial report on CE by 2023. In contrast to the previously prepared report, which primarily presented the results, this new document offers a more in-depth examination of the research methodology, incorporating a greater rigorous and critical analysis, as well as the discussion of the findings. In this regard, the objective of this study is to present a diagnostic assessment of the Circular Economy (CE) in the municipalities of Misiones, Argentina, supported by a detailed description of the methodology, including employed procedures and tools.

2 Materials and methods

This study follows a quantitative approach, relying on data collected through structured instruments; more specifically, a questionnaire, which enables the statistical analysis of observed patterns and relationships, along with surveys administered to the relevant stakeholders. Furthermore, this is applied research [9], as it is directly aimed at collecting information through orienting strategies for a concrete issue: diagnosing and generating empirical insights for designing useful public policies for household waste, regarding the circular economy in Misiones Province.

The study was developed through three primary stages: first, a round of exploratory surveys was conducted in randomly selected municipalities in Misiones Province. During the second stage, a formal survey was elaborated, and the representative sample of municipalities was determined by stratum.

In the third stage, surveys were administered to sample municipalities, private recycling companies, and some other relevant companies that could be accessed, with the aim of gathering this information. Ultimately, data analysis and conclusion discussions were carried out. Below, a brief description of the previously mentioned stages can be found:

2.1 Stage 1: Elaboration of the exploratory survey

The first phase consisted of a round of exploratory surveys designed through a Google Forms questionnaire to identify key topics and adjust the questions for the formal survey targeted to municipality stakeholders. These preliminary surveys were conducted with a small group of participants randomly selected from different municipalities. The results of this preliminary stage helped to refine the questionnaire and ensure the relevance and clarity of the questions, in order to obtain more useful answers and reduce errors as well as uncertainty among respondents.

2.2 Stage 2: Elaboration of the formal survey and determination of the sample

To define the formal questionnaire, questions from the sample version were redesigned. The items and questions that made up the final questionnaire [10] included:

-Municipality denomination.

-Individuals in charge of the Waste Management Area.

-WhatsApp contact.

-The following questions: 1. How many tonnes of bulky and Urban Solid Waste (USW) did the municipality generate in 2023?; 2. How many tonnes of this waste collected in 2023 were sent to the AESA transfer station?; 3. How many tonnes of waste were recovered to recycle and compost in 2023?; 4. Does the municipality have a final disposal site for bulky waste (such as pruning, wood, scrap materials, among others)?; 5 Name of the municipality government area that manages USW; 6. Does the municipality have a waste sorting facility?; 7. Does it have a composting program?; 8. If the previous question was answered affirmatively, how many tonnes of compost are produced every year?; 9. Does the municipality have "eco-points"? How many "eco-points" does the municipality have?; 10. What is the total number of municipality workers dedicated to waste management?; 11. Does the municipality articulate material recovery for recycling with urban waste recuperators?; 12. Are there any urban waste recuperators in the municipality? "Urban waste recuperators" are individuals who collect, select, recover, transform, trade, and reuse solid waste, previously known as "cartoneros" (in Argentina, similar to scrap dealers) or recyclers.; 13. If the previous question was answered affirmatively, please indicate the

estimated number of urban recuperators in the municipality.; 14. Does the municipality have any of the following programs? Please, only mark the programs that the municipality HAS: recovery of Used Cooking Oil (UCO), end-of-life tires, electrical and electronic devices, none, others; 14. Does it have a global figure representing the total amount of waste recovered by private actors or parties in the municipality? That is to say, it is asked to estimate the approximate kilograms that companies or organizations recycle in the municipality every month.; 15. Does the municipality have entrepreneurs or salespeople who reuse materials? Please, comment briefly. (For instance, 5 entrepreneurs using plastic bottles for decorations, 2 entrepreneurs using glass for local fairs or markets.)

Before distributing the formal survey, a sample of municipalities was selected from the entire population in Misiones to identify those that would receive the questionnaire. In order to do this, 78 municipalities were enlisted and selected as a representative list of Misiones Province population by following the steps described below.

2.2.1 Sample selection

The sample for this study has been selected employing the stratified sampling method to ensure that all relevant subgroups (municipalities categorized by zone and population size) were adequately represented, according to Sampieri *et al.* [9]. In which, for every stratum h:

- N_h: total population (inhabitants) of the stratum
- n_h: number of sample municipalities in the stratum
- w_i: weight for population-based weighting, applied by zone (z) and by population category (c):

$$wi = w(z) * w(c) \quad (1)$$

$$w(z) = \frac{Zone\ population}{Province\ population} \quad (2)$$

$$w(c) = \frac{Category\ population}{Total\ population\ of\ the\ zone} \quad (3)$$

Stratification was carried out by zone (z) and by category according to population size (c). Based on the total population of municipalities and weighting (1) by the province zone in which each municipality is located (South, Centre, or North) and (2) by population category (Low, Medium, or High), a certain number of municipalities were selected, constituting the sample after applying the corresponding formulas.

2.2.2 Data collection procedure

Providing the formal survey in Google Forms, officials who work on waste management for the sample municipalities were contacted one by one. Employed methods to obtain answers can be found below:

- Telephonic verbal communication: calls were made to contact officials who work on waste management for the sample municipalities (or those who are in charge of waste management in the localities). On the other hand, municipality agents or staff members who preferred this type of communication for any reason were also contacted by phone.

In different cases, detailed answers in this type of communication were transcribed directly into the questionnaire.

- Mobile phone communication: WhatsApp messages were sent to distribute the questionnaire and facilitate communication with participants, taking advantage of the popularity of the platform.
- E-mail: surveys were also sent through email. These means of communication allowed participants the ability to answer an online form, providing more thoughtful answers described in the questionnaire.

2.3 Stage 3: Analysis of the obtained answers

Once the information from the municipalities was collected, an analysis was carried out in order to identify patterns and trends in the answers. Microsoft Excel v.2022 and IBM SPSS Statistics v.29.0.2.0 software were used for this purpose, as it is a useful software to analyse data and elaborate graphics since information can be downloaded from Google Form and imported directly into this software.

The application of the previously described stages ensured the selection of a representative sample and the collection of relevant data, offering a comprehensive view of the population's perspectives and circular economy practices across the municipalities of Misiones Province.

3 Results and discussion section

The municipalities of Misiones Province have been the subjects of this study.

In addition, the initial exploratory survey was only targeted at 10 municipalities randomly selected. This pilot exercise made it possible to identify key topics, areas of interest, and potential difficulties in understanding certain questions.

The school research team worked on the creation of a formal questionnaire based on the exploratory survey findings for more than one week. The development of the formal questionnaire was carried out in collaboration between the School of Engineering, in Oberá, and the Undersecretary of Circular Economy of Misiones. The final version included both open and closed questions to gather information on the municipalities' perspectives and practices regarding the circular economy, as well as activities related to "eco-points", "clean points", composting, and engagement with urban recuperators or local cooperatives.

To ensure that the municipalities selected in the sample were representative, the following steps were taken:

Step 1: Municipality separation by strata
The municipalities of Misiones Province were classified by strata according to their geographic location (South, Centre, or North) and by category (Table 1), considering the population characteristics reflected in the last National Population and Dwelling Census carried out by the National Statistics Institute (INDEC) in 2022 [11].

Table 1: Sample stratification.

Stratum by zone (h)	Nh (Number of municipalities by zone)	Sample stratification	Stratum by population category: c (number of municipalities by category)
North	24	5 municipalities	High (1)-Medium (2)-Low (2)
Centre	38	12 municipalities	High (1)-Medium (6)-Low (5)
South	15	4 municipalities	High (1)-Medium (2)-Low (2)

Source: Prepared following Sampieri *et al*. [9]

The study population consisted of 78 municipalities (N).
The sampling error (E) is calculated by combining the errors by stratum (Eh) according to (4):

$$E = Z * Etotal \quad (4)$$

With a 95% confidence level (Z = 1.96), where p = 0.5 (maximum variance)
For $n_{h=north}$=5, $n_{h=centre}$=12, $n_{h=south}$=4
Therefore, for each zone (h):

$$Eh = \sqrt{\frac{p*(1-p)}{nh}} * \sqrt{\frac{Nh-nh)}{Nh-1}} \quad (5)$$

$$Wh = \frac{Nh}{N} \quad (6)$$

$$Etotal = \sqrt{\sum_h (Wh^2 * Eh^2)} \quad (7)$$

By substituting the values and performing the corresponding calculations, the sampling error is 18.8%, which is consistent with the methodological criteria proposed by Sampieri *et al*. [9] (the error must be lower than 25%). Therefore, the sample ensures an acceptable level of representativeness.

Step 2: Selection of sample municipalities
Within each stratum (Table 1), the cities with the largest populations were selected (60,000 inhabitants or more), as well as towns with medium populations (higher than 10,000 and less than 60,000 inhabitants) and low populations (peripheral municipalities[1] with less than 10,000 inhabitants), resulting in a total of 21 (sample) municipalities selected to participate in the formal survey. Sample municipalities represented almost 80% of the provincial population. Figure 1 shows municipalities integrating this sample and their estimated population based on INDEC data [11].

[1] Peripheral municipalities are those localities that have disadvantaged conditions due to poor infrastructure, basic public services, state investment, and socioeconomic opportunities for the inhabitants [12,13].

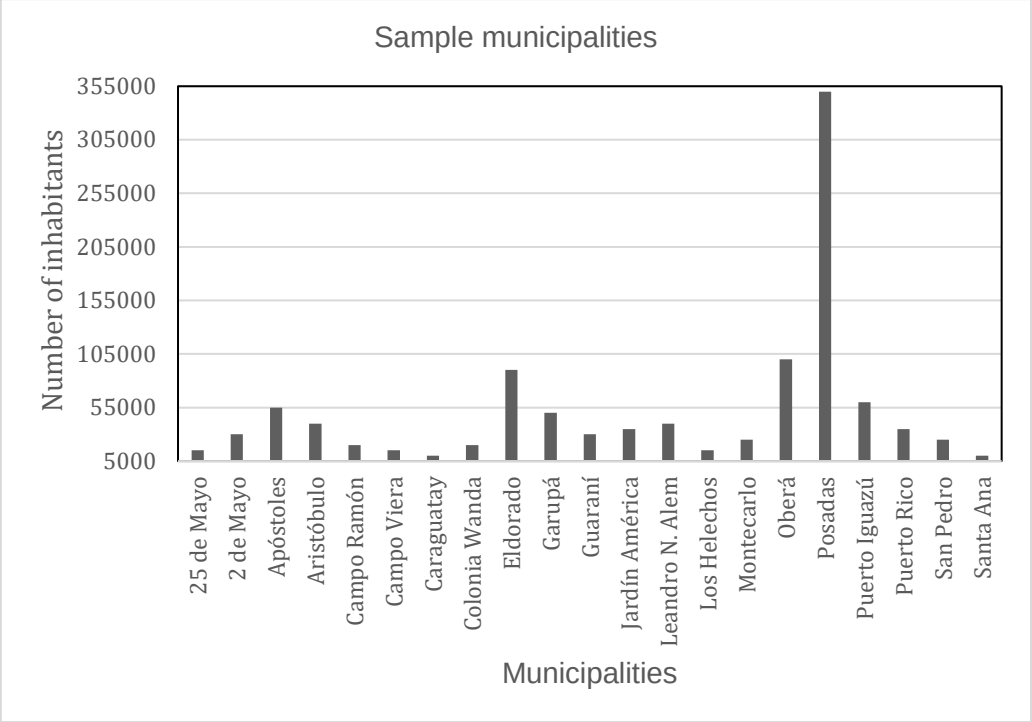

Figure 1: Sample municipalities and their respective populations by 2023. Source: Own elaboration using Microsoft Excel v.2022.

The survey process was carried out over 3 months and made it possible to capture a variety of experiences and perspectives regarding circular economy, by including both localities engaged in household waste management activities (typically larger towns) and other municipalities with isolated circular economy initiatives, as well as those lacking of plans to manage the waste they generate (generally smaller or peripheral municipalities).

Challenges during the data collection process included the lack of answers from some municipalities, and, therefore, it was necessary to send a formal request to the community authorities for them to participate. Apart from that, it was necessary to track persistently and individually several sample municipalities to obtain answers.

Step 3: Data purging and analysis

The information obtained from the questionnaire and its corresponding answers was verified one by one. In several instances, inconsistencies in units (kilograms and tonnes) were detected, and in some cases, it was necessary to contact the respondent. The section below presents the results in a graphical and tabular form, based on the information collected.

- The answers by the agents reveal that most municipalities do not have a specific area or department dedicated to waste management. Only the most populated cities (categorized as having a “high” population) have a specific department responsible for waste management. In most cases (municipalities with “low” and “medium” populations), the Secretary of Public Works is in charge of waste management.
- The disposal of household waste in the sanitary landfills of the province reached approximately 224,000 tons in 2023.

Collected data through this research (surveys for municipalities and other details about recycling from private companies) are presented in Table 2.

Table 2: Summary of collected data.

Variable	Value	Unit	Observations
Inhabitants included in the sample	942,277	inhabs.	Number of inhabitants for the included sample municipalities that answered the questionnaire
Tonnes managed by private recycling companies (2023)	7,419.32	t	Inorganic materials recovered by the sample municipalities
Tonnes managed by AESA (2023)	178,292.04	t	Amount of waste sent for final disposal based on the sample municipalities

Tonnes of organic waste for composting in the sample municipalities (2023)	793	t	Organic fraction recovered by the sample municipalities
Tonnes of pruning in the sample municipalities	13,640	t	Vegetal material managed by the sample municipalities
Recycled tonnes by the sample municipalities	1,075.6	t	Inorganic fraction managed by the sample municipalities
Managed tonnes of bulky waste (2023)	15,970	t	Furniture, appliances, and other waste managed by the sample municipalities
Total amount of waste generated by the sample municipalities	**249,378.44**	t	Including all the fractions

Source: Own elaboration.

Based on the data gathered in Table 2 and the individual responses from the municipalities, several indicators were evaluated.

Using the data on the amount of waste generated by each municipality during 2023 and their respective populations, the Per Capita Waste Generation (PCWG) index was estimated.

$$GPC\ \frac{[Kg{*}día]}{[persona]} = \frac{Cantidad\ total\ de\ residuos\ por\ [Kg{*}año]}{Cantidad\ de\ habitantes\ [persona]} * \frac{365\ [día]}{1\ [año]} \quad (8)$$

The estimates varied depending on the municipality assessed. It was determined that each person generates between 0.2 kg and 0.8 kg of waste per day.

As shown in Table 2, only a portion of the waste generated in the province is recycled or composted. This indicator is represented as the Circularity Index (CI), which is calculated as the ratio between the amount recovered through recycling and composting and the total amount generated during the same period.

$$IC = \frac{cantidad\ compostada + cantidad\ reciclada}{cantidad\ total\ generada} * 100\ \% \quad (9)$$

Of the 249,378.44 tons of waste generated in 2023 by the sample municipalities, approximately 15.36% returns to the productive or biological cycle, representing the percentage CI.

Figure 2 shows the composition of the CI, highlighting the difference between the amount of composted organics and recycled materials. Thus, those recyclables that enter the technical cycle (potentially recyclable inorganic materials such as plastics, cardboard, and metals, among others) have an indicator close to 10%, while organic waste, which is returned to the soil in the form of nutrients through the biological cycle, has a value below 6%. For this reason, the waste that attains a second life (either through recycling or by being returned to the soil) represents the combined total of both.

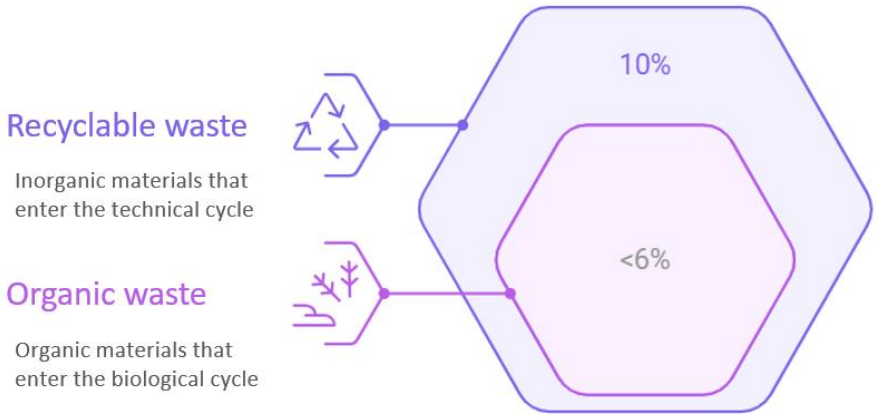

Figure 2: Circularity indexes differentiated from the sample.
Source: Own elaboration.

As it is shown in Figure 3, the analysis results and answers for the questionnaires indicated that a great number of inhabitants have access to an "eco-point" in the province (66.7%), while approximately 23% could access composting programs in 2023 (23.8%, to be specific).

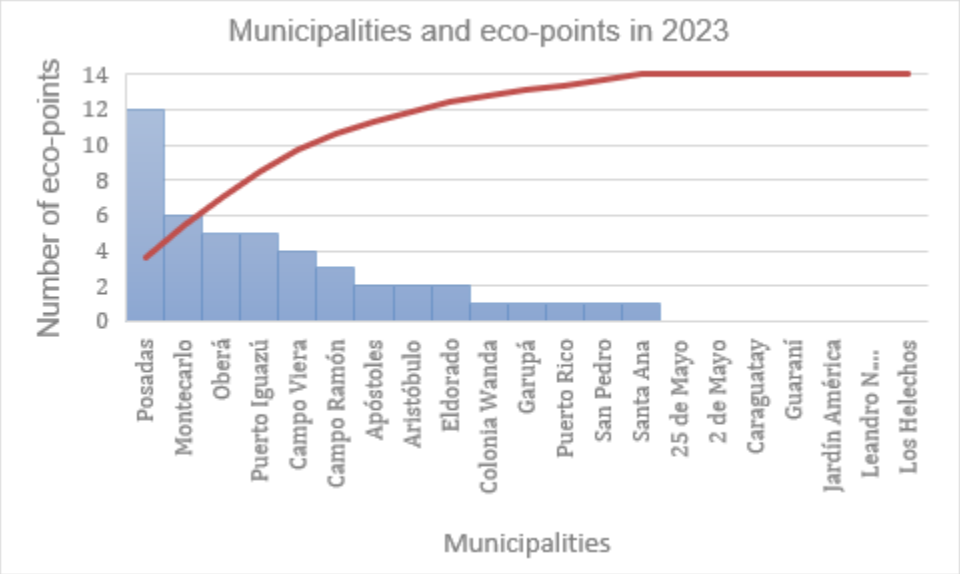

Figure 3: Eco-points in the municipalities of Misiones
Source: Own elaboration using Microsoft Excel v.2022.

Figure 3 shows that the number of "eco-points" corresponds directly to the most populated cities in the province: Oberá and Posadas.

More than 70% of the surveyed municipalities reported having urban waste recuperators who contribute to the circular flows of residual materials. Nevertheless, the answers to the questionnaire indicated that municipalities rarely coordinate their activities with companies or local cooperatives that manage waste within the area. Only the largest cities have plans that articulate some activities of the municipality with urban waste recuperators.

At the provincial level, according to data provided by recycling companies and the company responsible for landfill disposal in Misiones Province, over ten thousand tonnes of recyclable materials were circulated in 2023. This figure represents 4% of the waste disposed of in the province's landfills during this same year.

Undoubtedly, the activities carried out by each municipality on a "micro" scale contribute to the "macro" circularity rate if individuals and companies are taken into account, thus reducing the portion corresponding to sustainable behaviour. Evidently, circular initiatives can be achieved through small contributions from each actor or party, as the popular saying goes: "unity is strength" or "little streams make big rivers" (adapted from Calvo [14,15]).

According to studies conducted by the research team and by Sambiassi *et al.* [16], the largest amount of waste found in households in the largest cities of Misiones is compostable (around 50%).

It is important to note that in most municipalities, one of the most significant expenses is related to waste management, according to the "Manual for Calculating the Cost of Comprehensive Urban Solid Waste Management and the Use of the GIRSU Online Cost Matrix" [17]. Having said this, it is evident that waste management is a multi-criteria problem, where the best option is a plan tailored to the region and which is likely to be the result of environmental, economic, social, and technical dimensions.

Similar studies have been conducted using non-probabilistic samples, also known as purposive samples, in which the researcher deliberately selects the participants of the study (Sampieri, 2014) [9]. Among these studies, Camuci and Andrade Gonçalves (2020) [18] stand out, who investigated 25 municipalities, as well as Fratta *et al*. (2019) [19], who conducted a diagnosis of urban solid waste management in the municipalities of the ABC Paulista, Brazil, through the application of sustainability indicators.

Purposive studies aim to propose adaptations for those specific municipalities, while stratified evaluations can reach and diagnose larger regions. It is worth noting that the diagnosed region (Misiones Province) has two municipalities that implement differentiated collection and other practices. Nonetheless, in most municipalities, CE practices are still in their initial stages.

In this context, studies such as those carried out by Sá *et al*. (2022) [20] have evaluated the sustainability of selective collection programs in multiple Brazilian cities, using indicators across political, economic, social, and environmental dimensions. These methodological approaches make it possible to identify areas for improvement and guide public policies toward more efficient and sustainable urban solid waste management. Hence, it is relevant to note that, once the diagnosis is completed, it is possible to define the actions to be taken. For this purpose, several studies have employed multi-criteria analysis

techniques [21, 22, 23, 24, 25], which allow strategies to be prioritized while simultaneously considering environmental, economic, social, and technical criteria.

4 Conclusions

Thanks to this study, it was possible to determine the Circularity Index and to prepare the Circular Economy Report for Misiones for 2023.

The applied methodology made it possible to obtain quantitative information to understand the figures and practices of municipalities in Misiones, regarding the circular economy. A combined initial round of exploratory surveys with a formal survey targeted to a sample of representative municipalities facilitated the collection of variables and difficulties they face in managing their generated waste. In several instances, it has been necessary to contrast and validate part of the information through additional surveys for the respondents, ensuring the accuracy of the collected data in formal questionnaires.

Based on the information provided by municipalities, recycling companies, and the estimated tonnes of waste disposed of in sanitary landfills during the assessed period (2023), it has been possible to calculate the circularity index for the province. Results reflected clear patterns and trends of the differences regarding management for the largest and the smallest populations. It should be noted that those municipalities with a higher level of security circularity are generally the most populated. In spite of this, differentiated levels of commitment and adoption of circular strategies have also been identified among the different localities.

A common challenge these municipalities face is the absence of a local department responsible for waste management, particularly in smaller municipalities and those that still lack “eco-points” and “clean points”.

These findings not only enrich academic knowledge on the status of circular economy, but also provide key insights for designing public policies and formulating effective strategies for waste management in the municipalities of Misiones.

Recommendations

It is suggested to use simple questions in the questionnaire targeted to municipality officials for this type of study. In addition, it is suggested to standardize measurement criteria in the questions, such as expressing quantities only in tonnes or kilograms. It is also important to include clarifications in the questions (for example: 1 tonne = 1,000 kg) and to provide definitions of terms such as bulky waste, household waste, solid waste, organic waste, and inorganic waste. These aspects decrease the possibility of errors and clarify potentially doubts for the respondents.

Acknowledgements

The study hereby carried out has been possible through funding from the National Scientific and Technical Research Council (CONICET) as part of the doctoral thesis “Alternative Model for Household Solid Waste Management: Sustainable Development Application in Municipalities of Misiones Province, Argentina” developed within the project 6/I1486-PI of FI-UNaM. It has also been possible thanks to the cooperation agreement signed between the School of Engineering of the National University of Misiones (in Oberá, Misiones, Argentina) and the Ministry of Climate Change of the Misiones Province (Argentina), which enabled the creation of the First Report on Circular Economy of Misiones Province.

References

[1] Ellen Macarthur Foundation (2020). Circulytics - measuring circularity. Disponible en: https://www.ellenmacarthurfoundation.org/resources/apply/circulytics-measuring-circularity (Acceso: 11.10.24)

[2] Geissdoerfer, M., Savaget, P., Bocken, N.M.P., Hultink, E.J.(2017). The circular economy – a new sustainability paradigm? J. Clean. Prod. 143, 757 768.https://doi.org/10.1016/j.jclepro.2016.12.048

[3] Banco Interamericano de Desarrollo (2024). Development Effectiveness Overview 2024. Disponible en: https://www.idbinvest.org/en/publications/development-effectiveness-overview-deo-2024 (Acceso: 28.07.25)

[4] Akomea-Frimpong, I., Tetteh, P. A., Ofori, J. N. A., Tumpa, R. J., Pariafsai, F., Tenakwah, E. S., et al. (2024). A bibliometric review of barriers to circular economy implementation in solid waste management. Discover Environment, 2(20). Disponible en: https://link.springer.com/article/10.1007/s44274-024-00050-4 (Acceso: 28.07.25)

[5] Gallego-Schmid, A., López-Eccher, C., Muñoz, E., Salvador, R., Cano-Londoño, N. A., Vetroni Barros, M., Choconta Bernal, D., Mendoza, J. M. F., Nadal, A. y Guerrero, A. B. (2024). Circular economy in Latin America and the Caribbean: Drivers, opportunities, barriers and strategies. Sustainable Production and Consumption, 51, 118–136. https://doi.org/10.1016/j.spc.2024.09.006.

[6] Gobierno de Argentina. Plan GIRSU. Promovido por el ex Ministerio de Ambiente y Desarrollo Sostenible de la Nación Argentina.

Disponible en: https://www.argentina.gob.ar/interior/ambiente/erradicacion-de-basurales (Acceso: 27.07.24)

[7] Comisión Económica para América Latina y el Caribe – CEPAL (2021). Construir un futuro mejor: acciones para fortalecer la Agenda 2030 para el Desarrollo Sostenible. Cuarto informe sobre el progreso y los desafíos regionales. Disponible en: https://www.cepal.org/es/publicaciones/46670-cuarto-informe-sobre-el-progreso-los-desafios-regionales-la-agenda-2030-america (Acceso: 11.10.24)

[8] Niezwida,S.R; Santacruz F.A. Informe de economía circular de Misiones (2024). Disponible en: https://cambioclimatico.misiones.gob.ar/wp-content/uploads/2024/09/Misiones-Informe-Economia-Circular-2024.pdf (Acceso: 11.10.24)

[9] Hernández Sampieri, R., Fernández Collado, C., & Baptista Lucio, P. (2014). Metodología de la investigación. (CAPITULO 1) McGraw Hill México (PÁGINAS 70-120)

[10] Cuestionario original definitivo. Relevamiento de Economía Circular a Municipios de Misiones - Periodo 2023. Elaborado por los autores para fines de la investigación: https://docs.google.com/forms/d/1E9bEoU_38IIkUswZC8YhYmvcd2go9HbmFm-J8n69alM/edit#responses

[11] Instituto Nacional de Estadística y Censos. Censo Nacional de Población, Hogares y Viviendas 2022. Resultados Definitivos. 2023. Recuperado de: www.ipec.misiones.gov.ar/wp-content/uploads/2023/05/IPEC-Anuario-Estad%C3%ADstico-de-la-Provincia-de-Misiones-2021.pdf. (Acceso: 11.10.24)

[12] Berazategui, J., Carbonari, G., & Grinberg, J. (2023). Periferias urbanas en América Latina: Desafíos teóricos y metodológicos para la acción sociopolítica. Buenos Aires: CLACSO. https://doi.org/10.2307/j.ctv2z2w6h5

[13] Marjanović, M.; Williams, J. (2024). Mapeo del surgimiento de la economía circular dentro de las rutas de gobernanza de las ciudades y regiones en contracción: un estudio comparativo de Parkstad Limburg (NL) y Satakunta (FI), Cambridge Journal of Regions, Economy and Society , Volumen 17, Número 3, noviembre de 2024, Páginas 517–534, https://doi.org/10.1093/cjres/rsae019

[14] Calvo, J. L. (2024) Economía de la Conducta Sostenible. El efecto NIMBY. Behanomics, 2,153-166. DOI: https://doi.org/10.55223/bej (Acceso: 30.8.2024)

[15] García-Gómez, J. (2023). Buenas prácticas operativas de residuos sólidos un desafío complejo para la gestión pública.Revista investigación, transcomplejidad y ciencia, 4(2). Disponible en: https://revistasuba.com/index.php/INVESTIGACIONTRANSCOMPLEJIDADYCI/article/view/681. (Acceso: 10.7.2025)

[16] Sambiasi, C. G., Barrera, A. E., Pascual,Sambiasi, M. A.. (2022). Sustainable management of construction waste in the Metropolitan Area of Misiones. Revista de Ciencia y Tecnología, (37), 31-40. https://dx.doi.org/10.36995/j.recyt.2022.37.004

[17] Manual para el cálculo del costo de la gestión integral de residuos sólidos urbanos y para el uso de la matriz de costo girsu online. Argentina.gob, s.f. https://www.argentina.gob.ar/sites/default/files/resu-manual-calculo-costos-matriz-economico-financiera.pdf (Acceso: 30/8/2024)

[18] Camuci, M., & Andrade Gonçalves, M. (2020). Diagnóstico da situação dos resíduos sólidos urbanos nos municípios com área na Bacia do Rio Ivinhema – MS (Tesis de maestría, Universidade Federal de Mato Grosso do Sul). Recuperado de https://ppggeografiacptl.ufms.br/files/2021/03/DISSERTA%C3%87%C3%83O-MARISA.pdf

[19] Fratta, K. D. D. S. A., Toneli, J. D. C., & Antonio, G. C. (2019). Diagnóstico de la gestión de residuos sólidos urbanos en los municipios del ABC Paulista de Brasil mediante la aplicación de indicadores de sostenibilidad. Waste Management, 85, 11–17. https://doi.org/10.1016/j.wasman.2018.12.001

[20] Sá, A. C. N. de, Nóbrega, C. C., Alves, N. B. P., Silva, R. M. G., & Lacerda, G. L. B. (2023). Indicadores de sustentabilidade para avaliação de programas de coleta seletiva: Estudo de caso na cidade de João Pessoa, Paraíba, Brasil. Engenharia Sanitária e Ambiental, 28(3), e20220103. https://doi.org/10.1590/s1413-415220220103

[21] Ecco, MH, Matias, MS y de Castilhos Junior, AB. (2024). Análisis multicriterio como herramienta emergente para la gestión integrada de residuos biológicos: una revisión desde la prevención del desperdicio de alimentos hasta el uso de subproductos. J Mater Cycles Waste Manag (2024). https://doi.org/10.1007/s10163-024-02087-2

[22] Fratta Alcântara, K. (2022**)**. Análise multicritério da gestão de resíduos sólidos urbanos com enfoque nos sistemas de tratamento: um estudo de caso nos municípios do ABC Paulista (Tesis doctoral). Universidade Federal do ABC, Centro de Engenharias, Modelagem e Ciências Sociais Aplicadas, Pós-graduação em Energia. São Paulo, Brasil. Disponible en: http://biblioteca.ufabc.edu.br/index.php?codigo_sophia=122975&midiaext=80141&utm_source=chatgpt.com (Accedido: 12.7.2025)

[23] Rodrigues, T. D., & Mondelli, M. (2021). Assessment of integrated MSW management using multicriteria analysis in São Paulo City. Waste Management & Research, 39(12), 1711–1723.Disponible en: https://repositorio.unesp.br/entities/publication/26f914d0-2f91-40a3-ae7d-4ddcd152f074. (Accedido: 10.7.2025).

[24] Santos, S.M., Silva, M.M.; Melo, R.M. (2017). Análisis multicriterio para la gestión de residuos sólidos urbanos en un área metropolitana brasileña. *Environ Monit Assess* **189** , 561. https://doi.org/10.1007/s10661-017-6283-x

[25] Almeida, D. A., Costa, H. G., & de Almeida, L. M. W. (2024). Prioritization of alternatives in waste management: A case in Pernambuco State, Brazil. Pesquisa Operacional para o Desenvolvimento, 16(1), e240011. Disponible en: https://www.scielo.br/j/pope/a/4wcpQ3JZzWfwddn4MkxH47K (Accedido: 10.7.2025).

[26] Autodesk. (2024). IBM SPSS Statistics Versión 29.0.2.0. Versión educativa [software]. Disponible en: https://www.ibm.com/products/spss-statistics(Accedido: 3.7.2024).

[27] Autodesk. (2022). Microsoft Corporation. (2022). Versión educativa [software]. Microsoft Excel (versión 2022) [Hoja de cálculo]. Microsoft. (Accedido: 3.7.2024).

RECyT
Year 27 / Nº 44 / 2025 /
DOI: https://doi.org/10.36995/j.recyt.2025.44.003

Physicochemical characterization, viability and *in vitro* gastrointestinal resistance of probiotic *Bacillus* spp. in cheese bread

Caracterización fisicoquímica, viabilidad y resistencia gastrointestinal *in vitro* de *Bacillus* spp. probióticos en pan de queso

Mariana, Silva de Souza Malaquias[1]; Sara, Pereira Leandro[1]; Nataly, de Almeida Costa[1]; Isabela, Campelo Queiroz[1]; Wellingta Cristina A., do Nascimento Benevenuto[1]; Maurílio, Lopes Martins[1]; Eliane Mauricio, Furtado Martins[1,*]

1- Federal Institute of Education, Science and Technology of Southeast Minas Gerais, Rio Pomba campus, Avenue Doctor José Sebastião da Paixão - Lindo Vale, Rio Pomba, Minas Gerais, Brazil.
* E-mail: eliane.martins@ifsudestemg.edu.br

Received: 12/08/2024; Accepted: 02/07/2025

Abstract
The objective was to develop cheese bread doughs containing spores of *Bacillus coagulans* BC30 or *Bacillus clausii* and to evaluate the physicochemical characteristics (moisture, ash, proteins and lipids), viability and *in vitro* gastrointestinal resistance of the probiotics. The control and probiotic bread doughs were kept at -20 °C for 90 days, with the product being baked after 0, 30, 60 and 90 days to carry out the analyses. There was no difference ($p>0.05$) in moisture, ash, lipids and carbohydrates between the masses of the three treatments. The viability of *B. coagulans* in dough, after processing and 90 days was > 7.71 log CFU/g, while in baked bread it was 5.24 log CFU/g and 6.03 log CFU/g at 0 and 90 days, respectively. The viability of *B. clausii* in dough at times 0 and after 90 days was > 7.32 log CFU/g and in bread baked at the same times it was, respectively, 5.39 log CFU/g and 5.95 log CFU/g. In enteric phase II, at 90 days, the viability of *B. clausii* was 4.77 log CFU/g, while that of *B. coagulans* was 4.11 log CFU/g. The addition of these probiotics to cheese bread is a promising alternative for the market.

Keywords: Bacillus coagulans; *Bacillus clausii*; Dough; Thermal resistance.

Resumen
El objetivo fue desarrollar masas de pan de queso que contengan esporas de *Bacillus coagulans* BC30 o *Bacillus clausii* y evaluar las características fisicoquímicas (humedad, cenizas, proteínas y lípidos), viabilidad y resistencia gastrointestinal *in vitro* de los probióticos. Las masas de pan control y probiótico se mantuvieron a -20 °C durante 90 días, horneándose el producto a los 0, 30, 60 y 90 días para realizar los análisis. No hubo diferencia ($p>0.05$) en humedad, cenizas, lípidos y carbohidratos entre las masas de los tres tratamientos. La viabilidad de *B. coagulans* en masa, después del procesamiento y después de 90 días fue > 7,71 log UFC/g, mientras que en pan horneado fue de 5,24 log UFC/g y 6,03 log UFC/g a los 0 y 90 días, respectivamente. La viabilidad de *B. clausii* en masa en los tiempos 0 y después de 90 días fue > 7,32 log UFC/g y en pan horneado en los mismos tiempos fue, respectivamente, 5,39 log UFC/g y 5,95 log UFC/g. En la fase entérica II, a los 90 días, la viabilidad de *B. clausii* fue de 4,77 log UFC/g, mientras que la de *B. coagulans* fue de 4,11 log UFC/g. La adición de estos probióticos al pan de queso es una alternativa prometedora para el mercado.

Palabras clave: Bacillus coagulans; *Bacillus clausii*; Masa; Resistencia térmica.

INTRODUCTION

The eating habits of the population, especially those individuals who care about health and well-being, have been undergoing changes related to better nutrition and body maintenance. In this sense, functional foods increasingly attract consumers' attention because they provide health benefits and help reduce health risks [1].

Probiotics are functional ingredients that, when administered in adequate amounts, provide health benefits [2] such as improving the immune system through the synthesis of vitamins, and enhancing the health of the gastrointestinal tract, preventing allergic and cancer-related diseases, among other benefits. These microorganisms are represented mainly by bacteria of the genera *Lactobacillus*, *Streptococcus*, *Bifidobacterium*, *Enterococcus* and *Bacillus* [3; 4].

Bacillus coagulans is a species that presents strains with probiotic characteristics, such as *B. coagulans BC30*, which presents spores highly resistant to acids and able to adapt to

environments in the intestinal tract with a low presence of oxygen, remaining stable during processes involving heat treatment and when stored at low temperatures [5]. In addition to *B. coagulans*, *Bacillus clausii* is also a sporulated probiotic that is tolerant to heat, acid and salt, as well as resistant to the human gastrointestinal tract [6].

The addition of *Bacillus* probiotics has been studied in several food products, as the spores of these microorganisms are resistant to heat treatment and survive after industrial baking processes, which is an additional advantage compared to usual probiotics, such as lactobacilli. Thus, *Bacillus* have already been used in pasta [7; 8], breads [9; 10], cake mix [11], among other foods subjected to heat treatment.

Cheese bread is a widely consumed product in Brazil. Its formulation includes ingredients such as egg, cheese, cassava starch, milk or water, butter or vegetable oil and salt [12]. The addition of functional ingredients, such as probiotics resistant to heat treatment in bakeable products is an innovative idea and arouses interest among consumers and the food sector due to the scarcity of bakery and confectionery products containing probiotics. Therefore, this study aimed to develop cheese bread doughs added with *Bacillus coagulans* BC30 spores and *Bacillus clausii* spores, and to evaluate their physicochemical characteristics, as well as the viability of probiotics and their resistance to the simulated gastrointestinal tract (GIT) *in vitro* in baked cheese breads.

MATERIAL AND METHODS

Development of cheese breads

For the development of cheese breads, sunflower oil and salt were used, purchased from local stores in Rio Pomba – MG, Brazil; pasteurized liquid egg (Cecoti, Juiz de Fora, MG, Brazil); half-cured cheese; salted butter; and whole milk powder donated by Porto Alegre (Ponte Nova, MG, Brazil) and starch mix (Poduim Alimentos, Tamboara, PR, Brazil), according to Table 1. *B. clausii* (Enterogermina Plus®, Sanofi, São Paulo, SP, Brazil) was added to the formulation in suspension, and *B. coagulans* BC30 (Kerry/Ganeden Biotech BC30®, USA) was added in freeze-dried powder form.

Table 1. Formulation of cheese breads.

Treatments	Portions
Control cheese bread - CCB	500g of dough
Cheese bread with *B. coagulans* – CBBCO	500g of dough + 18 g of freeze-dried powder of *B. coagulans* BC30 with 1,0 x 10^9 CFU
Cheese bread with *B. clausii* – CBBCLA	500 g of dough + 5 mL with 4,0 x 10^9 spores of *B. clausii*

Initially, all powdered ingredients were transferred to a dough mixer (Arno, SX33, Brazil) and mixed until complete homogenization. Then, sunflower oil, butter, and liquid egg were added, while maintaining homogenization. Subsequently, water was added until the dough became consistent and homogeneous, and the cheese was added last. The mass obtained was divided into three portions as shown in Table 2.

Table 2. Percentages of ingredients used in the preparation of cheese bread.

Ingredients	CCB	CBBCO	CBBCLA
Mix of starches	33.98	33.98	33.98
Half cured Minas cheese	14.77	14.77	14.77
Butter with salt	1.85	1.85	1.85
Whole liquid egg	10.62	10.62	10.62
Whole milk powder	2.31	2.31	2.31
Salt	0.92	0.92	0.92
Sunflower oil	5.54	5.54	5.54
Water	30.01	30.01	30.01
B. clausii	-	-	5 mL
B. coagulans BC30	-	18 g	-

Source: adapted from Castro [13]. *The formulation was prepared for 100g of dough. However, CBBCLA dough contains 105g and CBBCO contains 118g.

The three treatments were weighed and formed into 25g portions. The dough from the different treatments was analyzed for the physicochemical characteristics and the viability of the probiotics at time zero (T0) of manufacturing.

At the same time, the bread samples from the different treatments were transferred to a stainless-steel pan and baked at 180 °C for 30 minutes in an oven that had been preheated (Arno, SX33, Brazil) for 10 minutes. The remaining cheese bread doughs prepared were stored in styrofoam trays covered with plastic film and frozen at -20 °C.

Physicochemical evaluation of cheese bread doughs during the storage period

The analyses of moisture, ash, proteins, and lipids were carried out at time 0 according to the methodology of the Association of Official Analytical Chemists [14] for the preparation of the cheese bread doughs (CCB, CBBCO e CBBCLA).

Humidity determination was conducted using the gravimetric method, based on the weight loss of the samples in an oven heated to 105 °C until constant weight was reached. The ash was obtained from fixed mineral residue after incineration of the sample in a muffle furnace at a temperature of 550 °C for 12 hours.

For protein determination, the *Kjeldahl* method was used with a nitrogen-to-protein conversion factor of 6.38, and the quantification of lipids was carried out using the *Soxhlet* method, with residues being weighed and quantified after removing the solvent.

After obtaining the results of the analyses described above, the carbohydrate content was determined by difference through the following calculation: % Carbohydrates = 100 – (% moisture + % ash + % lipid + % protein).

Viability of *B. coagulans* BC30 and *B. clausii* (Enterogermina Plus®) in cheese bread during the storage period

To determine the viability of probiotics, 10 g of dough and baked cheese bread from both treatments were diluted in 90 mL of peptone saline solution [0.85 % de NaCl (Synth, Diadema, São Paulo, Brazil) and 0.1 % of peptone (Acumedia, Michigan, EUA)], and the mixture was homogenized to carry out serial dilutions. The pour plate method was adopted by adding 1 mL of dilutions 10^2 to 10^6 into each Petri dish (Cial, Paulina, São Paulo, Brazil), followed by approximately 15-20 mL of TSA agar (Tryptone Soy Agar). They were incubated at 37 °C for 48 hours in the case of *B. clausii* and 72 hours in the case of *B. coagulans* BC30 [15]. At the end of the incubation period, the count of *B. coagulans* BC30 and *B. clausii* was expressed in Colony Forming Units (CFU) to determine the amount of probiotic bacteria in the product.

Viability was evaluated in the dough after formulation and after baking the breads (time 0), and after 30, 60, and 90 days of freezing the products at -20 ºC (CBBCO e CBBCLA).

Evaluation of the resistance of *B. coagulans* BC30 and *B. clausii* to simulated *in vitro* gastrointestinal conditions

To evaluate resistance to gastrointestinal conditions, baked cheese breads were subjected to *in vitro* testing by simulating gastric and enteric phases I and II, at times 0, 30, 60, and 90 days of storage at -20 °C, according to the methodology of Bedani, Rossi and Saad. [16].

At the end of each phase (gastric, enteric I and II), 1 mL aliquots were removed, and serial dilutions were made in saline solution (0.85% NaCl). Then, in-depth plating on TSA Agar was performed, and the counts of *B. coagulans* BC30 and *B. clausii* surviving the gastrointestinal conditions were determined.

The percentage of bacterial survival in relation to the initial counts prior to the assay, was also calculated according to Guo et al. (2009) [17], using the following equation: Survival rate (%) = (Log CFU N_1/Log CFU N_0) x 100; where N_1= probiotic cell counts at the end of the *in vitro* assay and N_0 = probiotic cell counts before the *in vitro* assay.

Statistical analysis

The experiment for the physicochemical characterization of moisture, ash, proteins, lipids, and carbohydrates of the products was performed under a in a Completely Randomized Design (CRD).

The viability of probiotics was also analyzed by CRD in a 3 × 4 factorial scheme (3 treatments: control and 2 probiotics × 4 times: 0, 30, 60, and 90 days). Analysis of variance (ANOVA) was performed at 5% probability. The means were generated and evaluated using the Tukey Test at a 5% probability level.

The simulated *in vitro* gastrointestinal resistance experiment was carried out in CRD, with comparisons made between phases at each time point and across time points within each phase. Counts were converted into log CFU/g and analysis of variance (ANOVA) was performed. The means were compared using the Tukey Test at a 5% probability level.

The analyses were carried out with the R Software (R CORE TEAM, 2021) and the ExpDes.pt Package [18].

RESULTS AND DISCUSSION

Physicochemical characteristics of control and cheese bread doughs added with *Bacillus* probiotics

There was no difference in moisture, ash, lipids and carbohydrates among the different treatments ($p>0.05$), indicating that the addition of probiotic *Bacillus* did not interfere with the physicochemical quality of the cheese bread dough. However, only the protein content of the control bread dough was lower ($p<0.05$) in relation to doughs containing probiotics (Table 3).

Table 3. Average percentages (%) of the physicochemical characteristics of control cheese bread doughs (CCB) and those added with *B. clausii* (CBBCLA) and *B. coagulans* BC30 (CBBCO).

Treatments	Moisture	Ashes	Protein	Lipids	Carbohydrates
CCB	41.56 ± 1.02[a]	2.56 ± 0.06[a]	5.30 ± 0.06[b]	13.12 ± 0.47[a]	38.38 ± 0.77[a]
CBBCLA	40.75 ± 3.33[a]	2.13 ± 0.05[a]	6.48 ± 0.36[a]	13.52 ± 0.04[a]	38.59 ± 2.29[a]
CBBCO	35.70 ± 0.06[a]	2.75 ± 0.86[a]	6.22 ± 0.16[a]	13.24 ± 0.46[a]	42.76 ± 2.62[a]

*Different letters in the same column indicate a significant difference ($p<0.05$) between treatments.

In the study by Almada-Érix et al. [10], the incorporation of *B. coagulans* BC30 also did not affect humidity or other evaluated characteristics, such as specific volume, texture and color parameters, water activity, and pH of the breads.

Bakery products and some baked foods are mostly composed of carbohydrates, having low nutritional value but high energy value [19]. In the present study, the addition of *Bacillus* probiotics did not affect the carbohydrate content of the samples.

Viability of *B. coagulans* and *B. clausii* in cheese bread during the storage period

A reduction in the viability ($p<0.05$) of *B. coagulans* and B. *clausii* was found after baking the cheese breads (Figure 1A and 1B). The viability of *B. coagulans* in cheese bread dough was 7.77 log CFU/g at T0 (after processing) and 7.71 log CFU/g after 90 days, whereas for the baked bread it was 5.24 log CFU/g at T0 and 6.03 log CFU/g after 90 days (Figure 1A). The viability of *B. clausii* in bread dough was 7.73 log CFU/g at T0 and 7.32 log CFU/g after 90 days, whereas in baked bread at the same times it was 5.39 log CFU/g and 5.95 log CFU/g, respectively (Figure 1B). It was also observed that the time factor did not interfere with the viability ($p>0.05$) of *B. coagulans* and *B. clausii* in either dough or baked bread (Figure 1A and 1B).

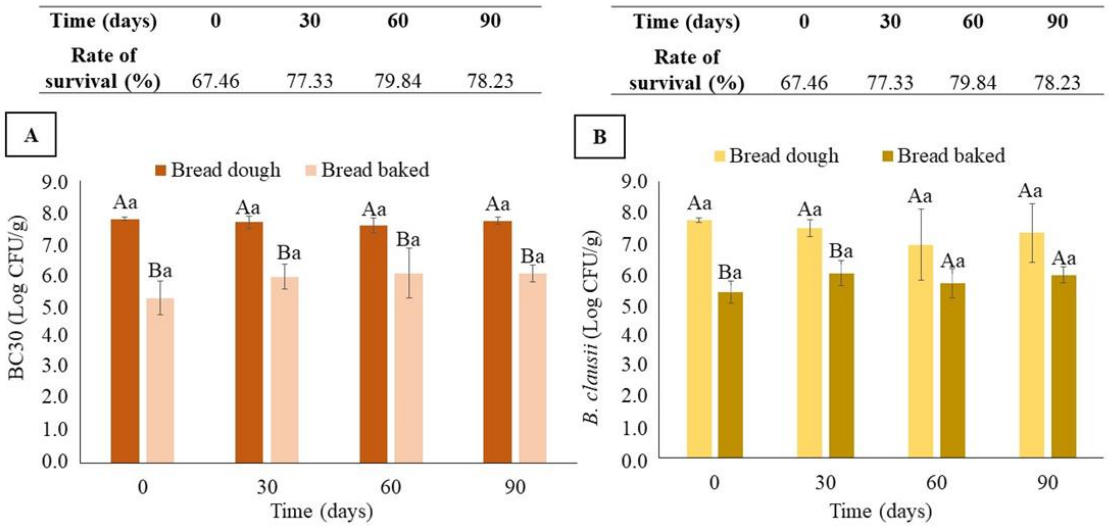

Figure 1. Viability in log CFU/g of *B. coagulans* BC30 (A) and *B. clausii* (B) in cheese bread dough and baked cheese bread over 90 days.

*Different capital letters indicate a significant difference ($p<0.05$) before and after baking at the same time. Different lowercase letters indicate significant differences ($p<0.05$) over time for each treatment.

Almada-Érix et al. [10] also found a significant reduction in the viability of *B. coagulans* BC30 in bread after baking at T0. During the baking stage, the researchers observed a significant difference in the probiotic counts between the crusts of white and wholemeal breads after baking, which decreased by 1.9 log CFU/g and 1.6 log CFU/g, respectively. In the crumb, reductions of 1.6 log CFU/g and 1.5 log CFU/g in probiotic counts were observed, respectively. In the entire slice of both breads, there was a reduction in the count of 1.5 log CFU/g.

Regarding the survival rate of probiotics, this was represented by the viability in the baked cheese bread (final count) in relation to the viability in the dough (initial count) at each time point. Thus, at T0 the survival rate of *B. coagulans* was above 67% and by the end of the storage period it was above 78%. For *B. clausii*, the rate was approximately 70% at T0 and above 82% after 90 days of storage (Figure 1A and 1B). Both probiotics showed an excellent survival rate throughout storage, this being higher for *B. clausii* (Figure 1B).

According to Cinbas, Tontul and Akin [20], the high content of oils and fats present in the formulation of some foods are capable of exerting a thermal insulating effect on the spores when subjected to high cooking temperatures, ensuring the stability of the probiotics.

Thus, the use of sporulated probiotics is considered to be of great industrial interest due to their ability to withstand processing steps, such as mechanical homogenization and heat treatment. Although the time-temperature binomial affected spore survival compared with the dough, counts above 10^5 log CFU/g of both probiotics were able to survive the high baking

temperatures to which the cheese breads were subjected (Figure 1). A portion of cheese bread is defined as 50 g, equivalent to two medium-sized units. Therefore, by consuming this portion daily, the consumer would be ingesting the internationally suggested amount of > 10^6 required to exert a beneficial effect on health [21; 22], suggesting that cheese bread can be considered a potential carrier matrix for these microorganisms. In the present study, frozen cheese breads were also found to be an excellent carrier matrix for probiotics, as storage at low temperatures maintained the viability of both probiotics over time.

Survival of *B. coagulans* and *B. clausii* in cheese bread after simulated *in vitro* gastrointestinal (GIT) conditions

When comparing the viability of *B. coagulans* after the *in vitro* test, a significant difference was observed between the phases at 0, 60, and 90 days ($p<0.05$) (Table 4).

During the first 30 days of storage, more than 5.6 log CFU/g remained viable in enteric phase II (FEII), which simulates the large intestine, whereas after 60 and 90 days, a reduction of more than 1.0 log CFU/g was observed. However, regardless of the shelf life, to guarantee consumer benefits, with counts >10^6 CFU/g, it is necessary to consume 100g of cheese bread, which is equivalent to 4 units, throughout the storage period.

When analyzing the breads containing *B. clausii*, a difference in viability between the gastric phase and the enteric phases I and II was observed only at day 30 ($p<0.05$). In enteric phase II, the viability was > 5.33 log CFU/g for *B. clausii* at 0, 30, and 60 days, and equal to 4.77 log CFU/g at 90 days, suggesting that only a 50 g portion of bread is sufficient to achieve satisfactory counts throughout the shelf life (Table 4).

Table 4. Viability of *B. coagulans* and *B. clausii* (log CFU/g) in cheese bread after *in vitro* gastrointestinal resistance test, at times 0, 30, 60 and 90 days of frozen storage for the gastric phase (GP), and enteric phase I (EI) and II (EII).

Probiotic	Phases	Times			
		0	30	60	90
B. coagulans	**GP**	6.76 ± 0.02^{a}	5.15 ±0.06^{a}	4.44 ± 0.05^{b}	4.20 ± 0.19^{b}
	EI	5.95± 0.1 6^{b}	5.33 ± 0.22^{a}	4.56 ± 0.01^{ab}	4.90 ± 0.07^{a}
	EII	5.62 ± 0.06^{c}	5.65 ± 0.03^{a}	4.61 ± 0.09^{a}	4.11 ± 0.06^{b}
B. clausii	**GP**	5.77 ± 1.78^{a}	5.12 ±1.16^{b}	5.80 ± 0.65^{a}	4.39 ± 5.27^{a}
	EI	5.73 ± 0.92^{a}	5.43 ± 0.57^{a}	5.71 ± 4.40^{a}	4.77 ± 1.46^{a}
	EII	5.60 ± 1.20^{a}	5.33 ± 2.01^{a}	5.37 ± 12.54^{a}	4.77 ± 1.47^{a}

*Different letters for each probiotic evaluated separately, in the same column, indicate a significant difference ($p<0.05$) between the phases at the same time.

In the EII phase (Figure 2A), *B. coagulans* presented approximately 108.09% viable cells at the initial time (T0). After 90 days of storage ($p<0.05$), around 69.37% of the probiotics remained viable at the end of the simulated GIT. On the other hand, the survival rate of *B. clausii* went from 96.53% at T0 to 77.63% at the end of 90 days of storage ($p>0.05$) (Figure 2B). Therefore, it is observed that *B. clausii* showed a higher survival rate in the final intestine phase (EII) after the bread storage period. However, both probiotics showed sufficient survival (> 69% of viable cells) to provide health benefits to the consumer after passing through the simulated GIT, indicating that their use is promising in bakery and bakeable products. Alves [9] developed breads with ora-pro-nobis flour and observed that the survival rate of *B. clausii* at the end of enteric phase II was 98.8% at time 0 and 101.9% after 4 storage days. These values further reinforce that *B. clausii* spores are capable of resisting the time and temperature stress involved in bread manufacturing and storage, as well as the simulated *in vitro* digestion process.

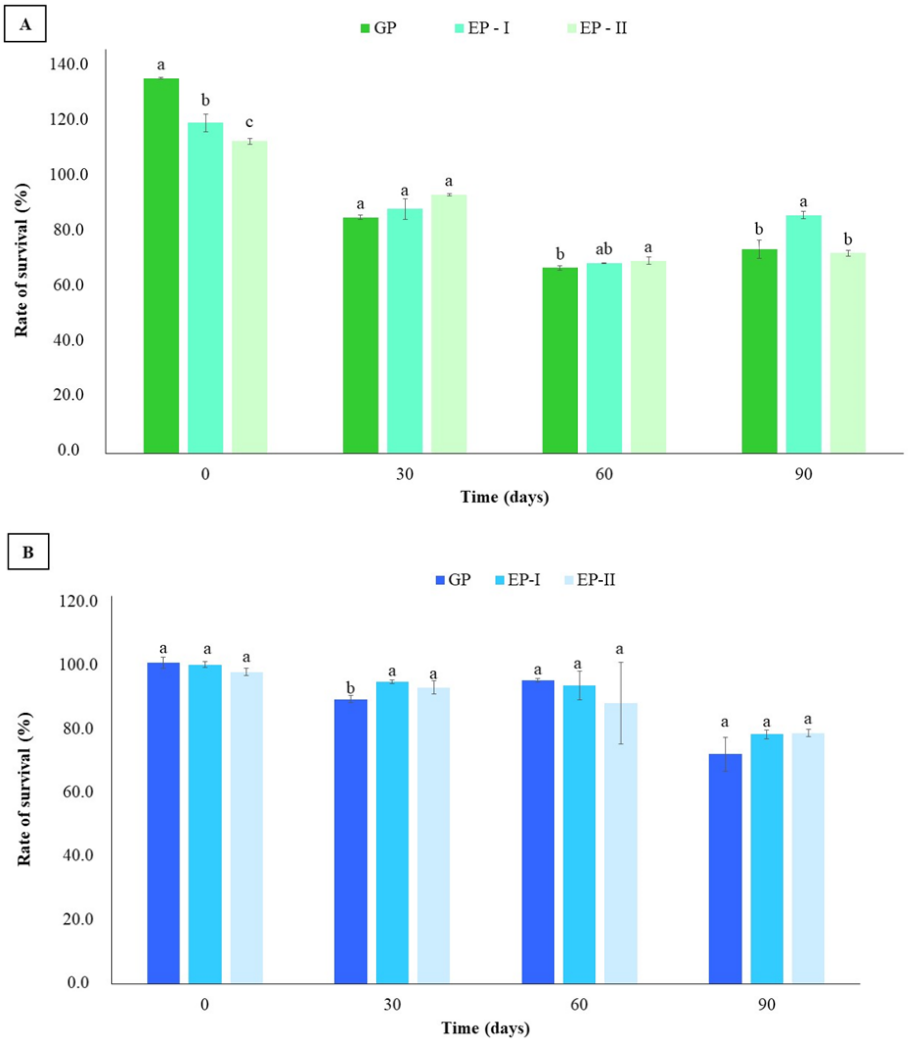

Figure 2. Survival rate of *B. coagulans* (A) and *B. clausii* (B) in cheese breads, after *in vitro* gastrointestinal resistance testing, at times 0, 30, 60, and 90 days of storage for the gastric phase and enteric phases I and II.

*Different letters in the same bars indicate a significant difference ($p<0.05$) between phases at the same time.

The ability of *Bacillus* species to form endospore is a crucial characteristic for their survival under environmental stress conditions, as it contributes to the tolerance of pH, bile fluid levels, high temperatures, dehydration, salt, among other environments [23].

Therefore, the addition of *B. coagulans* and *B. clausii* to cheese bread is advantageous, as they resist high baking temperatures as well as freezing conditions, thereby expanding the possibilities of their addition to baked products.

CONCLUSIONS

The addition of *B. coagulans* and *B. clausii* did not alter the moisture, ash, lipids and carbohydrates of the cheese breads.

The viability of probiotic *Bacillus* in raw cheese bread dough remained above 7.0 log CFU/g throughout the 90 days of storage. In baked breads, viability remained above 5.0 log CFU/g and storage time did not influence their viability either in raw dough or the baked breads.

The *in vitro* gastrointestinal simulation showed that, for more than 10^6 CFU/g of viable cells to reach the large intestine, it is necessary to consume 50 g of cheese bread containing *B. coagulans* at 0 and 30 days of storage, and 100 g at 60 and 90 days of storage. In contrast for cheese bread containing *B. clausii*, only a portion of 50 g, which is equivalent to two loaves of bread, is sufficient throughout the product's entire useful life for the consumer to obtain the benefits.

Both *Bacillus* probiotics resisted the cheese bread baking process, expanding the possibilities of their addition to bakery products subjected to heat treatment.

ACKNOWLEDGEMENTS

The authors are thankful to the IF Sudeste MG - Rio Pomba Campus for financial support.

CONFLICT OF INTEREST

There is no conflict of interest from the authors. The authors are solely responsible for the content of this article.

REFERENCES

1. **Lopez, R. B.; Tausen, B. M.; Traub, G.; Marathia, E.; Saunders, B**. Connecting to our future, healthier selves: Associations between self-continuity measures and eating behaviors in daily life. Current Research in Behavioral Sciences, v. 5, p. 1-10, 2023. Available in: https://doi.org/10.1016/j.crbeha.2023.100128.
2. **Hill, C.; Guarner, F.; Reid, G.; Gibson, G. R.; Merenstein, D. J.; Pot, B.; Morelli, L.; Canani, B. R.; Flint, H. J.; Salminen, S.; Calder, P. C.; Danders, M. E**. The International Scientific Association for Probiotics and Prebiotics consensus statement on the scope and appropriate use of the term probiotic. Nature Reviews Gastroenterology & Hepatology, v. 11, p. 506-514, 2014. Available in: https://doi.org/10.1038/nrgastro.2014.66.
3. **Altun, G. K.; Erginkaya, Z**. Identification and characterization of *Bacillus coagulans* strains for probiotic activity and safety. LWT – Food Science and Technology, v. 151, n. 112233, p. 1-10, 2021. Available in: https://doi.org/10.1016/j.lwt.2021.112233.
4. **Wu, Y-p.; Liu, D-m.; Zhao, S.; Huang, Y-y.; Zhou, Q-y**. Assessing the safety and probiotic characteristics of *Bacillus coagulans* 13002 based on complete genome and phenotype analysis. LWT – Food Science and Technology, v. 155, p. 1-9, 2022. Available in: https://doi.org/10.1016/j.lwt.2021.112847.
5. **Wang, Y.; Lin, J.; Cheng, Z.; Wang, T.; Chen, J.; Long, M**. *Bacillus coagulans* TL3 inhibits LPS-induced caecum damage in rat by regulating the TLR4/YD88/k Band Nrf2 signal pathways and modulating intestinal microflora. Oxidative Medicine and Cellular Longevity, v. 2022, p. 1-20, 2022. Available in: https://doi.org/10.1155/2022/5463290.
6. **Ghelardi, E.; Abreu, A. T. A. Y.; Marzet, C. B.; Calatayud, G. A.; Pereziii, M.; Castro, A. P. M**. Current progress and future perspectives on the use of *Bacillus clausii*. Microorganisms, v. 10, n. 6, p. 1-16, 2022. Available in: https://doi.org/10.3390/microorganisms10061246.
7. **Altun, G. K.; Erginkaya, Z**. Quality evaluation of probiotic pasta produced with *Bacillus coagulans* GBI 30. Innovative Food Science & Emerging Technologies, v. 66, p. 1-6, 2020. Available in: https://doi.org/10.1016/j.ifset.2020.102489.
8. **Majeed, M.; Majeed, S.; Arumugam, S.; Ali, F.; Beede, K**. Comparative evaluation for thermostability and gastrointestinal survival of probiotic *Bacillus coagulans* MTCC 5856. Bioscience, biotechnology and biochemistry, v. 85, n. 4, p. 962-971, 2020. Available in: https://doi.org/10.1093/bbb/zbaa116.
9. **Alves, D. T**. Pães contendo farinha de ora-pro-nóbis e esporos de *Bacillus clausii*: estudo de percepção do consumidor, elaboração, caracterização físico-química e microbiológica e resistência ao trato gastrointestinal *in vitro*. 81f. 2022. Dissertação (Mestrado Profissional em Ciência e Tecnologia de Alimentos). Instituto Federal de Educação, Ciência e Tecnologia do Sudeste de Minas Gerais, Rio Pomba, MG, 2022.
10. **Almada-Érix, C. N.; Almada, C. N.; Pedrosa, G. T. S.; Biachi, J. P.; Bonatto, M. S.; Schmiele, M.; Nabeshima, E. H.; Clerici, M. T. P. S.; Magnani, M.; Sant'ana, A. S**. Bread as probiotic carriers resistance *of Bacillus coagulans* GBI-30 6086 spores through processing steps. Food Research International, v. 155, p. 1-6, 2022. Available in: https://doi.org/10.1016/j.foodres.2022.111040.
11. **Amini, K.; Sharifan, A.; Tarzi, B. G.; Azizinezhad, R**. Preparation of a low calorie, gluten-free all-in-one cake mix, containing *Bacillus coagulans* using quinoa and inulin functionality. Journal of Food Quality, v. 2022, n. 8550086, p. 1-12, 2022. Available in: https://doi.org/10.1155/2022/8550086.
12. **Zapata, F.; Zapata, E.; Rodríguez-Sandoval, E**. Influence of guar gum on the baking quality of gluten-free cheese bread made using frozen and chilled dough. International Journal of Food Science and Technology, v. 54, p. 1-12, 2018. Available in: https://doi.org/10.1111/ijfs.13936.
13. **Castro, M. P. N. de**. Desenvolvimento e caracterização de pão de queijo funcional pela incorporação de inulina e isolado proteico de ervilha. 85f. 2022. Dissertação (Mestrado Profissional em Ciência e Tecnologia de Alimentos). Instituto Federal de Educação, Ciência e Tecnologia do Sudeste de Minas Gerais, Rio Pomba, MG, 2022.
14. AOAC. ASSOCIATION OF OFFICIAL ANALYTICAL CHEMISTS. **Official methods of analysis of the Association of Official Analytical Chemists**. 20 ed. Washington, DC., v. 2. 2016.
15. **Silva, N.; Junqueira, V. C. A.; Silveira, N. F. A.; Taniwaki, M. H.; Gomes, R. A. R.; Okazaki, M. O**. Manual de métodos de análise microbiológica de alimentos e água. 5. ed. São Paulo: Blucher, p. 560, 2017.
16. **Bedani, R.; Vieira, A. D. S.; Rossi, E. A.; Saad, S. M. I**. Tropical fruit pulps decreased

probiotic survival to *in vitro* gastrointestinal stress in symbiotic soy yoghurt with okara during storage. LWT – Food Science and Technology, v. 55, p. 436- 443, 2014. Available in: https://doi.org/10.1016/j.lwt.2013.10.015.

17. **Guo, Z.; Wang, J.; Yan, L.; Chen, W.; Liu, X-M.; Zhang, H-P**. *In vitro* comparison of probiotics properties of *Lactobacillus casei* Zhang, a potential new probiotic, with selected probiotic strains. LWT – Food Science and Technology, v.42, p. 1640-1646, 2009. Available in: https://doi.org/10.1016/j.lwt.2009.05.025.

18. **Ferreira, E.; Cavalcanti, P.; Nogueira, D**. ExpDes: An R Package for ANOVA and Experimental Designs. Applied Mathematics, v. 5, p. 2952-2958, 2014.

19. **Pereira, B. da S.; Pereira, B. da S.; Cardos, É. Dos S.; Mendonça, J. O. B.; Souza, L. B. de.; Santos, M. P. dos; Zago, L.; Freitas, S. M. de L**. Physical, chemical and sensory analysis of gluten-free potato bread enriched with chia flour. Demetra: Alimentação, Nutrição & Saúde, v. 8, n. 2, p. 125-136, 2013.

20. **Cinbas, G.; Tontul, S. A.; Akin, N**. Effect of bread and baking techniques on *Bacillus coagulans* GBI-30 viability during and in vitro digestion. Journal of cereal Science, v. 117, p. 1-6, 2024. Available in: https://doi.org/10.1016/j.foodres.2022.111040.

21. **Hassan, A. A-M.; Elenany, Y. E.; Nassrallah, A.; Cheng, W.; El-Maksoud, A. A. A**. Royal jelly improves the physicochemical properties and biological activities of fermented milk with enhanced probiotic viability. LWT – Food Science and Technology, v. 155, p. 1-8, 2022. Available in: https://doi.org/10.1016/J.LWT.2021.112912.

22. **Sultana, M.; Chan, E. S.; Janarthanan, P.; Choo, W. S**. Functional orange juice with *Lactobacillus casei* and tocotrienol-enriched flaxseed oil co-encapsulation: Physicochemical properties, probiotic viability, oxidative stability, and sensorial acceptability. LWT – Food Science and Technology, v. 188, p. 1-12, 2023. Available in: https://doi.org/10.1016/j.lwt.2023.115388.

23. Łubkowska, B.; Jeżewska-Frąckowiak, J.; Sroczyński, M.; Dzitkowska-Zabielska, M.; Bojarczuk, A.; Skowron, P. M.; Cięszczyk, P. Analysis of industrial *Bacillus* species as potential probiotics for dietary supplements. Microorganisms, v. 11, n. 488, p. 1-12, 2023. Available in: https://doi.org/10.3390/microorganisms11020488.

RECyT
Year 27 / Nº 44 / 2025 /
DOI: https://doi.org/10.36995/j.recyt.2025.44.004

Gastrointestinal nematodes in small ruminants: genus identification and evaluation of anthelmintic resistance in Misiones, Argentina

Nematodos gastrointestinales en pequeños rumiantes: identificación de géneros y evaluación de resistencia antihelmíntica en Misiones, Argentina

Samuel O., Miño[1, 2, *]; Aylén R., Díaz[2]; Cristian, Miño[3]; Ricardo, Díaz Alarcón[1, 4]; Domingo J., Liotta[2, 5]; Miguel, Da Luz[3]

1- Instituto Nacional de Tecnología Agropecuaria (INTA). Centro Regional Misiones, EEA Cerro Azul. Ruta Nacional 14, Km836,5, Cerro Azul, Misiones, Argentina.
2- Laboratorio de Biología Molecular Aplicada (LaBiMAp). Facultad de Ciencias Exactas, Químicas y Naturales. Universidad Nacional de Misiones. Av. Mariano Moreno 1375, Posadas, Misiones.
3- Instituto de Macroeconomía Circular (IMAC). San Lorenzo 2152, Posadas, Misiones.
4- Consejo Nacional de Investigaciones Científicas y Técnicas (CONICET).
5- Instituto Nacional de Medicina Tropical (INMeT) - ANLIS "Dr. Carlos Malbrán", Puerto Iguazú, Misiones, Argentina.

* E-mail: mino.samuel@inta.gob.ar

Received: 04/11/2024; Accepted: 24/07/2025

Abstract
Infections by gastrointestinal nematodes (GIN) are a significant cause of productivity losses in sheep and goat farming. Anthelmintic resistance is a growing issue, driven by the indiscriminate use of these products. This study examines the GINs in sheep and goats in the province of Misiones, Argentina, and the resistance to anthelmintic drugs. Ten farms from southern Misiones were analyzed, with fecal egg counts (FEC) and drug resistance tests were performed. A wide variability in parasite burden was observed both between and within herds, highlighting the importance of customizing treatments. The average FEC was 309 and was established as the threshold above which an individual should be treated. Strategic treatment is proposed, targeting animals with high parasite loads, considered "spreaders" of infection. This approach optimizes the use of anthelmintics, reducing selection pressure on the parasite population and helping prevent resistance. Resistance to ivermectin was detected in all evaluated farms, as well as to benzimidasole and closantel, confirming the need for laboratory diagnostics before administering treatments. The predominant GIN genus was *Haemonchus*, represented by *H. contortus* and *H. placei*, followed by *Cooperia.* Additionally, a Polymerase Chain Reaction (PCR) technique was adapted for the rapid detection of the most common genera, which will improve parasite diagnosis and characterization. This study describes the GIN and anthelmintic resistance in sheep and goats in the province of Misiones, and underscores the need for continued research to adapt control strategies to local conditions and ensure the sustainability of production.

Keywords: Gastrointestinal parasites, *Haemonchus*, FEC, Anthelmintic resistance, Strategic control.

Resumen
Las parasitosis por nematodos gastrointestinales (NGI) son una causa significativa de pérdidas productivas en la ganadería ovina y caprina. La resistencia a los antihelmínticos es un problema creciente, impulsada por el uso indiscriminado de estos productos. Este trabajo estudia a los NGI en ovinos y caprinos de la provincia de Misiones, Argentina, y la resistencia a las drogas antihelmínticas. Se analizaron 10 establecimientos del sur de Misiones, obteniendo valores de huevos por gramo (HPG) y realizando test de resistencia a drogas. Se observó una amplia variabilidad de la carga de parásitos entre y dentro de cada rebaño, destacando la importancia de personalizar los tratamientos. El valor promedio del HPG fue de 309, estableciéndose como umbral a partir del cual un individuo debe ser tratado. Se propone el tratamiento estratégico, dirigido a aquellos animales con cargas parasitarias elevadas, considerados como "diseminadores" de la infección. Esto permite optimizar el uso de antihelmínticos, reduciendo la presión de selección sobre la población de parásitos y contribuyendo a evitar la resistencia. Se detectó entre un 90,3% y 35% de resistencia a la ivermectina en los dos campos evaluados, así como un 60,7% y 32,2% al febendazol y 25,9% al closantel, lo que confirma la necesidad de implementar diagnósticos de laboratorio antes de proceder con tratamientos. El género de NGI predominante fue *Haemonchus*, representado por *H. contortus y H. placei*, seguido por *Cooperia*. Además, se puso a punto una técnica de Reacción en Cadena de la Polimerasa para la detección rápida de los géneros más comunes, lo que permitirá mejorar el diagnóstico y caracterización de los parásitos. Este trabajo describe los NGI y la resistencia a los antihelmínticos en ovinos y caprinos en la provincia de Misiones, y destaca la necesidad de continuar realizando investigaciones para adaptar las estrategias de control a las particularidades locales y garantizar la sustentabilidad de la producción.

Palabras clave: Parásitos gastrointestinales, *Haemonchus*, HPG, Resistencia antihelmíntica, Cabras, Ovejas.

INTRODUCTION

Gastrointestinal nematodiasis, or verminous gastroenteritis, is a multifactorial disease caused by gastrointestinal nematodes (GIN) of various genera and species that affect ruminants in different segments of their digestive tract [1]. The disease is generally subclinical and constitutes an important cause of production losses [2]. These infections trigger a series of harmful signs such as weakness, depression, intestinal inflammation, diarrhea, edema, general debilitation, hemorrhages in the gastrointestinal tract, and metabolic alterations in protein processing, leading to reduced weight gain and, in severe cases, death [3]. Infection with GIN has direct effects on weight gain, body development, reproductive performance, and milk production, as well as indirect effects such as underutilization of forage resources and increased susceptibility to diseases. In addition, the costs associated with veterinary treatments contribute to higher production expenses, ultimately reducing profitability [4], [5].

GIN are considered endemic and do not have significant regulatory or commercial implications; therefore, their control remains largely the responsibility of farmers and/or veterinarians [6]. The main GIN species affecting sheep and goats include *Haemonchus spp., Cooperia spp., Teladorsagia (Ostertagia) circumcincta, Trichostrongylus spp., Nematodirus spp., and Oesophagostomum spp.*, which may be located in different segments of the ruminant digestive tract [7].

Diagnosis of GIN parasitism is performed through a fecal egg count (FEC), which is an indicator of the parasitic load carried by the animal [8].

Control of gastrointestinal parasitoses is achieved through the use of anthelmintic drugs and parasite management strategies, which encompass all grazing system measures aimed at reducing pasture contamination with eggs or L3 larvae infestations [9], [10]. Benzimidazoles (albendazole and fenbendazole), imidazothiazoles (levamisole), salicylanilides (closantel), and macrocyclic lactones (ivermectin) are broadly employed nematicidal compounds commonly used in ruminants both in the province of Misiones and throughout Argentina [11]. Anthelmintic drugs have recommended dosages according to their pharmacological use in cattle and sheep. However, in goats, the absorption of anthelmintics is lower than in other ruminants, and they are metabolized and excreted more rapidly; therefore, the recommended dose is twice that used for sheep [12]. It is well known that the use of anthelmintic drugs favors the multiplication of resistant individuals, representing a threat to the livestock industry [9], [10]. GIN have genetic characteristics that promote the rapid development of resistance to different drugs (10). At present, resistance has been detected to all drugs available on the market, including those of the latest generation. Worldwide [13]–[15], as well as in our country and in the NEA region (Northeast Argentina) [7], [11], [12], [16]–[21], the implementation of appropriate control strategies and treatments based on laboratory analyses has become both a necessity and an active field of research [17], [22].

In Argentina, studies on GIN have been conducted in several provinces, with the exception of Misiones [2], [4], [28], [11], [12], [20], [23]–[27]. Misiones has a production system based on smallholdings, where most producers operate small farms that are often not self-sustaining [29]. This situation encourages the formation of associations, giving rise to production basins, among which the Sheep and Goat Production Basin (COC) of Southern Misiones serves as the prime example [30]. This basin encompasses more than 25,000 head of sheep and goats distributed among approximately 450 producers from the municipalities of Candelaria, Garupá, Cerro Corá, Cerro Azul, Santa Ana, Fachinal, Profundidad, Olegario Víctor Andrade, and San José [31]. Although preliminary studies on GIN parasitoses have been conducted [18], [32], their impact on local herds remains unknown.

Therefore, the aim of this study was to investigate gastrointestinal nematodes in sheep and goats from Misiones, to evaluate resistance to anthelmintic drugs (ivermectin, closantel, fenbendazole, and levamisole), and to establish a molecular biology assay for genus characterization. The research focused on fecal egg count (FEC) analysis in farms within the COC, with the objective of generating key information to improve parasite control in the region.

MATERIALS AND METHODS

Experimental design

Ten farms from the Sheep and Goat Production Basin (COC) in southern Misiones were selected based on their proximity and/or at the owner's request (convenience sampling) [33], during September 2022 and March 2023 (Figure 1). A management survey was conducted at each farm to determine management conditions. Fecal samples (FS) from sheep and goats were collected to evaluate the number of GINs through fecal egg counts. In addition, fecal samples were pooled by farm to perform coprocultures and identify nematode genera under an optical microscope. From each pool, a sample was also processed to determine the genera present by PCR. After establishing the average FEC threshold, resistance testing was performed on farms that exceeded this value.

Sample collection
Fecal samples were collected directly from the rectum of adult animals (both females and males) showing no signs of disease, using clean, labeled polyethylene bags, and stored in insulated containers for transport. As an inclusion criterion, animals must not have received anthelmintic treatment during the three months prior to sampling.

Fecal Egg Counts
The fecal egg count (FEC) was performed using the modified INTA McMaster chamber technique [2]. This method is based on the flotation principle, in which the eggs present in a fecal sample—when mixed with a supersaturated sodium chloride (NaCl) solution—separate from the fecal mass and rise to the surface of the aqueous solution [2]. A supersaturated (SS) NaCl solution was prepared, and feces were mixed at a 1:20 (w/v) ratio, corresponding to 2.5 g of feces in 50 ml of SS NaCl. The mixture was vortexed until the feces were completely disaggregated, then left to stand for 5 minutes. A sample from the upper portion of the supernatant was collected and loaded into the McMaster chamber, and the fields were then counted. The resulting value was multiplied by the dilution factor (20), thereby obtaining the helminth fecal egg count (FEC).

Coproculture
Coprocultures were performed for the identification of L3 larvae in a set of samples [2]. From farms with an average FEC above the threshold and sufficient sample volume, pooled fecal material was collected in a container, and granulated Styrofoam® was added until a light, crumbly consistency was achieved. The coprocultures were prepared in plastic cups following the recommendations of Fiel et al. (2011) [2]. The cultures were incubated for 21 days at room temperature (20–28 °C), ensuring that moisture was maintained. After incubation, the culture was transferred to a conical beaker, submerged in chlorine-free warm water, and allowed to settle at room temperature for 12–24 hours. Infective larvae were recovered from the bottom of the conical beaker, and identification was performed under an optical microscope after immobilizing the samples with Lugol's solution. Identification was carried out based on morphological characteristics [2]. A total of 300 L3 larvae from each of the four fecal sample batches were counted, resulting in 1,200 infective L3 GIN larvae in total.

Genus Identification by Polymerase Chain Reaction (PCR)

Analytical samples
For the extraction of DNA from GIN eggs, 50 mL of the processed supernatant from pooled fecal samples were used. The material was distributed into three 15 mL tubes and centrifuged for 5 minutes at medium speed (first cycle). The supernatant was retained (discarding the pellet) and examined under an optical microscope to confirm the presence of parasite eggs. The procedure was then repeated (second cycle). During the third cycle, the supernatant was diluted 1:1 with distilled water and centrifuged for 5 minutes at medium speed. The supernatant was discarded, and the resulting pellets were combined into a single 1.5 mL microtube for subsequent DNA extraction.

DNA extraction
A volume of 200 µL of concentrated eggs and 600 µL of Isotonic Lysis Solution (ILS) were placed into a 1.5 mL microtube, homogenized by inversion three times, and incubated for 3 minutes. The sample was centrifuged at 6,500 ×g for 1 minute, and the supernatant was discarded. Then, 20 µL of Proteinase K solution and 150 µL of PBS were added, and the sample was vortexed for 1 minute to resuspend the pellet completely. Next, 200 µL of BL buffer were added and mixed in a vortex for 30 seconds. The mixture was incubated for 15–30 minutes at 56 °C. After incubation, 200 µL of ethanol (96%) were added, mixed by inversion three times, and briefly centrifuged again. The entire contents were then transferred onto a silica minicolumn placed over a 2 mL collection tube from the "ADN PuriPrep-T Kit" (Inbio Highway, Tandil, Argentina). DNA extraction was performed according to the manufacturer's instructions. The eluted DNA was stored at −20 °C.

PCR Reactions
PCR reactions were performed using the primers described by Zarlenga et al. (2001) [34], which amplify specific regions corresponding to five genera of GIN (Table 1). Each reaction was carried out in a final volume of 50 µL, containing 1X buffer, $MgCl_2$ (1.5 mM), 0.2 µM of each primer, 200 µM dNTPs, 1% dimethyl sulfoxide (DMSO), 1.25 µU of DNA polymerase, and 1 µL of target DNA. The cycling profile consisted of the following: 94 °C for 5 minutes, followed by 40 cycles at 94 °C for 1 minute, 60 °C for 1 minute, and at 72 °C for 2 minutes, with a final extension at 72 °C for 7 minutes.
Amplification products were separated on a 1.8% agarose gel, stained with ethidium bromide, and visualized under UV transillumination.

Table 1. Primers used for PCR.

Name	Target genus and species	Orientation	Amplicon size (pb)	Sequence orientation 5' → 3'
NGI-I	*Ostertagia ostertagi*	F-417	257	TAAAAGTCGTAACAAGGTATCTGTAGGT
		R-526		GTCTCAAGCTCAACCATAACCAACCATTGG
NGI-II	*Haemonchus placei*	F-628	176	CATTTTCGTCTTGGGCGATAT
		R-627		TGAGACCGCACGCGTTGATTCGAA
NGI-III	*Oesophagostomum radiatum*	F-595	329	GCAGAACCGTGACTATGGTC
		R-653		GACAAGGAGATCACGACATCAGCAT
NGI-IV	*Trichostrongylus colubriformis*	F-708	243	CAGGGTCAGTGTCGAATGGTCATTGTCAAATA
		R-707		CAGGGTCAGTGGTTGCAATACAAATGATAATT
NGI-V	*Cooperia oncophora*	F-618	151	TCGATGAAGAGTTTTCGGTGTTC
		R-641		TTCACGCTCGCTCGTGACTTCA

Information adapted from Zarlenga et al. (2001) [34].

Anthelmintic Resistance Test

In herds that exhibited a high average FEC value, an anthelmintic resistance test is (ART) was performed to determine which anthelmintic drug showed the greatest effectiveness.

In each herd, the test was conducted as follows: five groups of ten animals each, belonging to the same species, were randomly selected from within the herd (G1: Control, G2: Closantel, G3: Levamisole, G4: Ivermectin, and G5: Fenbendazole). Each group received only one drug, except for the control group, which received no treatment. The drugs were administered at the manufacturer's recommended dosage. Fecal samples were collected from each group before treatment (time 0) and 14 days post-treatment. For each sample, the FEC was determined; and the fecal egg count reduction (FECR) at 14 days was calculated using the formula recommended by Coles et al. (1992) (8):

FECR %: ((C – T) / C) x 100

Where T is the arithmetic mean of each treated group, and C is the arithmetic mean of the untreated control group 14 days post-treatment. In cases where an untreated control group could not be used, the reduction was calculated based on the initial (day 0) count, which served as the control reference [2].

RESULTADOS

Samples were collected from 10 farms located in the municipalities of Cerro Corá (N=4), Fachinal (N=1), and Profundidad (N=5), in the province of Misiones, Argentina (Figure 1).

Figure 1. Map of the province of Misiones showing its political division and highlighting the municipalities where samples were collected (gray). The upper left inset shows a map of Argentina indicating the location of the Misiones Province (green).

Survey results

Of the 10 farms sampled, 30% (3/10) were goat farms, and 70% (7/10) were sheep farms. Samples were collected from 36% (422/1177) of the animals. Of this total, 81% (343/422) corresponded to sheep and 19% (79/422) to goats. The mean Fecal Egg Count (FEC) was 309, while the mean of the maximum counts reached 2680. Except for Farm 1, non-parasitized animals (FEC = 0) were found on all farms (Table 2).

According to the survey responses related to deworming practices, only 10% (1/10) of producers had an established deworming plan, while 80% (8/10) reported deworming their animals at their convenience, with frequencies ranging from every 2 to 6 months. Regarding the

deworming strategy, in 80% (8/10) of the farms, the entire herd was treated with anthelmintics, while in 20% (2/10), treatment was administered only to animals showing clinical signs. For newly introduced animals, 60% (6/10) of the producers reported administering anthelmintics upon entry to the farm, and 40% (4/10) reported doing so to offspring at the time of weaning.

To calculate the anthelmintic dose, 60% of producers reported visually estimating the weight of each animal, whereas 30% used the heaviest animal in each category as a reference.

Among the farms analyzed, 30% (3/10) of producers reported using ivermectin in their most recent deworming, 20% (2/10) used closantel, 20% (2/10) levamisole, and 10% (1/10) fenbendazole, while 20% did not know or could not recall which antiparasitic drug had been used most recently (Table 3).

Table 2. Number of animals analyzed.

				FEC		
Farm ID	**N**	**n**	**%**	**$\bar{x}$**	**Max.**	**Min.**
Farm 1*	150	22	15%	450	1500	60
Farm 2*	17	17	100%	119	520	0
Farm 3^{s}	150	32	21%	266	1840	0
Farm 4*	280	40	14%	244	1920	0
Farm 5^{s}	108	60	56%	94	1440	0
Farm 6^{s}	42	42	100%	202	3260	0
Farm 7^{s}	60	43	72%	235	1340	0
Farm 8^{s}	75	69	92%	35	280	0
Farm 9^{s}	200	54	27%	749	8600	0
Farm 10^{s}	95	43	45%	691	6100	0
	Σ: 1177	Σ: 422	$\bar{x}$: 36%	$\bar{x}$: 309	$\bar{x}$: 2680	

*: Goat farms. s: Sheep farms. N= herd size. n= sampled animals. %: Percentage of animals analyzed. $\bar{x}$= Mean. Σ= sum.

Table 3. Survey results. Drugs and strategies used by producers for deworming.

Farm ID	Cálculo de la dosis	Animales tratados	Droga utilizada
Farm 1	Individual weight	Entire herd	Ivermectin
Farm 2	Individual weight	Entire herd	ND*
Farm 3	Heaviest animal	Entire herd	Closantel
Farm 4	Individual weight	Entire herd	Closantel
Farm 5	Heaviest animal	Entire herd	Ivermectin
Farm 6	Heaviest animal	Entire herd	ND*
Farm 7	Individual weight	Animals with clinical signs	Levamisole
Farm 8	Heaviest animal	Entire herd	Ivermectina
Farm 9	Individual weight	Animals with clinical signs	Levamisole
Farm 10	Individual weight	Entire herd	Fenbendazole

*ND: Producer did not know or could not recall which drug was used for deworming.

Parasitic load

The distribution of the FEC in each herd shows that the parasitic load of the population tends to cluster around the mean. Isolated points (far from the mean value for each farm) represent the so-called “disseminating individuals,” except in Farm 1. These isolated points (outliers) within each dataset indicate the disseminating individuals in each herd. Additionally, Farms 5 and 8 exhibited low FEC values, likely as an effect of a recent deworming treatment (not reported by the producer). As a result, the entire herd showed a low mean count, with few disseminating individuals observed (Figure 2).

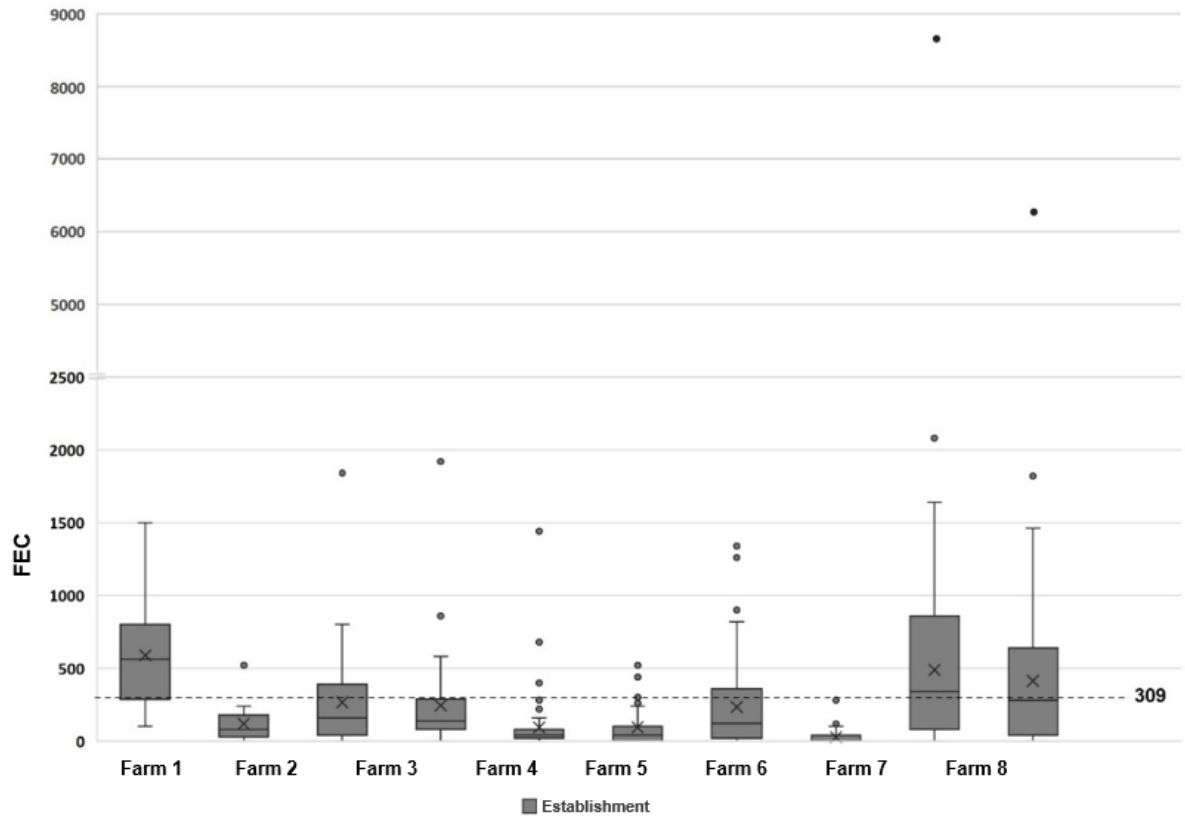

Figure 2. The box-and-whisker plot shows the farms where the parasite load was high (values above the dashed line: 309). The line dividing each box represents the median, while the "x" inside the box indicates the mean value. Additionally, the disseminating individuals in each farm are shown, which appear as "outliers" or isolated points (•) distant from the mean (x).

The distribution of FEC values shows that 71% of the animals had parasite loads below the overall mean (309). The remaining 29% had loads above the mean, with a maximum value of 8600 observed (Figure 3).

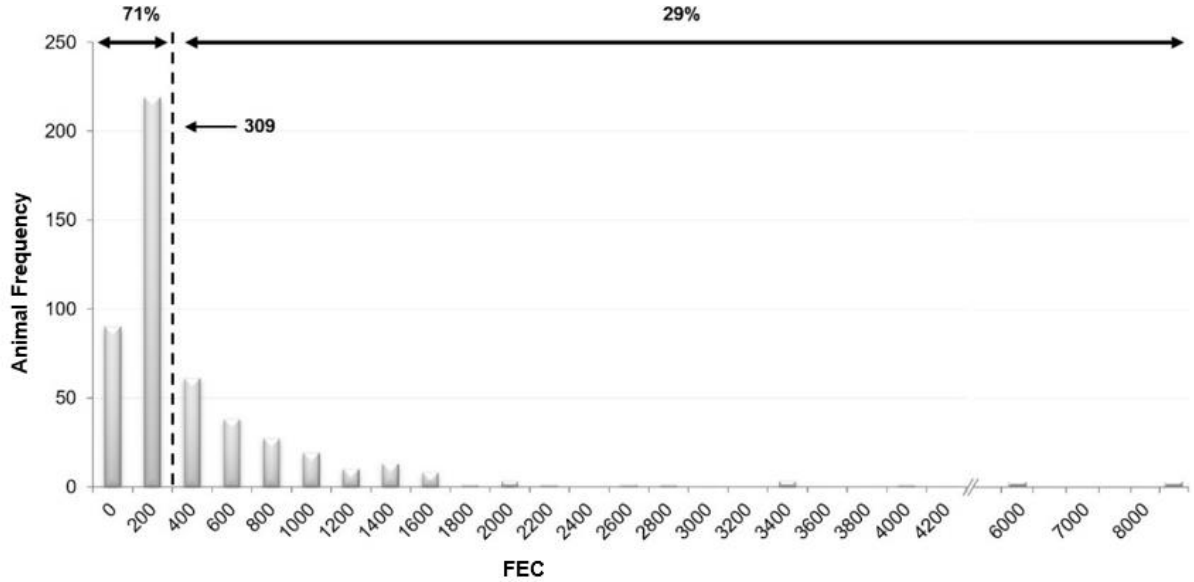

Figure 3. Fecal Egg Count distribution. The dashed line indicates the overall mean FEC value (309). The upper arrows show the 71% and 29% proportions, respectively.

Anthelmintic Resistance Test

Out of all the farms studied, the anthelmintic resistance test could be performed on 20% (2/10) of them (Farms 1 and 7), determined by the availability of a livestock scale at the time of the assays.

In Farm 1, the effectiveness of ivermectin and fenbendazole was 9.7% and 39.3% (corresponding to 90.3% and 60.7% resistance), respectively. In contrast, closantel showed 94.2% effectiveness (5.8% resistance). Data for the group treated with levamisole were unavailable for reasons beyond the scope of this study.

In Farm 7, effectiveness values of 65.0%, 67.8%, and 74.1% (35.0%, 32.2%, and 25.9% resistance) were observed for ivermectin, fenbendazole, and closantel, respectively. In contrast, levamisole showed 96.7% effectiveness (3.3% resistance) (Table 4).

Table 4. Resistance test.

Farm ID		G1-NT	G2-CSL	G3-LVM	G4-IVM	G5-BZM*
Farm 1	N*i*	8	8	-	8	8
	%FECR	-	**94,2**	-	9,7	39,3
	VR	-	0,24	-	0,21	0,18
	CI95 [min-max]	-	79 – 97	-	0 – 67	0 – 76
Farm 7	N*i*	10	10	-	10	10
	%FECR	-	*74,1*	**96,7**	*65,0*	*67,8*
	VR	-	0,30	0,33	0,74	0,35
	CI95 [min-max]	-	0 – 93	88 – 99	0 – 96	0 – 94

G1-NT: Group 1, untreated. G2-CSL: Group treated with Closantel. G3-LVM: Group 3, treated with Levamisole. G4-IVM: Group 4, treated with Ivermectin. G5-BZM: Group 5, treated with Benzimidazole. N*i*: Number of animals. %FECR: Percentage reduction in fecal egg count. VR: Variance of the reduction, representing the variance of the data with respect to the mean and among themselves. CI95: 95% confidence interval. Values in **bold** indicate >94% effectiveness; values in *italics* indicate effectiveness between 65–94%.

Coproculture and Larval Identification

From the four cultured samples, 300 L3 larvae were counted from each (total = 1,200 L3 larvae). Five genera were identified: *Haemonchus* 43% (516) — (*H. contortus* 30% [360] and *H. placei* 13% [156]) — *Cooperia* 35% (420), *Trichostrongylus* 12% (144), *Oesophagostomum* 6% (72), and *Ostertagia* 4% (48) (Figure 4).

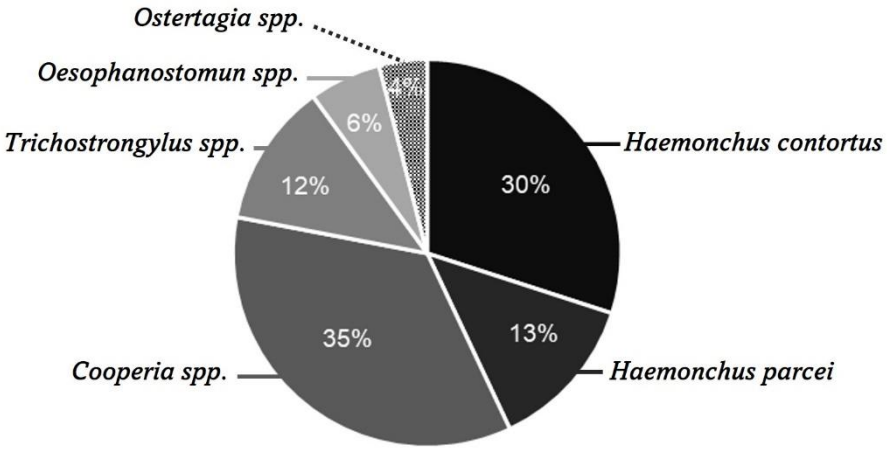

Figure 4. Pie chart showing the proportion of gastrointestinal nematode (GIN) genera and species detected in the coproculture.

Molecular Detection of Genera

The cultured larvae were used to prepare the PCR assay described by Zarlenga et al. (2001). The following species were detected: *Ostertagia ostertagi*, *Haemonchus* spp., *Oesophagostomum radiatum*, *Trichostrongylus colubriformis*, and *Cooperia oncophora*. No nonspecific amplifications were observed in any of the reactions.

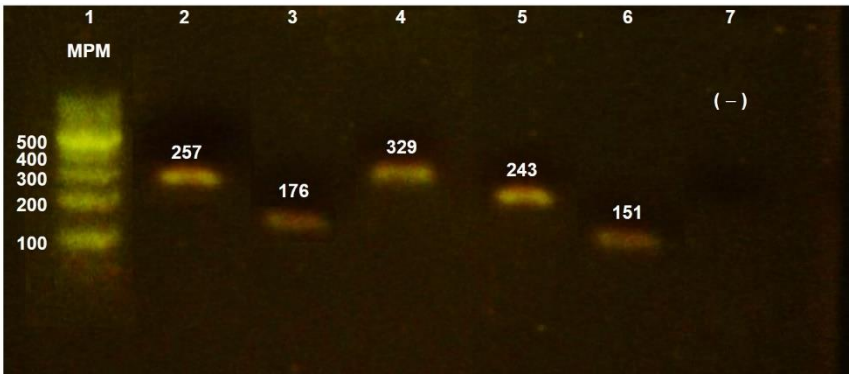

Figure 5. 2% agarose gel showing the bands corresponding to the GIN genera detected.

DISCUSSION

Gastrointestinal nematode (GIN) infections represent a global issue in sheep and goat farming [10]. They have a significant impact in productive regions, and the drive to control them without proper diagnosis has led to the proliferation of anthelmintic drug resistance [10, 35]. This study constitutes the first report describing GINs in sheep and goats from the province of Misiones. It allowed the determination of the average fecal egg count (FEC) in sheep and goats, as well as the implementation of resistance tests and the characterization of the main GIN genera present in the farms studied. In this manner, the data obtained complement the findings previously reported by Fiel et al. (2014) [32], Lobayan et al. (2016) [18], and Da Luz (2020, unpublished data). Our study reveals variability in herd sizes across farms (ranging from 17 to 280 animals), reflecting the smallholder nature [29] of sheep and goat production in the region (Table 2).

The distribution of FEC values varies among animals, with a few individuals responsible for spreading parasites within the farm and the population [6, 36]. Our results show similar variability within and between farms (Figure 2), supporting the idea that treatments should be tailored to each establishment. Thus, determining the herd's FEC makes it possible to identify animals with extreme values (disseminators), which should be the focus of treatment [23]. Furthermore, when analyzing the FEC distribution of all examined animals, most of the population (71%) shows an FEC ≤ 309, while only 29% require antiparasitic treatment, as they are the disseminators of infection within the herd. These findings are consistent with previous reports in sheep [6], [37] and suggest the need for selective or strategic treatment approaches.

The sanitary conditions of sheep and goat farms in Misiones are similar to those described for other provinces in Argentina [28], [38]. These systems are characterized by small-scale, low-efficiency production, feeding mainly on natural pastures, precarious infrastructure, and limited technical assistance [29], [38]. Under these conditions, parasitic infections are treated without laboratory diagnosis, which contributes to the spread of resistance since drug selection is based on tradition, price, or recommendation rather than on efficacy. In this study, two in vivo resistance tests were performed using the Fecal Egg Count Reduction Test (FECRT) [17]. In both farms, populations of parasites resistant to ivermectin were detected (Table 4), a situation already reported in other regions of Argentina [4], [5], [9], [18]–[20], [28], [32], [37]. In addition, one farm showed resistance to fenbendazole, where closantel proved to be the most effective drug. In the second farm, resistance was observed to both closantel and fenbendazole, with levamisole being the effective drug (Table 4). This indicates that each farm presents a distinct situation, and treatments should therefore be based on specific diagnostic testing tailored to each case.

Anthelmintic resistance is a growing global issue driven by the indiscriminate (or improper) use of these drugs, which compromises their long-term efficacy [10]. GIN show high genetic variability, enabling them to quickly adapt to treatments and spread resistance genes within their populations [22]. This phenomenon, documented both worldwide and in Argentina, underscores the need to implement comprehensive health management practices that include laboratory-based diagnoses and selective treatment control strategies. Such measures would help preserve drug efficacy and reduce the spread of resistance within herds [10], [11].

Regarding the genera identified, coproculture analyses revealed the mixed nature of gastrointestinal nematode (GIN) infections, since the different worms inhabit distinct regions of the digestive tract [4] (Figure 4). Among this diversity, the genus *Haemonchus* was predominant (43%), with two species identified: *H. contortus* (30%) and *H. placei* (13%). While *H. contortus* has been widely reported in the literature as the predominant species in sheep and goat herds [4], [11], [17], [18], [23], [26], [28], [32], [38], [39], there are few reports of *H. placei* [17]. Therefore,

ongoing studies are being conducted to further investigate this finding.

In addition, *Haemonchus sp*. and *Cooperia sp*. were detected in 35% of the samples, drawing further attention to the presence of these parasites in the region.

Currently, the use of molecular techniques for monitoring veterinary parasites remains limited in low-resource subsistence farming areas, both in Argentina and worldwide [40]. The evaluation of GIN genera traditionally requires the culture and isolation of L3 larvae [2], although eggs and L1 larvae are sufficient for molecular analyses and may help avoid potential biases associated with culturing [41]. To advance in this area and accelerate the characterization of the most prevalent GINs, a PCR assay was successfully prepared for the detection of *Ostertagia ostertagi*, *Haemonchus sp.*, *Oesophagostomum radiatum*, *Trichostrongylus colubriformis*, and *Cooperia oncophora* [34]. Although additional genera remain to be detected, this assay represents a first step towards modernizing veterinary diagnostics in the region.

CONCLUSIONS

This study highlights the importance of proper diagnosis for the control of GIN infections in the province of Misiones, Argentina. It constitutes the first report describing GINs in sheep and goats from this region, revealing variability in fecal egg count (FEC) among animals and farms, which underscores the need for selective treatments tailored to each establishment. Resistance testing demonstrated the presence of nematode populations resistant to anthelmintic drugs such as ivermectin, fenbendazole, and closantel, confirming the urgency of implementing control strategies based on laboratory analyses to avoid the indiscriminate use of anthelmintics and to prevent the spread of resistant parasites.

Moreover, the characterization of GIN genera—where *Haemonchus* and *Cooperia* were the most prevalent—and the preparation of a PCR assay for the rapid detection of the main parasitic genera represent significant advances for managing these infections.

In conclusion, this study emphasizes the need for more precise health management in the region, incorporating diagnostic-based and strategic treatment approaches to improve animal health and the profitability of local producers. Ultimately, continued monitoring of GIN populations and anthelmintic resistance is essential to adapt control strategies and ensure the sustainability of small ruminant production in the region.

ACKNOWLEDGEMENT

This work was carried out under the Scientific Cooperation Agreement between INTA and UNaM and funded by the INTA projects PE-I044 and RIST-I111 (2023 portfolio).

We thank the Municipality of Profundidad and Mayor Silvita Estigarribia for her support and collaboration.

We are especially grateful to the producers of the Sheep and Goat Production Basin of Southern Misiones, whose willingness to open the gates of their farms made this study possible.

REFERENCES

[1] M. K. Nielsen, “Internal Parasite Screening and Control,” in *Robinson’s Current Therapy in Equine Medicine: Seventh Edition*, Seventh Ed., Elsevier Inc., 2015, pp. 336–340.

[2] C. Fiel, P. Steffan, and D. Ferreyra, *Diagnóstico de las parasitosis más frecuentes de los rumiantes*, 1º. Tandil, Buenos Aires: Facultad de Ciencias Veterinarias, UNCPBA Tandil, 2011.

[3] T. Tesfaye, “Prevalence, species composition, and associated risk factors of small ruminant gastrointestinal nematodes in South Omo zone, South-western Ethiopia,” *J. Adv. Vet. Anim. Res.*, vol. 8, no. 4, pp. 597–605, 2021, doi: 10.5455/javar.2021.h550.

[4] M. Habela, R. G. Sevilla, E. Corchero, J. M. Fruto, and J. Peña, “Nematodosis gastrointestinales en ovinos,” *Mundo Ganad.*, no. Mayo, pp. 1–6, 2002.

[5] A. Almada, “Parasitosis: pérdidas productivas e impacto económico,” *Boletín Técnico, MERIAL LATAM*, 2015. https://www.ganaderia.com/destacado/Parasitosis:-Pérdidas-productivas-e-impacto-económico.

[6] A. Bosco *et al.*, “The threat of reduced efficacy of anthelmintics against gastrointestinal nematodes in sheep from an area considered anthelmintic resistance-free,” *Parasites and Vectors*, vol. 13, no. 1, pp. 1–12, 2020, doi: 10.1186/s13071-020-04329-2.

[7] R. Z. Salas, R. V. Vélez, L. V. H. Ospina, L. R. Osorio, and D. N. P. Echeverry, “Prevalence of gastrointestinal nematodes in sheep and goat production systems under confinement, semi-confinement and grazing in municipalities of antioquia, Colombia,” *Rev. Investig. Vet. del Peru*, vol. 27, no. 2, pp. 344–354, 2016, doi: 10.15381/rivep.v27i2.11647.

[8] G. C. Coles *et al.*, “World Association for the Advancemente of Veterinary Parasitology (WAAVP) methods for the detection of antihelmintic resistance in nematodes of veterinary importance,” *Vet. Parasitol.*, vol. 44, pp. 35–44, 1992, doi: 10.1016/0304-4017(92)90141-u.

[9] J. Bonino Morlán, “RESISTENCIA ANTIHELMINTICA EN OVINOS: Antecedentes y situación actual,” in *INIA Tacuarembo*, 2004, no. Seminario Parasitología, pp. 20–31.

[10] J. Charlier *et al.*, “Anthelmintic resistance

in ruminants: challenges and solutions," 2022, pp. 171–227.
[11] O. S. Anziani and C. A. Fiel, "Resistencia a los antihelmínticos en nematodos que parasitan a los rumiantes en la Argentina," *Rev. Investig. Agropecu.*, vol. 41, no. 1, pp. 34–46, 2015.
[12] M. Chocobar *et al.*, "Determinación de la eficacia de antihelmínticos para el tratamiento de la gastroenteritis verminosa en caprinos de la provincia de Tucumán," *FAVE Sección Ciencias Vet.*, vol. 19, no. 2, pp. 69–73, 2020, doi: 10.14409/favecv.v19i2.9775.
[13] H. Rose Vineer *et al.*, "Increasing importance of anthelmintic resistance in European livestock: Creation and meta-analysis of an open database," *Parasite*, vol. 27, 2020, doi: 10.1051/parasite/2020062.
[14] R. M. Kaplan *et al.*, "World Association for the Advancement of Veterinary Parasitology (W.A.A.V.P.) guideline for diagnosing anthelmintic resistance using the faecal egg count reduction test in ruminants, horses and swine," *Vet. Parasitol.*, vol. 318, no. April, p. 109936, 2023, doi: 10.1016/j.vetpar.2023.109936.
[15] H. Jung, D. Zarlenga, J. C. Martin, P. Geldhof, K. Hallsworth-Pepin, and M. Mitreva, "The identification of small molecule inhibitors with anthelmintic activities that target conserved proteins among ruminant gastrointestinal nematodes," *MBio*, vol. 15, no. 3, 2024, doi: 10.1128/mbio.00095-24.
[16] A. Díaz, R. Díaz Alarcón, C. Miño, M. Da Luz, D. J. Liotta, and O. S. Miño, "Evaluación de la eficacia de drogas antihelmínticas en ovinos y caprinos de la Provincia de Misiones.," 2022.
[17] B. Cetrá, M. Pereira, M. Pereyra, and J. C. Ramírez, "Resistencia antihelmíntica en bovinos: Situación en la provincia de Corrientes, Argentina," *INTA Ediciones*, Mercedes, Corrientes, pp. 1–5, May 2016.
[18] S. I. Lobayan, T. M. Tuzinkievicz, C. A. Fiel, J. N. Nápoli, and A. P. Dalzotto, "Relevamiento de nematodes gastrointestinales en bovinos del sur de Misiones y nordeste de Corrientes (Argentina)," *Rev. Vet.*, vol. 27, no. 2, p. 137, 2016, doi: 10.30972/vet.2721091.
[19] R. D. Irigoyen, R. M. Larsen, and C. A. Fiel, "Determinación de resistencia antihelmíntica en Cría y Recría de un sistema productivo del partido de Azul .," Universidad Nacional del Centro de la Provincia de Buenos Aires, 2019.
[20] V. H. Suárez, F. Echazú, J. Alfonso, Q. Roger, and A. E. Viñabal, "Parásitos internos de caprinos y ovinos en las regiones de quebradas áridas y la Puna de Jujuy (Argentina)," *Rev. med. vet. (B. Aires)*, vol. 99, no. 2, pp. 112–116, 2018.
[21] J. A. Salgado and C. de P. Santos, "Panorama da resistência anti-helmíntica em nematoides gastrointestinais de pequenos ruminantes no Brasil," *Rev. Bras. Parasitol. Vet.*, vol. 25, no. 1, pp. 3–17, 2016, doi: 10.1590/S1984-29612016008.
[22] W. Fissiha and M. Z. Kinde, "Anthelmintic Resistance and Its Mechanism : A Review," *Infect. Drug Resist.*, vol. 14, pp. 5403–5410, 2021, doi: 10.2147/IDR.S332378.
[23] J. Papaleo and M. Lloberas, "Ovinos : seleccionan genotipos con resistencia a parásitos," *INTA EEA Balcarce*, no. 11 de Junio, pp. 1–3, 2019.
[24] M. Bulman, "Pérdidas económicas directas e indirectas por parásitos internos y externos de los animales domésticos," *Rev. Vet. Argentina*, vol. XXXII, no. 330, p. 95, 2015.
[25] PROSAP, "EVALUACIÓN DE IMPACTO AMBIENTAL Y SOCIAL PROYECTO DESARROLLO INTEGRAL GANADERO," PROVINCIA DE RÍO NEGRO, 2010.
[26] V. Suárez, M. Fondraz, A. Viñabal, G. Martínez, and A. Salatín, "Epidemiología de los nematodes gastrointestinales en caprinos lecheros en los valles templados del NOA, Argentina," *RIA*, vol. 39, no. 2, pp. 191–198, 2013.
[27] J. Romero and C. Boero, "Epidemilogía de la gastroenteritis verminosa de los ovinos en las regiones templadas y cálidas de la Argentina," *Analecta Vet.*, vol. 21, no. 1, pp. 21–37, 2001.
[28] A. Petryna, J. J. Gioffredo, W. Bayer, H. Lovera, and M. Galetto, "Especies prevalentes de nematodes gastrointestinales en ovinos en el sur de la provincia de Córdoba, Argentina.," *Rev. Vet. Argentina*, vol. 32, no. 323, pp. 1–12, 2015.
[29] R. J. Viana and P. L. Büttenbender, "La Administración Y Perspectivas En Los Minifundios De La Provincia De Misiones – Argentina.," *Rev. GESTO Rev. Gestão Estratégica Organ.*, vol. 9, no. 2, pp. 55–73, 2021, doi: 10.31512/gesto.v9i2.321.
[30] J. L. Garay *et al.*, "Constitución de la mesa de gestión de la Cuenca Ovino Caprina de la Zona Sur de la Provincia de Misiones," *Carta de Intención. Acta y Reglamento Constitutivo*. p. 4, 2016.
[31] S. Estigarribia, M. Benítez, D. Pedrozo, and C. Arce, "La 3° Expo de la Cuenca Ovino Caprina mostró el crecimiento del sector.," 2023, pp. 17–19.
[32] C. A. Fiel *et al.*, "Epidemiología de Nematodos Gastrointestinales y resistencia a los antiparasitarios en uso de la zona sur de la Provincia de Misiones.," *Anu. Investig. USAL*, vol. 1, pp. 1–6, 2014.
[33] A. S. Acharya, A. Prakash, P. Saxena, and A. Nigam, "Sampling: why and how of it?," *Indian J. Med. Spec.*, vol. 4, no. 2, pp. 330–333, 2013, doi: 10.7713/ijms.2013.0032.
[34] D. S. Zarlenga, M. Barry Chute, L. C. Gasbarre, and P. C. Boyd, "A multiplex PCR assay for differentiating economically important gastrointestinal nematodes of cattle," *Vet.*

Parasitol., vol. 97, no. 3, pp. 201–211, 2001, doi: 10.1016/s0304-4017(01)00410-1.
[35] R. M. Kaplan and A. N. Vidyashankar, “An inconvenient truth: Global worming and anthelmintic resistance,” *Vet. Parasitol.*, vol. 186, no. 1–2, pp. 70–78, May 2012, doi: 10.1016/j.vetpar.2011.11.048.
[36] P. R. Torgerson, M. Paul, and F. I. Lewis, “The contribution of simple random sampling to observed variations in faecal egg counts,” *Vet. Parasitol.*, vol. 188, no. 3–4, pp. 397–401, 2012, doi: 10.1016/j.vetpar.2012.03.043.
[37] G. Morales, A. T. Guillen, A. Pinho, L. Pino, and F. Barrios, “Clasificación por el método Famacha y su relación con el valor de hematocrito y recuento de h.p.g. de ovinos criados en condiciones de pastoreo,” *Zootec. Trop.*, vol. 28, no. 4, pp. 545–555, 2010.
[38] F. Angeloni, V. Orcellet, D. Plaza, and R. Marengo, “Prevalencia y géneros de nematodos gastrointestinales en pequeños rumiantes de los Departamentos Feliciano y Federal , Entre Ríos,” in *VI Jornada de Difusión de la Investigación y la Extensión*, 2018, vol. Noviembre, no. Salud Animal, pp. 2–3.
[39] G. López-Rodríguez, A. Zaragoza-Bastida, A. Olmedo-Juárez, C. Rosenfeld Miranda, and N. Rivero-Perez, “Gastrointestinal nematodes in sheep and their anthelmintic resistance. A subject under discussion in Mexico,” *J. Selva Andin. Anim. Sci.*, vol. 10, no. 2, pp. 116–129, 2023, doi: 10.36610/j.jsaas.2023.100200116x.
[40] P. M. Airs *et al.*, “Low-cost molecular methods to characterise gastrointestinal nematode co-infections of goats in Africa,” *Parasites and Vectors*, vol. 16, no. 1, pp. 1–15, 2023, doi: 10.1186/s13071-023-05816-y.
[41] E. Redman, C. Queiroz, D. J. Bartley, M. Levy, R. W. Avramenko, and J. S. Gilleard, “Validation of ITS-2 rDNA nemabiome sequencing for ovine gastrointestinal nematodes and its application to a large scale survey of UK sheep farms,” *Vet. Parasitol.*, vol. 275, no. September, p. 108933, 2019, doi: 10.1016/j.vetpar.2019.108933.

RECyT
Year 27 / Nº 44 / 2025 /
DOI: https://doi.org/10.36995/j.recyt.2025.44.005

Functional microsatellites in cassava (*Manihot esculenta* Crantz): genomic mapping and genetic characterisation in cultivars from Misiones

Microsatélites funcionales en mandioca (*Manihot esculenta* Crantz): mapeo genómico y caracterización genética en cultivares de Misiones

César Adrián, Preussler[1]; Patricia Mabel, Aguilera[2]; María Isabel, Fonseca[3, 4, *]

1- Montecarlo Centre of Experimental Agriculture (EEA) (National Agricultural Technology Institute [INTA]). Montecarlo, Misiones, Argentina.
2- Institute of Subtropical Biology (IBS). School of Exact, Chemical and Natural Sciences. National University of Misiones. Misiones, Argentina.
3- Misiones' Institute of Biotechnology "Dra. María Ebe Reca" (INBIOMIS). School of Exact, Chemical and Natural Sciences. National University of Misiones. Misiones, Argentina.
4- CONICET. Buenos Aires, Argentina.
* E-mail: fonsecamariaisabel@yahoo.com.ar

Received: 22/12/2024; Accepted: 18/09/2025

Abstract
Cassava is a perennial root crop cultivated for human nutrition and livestock feeding. Its roots are consumed peeled and cooked, while the raw roots are processed industrially to obtain starch. In Misiones, farmers have traditionally preferred and preserved several cassava cultivars for specific traits, such as cooking quality, texture of boiled roots, or starch yield. Our objectives were to employ seven EST-SSR primer pairs to map them *in silico* onto the reference genome of *M. esculenta*, and to characterise a group of traditional and new cassava cultivars and lines for Misiones by PCR amplification. Each primer pair mapped uniquely to the expected locus and, for the first time, revealed the corresponding chromosome, gene identity, and primer-mapped region in the reference genome. The functional SSR marker was contained within the region delimited by both primers of each pair. In all 20 studied cassava accessions, these primers produced satisfactory amplification profiles showing bands of expected size. The assayed set of markers yielded a characteristic amplification pattern for each accession, allowing them to be differentiated by this seven-primer combination. This analysis aims to assist the initial steps of genetic characterisation for selection and breeding programs of cassava cultivars in Misiones.

Keywords: Aipim; Cassava; Yuca; Gene markers; Cultivar diversity; NE Argentina.

Resumen
La mandioca es un arbusto perenne cultivado para alimentación humana y del ganado. Sus raíces son consumidas como hortaliza o destinadas a la producción de fécula. En Misiones, tradicionalmente los productores han preferido y preservado varios cultivares según ciertas características, como calidad y textura de cocción, o rinde de fécula. Nuestros objetivos fueron utilizar siete pares de cebadores EST-SSR para localizarlos *in silico* en el genoma de referencia de *M. esculenta*, y caracterizar un grupo de cultivares y líneas tradicionales y nuevas para Misiones mediante amplificación por PCR. Cada par de cebadores mapeó únicamente en el locus esperado, revelando por primera vez el cromosoma correspondiente, el gen asociado y la región blanco de los cebadores en el genoma de referencia. Además, la región delimitada por ambos cebadores de cada par incluyó al respectivo marcador funcional SSR. Los cebadores produjeron perfiles de amplificación satisfactorios en las 20 accesiones estudiadas, con bandas del tamaño esperado. El conjunto de marcadores ensayado produjo un patrón de amplificación característico para cada accesión, permitiendo diferenciarlas con esta combinación de siete marcadores. Este análisis pretende asistir los pasos iniciales de caracterización genética para selección y programas de mejoramiento de mandioca en Misiones.

Palabras clave: Aipim; Mandioca; Yuca; Marcadores génicos; Diversidad de cultivares; NE de Argentina.

Introduction

Cassava (*M. esculenta* Crantz, Euphorbiaceae) is a perennial root crop naturally distributed from the southern United States of America to northern Argentina, and cultivated in tropical and subtropical regions of America, Africa, and Asia for both human nutrition and livestock feeding. This species, also known as *mandioca*, manioc, *aipim*, *macaxeira*, *yuca,* or *cuauhcamotli*, is a major worldwide staple food crop [1, 2]. Its roots are rich in complex carbohydrates and are a valuable source of gluten-free starch. They are consumed peeled and cooked, while the raw roots are processed industrially to obtain starch.

Cooked leaves are often consumed as a vegetable [3, 2].

Significant advances have been made in the genetic and genomic characterisation of this crop to assist selection and breeding programs. In this sense, genetic maps and even a dense composite reference map, comprising thousands of genetic markers, have been constructed [4, 5]. Functional [6] and random [5, 7] SSR markers have also been developed from this species. More recently, several genomic resources have become accessible [8, 4, 9, 10, 11], allowing the characterisation of cassava cultivars, wild accessions, and related species. Moreover, the sequenced, assembled, and annotated genome of the cassava cultivar AM560-2 from Colombia has been designated as a chromosome-level assembly reference genome [12], serving as the most up-to-date unifying platform for cassava genetics and genomics.

As is common worldwide, cassava is mainly cultivated in small-scale farming systems in the provinces of northeastern Argentina. In this region, it is a daily staple used to prepare various traditional dishes, with increasing demand nationwide [2, 13]. In Argentina, Misiones is the leading producer of this crop, and most growers are smallholder families who cultivate it mainly for home consumption but also for commercial purposes, highlighting its economic and sociocultural importance. In this province, cassava production reached 100,000 t in 2024, which was processed exclusively by the starch industry [14].

Traditionally, farmers in Misiones have preserved several cassava cultivars for specific traits, such as cooking quality, texture of boiled roots, and starch yield, to cover the wide range of potential uses. For example, sweet cultivars that are easy to peel and cook are preferred for vegetable consumption, while those with higher starch content are preferred for industrial use [15]. To increase yield and also overcome some issues of traditional cultivars related to biotic stresses, several cultivars and hybrid lines from diverse origins have recently been introduced from the Alliance of Biodiversity International and CIAT (Colombia) through the Clayuca Corporation [16], by the primary starch-producing agricultural cooperatives from Misiones. These cultivars and lines, although introduced for cultivation in NE Argentina, have not yet been included in local trial programs.

Despite the large number of popularly known traditional cultivars and novel accessions available, a comprehensive characterisation of this cassava germplasm remains lacking. Therefore, a depiction of cultivars currently being grown and those that would be brought into cultivation is required for conservation, selection, and breeding purposes [17]. In this regard, molecular markers can provide valuable information on their potential linkage to agronomically interesting genes, genomic context, and genetic variability.

The objectives of this work were i) to localise *in silico* a group of previously developed functional microsatellite markers onto the annotated reference genome of *M. esculenta* and ii) to assay and test their applicability to characterise a group of traditional and new cassava cultivars and lines in Misiones.

Materials and methods

Genomic mapping of functional microsatellite primers: The chromosome-level assembly reference genome GCA_001659605.2 (*M. esculenta*_v8) of cassava cultivar AM560-2 (Colombia) was downloaded from the NCBI Genome Datasets [12]. This genome was employed for *in silico* mapping of a group of seven selected EST-SSR primer pairs (MeESSR8, 15, 19, 22, 23, 28, and 29) developed by Raji et al. [6] (Table 1).

Table 1: Main features of EST-SSR primers mapped in the *M. esculenta* GCA_001659605.2 genome and assayed in traditional cassava cultivars from Misiones and accessions introduced from CIAT.

Marker name	Forward primer/ Reverse primer	Repeat type	Product size (bp)
MeESSR8	ATTGAAATTGGCTTCCGTCA AACCCCCACACCGTACAATA	$TAC(AT)_5T$	166
MeESSR15	TTCGCCTTTCTCATAGCTCAA ATGCATCTGCATGCCTATTT	$(AT)_8$	157
MeESSR19	TTCTCGTCGGCTCCTTTCTA CCCCACTTGATCTGCCTTTA	$(AT)_{10}$	208
MeESSR22	CGACGCATTTTACGTTTTCC CCCCCTCTCATGAATTGAAA	$(CT)C(CT)T(CT)_3CC$	183
MeESSR23	GCTGAGGTTCTGCTGGTTTC CGGAGGATTTCACTGAGGAC	$TT(CT)_4A(TC)_3T$	212
MeESSR28	TTCGATTCAAGAAGGTATTCCA CCTGAAGTACTCGCCTGAGC	$(CT)_{12}$	190
MeESSR29	AATTCTAGGGTCGCCGATTT TGCCATAATAAACCACCTTGG	$(CT)_{11}$	150

The primer pairs were mapped using the Geneious platform (Biomatters Ltd.) with the Geneious mapper at default parameters, except allowing sequence mismatches of 0-10% and a

random number of genomic matches. For each primer pair, we analysed matches to cassava chromosomes, genic loci, gene identity, and the identification of expected simple sequence repeats (SSRs).

Amplification of microsatellite markers in cassava cultivars

Plant material: Seven *M. esculenta* cultivars traditionally grown in Misiones, Argentina, were used. Among them, five cultivars known as *Rocha/Petroski*, *Tacuara/Tacuarita*, *Pomberí/Blanca/Pombero*, *Coloradita/Horquetuda* and *Concepción/Conche* are preferred for both fresh consumption and the starch industry. Additionally, CA 25-1 and IAC-90 are typically intended for industry. In addition, 13 accessions (cultivars and hybrid lines) introduced as a novelty for NE Argentina from CIAT, Colombia, were also considered: PAR 1, PAR 105, BRA 899, BRA 1197, CHN 1, ARG 2, BRA 29, BRA 31, BRA 33, BRA 894, CM321-188, TAI 8, and TAI 16. All these plant materials were maintained in the field and greenhouse at Laharrague Annexe Experimental Field (EEA, INTA, Montecarlo), located in Misiones, Argentina (26°33'36"S 54°40'19"W) (Figure 1).

DNA extraction: Genomic DNA was isolated from 1.5 g of fresh leaves of one individual from each of the 20 cassava cultivars under study, according to Doyle & Doyle [18], with the following modifications. Leaf tissue was ground in a mortar using 4 ml of 2X CTAB isolation buffer. Ground material was poured into a 2 ml tube, and the mortar was rinsed with 4 μl of 2-mercaptoethanol and added to the same tube. 10 μl of proteinase K was added to each sample, followed by a sufficient volume of CTAB buffer to bring the total volume to 2 ml. Samples were incubated at 65 °C with gentle swirling for 15 min and then centrifuged at 3000 rpm for 5 min. About 0.9 ml of the supernatant was recovered and transferred into a new 2 ml tube, and 0.9 ml of chloroform-isoamyl alcohol (24:1, v/v) was added. Samples were then centrifuged at 13000 rpm for 8 min. About 0.9 ml of the supernatant was transferred to a clean tube, and 540 μl of isopropanol was added, gently mixed by hand for about 1 min. Samples were kept at -20 °C for 30 min and then centrifuged at 13000 rpm and 4 °C for 12 min. Finally, the supernatant was gently poured off, and the pellet containing DNA was washed twice with 1 ml of 70% cold ethanol. Finally, the ethanol was discarded, and tubes containing pellets were allowed to dry in a thermal block at 65 °C for 30 min. Then, 100 μL of UP water and 2 μL of RNase were added to each sample. Samples were incubated at 37 °C for 30 min. Sample quality controls were performed by measuring absorbance at 260 and 280 nm in a spectrophotometer and by electrophoresis at 25 V and 1X TBE in 1% agarose gels. DNA samples were stored at -20 °C.

PCR for functional microsatellite amplification: Seven EST-SSR primer pairs (Table 1) previously developed from the *M. esculenta* cultivar TME117 *Isunikankiyan* (Nigeria) [19, 6] were tested in 20 cassava cultivars and lines by PCR amplification. For each cassava cultivar, the amplification reaction was performed using 52.7 ng/μl of template DNA, 1X reaction buffer (PB-L), 5 mM $MgCl_2$, 0.2 μM dNTPs, 0.2 μM of each primer F and R, 0.1 U/μl of Taq DNA polymerase (TAQ Pegasus), and distilled water to a final volume of 20 μl (all final concentrations). Reactions were performed using an Ivema-T21 thermocycler under the following cycle profile: (I) 3-min initial denaturation at 94 °C; (II) 35 cycles of: 30 s at 94 °C, 30 s at 52 °C, 30 s at 72 °C; (III) 5-min final extension at 72 °C.

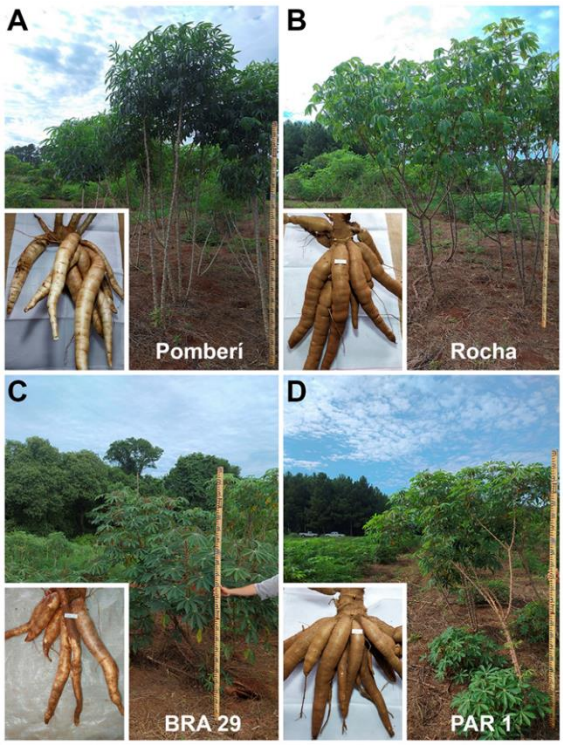

Figure 1: Plants and roots of some *M. esculenta* plant material employed in this work, growing in Montecarlo, Misiones, Argentina. A, B: Misiones' traditional cultivars *Pomberí* and *Rocha*; C, D: line BRA 29 and cultivar PAR 1 imported from CIAT. Note the variability in plant appearance, root number and size, and peel colour.

Polyacrylamide gels for marker visualization: 12% polyacrylamide gels were prepared using 8.871 ml of distilled water, 7.5 g of urea, 1 ml of TBE 5X buffer, 4.5 ml of acrylamide: bisacrylamide (38:2, 40%, w/v) stock solution, 10 μl of N,N,N',N'-tetramethylethylenediamine (temed), and 100 μl of 10% ammonium persulfate (APS) solution. The samples were denatured by formamide treatment at 95 °C for 5 min and then abruptly cooled to 4 °C. Then, 4 μl (containing 1 μl of PCR product and 3 μl of loading buffer) of the denatured samples, and 1 μl of DNA ladder (1 μl PB-L 100 bp DNA ladder, and 3 μl of loading buffer) were loaded onto denaturing 12% polyacrylamide gels. Electrophoresis was carried out at 120 W for 1 h 20 min using a Scie-Plas electrophoresis cell connected to a PowerPac/3000 power supply. After electrophoresis, the gels were fixed in a solution of 10% ethanol and 0.75% acetic acid for 5 minutes. The amplification products were then visualised using silver nitrate according to the Silver Staining-System protocol (Promega, USA), digitised with a Samsung A23 digital camera, and visually analysed.

Results and discussion

Genomic mapping of functional microsatellite primers in cassava

The mapping of seven EST-linked primers to the *M. esculenta* reference genome (GCA_001659605.2) revealed, as expected, seven genomic loci (Figure 2, Table 2). These primers, which were assayed *in silico*, were initially developed by Raji et al. [6] from a set of expressed sequence tags (ESTs) containing microsatellite repeats, obtained from a dehydration-stress transcriptome analysis of TME117, a cassava accession from Nigeria [19]. Since this reference genome represents a consensus of maternal and paternal haplotypes, a unique genomic locus linked to a genic region is expected to be revealed when mapping a primer pair derived from an expressed functional region. The availability of a reference genome sheds light on the target region of these primers, and genomic mapping revealed, for the first time, the corresponding *M. esculenta* chromosome, the gene identity, and the primer-mapped region (mRNA, gene-adjacent genomic region, or ncRNA) for each primer pair. Importantly, each of the seven EST-derived primer pairs was uniquely mapped to the expected genome region, and the region delimited by both primers contained the SSR, in agreement with Raji et al. [6]. (Figure 2).

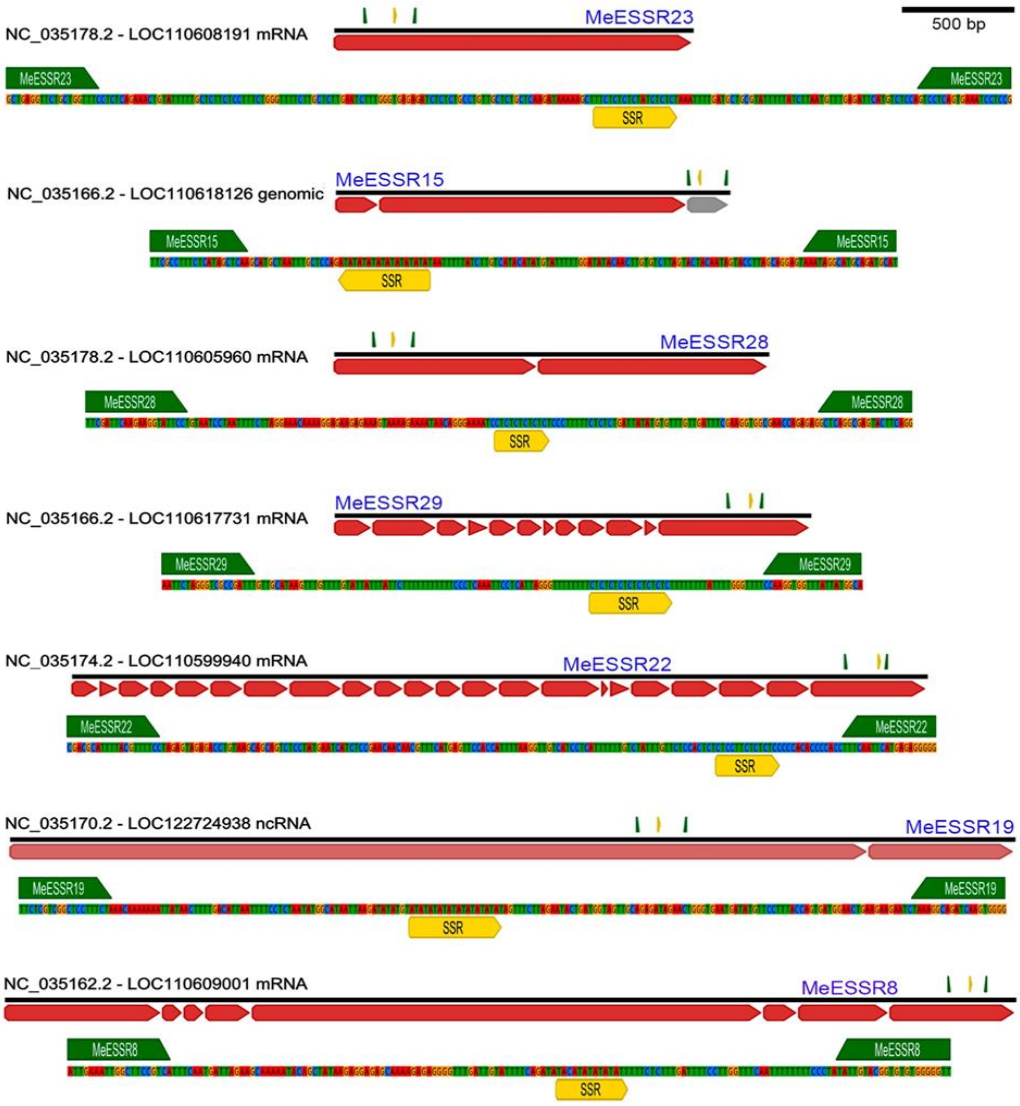

Figure 2: Mapping of EST-linked primers and their products containing SSR markers into the reference genome of *M. esculenta* GCF_001659605.2. Primers were uniquely mapped to expected genome regions encompassing mRNA or adjacent regions, and to ncRNA sequences; NC=chromosome; LOC=gene. Note the detailed amplified region containing SSR markers for each primer pair.

According to the reference genome [12] each primer pair mapped as follows: MeESSR8 to chromosome 2 (NC_035162.2), into the mRNA region of LOC110609001; MeESSR15 to chromosome 6 (NC_035166.2), into the genomic region adjacent to the mRNA of LOC110618126; MeESSR19 to chromosome 10 (NC_035170.2), into an ncRNA of LOC122724938; MeESSR22 to chromosome 14 (NC_035174.2), into the mRNA of LOC110599940; MeESSR23 and MeESSR28 to chromosome 18 (NC_035178.2), into mRNA regions of LOC110608191 and LOC110605960, respectively; and MeESSR29 to chromosome 6 (NC_035166.2), into mRNA of LOC110617731 (Table 2). The gene product encoded by each primer-targeted gene is depicted in Table 2. These results are consistent with the putative functions assigned by Raji et al. [6] through BlastX searches aimed at annotating the respective EST and with gene annotations for coding protein genes from reference genome GCF_001659605.2 via Eggnog-mapper by Aguilera & Grabiele [11] and the NCBI Gene section [20]. Future *in silico* assays of the cassava reference genome that consider functional microsatellite primers not included in this study could reveal their linkage to other agronomically interesting genes and cost-effectively assist selection programs.

Table 2: Summary of seven EST-linked primers *in silico* mapped to the reference genome of *M. esculenta* GCF_001659605.2. The primer target regions are shown relative to the chromosome and gene ID, gene model-related regions, gene products, and the SSR motif contained therein.

Chromosome-Gene ID	Primer-mapped region	Gene product	Primers	SSR motif

NC_035162.2 - LOC110609001	mRNA	PH, RCC1 and FYVE domains containing protein 1	MeESSR8	TACATATATATATT
NC_035166.2 - LOC110618126	Genomic-adjacent to mRNA	chaperone protein dnaJ 49	MeESSR15	ATATATATATATATATATAT
NC_035170.2 - LOC122724938	ncRNA	uncharacterized LOC122724938	MeESSR19	ATATATATATATATATATAT
NC_035174.2 - LOC110599940	mRNA	ATPase 11, plasma membrane-type	MeESSR22	CTCCTTCTCTCTCC
NC_035178.2 - LOC110608191	mRNA	bZIP transcription factor 44	MeESSR23	TTCTCTCTCTATCTCTCT
NC_035178.2 - LOC110605960	mRNA	AP2/ERF transcription factor ABR1	MeESSR28	CTCTCTCTCTCT
NC_035166.2 - LOC110617731	mRNA	chaperone protein dnaJ 15	MeESSR29	CTCTCTCTCTCTCTCTCT

Total DNA extraction and functional microsatellite amplification in cassava

Using the described protocol, total genomic DNA was successfully extracted from all 20 cassava accessions, with concentrations ranging from 377.18 to 707.09 ng/μl (Pomberí and C321-188, respectively).

Amplification reactions using functional microsatellite markers were performed across all 20 cassava cultivars and hybrid lines, including seven traditional from Misiones and 13 newly introduced for field trials in NE Argentina. PCR products were visualised on 12% polyacrylamide gels. A total of seven primer pairs for EST-SSRs were assayed in all samples (Table 1, Figure 3). This same set of primers also successfully mapped to the *M. esculenta* reference genome (Figure 2). In all 20 studied cassava accessions, these primers produced satisfactory amplification profiles, mostly showing clear bands.

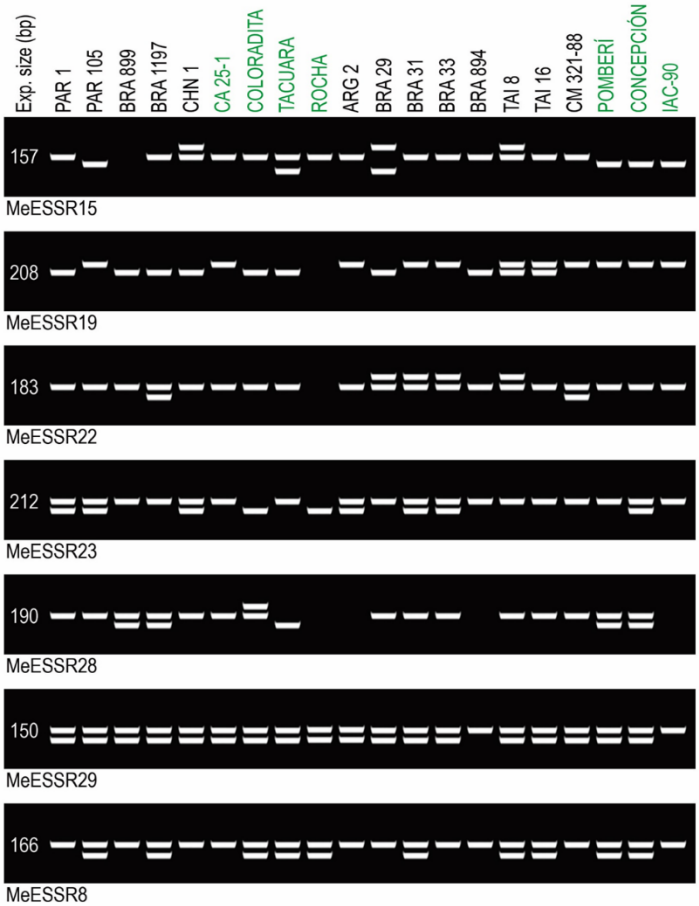

Figure 3: Schematic representation of the EST-linked PCR products assayed in 20 cultivars of *M. esculenta*; in green, traditional cultivars from Misiones. Note the variability in the number and size of amplified DNA bands for each cultivar regarding each pair of primers.

As expected, bands ranging in size from 150 bp (MeESSR29) to 212 bp (MeESSR23) were observed (Figure 3) [6].

Since *M. esculenta* is considered an allotetraploid with disomic inheritance [21, 22] and functional microsatellites are locus-specific [6], the

amplification of one or two bands per locus is expected in each accession. Consistent with this, one or two bands were observed across accessions depending on the primer pair used, thereby indicating a homozygous (one band) or heterozygous (two bands) condition at the respective locus (Figure 3).

Unexpectedly, the traditional cultivar Rocha from Misiones failed to produce many bands for the markers MeESSR19, 22, and 28. Although primers designed to reveal functional markers are from highly conserved regions, slight sequence variations in the target regions, i.e., SNPs, may occur in some cultivars or hybrid lines. Furthermore, if the genotype, *M. esculenta* cultivar TME117 ´Isunikankiyan´ from which these primers were developed, has an SNP/deletion/insertion relative to other members of the species, or if other members have an SNP/insertion/deletion, the corresponding sequence data from those individuals may not align to TME117 [4] and vice versa. Thus, possible sequence differences between the accession TME117 from which the primers were developed and our cultivar *Rocha* from Misiones could explain the lack of amplification products for specific markers in the latter. Different PCR amplification conditions to ensure hybridisation of these primer pairs could help overcome this issue.

Additionally, a different number of total alleles per locus was observed compared to those reported by Raji et al. [6]. In this work, we observed 2, 4, 3, 2, 3, and 2 alleles per locus revealed by markers MeESSSR8, 15, 19, 22, 23, 28, and 29, respectively, while 4, 8, 6, 3, 5, 3, and 5 were previously reported by these authors for the same markers in cassava [6]. Our observations on the number of alleles per locus are coincident with those of Raji et al. [6] only for marker MeESSR28 (3 alleles). These authors developed the primers used and scored them in a group of 24 *M. esculenta* cultivars from Africa, Asia, and Latin America, including landraces, elite breeding lines, putative interspecific hybrids, wild *Manihot* species, and related Euphorbiaceae [6]. Considering the wide range of genotypes, the diversity of accessions we tested here seems to be narrowed by the more limited origins of our material. Most of our studied accessions included cultivars and hybrid lines from Argentina (ARG 2), particularly traditional ones from Misiones, Argentina (*Rocha, Tacuara, Pomberí, Coloradita*, CA 25-1, IAC-90, *Concepción*), Paraguay (PAR 1, PAR 105), Brazil (BRA 899, BRA 1197, BRA 29, BRA 31, BRA 33, BRA 894), Colombia (CM321-188), China (CHN 1), and Thailand (TAI 8, and TAI 16). Thus, most of the plant material we studied represents only a portion of the Latin American diversity of cassava. The lower number of alleles per locus could indicate a constricted diversity of these materials compared to those of Raji et al. [6].

Interestingly, the set of seven assayed markers yielded a characteristic amplification pattern for each of the 20 tested cassava accessions, enabling their differentiation based on this primer combination (Figure 3). Considering the absence of previous variability characterisation experiments for traditional cultivars from Misiones and the need to compare them with new cultivars or lines introduced for cultivation, this type of functional marker may be particularly useful.

By mapping a new set of functional microsatellite primers to the cassava reference genome, it would be feasible to select EST-SSRs linked to other agronomically interesting genes. After accurately selecting an array of interesting and informative primers, this analysis could be extended to other valuable cassava accessions.

Conclusions

Seven EST-SSR primer pairs were mapped *in silico* on the reference genome of *M. esculenta*. Each primer pair mapped uniquely to the expected locus and, for the first time, revealed the corresponding chromosome, the gene identity, and the primer-mapped region (mRNA, genomic-adjacent to a gene model, or ncRNA). As expected, the SSR marker was contained within the area delimited by both primers of each pair.

In all 20 studied cassava accessions, these primers produced satisfactory amplification profiles with bands of the expected sizes. This set of assayed markers yielded a characteristic amplification pattern for each accession, effectively enabling their differentiation through this primer combination.

Acknowledgements

This contribution is part of the doctoral thesis of C. A. Preussler (DCA-UNaM). We are grateful to the National Agricultural Technology Institute, the National University of Misiones and the National Scientific and Technical Research Council in Argentina (CONICET), from which C. A. Preussler (INTA), P.M. Aguilera and M. I. Fonseca (UNaM-CONICET) are researchers, for their continuous support.

Bibliography

1. **Howeler, R.; Lutaladio, N.; Thomas, G.** (2013) *Save and grow: Cassava, a guide to sustainable production intensification*. FAO of the United Nations. Disponible en: https://www.fao.org/4/i3278e/i3278e.pdf. Diciembre 2024.

2. **Feltan, R.; Villasanti, A.; Padawer, A.** (2016) *La cassava. Tecnología en alimentos para la economía social.* Ministerio de Ciencia,

Tecnología e Innovación Productiva, Presidencia de la Nación, Argentina. Disponible en: https://cyt.rec.uba.ar/wp-content/uploads/La-Cassava.pdf. Diciembre 2024.

3. **Cassava, un alimento con potencialidad** (2015) *Nutrición y educación alimentaria, ficha n° 46.* Ministerio de Producción y Trabajo, Presidencia de la Nación, Argentina. Disponible en: https://alimentosargentinos.magyp.gob.ar/HomeAlimentos/seguridad-alimentaria-y-nutricion/fichaspdf/Ficha_46_Cassava.pdf. Diciembre 2024.

4. **Lyons, J.; Bredeson, J.; Mansfeld, B.; Bauchet, G.; Berry, J.; Boyher, A.; et al.** (2022) *Current status and impending progress for cassava structural genomics*. Plant Molecular Biology. Vol. 109. p. 177 – 191.

5. **Chavarriaga-Aguirre, P.; Maya, M.; Bonierbale, M.; Kresovich, S.; Fregene, M.; Tohme, J.; et al.** (1998) *Microsatellites in Cassava (Manihot esculenta Crantz): discovery, inheritance and variability*. Theoretical and Applied Genetics. Vol. 97. p. 493 – 501.

6. **Raji, A.; Anderson, J.; Kolade, O.; Ugwu, C.; Dixon, A.; Ingelbrecht, I.** (2009) *Gene-based microsatellites for cassava (Manihot esculenta Crantz): prevalence, polymorphisms, and cross-taxa utility.* BMC Plant Biology. Vol. 9. p. 118.

7. **Mba, R.; Stephenson, P.; Edwards, K.; Melzer, S.; Nkumbira, J.; Gullberg, U.; et al.** (2001) *Simple sequence repeats (SSR) markers survey of the cassava (Manihot esculenta Crantz) genome: towards an SSR-based molecular genetic map of cassava.* Theoretical and Applied Genetics. Vol. 102. p. 21 –31.

8. **Iragaba, P.; Kawuki, R.; Bauchet, G.; Ramu, P.; Tufan, H.; Earle, E.; et al.** (2020) Genomic characterization of Ugandan smallholder farmer-preferred cassava varieties. Crop Science. Vol. 60. p. 1450 – 1461.

9. ***Manihot esculenta***. *Genome Datasets section.* National Library of Medicine, National Center for Biotechnology Information. Disponible en: https://www.ncbi.nlm.nih.gov/datasets/genome/?taxon=3983. Noviembre 2024.

10. **Ogbonna, A.; Braatz de Andrade, L.; Mueller, L.; Oliveira, E.; Bauchet, G.** (2021) *Comprehensive genotyping of a Brazilian cassava (Manihot esculenta Crantz) germplasm bank: insights into diversifcation and domestication.* Theoretical and Applied Genetics. Vol. 134. p. 1343 – 1362.

11. **Aguilera, P.; Grabiele, M.** (2024) *Annotated genes in cassava/cassava/yuca (Manihot esculenta) via Eggnog-mapper, iTAK and PlantTFDB*. Mendeley Data V1. Disponible en: doi 10.17632/kmjg84z8cj.1. Noviembre 2024.

12. ***Manihot esculenta,* Genome assembly M.esculenta_v8 (reference)** *Genome Datasets section.* National Library of Medicine, National Centre for Biotechnology Information. Disponible en: https://www.ncbi.nlm.nih.gov/datasets/genome/GCF_001659605.2/. Noviembre 2024.

13. **Burgos, A**. (2018) *Estado actual del cultivo de cassava en la República Argentina*. Agrotecnia. Vol. 27. p. 14 – 18.

14. **Agro: La producción de cassava en Misiones creció un 65% en 2024** (2024) *Gobierno de la Provincia de Misiones*. Disponible en: https://comunicacion.misiones.gob.ar/agro-la-produccion-de-cassava-en-misiones-crecio-un-65-en-2024/. Noviembre 2024.

15. **Cuadernillo de producción de cassava y sus usos** (2008) *INTA EEA Montecarlo y Secretaría de Desarrollo Económico de la Municipalidad de Montecarlo*. Misiones, Argentina. 23 p.

16. **Clayuca**. Disponible en: https://clayuca.org/nosotros/#:~:text=Es%20el%20organismo%20encargado%20de,cumplimiento%20de%20su%20objeto%20social. Noviembre 2024.

17. **Shindoi, M.; Avico, E.; Sarco, P.** (2018) *Comportamiento agronómico de diez cultivares de cassava (Manihot esculenta Crantz) en Colonia Benítez, Chaco*. Agrotecnia. Vol. 27. p. 9 – 13.

18. **Doyle, J; Doyle, J.** (1987) *A rapid DNA isolation procedure for small quantities of fresh leaf tissue*. Phytochemical Bulletin. Vol. 19. p. 11 – 15.

19. **Lokko, Y.; Anderson, J.; Rudd, S.; Raji, A.; Horvath, D.; Mikel, M.; et al.** (2007) *Characterization of an 18,166 EST dataset for cassava (Manihot esculenta Crantz) enriched for drought-responsive genes.* Plant Cell Reports. Vol. 26. p. 1605 – 1618.

20. **Gene section**. *National Library of Medicine, National Center for Biotechnology Information.* Disponible en: https://www.ncbi.nlm.nih.gov/gene. Diciembre 2024.

21. **Jennings, D.** (1963) *Variation in pollen and ovule fertility in varieties of cassava and the effect of interspecific crossing on fertility*. Euphytica. Vol. 12. p. 69 – 76.

22. **Umanah, E.; Hartmann, R.** (1973) *Chromosome numbers of karyotypes of some Manihot species*. Journal of the American Society for Horticultural Science. Vol. 98. p. 272 – 274.

RECyT
Year 27 / Nº 44 / 2025 /
DOI: https://doi.org/10.36995/j.recyt.2025.44.006

In vitro and *ex vitro* germination of *Jatropha gossypiifolia* and initiation of *in vitro* cultivation

Germinación *in vitro* y *ex vitro* de *Jatropha gossypiifolia* e inicio del cultivo *in vitro*

Germinação *in vitro* e *ex vitro* de *Jatropha gossypiifolia* e iniciação de cultivo *in vitro*

Jack B. S., Rojas[1]; Maria da P. F., Silva[1]; Adriano. P., Guilherme[1]; Milena. G., Malosso[1,*]
1- Instituto de Saúde e Biotecnologia de Coari. Universidade Federal do Amazonas (ISB/UFAM). Brazil.
* E-mail: milena@ufam.edu.br

Received: 12/09/2023; Accepted: 22/09/2025

Abstract
Jatropha gossypiifolia L. is a widely used medicinal plant in the Amazon region. Commonly known as pião-roxo, it produces luteol, a compound with healing properties, and has therefore been included in the National List of Medicinal Plants of Interest to the Brazilian Unified Health System (SUS). Despite its potential as a herbal medicine, there are no phytotechnical studies supporting its large-scale propagation, making seed germination trials essential. For the *ex vitro* germination test, seeds were placed in different substrates over a period of 180 days to determine the most suitable soil type for germination. For the *in vitro* germination test, three concentrations of sodium hypochlorite were evaluated: 0.1%, 0.5%, and 1.0%. Nodal segments were subjected to the same aseptic treatments. As a result, clayey soil was identified as the most effective substrate, presenting the highest seed germination speed index. Since *in vitro* seed germination was not achieved, cultivation of the species was initiated using nodal segments, with the most effective treatment being 1.0 mg/L of sodium hypochlorite. Thus, it was demonstrated that biomass production of this species is feasible for pharmaceutical industry applications through both *ex vitro* and *in vitro* methods.

Keywords: Conservation; Medicinal plant; Germination test; Pião-roxo; Biomass production.

Resumen
Jatropha gossypiifolia L. es una planta medicinal común en el Amazonas. Conocida popularmente como punta morada, produce luteol que tiene actividades curativas y, por eso, fue incluida en la Lista Nacional de Plantas Medicinales de Interés para el SUS. Tiene potencial como medicina herbaria, pero no existen estudios fitotécnicos para su reproducción a gran escala y, por tanto, son necesarias pruebas de germinación de semillas. Para la prueba de germinación *ex vitro*, las semillas se colocaron en diferentes sustratos durante 180 días para determinar el mejor tipo de suelo para la germinación. Para la prueba de germinación *in vitro* se probaron tres concentraciones diferentes de hipoclorito de sodio: 0,1; 0,5 y 1,0%. Los segmentos nodales fueron sometidos a la misma asepsia. Como resultado, se indicó suelo arcilloso por presentar el mayor índice de velocidad de germinación de las semillas. Al no obtenerse germinación de semillas *in vitro*, se decidió iniciar el cultivo de esta especie utilizando segmentos nodales y el mejor tratamiento fue 1,0 mg/L de hipoclorito de sodio. Así, se encontró que es posible producir biomasa vegetal de esta especie para satisfacer las necesidades de la industria farmacéutica tanto *ex vitro* como *in vitro*.

Palabras clave: Conservación; Planta medicinal; Prueba de germinación; Peonza morada; Producción de biomosa.

Resumo
A *Jatropha gossypiifolia* L., é uma planta medicinal comum no Amazonas. Popularmente conhecida como pião-roxo, produz luteol que apresenta atividades cicatrizantes e, por isso, foi inserido na Relação Nacional de Plantas Medicinais de Interesse ao SUS. Apresenta potencial como fitoterápico, mas não possui estudos fitotécnicos para reprodução em larga escala e, por isso, testes de germinação de sementes são necessários. Para o teste de germinação *ex vitro*, sementes foram colocadas em diferentes substratos por 180 dias para averiguar o melhor tipo de solo para germinação. Para o teste de germinação *in vitro*, foram testadas três diferentes concentrações de hipoclorito de sódio: 0,1; 0,5 e 1,0%. Segmentos nodais foram submetidos à mesma assepsia. Como resultado, foi indicado o solo argiloso por apresentar o maior índice de velocidade de germinação de sementes. Como não foi obtido germinação de sementes *in vitro*, optou-se por iniciar o cultivo desta espécie utilizando segmentos nodais e obteve-se como melhor tratamento o de 1,0 mg/L de hipoclorito de sódio. Assim, verificou-se que é possível produzir biomassa vegetal desta espécie para suprir as necessidades da indústria farmacêutica tanto *ex vitro* como *in vitro*.

Palavras-chave: Conservação; Planta medicinal; Teste de germinação; Pião-roxo; Produção de biomassa.

Introduction

The Euphorbiaceae family encompasses the Crotonoideae subfamily, which includes the Jatropheae L. tribe, part of the Jatropha L. genus. This genus comprises between 165 and 175 species, distributed across Africa, India, the West Indies, Central America, the Caribbean, and South America (LEAL and AGRA, 2005) [1]. Among these species is *Jatropha gossypiifolia*, which is found throughout Brazil (BIGIO, 2023) [2].

Jatropha gossypiifolia L. is a subshrub that can reach up to 5 meters in height, with purplish branches and leaves during its juvenile stage, and secretes a milky, acrid latex. Its leaves are simple and lobed, its flowers are arranged in purple paniculate inflorescences, and its fruit is a capsule (ARAÚJO *et al.*, 2023) [3].

This species, commonly known in northern Brazil as pião-roxo, possesses medicinal properties (VARELA, 2021) [4], which, according to Bastos (2019) [5], include healing and anti-inflammatory biological activities. Lemos *et al.* (2021) [6] attribute these properties to the triterpene luteol, and as noted by Ferreira (2022) [7], the plant has been included in the National List of Medicinal Plants of Interest to the Brazilian Unified Health System.

Pião-roxo exhibits significant phytotherapeutic potential, and as such, research into its various biological and agronomic aspects has been encouraged, given the limited knowledge available regarding its life cycle. Consequently, studies on seed germination are essential.

As stipulated by the Ministry of Agriculture, Livestock and Supply through the Rules for Seed Analysis, the evaluation of light, temperature, humidity, oxygen availability, and substrate type is fundamental for conducting seed germination tests (BRASIL, 2009) [8]. According to Lima Júnior (2010) [9], the most commonly used substrates for such tests include coconut fiber, soil, and sand, which must be adequately moistened to ensure sufficient water availability for seed germination.

Mendes *et al.* (2019) [10] state that the ideal substrate must meet the specific requirements of the seed in terms of size, shape, and desiccation tolerance, while also allowing for the assessment of its availability, economic viability, standardization, and uniformity. Furthermore, it should possess suitable physical and chemical properties. According to these authors, an appropriate substrate must offer adequate structure, consistency, and porosity to facilitate water drainage, good capillarity for moisture retention, and be free of toxic substances, pathogens, invasive plants, or other pests.

As Queiroga *et al.* (2021) [11] emphasize, the substrate must not impede oxygen penetration and should not retain excessive moisture, which could result in a water film surrounding the seed. Therefore, the ideal substrate must maintain a balance between water availability and aeration.

Accordingly, the substrate selected should be the one that yields the best results in seed germination tests and seedling establishment (DE PETRI *et al.*, 2020) [12].

Modern biotechnological methodologies are increasingly employed in seed germination studies (JOÃO *et al.*, 2021) [13]. Through plant tissue culture and micropropagation techniques, it is possible to rapidly produce plant biomass on a large scale and at low cost (SANTOS, 2020) [14], for use in the pharmaceutical industry.

The initial step in obtaining inputs through this technique involves the production of axenic seedlings *in vitro* (HOFFMANN *et al.*, 2022) [15], typically derived from explants such as seeds, nodal or apical segments, leaves, roots, among others (LIMA *et al.*, 2022) [16]. These explants are placed in culture media that generally contain an auxin to promote cell elongation and a cytokinin to stimulate cytokinesis, thereby inducing rapid formation and growth of the aerial parts of the plant (PORFÍRIO *et al.*, 2019) [17].

According to Docha *et al.* (2020) [18], the first stage of micropropagation is explant asepsis, aimed at the complete elimination of microorganisms. This process typically involves the use of antibacterial agents such as sodium and calcium hypochlorite, in concentrations ranging from 0.1% to 1.0%, and various antibiotics. Additionally, 70% ethanol serves an astringent function, detaching microbial hyphae and spores from the explants. Systemic fungicides such as Derosal or Benomyl at 1% are also commonly employed.

Asepsis protocols are considered effective when they induce seed germination or promote the growth of pathogen-free nodal segments. It is customary to identify the treatment that yields the highest germination rate and the lowest contamination rate. Upon successful asepsis, the process advances to the multiplication phase, where plant biomass is produced on a large scale. Therefore, *in vitro* germination tests are as necessary and significant as *ex vitro* tests.

In light of the need to produce biomass for use in the phytotherapeutic industry, the objective of this study was to determine the most suitable substrate for seed germination and the most effective asepsis protocol for initiating *in vitro* cultivation of *Jatropha gossypiifolia* L., with a view toward large-scale biomass production for pharmaceutical applications.

Material and Methods

1. *Ex vitro* germination test:

To conduct this experiment, ripe fruits were collected in November 2012 from the parent plant located in the garden of the Institute of Health and Biotechnology at the Federal University of Amazonas, specifically in front of the Plant Tissue Culture Laboratory. The fruits were taken to the laboratory, depulped, and the seeds were sown in different types of substrates.

Four types of substrates were used in this experiment: coconut fiber, sand, clay, and a 1:1 mixture of sand and clay. These substrates were autoclaved for 40 minutes at 121 ºC and distributed in plastic trays measuring 25.0 cm × 39.0 cm × 7.5 cm, which were kept in the greenhouse of the Plant Tissue Culture Laboratory at the Institute of Health and Biotechnology of the Federal University of Amazonas.

In each substrate, 30 seeds were placed, as shown in Figure 1, totaling 120 seeds of *Jatropha gossypiifolia* L.

Figure 1 - *Ex vitro germination experiment of Jatropha gossypiifolia L., showing seed distribution in the substrate composed of equal parts sand and clay*.

The trays containing the substrates and seeds were installed in a covered outdoor area of the laboratory, where they were irrigated daily and monitored for 180 days post-sowing.

Every 15 days, data were collected on the number of germinated seeds in each substrate type to evaluate the Seed Germination Speed Index.

The Germination Speed Index (GSI) was calculated as described by Maguire (1962) [19].

The results were expressed as mean and standard deviation and analyzed using Tukey's test.

2. *In vitro* germination test:

2.1. Seed asepsis:

Fruits of *J. gossypiifolia* L. were collected from the nursery of the Plant Tissue Culture Laboratory at the Coari Institute of Health and Biotechnology, Federal University of Amazonas. In the laboratory, the fruits were depulped and the seeds washed with neutral detergent and rinsed under running water. Subsequently, they were immersed in three different concentrations of sodium hypochlorite—0.1%, 0.5%, and 1.0%—for 30 minutes under constant orbital agitation at 100 rpm. They were then immersed in 70% ethanol for 1 minute and in a 1% Benomyl solution for 1 hour, also under orbital agitation. At the end of the process, the seeds were rinsed four times with sterile distilled water and inoculated into test tubes containing MS/2 culture medium supplemented with 30.0 g/L sucrose and adjusted to pH 6.0.

The seeds were maintained in a growth chamber under a 16-hour photoperiod with cold white fluorescent lighting, at a temperature of 25 ± 2 ºC and relative humidity of 65% for 180 days to determine the germination rate. However, contamination rate was assessed only once, 30 days after *in vitro* inoculation.

Thirty seeds were used for each sodium hypochlorite treatment.

2.2. Asepsis of nodal segments:

Nodal segments of *J. gossypiifolia* L. were obtained from branches collected from mother plants in the nursery of the Plant Tissue Culture Laboratory at the Institute of Health and Biotechnology of Coari, Federal University of Amazonas. In the laboratory, the branches were cut into nodal segments shaped like small "Y" structures, washed with neutral detergent using a soft toothbrush, and thoroughly rinsed under running water.

The nodal segments underwent the same aseptic treatment as the seeds, with the addition of 5.0 mg/L of ascorbic acid to the culture medium. This experiment was conducted under the same conditions as the previous one.

The results of these experiments were analyzed using simple percentage calculations followed by Tukey's test.

Results and Discussion

1. E*x vitro* germination test:

When selecting a substrate, it is essential to consider seed size, moisture requirements, light sensitivity, and the ease with which seedling development and evaluation can be conducted (SOUZA *et al.*, 2020) [20].

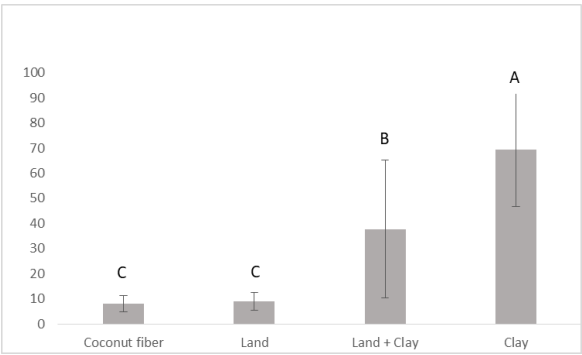

Graph 1: Germination rate of *Jatropha gossypiifolia* L. in different substrates.

As shown in Graph 1, after 180 days of sowing, coconut fiber and sandy soil exhibited low

germination rates, respectively (7.99 ± 3.22) and (8.99 ± 3.53), due to the limited water retention capacity of these substrates. Gonçalves *et al.* (2022) [21] reported similar findings with cedar seeds. Furthermore, as explained by Menegaes *et al.* (2017) [22], this phenomenon occurs because *Jatropha gossypiifolia* L. seeds do not encounter optimal conditions in these substrates in terms of density, total porosity, aeration space, moisture, water retention capacity, proportion of solid pores, and appropriate water pH.

Both the substrate composed of equal parts sand and clay (37.66 ± 27.44) and the clayey soil (69.33 ± 22.49) demonstrated a progressive germination rate that stabilized after 90 days (data not shown), indicating high germination performance. Silva *et al.* (2020) [23] explains that substrates composed of larger particles possess greater void space and, consequently, lower compaction and apparent density, which enhances soil aeration and facilitates seedling germination. Dutra *et al.* (2016) [24] also identified these two substrate types as ideal for the germination of Luehea divaricata Mart. et Zucc. seeds.

2. *In vitro* germination test:

Asepsis is a critical step in the *in vitro* plant cultivation process, as the absence of an effective protocol for microorganism elimination results in an insufficient number of seedlings to proceed with biomass multiplication (VIEIRA *et al.*, 2021) [25].

Although the *in vitro* germination experiment for *Jatropha gossypiifolia* L. seeds was repeated three times in triplicate, axenic seeds could not be obtained, and no germination was observed even after 180 days, indicating low viability of this species under stress conditions. Similar results were reported by Lattuada *et al.* (2019) [26] with oregano.

Due to the unsatisfactory germination results and the need to address biomass production for pharmaceutical applications, a new asepsis experiment was conducted using nodal segments. However, this resulted in 100% mortality of explants due to oxidation. This outcome can be attributed to the relationship between explant size and the action of the disinfectant agent, as small tissues are highly susceptible to degeneration caused by sodium hypochlorite, leading to phytotoxicity (SILVA *et al.*, 2021) [27].

Moreover, the progressive darkening that culminated in complete carbonization of the nodal segments may also be explained by the release of phenolic compounds, highlighting the need to retest this cost-effective asepsis method with the addition of an antioxidant agent and/or under light-exclusion conditions.

Subsequently, a second experiment identical to the first was conducted, incorporating 5.0 mg/L of ascorbic acid into the culture medium to mitigate phenolic oxidation caused by explant excision (RONDON *et al.*, 2023) [28]. The results are presented in Table 1.

Table 1: Asepsis of nodal segments of *Jatropha gossypiifolia* L.

Treatment	Live explants (%)	Bacterial contamination (%)	Fungal contamination (%)
0.1% sodium hypochlorite	100,0 a	13,33 b	50,0 c
0.5% sodium hypochlorite	100,0 a	13,33 b	30,0 b
1.0% sodium hypochlorite	100,0 a	3,33 a	10,0 a

In this second experiment, as shown in Table 1, 100% of the nodal segments survived across all treatments, indicating that ascorbic acid exerted an effective antioxidant action on this type of explant. Similar results were reported by Oliveira *et al.* (2021) [29] in studies with olive trees.

According to the table, bacterial contamination of *Jatropha gossypiifolia* L. nodal segments was 13.33% in treatments with 0.1% and 0.5% sodium hypochlorite, and 3.33% in the 1.0% treatment, demonstrating the disinfectant's efficacy against bacterial infestations in this species. As noted by Silva *et al.* (2021) [27], acceptable contamination rates are those below 10.0%.

Table 1 also shows that fungal contamination decreased proportionally with increasing sodium hypochlorite concentration—50.0%, 30.0%, and 10.0%, respectively—confirming its effectiveness against fungal contaminants. Messias *et al.* (2019) [30] reached similar conclusions in their studies with *Paulinia melifolia*.

Therefore, treatment with 1.0% sodium hypochlorite is currently recommended for initiating *in vitro* cultivation of this species using nodal segment explants.

Conclusion

Based on the findings of this study, it is concluded that high germination rates of *Jatropha gossypiifolia* L. can be achieved *ex vitro* when using clay-based substrates. However, it is recommended that further trials be conducted with nutrient-rich substrates to investigate the potential for even higher germination rates.

It is also advised that new *in vitro* seed germination tests be undertaken, as the experiments conducted in this study did not result in successful *in vitro* germination of *J. gossypiifolia* L. seeds. Nevertheless, it was possible to initiate axenic *in vitro* cultivation of this species using nodal segments, which may be employed for

large-scale biomass production to meet the demands of the pharmaceutical industry.

Acknowledgments
We extend our sincere gratitude to the Fundação de Amparo à Pesquisa do Estado do Amazonas (FAPEAM) for financial support provided through the Scientific Initiation Scholarship Program. We also wish to thank Dr. Thierry Ray Jehlen Gasnier for his invaluable guidance in conducting the statistical analyses.

REFERENCES

[1]LEAL, Crislaine Kieva Abreu; AGRA, Maria de Fátima. Estudo farmacobotânico comparativo das folhas de *Jatropha molissima* (Pohl.) Baill. e *Jatroplha ribifolia* (Pohl.) Baill. (Euphorbiaceae). **Acta Farm. Banaerense.** v. 24, n. 1, p. 5 – 13, 2005. Disponível em: http://www.latamjpharm.org/trabajos/24/1/LAJOP_24_1_1_1_6WQ842B4X2.pdf. Acesso em 24 ago. 2023.

[2] BIGIO, N. C.; SECCO, R. S.; MOREIRA, A. S. *Jatropha in* **Flora e Funga do Brasil.** Jardim Botânico do Rio de Janeiro. Disponível em: <https://floradobrasil.jbrj.gov.br/FB17581>. Acesso em: 24 ago. 2023.

[3] ARAÚJO, Paloma Andrade Santos; de OLIVEIRA, Vinícius Araújo; PONTES, Márcio Michel; de GÓIS, Alexsandro Melquiades; da SILVA, Gisele Nayara Bezerra. FALCÃO, Rosângela Estevão Alves. **Pinhão-roxo (*Jatropha gossypiifolia* L.): uma revisão de literatura dos usos tradicionais, atividade biológica e caracterização fitoquímica**. *In*: Pesquisas e avanços e química de produtos naturais. 1º Edição. Jardim do Serindó: Agro Science. 463 p., 2023. Disponível em: https://agronscience.com/livro-cbqnat/. DOI: doi.org/10.53934/9786599965814. Acesso em: 24 ago. 2023.

[4] VARELA, Alex Gonçalves. A trajetória de Joaquim Monteiro Caminhoá: um botânico no império do Brasil. **Brasilian Journal of Development**. v. 7, n. 1, p. 9905-9924. Disponível em: file:///C:/Users/MIlena/Downloads/admin,+672.pdf. DOI:10.34117/bjdv7n1-672. Acesso em 24 ago. 2023.

[5] BASTOS, Maria Lysete de Assis. Evidências científicas acerca das atividades biológicas de uma planta nativa do Nordeste Brasileiro – o pião roxo. **Revista Enfermagem Atual in Derm**. Suplemento, 2019;87, 9 p., 2019.

[6] LEMOS, Ari Sérgio de Oliveira; de OLIVEIRA, Naiara Norberto Tavares; NETTO, Lívia Lacerda; REIS, Samara Evangelista; de MEDEIROS, Valquíria Pereira; FABRI, Rodrigo Luiz; CHEDIER, Luciana Moreira. Avaliação do perfil químico e citotóxico de *Jatropha multifida* L. (Euphorbiaceae). **Brasilian Journal of Development**. v. 7, n. 10, p. 94971 – 94984, 2021. Disponível em: https://d1wqtxts1xzle7.cloudfront.net/79162067/pdf-libre.pdf?1642689252=&response-content-disposition=inline%3B+filename%3DAvaliacao_do_perfil_quimico_e_citotoxico.pdf&Expires=1692934763&Signature=F9301XHPCRTOgl880kZIABgSCFoHoslJT-egiBxDM2vEdt82753zv4LNN2BgChM87sjk5tFB7-bTpy-SAF-O0kOaYEIKtZlR~rFOwRiIbCf58qjpVUB7R6Sod2bYm~U8bfw42MfkzCAGzx6I5~eUAOvt0nVoMiJBF2pXwy-6hNsnQ5G9RVMmC7WNbDoMr3Pbxhl3j1ze~UhclIA37phqEa1edK4MEbN3E7w8lzXBSKbQNry0OIwSJ-QRx-eftwQ~sB0tvEksIEzbgg9zV9VxbXprJNEF21XwSO-jZGWD0IJ1AdJ7W5djlG9KN3Lb5ORwDZJhd9mQ1EKMIAvizo1vXw__&Key-Pair-Id=APKAJLOHF5GGSLRBV4ZA . DOI:10.34117/bjdv7n10-010. Acesso em: 24 ago. 2023.

[7] FERREIRA, Ilke Mara Rodrigues. Estudo farmacológico e toxicológico da *Jatropha gossypiifolia*: uma revisão integrativa. **Revista Ciência (In) Cena**. v. 1, n. 16, p. 71 – 87, 2022. Disponível em: https://estacio.periodicoscientificos.com.br/index.php/cienciaincenabahia/article/view/1311/1110. Acessado em 24 ago. 2023.

[8]BRASIL, Ministério da Agricultura, Pecuária e Abastecimento. **Regras para análise de sementes.** 1º Edição. Brasília: MAPA, 398 p., 2009. Disponível em: regras-para-analise-de-sementes.pdf. Acesso em 25 ago. 2023.

[9]LIMA JUNIOR, Manoel de Jesus. **Manual de procedimentos para a análise de sementes florestais.** 1ª Edição. Manaus: EDUFAM, 146 p., 2010. Disponível em: Layout 1 (researchgate.net). Acesso e, 25 ago. 2023.

[10]MENDES, Rafaella Gouvea; BONETTI, Leila Leal d Silva; GASTL-FILHO, Josef; de MENEZES, Danylla Paula; de SANTI, Sávio Luiz; REZENDE, Arthur Silva; MENEZES, Leonardo Henrique Queiroz; SILVA, Aurélio Freitas Pereira. Germinação e vigor de sementes de Araticum-cagão influenciadas por GA3 em diferentes substratos. **Bazilian Journal of Animal and Enviromental Research**. v. 2, n. 1, p. 632 – 645, 2019. Disponível em: Vista do Germinação e vigor de sementes de Araticum-Cagão influenciados por GA3 em diferentes substratos (brazilianjournals.com.br). Acesso em 25 ago. 2023.

[11]QUEIROGA, Vicente de Paula; GOMES, Josivalda Palmeiras; FIGUEIREDO NETO, Acácio; QUEIROZ, Alexandre José de Melo; MENDES, Nouglas Veloso Barbosa; de

ALBUQUERQUE, Ester Maria Barros. Mirtilo (*Vaccinum spp.*) tecnologias de plantio em típicas regiões serranas. **Revista Eletrônica A Barriguda**. 237 p., 2021. Disponível em: Capa Mirtilo.cdr (researchgate.net). Acesso em 25 ago. 2023.

[12]DE PETRI, Eliane Cristina Moreno; CARDOSO, Elisa dos Santos; TIAGO, Auana Vicente; DA ROCHA, Vinícius Delgado; ROSSI, Ana Aparecida Bandini. Influência do armazenamento e substrato na emergência de plântulas de maracujá-amarelo. **South American Journal of Basic Education, Technical and Technological.** v. 7, n. 2, p. 458 – 468, 2020. Disponível em: 2528-libre.pdf (d1wqtxts1xzle7.cloudfront.net). Acesso em 08 set. 2023.

[13]JOÃO, Amanda Aparecida; FERRERA, Lucas Fantin Machado; CORRÊA, Pedro Henrique Florêncio; LUIZ, Rita de Cássia Portes; DE OLIVEIRA NETO, Sebastião Soares. Biotecnologia Vegetal 4.0: uma abordagem sobre "speed breeding**". Research, Society and Development**. v. 10, n. 12, 2021. Disponível em: View of Plant biotechnology 4.0: an approach to "Speed Breeding" (rsdjournal.org). Acessado em 08 set. 2023.

[14]SANTOS, Cleberson Corrêa (Org.). **Agrobiodiversidade: manejo e produção sustentável**. Volume 1. 1º Edição. Mato Grosso: Editora Pantanal. 146 p. 2020. Retirado de: ebook.pdf (editorapantanal.com.br). Acessado em 08 set. 2023.

[15]HOFFMANN, Luana Tiara; BITTENCOURT, Ricardo; GROTTI, Yasmin Tassi; SPELICH, Carmen Lúcia. Germinação in vitro de *Raulinoa echinata* R. S. Cowan (Rutaceae): sementes e embriões zigóticos. Ciência Florestal, v. 32, n. 3, p. 1187 – 1204, 2022. Disponível em: EBSCOhost | 160108573 | Germinação in vitro de Raulinoa echinata R. S. Cowan (Rutaceae): sementes e embriões zigóticos. Acesso em 08 set. 2023.

[16]LIMA, Cláudia Simone Madruga; DA ROSA, Gabriela Gerhardt; BONOME, Lisandor Tomas da Silva. **Aspectos técnicos da cultura de Romanzeira**. 1ª Edição. Chapecó: Editora UFFS. 138 p. 2022. Disponível em: Aspectos técnicos da Cultura da Romãzeira (PDF).pdf (uffs.edu.br). Acesso em: 08 set. 2023.

[17]PORFÍRIO, Kennedy de Paiva; TITON, Miranda; DE CASTRO, Ana Carolina Macedo; PEREIRA, Israel Marinho; PFEILSTICKER DE KNEGT, Rafael Antoniu. Multiplicação *in vitro* de Xyolopedia aromatica em diferentes meios de cultura e concentrações de BAP. **Pesquisa Florestal Brasileira.** v. 39, n. 1, 7 p. Disponível em: Vista do Multiplicação in vitro de Xylopia aromatica em diferentes meios de cultura e concentrações de BAP (embrapa.br). Acesso em 08 set. 2023.

[18]DOCHA, Anna Luiza Mota; DE OLIVEIRA, Leandro Silva; DE SOUZA, Naiara dos Santos; BRONDANI, Gilvano Ebling. Estabelecimento in vitro de *Ceiba riboflora* Carb.-Sobr. e L. P. Queiroz: uma espécie endêmica do vale do rio São Francisco. **Caderno de Ciências Agrárias**. v. 12, p. 1 – 5, 2020. Disponível em: 988d28083d46dcceede70253104fe4d55cee.pdf (semanticscholar.org). Acesso em 08 set. 2023.

[19]MAGUIRE, James D. Speed of germination: aid in selection and evaluation for seedling emergence and vigour. **Crop Science**, v. 2, n. 2, p. 176-177, 1962. Disponível em: **https://doi.org/10.2135/cropsci1962.0011183X000200020033x**. Acesso em 28 ago. 2023.

[20]SOUZA, Gilda Gonçalves; REDIG, Meirevalda do Socorro Ferreira; BRITO, Sinara de Nazaré Santana; MONTEIRO, Arlesson Sidney Almeida; BRONZE, Antônia Benedita da Silva; LOPES, Elessandra Laura Nogueira; VASCONCELOS, Omar Machado. Determinação do índice de velocidade de germinação e dos parâmetros genéticos de sementes de Bacaba em diferentes substratos na Amazônia Oriental**. Brazilian Journal of Development**. v. 7, n. 3, p. 25887 – 25898, 2020. Disponível em: admin,+BJD+340.pdf. Acesso em 28 ago. 2023.

[21]GONÇALVES, Viviane Evellyn Costa; de CARVALHO, Cleverson Agueiro; de BRITO, Rychaellen Silva; da SILVA, Márcio Chaves; ANDRADE, Reginaldo Almeida. **Influência de diferentes níveis de umidade para a germinação de cedro (*Cedrela fissilis*)**. *In*: Anais do 9º Congresso Florestal Brasileiro. p. 582 – 585, 2020. Disponível em: 5596f81d-cd02-45ee-b535-fb5c0ac4a0fb.pdf. Acesso em: 28 ago. 2023.

[22]MENEGAES, Janine Farias; NUNES, Ubirajara Russi; BALLÉ, Rogério Antônio, LUDWIG, Eduardo José; SANGOIO, Pablo Reno; SPEROTTO, Lucas. Germinação de Sementes de *Cartamus tinctorius* em diferentes substratos. **Acta Iguazu**. v. 6, n. 3, p. 22 – 30, 2017. Disponível em: https://saber.unioeste.br/index.php/actaiguazu/article/view/17705/11728. Acesso em: 28 ago. 2023.

[23]SILVA, Jailton Jaime das Neves; NAVROSKI, Maricio Carlos; DE AQUINO, Marina Gabriela Cardoso; DENEGA, Lucas; DA FONSECA, Pedro Herique Tavares; DE OLIVEIRA, Luciana Magda; PEREIRA, Mariane de Oliveira. Ciência Florestal. v. 33, n. 1, p. 21 – 25, 2023. Disponível em: scielo.br/j/cflo/a/CXZ46ZrRhYqkPwK9nDXb5YN/?format=pdf&lang=pt. Acesso em 08 set. 2023.

[24]DUTRA, Adriana Falcão; ARAÚJO, Maristela Machado; RORATO, Daniele Guariente, MIETH, Patrícia. Germinação de sementes e emergência de plântulas de *Luehea divaricata* Mart. et. Zuc. em diferentes substratos. **Ciência Florestal**. v. 26, n. 2, p. 411 – 418. Disponível em:

https://www.scielo.br/j/cflo/a/bcMxMcp9kyfN3bWqKJ4HRgg. Acesso em 28 ago. 2023.
[25]VIEIRA, Michel Rafael Soares; SILVESTRIM, Eneida Guerra; DE LIMA FILHO, Arlindo Almeida; LOPES, Aixa Braga; SILVESTRIM, Fernanda Guerra. Métodos de assepsia na multiplicação *in vitro* da bananeira ´Pacovan´(*Musa* spp.). **Research, Society and Development**. v. 10, n. 16, 9 p., 2021. Disponível em: View of Methods in the in vitro multiplication of 'Pacovan' banana (Musa spp.) (rsdjournal.org). Acesso em 08 set. 2023.
[26]LATTUADA, Daiane Silva; GUASSO, Leonardo Zucuni; DE OLIVEIRA, Kédima Melo; DA SILVA, Valmira Machado; DE SOUZA, Paulo Vitor Dutra. Tipos de explantes para estabelecimento *in vitro* para orégano e hortelã. **Pesquisa Agropecuária Gaúcha**. v. 25, n. 3, p. 91 – 103, 2019. Disponível em: Vista do Tipos de explantes para estabelecimento in vitro de orégano e hortelã (agricultura.rs.gov.br). Acesso em 08 set. 2023.
[27]SILVA, Ana Cláudia Lopes; MANFIO, Cândida Elisa; LEÃO, José Ricardo Avelino; DE CARVALHO, Josiane Celerino; GONÇALVES, José Francisco de Carvalho; RAPOSO, Andréa. Indução de calogênese em segmentos foliares de seringueira (*Hevea* spp.) na Amazônia Sul Ocidental. **Research, Society and Development**. v. 10, n. 9, p. 1 – 10, 2021.
[28]RONDON, Melaca Juliana Peixoto; DE SOUZA, Tacia Ivila; ARAÚJO, Danielly Aparecida Amorim; ARAÚJO, Ingrid Slusarski; FERNANDES, Daiane Ávila. Benefícios do carvão ativado no meio de cultura para os explantes de banana prata, nanica e terra. **Connectionline**. n. 21, p. 71 – 81, p. 2019. Disponível em: BENEFÍCIOS DO CARVÃO ATIVADO NO MEIO DE CULTURA PARA OS EXPLANTES DE BANANA PRATA, NANICA E TERRA. | Rondon | CONNECTION LINE - REVISTA ELETRÔNICA DO UNIVAG. Acesso em 08 set. 2023.
[29]OLIVEIRA, Nilma Portela; RIBEIRO, Santuza Aparecida Furtado; de Souza, Marília Maia. Controle de contaminação e oxidação no cultivo *in vitro* de oliveira (*Olea europaea* L.) cv. “Koroneiki”. **Research, Society and Development**. v. 10, n. 5, p. 1 – 10, 2021. Disponível em: View of Control of contamination and oxidation in the in vitro cultivation of olive tree (Olea Europaea L.) cv. "Koroneiki " (rsdjournal.org). Acesso em 08 set. 2023.
[30]MESSIAS, Thiago da Silva; REZENDE, Rodrigo Kelson Silva; da Silva, Luciely Faustino; NUNES, Geissiany Pereira; JESUS, Mailson Vieira. Estabelecimento de protocolo para descontaminação de explantes foliares de *Paullinia meliifolia*. Saber Científico. v. 8, n. 1, p. 9 – 14, 20219. Disponível em: Vista do ESTABELECIMENTO DE PROTOCOLO PARA DESCONTAMINAÇÃO DE EXPLANTES FOLIARES DE PAULLINIA MELIIFOLIA (saolucas.edu.br). Acesso em: 08 set. 2023.

RECyT
Year 27 / Nº 44 / 2025 /
DOI: https://doi.org/10.36995/j.recyt.2025.44.007

Mycoinsecticide capacity of five strains of *Beauveria bassiana* isolated from Misiones (Argentina)

Capacidad micoinsecticida de cinco cepas de *Beauveria bassiana* aisladas de Misiones (Argentina)

Marilyn R. V. Silva[1, 2, *]; Gustavo A. Bich[1, 2]; Marcela A. Sadañoski[1, 2]; María L. Castrillo[1, 2]; Pedro D. Zapata[1, 2]; Laura L. Villalba[1]; María I. Fonseca[1, 2]

1- Laboratorio de Biotecnología Molecular. Instituto de Biotecnología Misiones "Dra. María Ebe Reca" (INBIOMIS). Facultad de Ciencias Exactas, Químicas y Naturales. Universidad Nacional de Misiones. Posadas, Misiones, Argentina.
2- Consejo Nacional de Investigaciones Científicas y Técnicas (CONICET). Buenos Aires, Argentina.
* E-mail: marisr424@gmail.com

Received: 23/06/2025; Accepted: 03/10/2025

Abstract
This study aimed to isolate and identify entomopathogenic fungal strains of the genus *Beauveria* from agricultural soils and to evaluate their pathogenic potential as mycoinsecticides. Fungal identification was based on a multifaceted approach that included macro- and micromorphological characterization, scanning electron microscopy, and analysis of nuclear ribosomal DNA, ITS, and EF-1α sequences. Pathogenicity tests were conducted against the larval stage of *Tenebrio molitor*. Among all isolates examined, two fungal strains collected from yerba mate plantations in southern Misiones were identified as *Beauveria bassiana* (HEP 32 and HEP MSO2). Larval mortality of *T. molitor* was significantly affected, particularly by the *B. bassiana* HEP MSO2 strain, suggesting its potential as an effective mycoinsecticide for integration into crop pest management strategies.

Keywords: Entomopathogenic fungus, Biocontrol, Pathogenicity.

Resumen
Este estudio tuvo como objetivo aislar e identificar cepas de hongos entomopatógenos del género *Beauveria* a partir de suelos agrícolas y evaluar su capacidad patogénica. La identificación fúngica se basó en un enfoque multifacético que incluyó el reconocimiento macro- y micromorfológico, microscopía electrónica de barrido y análisis del ADN ribosomal nuclear, secuencias ITS y EF-1α. Las pruebas de patogenicidad se realizaron sobre larvas de *Tenebrio molitor.* De todos los aislamientos estudiados, dos cepas fúngicas recolectadas en plantaciones de yerba mate del sur de Misiones fueron identificadas como *Beauveria bassiana* (HEP 32 y HEP MSO2). La mortalidad de las larvas de *T. molitor* se vio significativamente afectada, principalmente por la cepa HEP MSO2, lo que sugiere su potencial como micoinsecticida eficaz para integrar en estrategias de manejo de plagas en cultivos.

Palabras clave: Hongos entomopatógenos, Biocontrol, Patogenicidad.

INTRODUCTION

Insect pest management continues to pose a persistent global challenge (1). Due to their ongoing interactions, fungi and insects have co-evolved over thousands of years. These multifaceted relationships include antagonistic interactions, which render fungi valuable agents for biological control (2). A variety of practices enhance crop management, reinforce soil stability, and support environmentally sound actions, all of which are essential components of Integrated Pest Management (IPM) (3). In this context, entomopathogenic fungi (EPF) are key biological control agents against numerous insect pests, particularly those of significant sanitary relevance when incorporated into integrated management strategies (4).

Unlike other entomopathogens that require ingestion to infect, EPF typically penetrate the insect cuticle actively, irrespective of the insect's feeding behavior (5). The most prominent genera of entomopathogens include *Beauveria*, *Metarhizium*, and *Purpureocillium*, all belonging to the phylum Ascomycota (Order: Hypocreales) (6). These fungi are ubiquitous, saprotrophic filamentous organisms frequently isolated from soil, vegetation, decaying matter, or parasitized arthropods. They exhibit infective and lethal properties against insects across diverse geographic, climatic, and agroecological regions, offering promising prospects for the development of integrated management techniques that provide long-term solutions (7).

Mycobiocontrol, or the use of mycoinsecticides, plays a crucial role in environmental protection and food safety. It represents a valuable tool within IPM by reducing dependence on chemical insecticides. However, the current pathogenic

mechanisms of entomopathogens are relatively slow and require further refinement to enhance their efficacy (8). One strategy to address this limitation involves isolating and selecting fungi from environments that have remained largely undisturbed by chemical agents over extended periods, favoring traits such as rapid growth and heightened virulence.

Biotechnology contributes significantly to understanding the pathogenicity and mechanisms of action of EPF during pest control. Moreover, ecological insights into EPF are essential for designing strategies that enhance their effectiveness in field applications, including determining appropriate bioinsecticide dosages, identifying optimal application sites and timing, and recognizing the onset of insect attacks on crops (9). The vast microbial diversity present in natural ecosystems remains largely untapped and could serve as a valuable reservoir for future EPF candidates (10).

Beauveria bassiana is one of the principal EPF species. It causes white muscardine disease and can infect and parasitize insects until death, making it a highly promising bioinsecticide (11).

The objective of this study was to isolate and identify *Beauveria* strains from agricultural soils in Misiones and to evaluate their pathogenic potential as potent mycoinsecticides.

MATERIALS AND METHODS

Soil sampling

A total of 55 soil samples were collected from eleven Ilex paraguariensis (yerba mate) plantations located in the central and southern regions of Misiones province (Argentina) (Table 1). The area is characterized by a humid subtropical climate, with average annual maximum and minimum temperatures of 21 °C and 10 °C, respectively, rainfall of approximately 79.38 mm, and relative humidity around 77.38%. Soil samples (500 g) were taken at depths of 5–10 cm adjacent to yerba mate plants and 10–15 cm from the surface, using a previously disinfected shovel. Five randomly selected locations were sampled per site. Samples were stored in sterile polyethylene bags and transported to a laboratory in Posadas, Misiones, Argentina, for immediate processing.

Table 1: Sampling sites in yerba mate plantations in Misiones province (Argentina).

N°	Location	Geolocation	Type of management	Date
1	**Garupá**	27°27'10.4"S 55°50'17.0"W	conventional	15/10/2018
2	**Candelaria**	27°28'12.9"S 55°45'56.9"W	organic	2/12/2018
3	**Santo Pipó**	27°09'44.2"S 55°20'12.6"W	organic	7/11/2018
4	**Montecarlo**	26°53'26.0"S 54°76'23.2"W	organic	5/11/2018
5	**Aristóbulo del Valle**	27°02'09.8"S 54°47'26.3"W	conventional	24/7/2018
6	**Colonia Acaraguá**	27°29'24"S 54°50'13"W	organic	12/1/2019
7	**Posadas/El Porvenir I**	27°31'41.8"S 55°58'25.2"W	conventional	2/2/2019
8	**Posadas/El Porvenir II**	27°34'15.5"S 55°50'46.2"W	conventional	2/2/2019
9	**Parada Leis**	27°34'15.5"S 55°50'46.2"W	conventional	15/2/2019
10	**San José I**	27°45'27.9"S 55°46'27.9"W	conventional	15/2/2019
11	**San José** II	27°35'05.2"S 55°50'30.8"W	organic	15/2/2019

Isolation from soil: Soil dilution plating

Fungal isolation was performed using the dilution plate technique. One gram of each soil sample was suspended in 9 mL of distilled water and vortexed vigorously for 5 minutes. Subsequently, 0.1 mL of the suspension was plated at the center of a Petri dish and spread using a sterile glass spreader. Samples were cultured on a semi-selective medium for *Beauveria*, as described by Doberski and Tribe (12), with modifications (13): glucose 40 g/L, peptone 10 g/L, thiabendazole 0.004 g/L, chloramphenicol 0.5 g/L, crystal violet 0.01 g/L, agar 15 g/L, distilled water 1 L, pH 6. The medium was supplemented with 0.2 g/L ampicillin. Plates were incubated at 28 °C for 7–10 days. Colonies with expected morphology were subcultured onto Potato Dextrose Agar (PDA) plates. Axenic strains were identified based

on cultural and morphological characteristics described in the literature and stored on PDA at 4 °C.

Isolation of Beauveria species from insect cadavers

Collected insects were placed in sterile conical flasks and kept at room temperature for transport to the laboratory. Specimens were disinfected with 70% ethanol, and conidia from the surface of infected insects were transferred to the semi-selective medium for *Beauveria* (see section 1.2). Cultures were incubated in 9-cm Petri dishes at 28 ± 2 °C in darkness for 10 days. Pure cultures were then transferred to PDA, maintained at 28 °C, and subcultured every 2–3 weeks. Identification of the isolate obtained from the insect cadaver was performed using microscopy and molecular techniques (PCR and sequencing). Conidial suspensions of this isolate were used in bioassays.

Morphological and microscopic identification

Morphological identification of the isolates was based on macroscopic observation of colony characteristics (color, shape, and size) and microscopic examination of mycelium and reproductive structures. Identification keys by Samson et al. (14), Alves (15), and Humber (16) were used to classify the isolates at the genus level.

Microphotographs of the fungal surface were obtained using Scanning Electron Microscopy (SEM). Mycelium was fixed in a solution of formaldehyde, ethanol, and acetic acid (10:50:5). After critical point drying with CO_2 and gold coating, samples were examined using a JEOL 5800LV scanning electron microscope.

Molecular identification

Genomic DNA was extracted from 7-day-old axenic cultures grown on PDA supplemented with chloramphenicol, following the protocol by Fonseca et al. (17). The ITS and EF-1α regions were amplified via PCR under standard conditions and thermal cycling parameters (Table 2). Amplicons were sequenced bidirectionally by Macrogen (Korea), and consensus sequences were assembled using Chromas and BioEdit Sequence Alignment Editor v7.0.5. Alignments were performed and concatenated using MEGA v7.0, and phylogenetic analysis was conducted using the Neighbor Joining method with the Tamura model and 1000 bootstrap replicates. *Isaria* sp. sequences were used as outgroups. Final sequences were deposited in GenBank, and clades with <50% bootstrap support were collapsed in the consensus tree.

Table 2: Primers used for molecular identification of entomopathogenic fungi

Primer name	Oligonucleotide sequence 5′- 3′	Amplified región	Reference
ITS-1	TCC GTA GGT GAA CCT GCG G	ITS1-5.8 S-ITS2	(18)
ITS-4	TCCTCCGCTTATT GATATGC	ITS1-5.8 S-ITS2	(18)
EF1-728F	CATCGAGAAGTT CGAGAAGG	EF1-α	(19)
Tef1-R5	CCTTGGAGATAC CAGC	EF1-α	(19)

Viability tests

Spore viability was assessed prior to each pathogenicity test on *T. molitor* larvae. For each trial, 100 µL of conidial suspension was spread on 60-mm PDA plates using a sterile bent glass rod (Drigalski spatula). Plates were incubated in darkness at 28 °C for 24 hours. Spore viability was evaluated under a compound light microscope (20). One hundred conidia were randomly selected per plate (21) and considered viable if a germ tube at least half the conidial diameter was observed.

Pathogenicity tests

The *B. bassiana* strains under study were used. *T. molitor* insects (Piantieri Insect Farm, Argentina) were reared weekly in plastic trays containing approximately 200 individuals (eggs, larvae, pupae, and adults). Insects were maintained in a germination chamber at 25 ± 2 °C, 65% humidity, and a 14:10 h light-dark photoperiod. Larvae measuring 18–22 mm were selected under laminar flow conditions and placed in sterile cylindrical plastic containers with four lateral perforations and screw-on lids. Containers were refrigerated at 4 °C for 24 hours to reduce larval metabolism and prevent molting during the bioassay. Forty-eight larvae were selected per treatment, with fifteen treatments performed in triplicate. Larvae were transferred to sterile plastic flasks containing sterile carrot slices and inoculated with *B. bassiana* at concentrations of 1×10^5, 1×10^6, and 1×10^7 conidia/mL using an airbrush connected to an air compressor at a distance of 10 cm. Control groups were inoculated with distilled water. Flasks were kept in a climate chamber at 25 °C, with a 14:10 h photoperiod and 65% humidity, and monitored daily for 14 days. Dead larvae were recorded, and mortality percentages for each isolate were calculated. Deceased larvae were placed on PDA plates supplemented with chloramphenicol (10 mg/L) at 28 °C, and fungal development was monitored daily.

Larvae disinfection protocol

To eliminate external microbiota, *T. molitor* larvae were disinfected following a modified protocol by Cummings et al., involving sequential washes with ethanol, bleach, and sterile water. Disinfection was verified by culturing the final rinse and

performing an imprint on PDA. Larvae were dried on sterile paper and incubated at 28 °C in darkness to confirm mycosis.

Statistical analysis

Data were analyzed using Statgraphics Centurion software (StatPoint, Inc., version 15.2.05). Analysis of variance (ANOVA) followed by Fisher's Least Significant Difference (LSD) post-hoc test at $p<0.05$ was used to determine the significance of fungal strain tolerance to the three fungicide concentrations.

The time required to cause 50% and 90% mortality (T_{50} and T_{90}) of insect larvae in laboratory conditions was determined for the most pathogenic entomopathogenic fungus using simple regression analysis in Statgraphics. The equation used was $Y = a + b \cdot X$.

RESULTS

Eleven samples were collected from yerba mate plantations in Misiones province between 2018 and 2019. Approximately 72% of the fungal isolates were identified at the genus level. Of the total fungi recovered, 63.4% were non-entomopathogenic, and only 9% were entomopathogenic (Figure 1).

Among the non-entomopathogenic fungi, the most frequently identified genera were *Aspergillus* (17.5%), *Fusarium* (10.3%), *Mucor* (6.3%), *Penicillium* (19%), *Rhizopus* (3.2%), and *Trichoderma* (7.1%). The entomopathogenic fungi identified included *Clonostachys* (1.6%), *Purpureocillium* (5.6%), and *Beauveria* (1.6%) (Figure 1). The isolates of interest for this study, belonging to the genus *Beauveria* (HEP MSO2 and HEP 32), were collected from yerba mate plantations located in Candelaria and Colonia Acaraguá, in the southwest and southeast regions of Misiones province, Argentina, respectively.

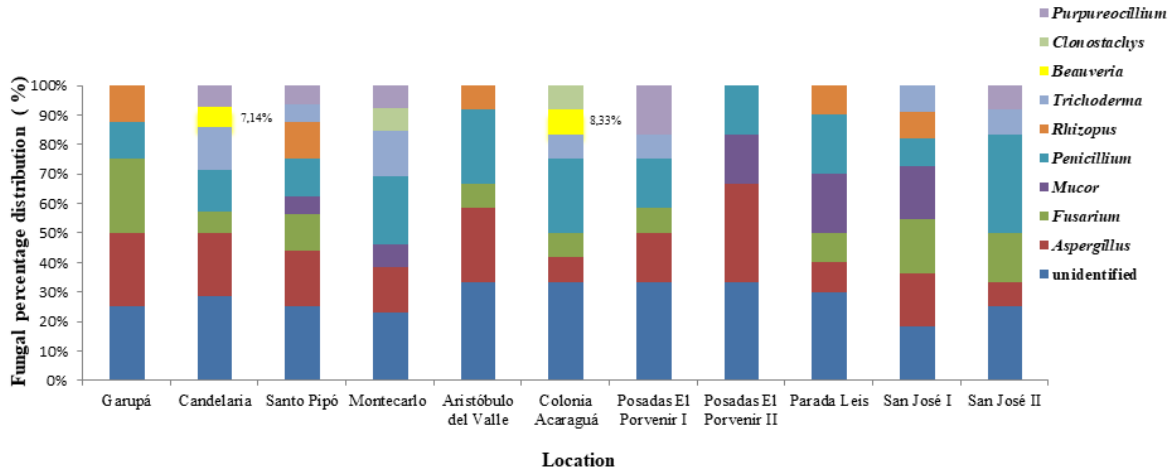

Figure 1. Percentage distribution of the fungal community at the genus level in soil samples and leaf litter from yerba mate plantations located in Misiones province.

Morphological identification of entomopathogenic fungi

Among the samples collected from yerba mate plantation soils, only the HEP MSO2 strain exhibited the typical characteristics of the *Beauveria* genus. HEP MSO2 was isolated from the Colonia Acaraguá plantation, an organic cultivation site (Figure 2a). This isolate displayed white to cream-colored colonies with irregular edges and a powdery texture, which are macroscopic traits characteristic of the *Beauveria* genus (Figure 2b). Microscopic observations revealed reproductive structures and conidia with morphology, size, and coloration consistent with the species *B. bassiana*. The conidiogenous cells measured 5.5 to 8.8 µm (SD 0.5 to 1.1 µm) × 2.0 to 2.7 µm (SD 0.1 to 0.8 µm), featuring a broad base and a tapered apex from which multiple conidia emerged in chains along a zigzag-shaped rachis. The conidia were hyaline and smooth, with a globose to subglobose structure. Their diameters ranged from 1.7 to 2.3 µm (SD 0.5 to 0.6 µm) (Figure 2c). Under scanning electron microscopy, hyphae with diameters of 1.12 to 1.41 µm and spherical conidia measuring 1.32 to 1.71 µm were observed on conidiophores with zigzag phialides (Figure 2d).

The HEP 32 isolate was obtained from parasitized insects of the genus *Brassolis* (Figure 2e), extracted from the soil surface and leaf litter of an organic yerba mate plantation in Candelaria (Table 1), surrounded by pine trees (*Pinus* spp.). This isolate exhibited macroscopic characteristics similar to those of HEP MSO2 (Figure 2f), although its colonies were slightly more flattened. Under electron microscopy, hyphae with

diameters ranging from 1.25 to 1.55 µm and spherical conidia measuring 1.1 to 1.2 µm were observed on conidiophores with zigzag phialides (Figure 2h). Both isolates produced and exuded structures known as synnemata as they aged.

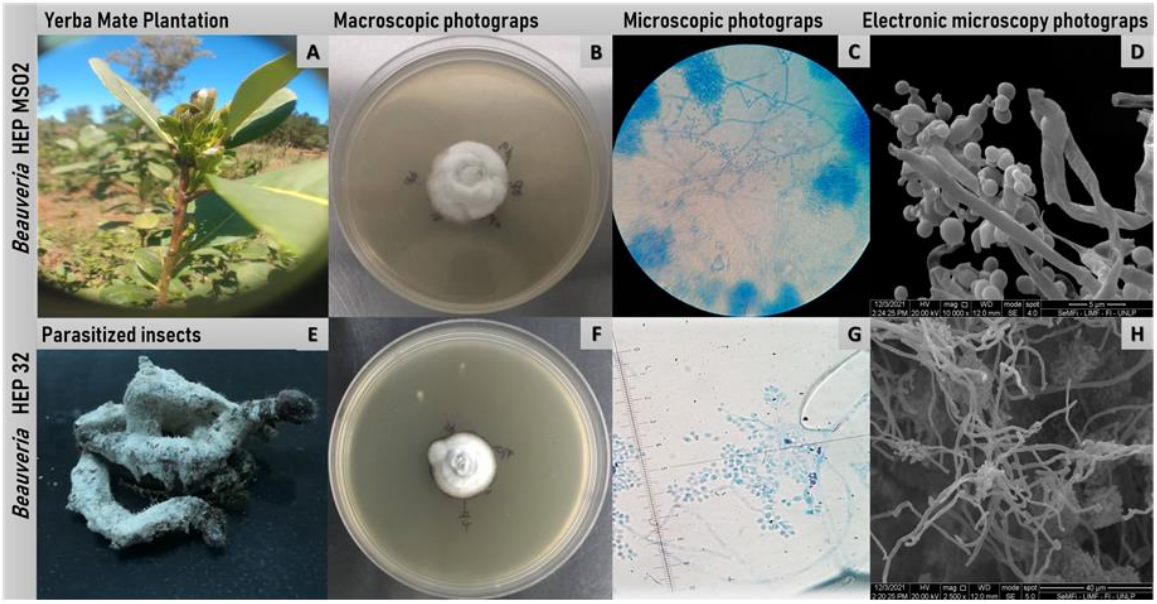

Figure 2. Fungal strains isolated from yerba mate plantation soil and parasitized insects. A) Fungi extracted from soil sample. B and C) Macroscopic and microscopic images of *B. bassiana* strain HEP MSO2. Photographs of colonies grown on PDA medium (Scale bar = 1 cm). Microphotographs stained with lactophenol cotton blue. E) Sample of parasitized insect (Lepidoptera). F and G) Macroscopic and microscopic images of *B. bassiana* strain HEP 32. D and H) Scanning electron microscopy images.

Molecular identification of entomopathogenic fungi

PCR amplification of the ITS and EF1-α regions from the DNA of the isolated entomopathogenic fungi yielded fragments of approximately 555 bp and 986 bp, respectively. Sequence identity analysis of the strains HEP MSO2 and HEP 32, which had been morphologically identified as *B. bassiana*, confirmed their taxonomic classification. The identity indices were 99.65% and 100% for the ITS regions (MK049987.1; MN428795.1), and 99.63% and 100% for the EF1-α regions (MK550625.1; KJ500423.1).

Phylogenetic tree analysis revealed that the fungal strains HEP MSO2 and HEP 32 clustered with other *B. bassiana* strains and their reference sequence (NR_111594), with bootstrap support values exceeding 99% (Figure 3).

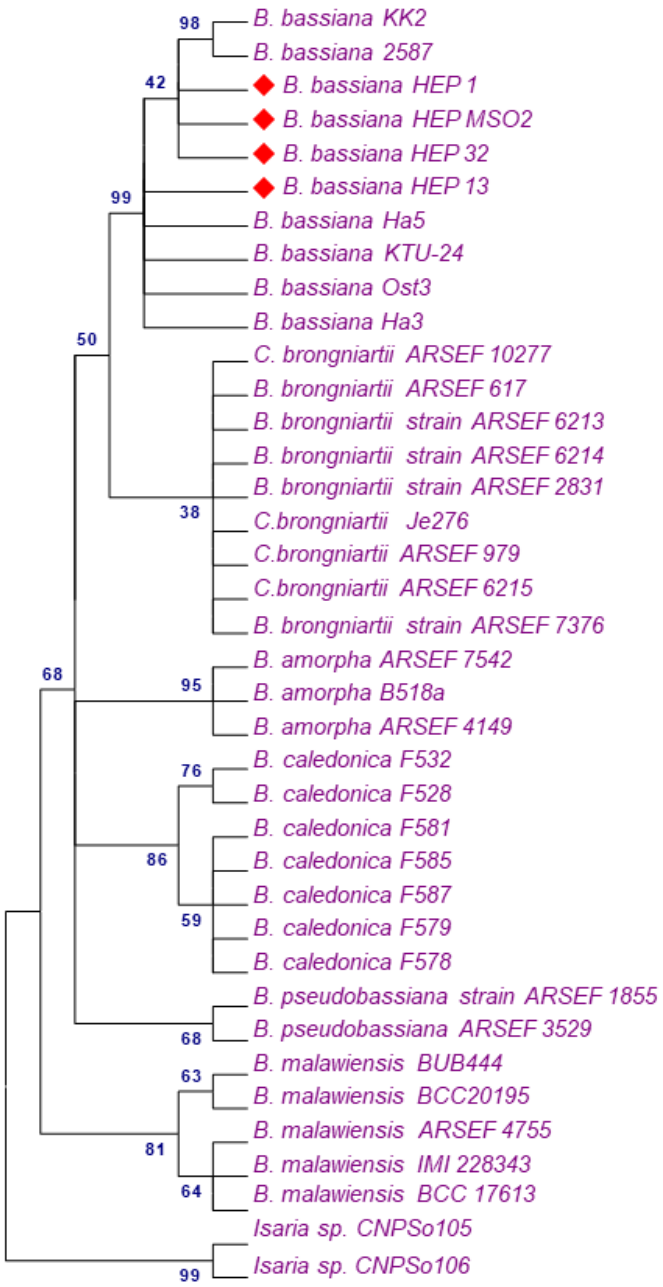

Figure 3. Concatenated phylogenetic tree constructed using the Neighbor Joining method, showing the relationship between the entomopathogenic fungal strains obtained in Misiones province and related species deposited in the GenBank–NCBI database. The sequences used correspond to the ITS and EF1α regions. The tree was built using MEGA 7.0 software. Bootstrap values from 1,000 replicates are indicated next to the branches. *Isaria* sp. sequences were designated as the outgroup to root the tree.

Pathogenicity tests

Spore viability was assessed prior to conducting pathogenicity tests on *T. molitor* larvae, with germination rates exceeding 90% in all trials.

Laboratory pathogenicity assays demonstrated that all five *B. bassiana* strains isolated in Misiones exhibited pathogenic activity, causing mortality in *T. molitor* larvae. Disease symptoms in the larval population varied depending on the fungal strain and conidial concentration. Initial symptoms appeared 48 hours after inoculation, with a marked reduction in insect activity leading to complete rigidity. In some cases, fungal structures emerged from the insect bodies 96 hours post-mortem, a characteristic confirming mortality due to fungal infection (Figure 4).

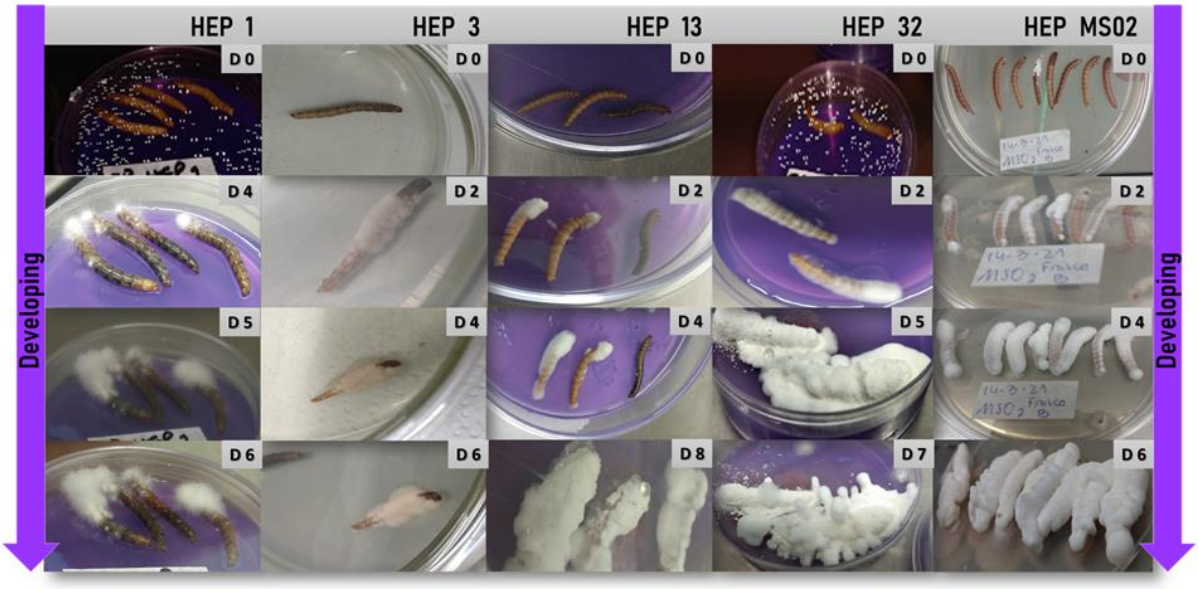

Figure 4. Images of deceased insects and fungal development from different *B. bassiana* strains at a concentration of 10^7 conidia/mL. Day 0 corresponds to the day of insect death. For HEP 1, death occurred on day 3 of the trial; for HEP 3, on day 4; for HEP 13, on day 4; for HEP 32, on day 4; and for HEP MSO2, on day 3.

Larvae disinfection protocol

The disinfection protocol applied at the conclusion of the pathogenicity tests with the five HEP strains successfully eliminated surface microbiota from the *T. molitor* larvae and confirmed that death was caused by pre-mortem mycosis. This procedure validated both the effective disinfection of the larvae and their mortality due to fungal infection. The fungal morphology observed in the insect cadavers was consistent with the colonial growth patterns on PDA medium (Figure 2e, f). Notably, no mycelial growth was detected on the plates used for the insect imprint tests.

Statistical analysis

The mortality rate was dependent on the concentration of *B. bassiana* (Table 3, Figure 5). At a concentration of 10^5 conidia/mL, the strains HEP 3, HEP 13, and HEP MSO2 induced the highest mortality rates in *T. molitor* larvae from the seventh day onward ($p < 0.00$) (Figure 5a). At a concentration of 10^6 conidia/mL, the isolates *B. bassiana* HEP 32 and HEP MSO2 exhibited the greatest larval mortality by the end of the trial ($p < 0.00$) (Figure 5b).

At the highest concentration tested (10^7 conidia/mL), HEP MSO2 demonstrated the most pronounced pathogenic effect, with mortality observed from day 6 onward ($p < 0.00$) (Figure 5c). All *B. bassiana* isolates at this concentration caused larval mortality exceeding 65% after eight days of treatment. Notably, HEP MSO2 achieved 100% mortality, distinguishing itself as the most virulent strain among those evaluated.

A simple regression analysis was employed to determine the time required to reach 50% and 90% mortality (T_{50} and T_{90}) in larvae exposed to the HEP MSO2 strain. The calculated values were 6.73 days for T_{50} and 14 days for T_{90}, respectively.

Table 3. Fisher's LSD Method, 95.0% Confidence Level

Treatment	Average LS	Sigma LS	Homogeneous Groups				
Control	0	1.12933	X				
HEP 1	29.8245	1.45796		X			
HEP 3	33.3961	1.45796			XX		
HEP 32	35.5135	1.45796				XX	
HEP 13	38.8192	1.45796				X	
HEP MSO2	56.4121	1.45796					X

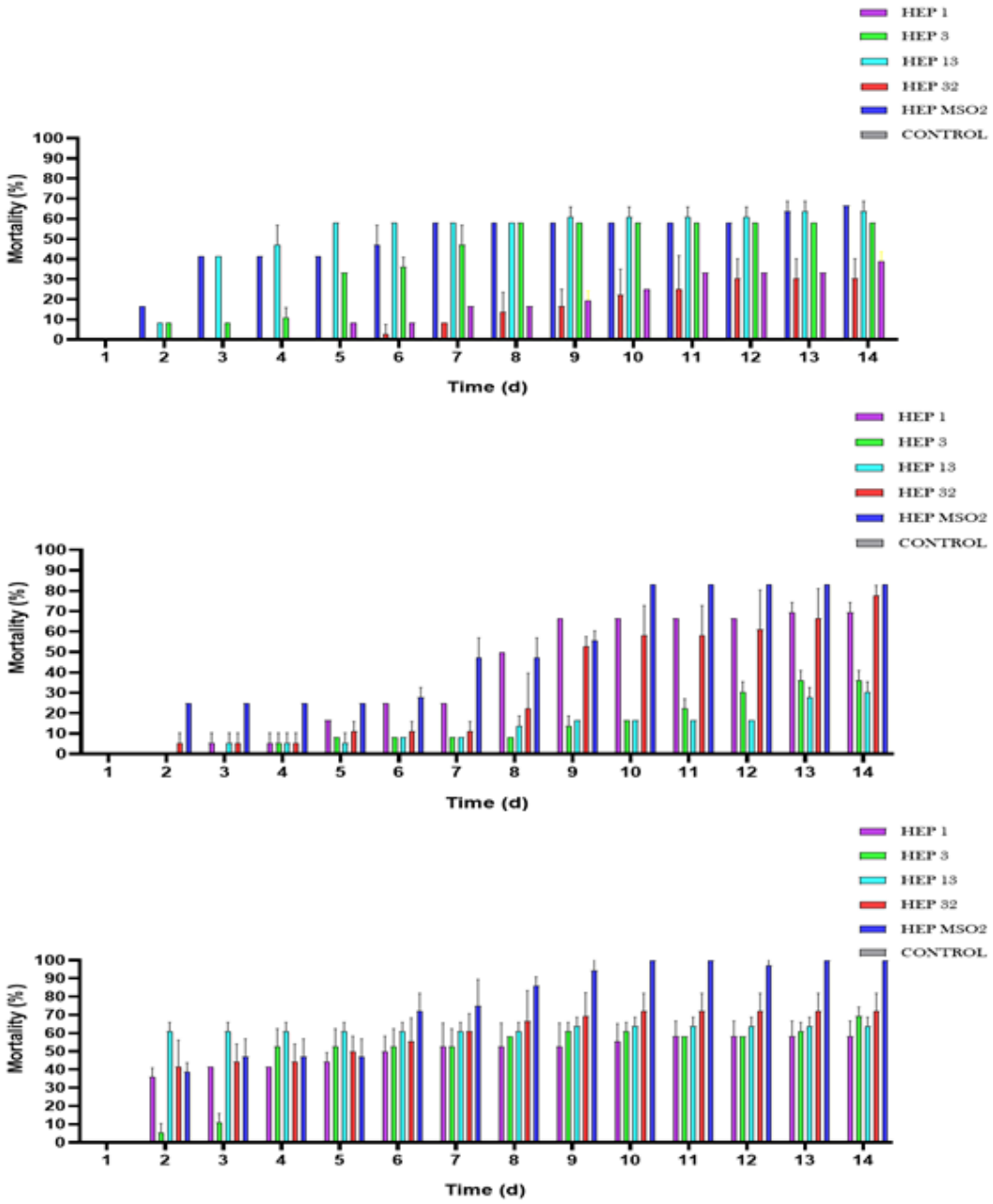

Figure 5. Mortality versus Lethal Time of *B. bassiana* Strains on *T. molitor* Larvae at Different Concentrations. A) 10^5 conidia/mL concentration B) 10^6 conidia/mL concentration C) 10^7 conidia/mL concentration

DISCUSSION

The growing global demand for food has intensified crop production (Lecuona & Posadas, 2019), positioning Argentina among the leading agricultural producers, with Misiones as the foremost global producer of Ilex paraguariensis (22). However, conventional pest control methods in yerba mate plantations, which rely heavily on agrochemicals, have resulted in detrimental effects such as soil degradation and increased pest susceptibility (23), thereby prompting the pursuit of sustainable alternatives.

Entomopathogenic fungi (EPF), particularly those isolated from native environments, offer promising potential as biological control agents due to their ability to infect insects via cuticular penetration (24; 25). In the present study, two *B. bassiana* strains (HEP MS02 and HEP 32) were isolated from organic yerba mate plantations in Misiones. Their origin in organically managed systems aligns with previous findings that report greater EPF diversity in soils devoid of chemical inputs (26; 27).

Although *Metarhizium* spp. are generally more frequently recovered from soil (28), *Beauveria* was more prevalent in the samples analyzed. Its presence was restricted to organic soils, corroborating studies that associate fungal

diversity with practices such as cover cropping and minimal soil disturbance (29; 30). Routine cleaning in yerba mate plantations has also been identified as a factor contributing to the loss of soil biodiversity (31). Environmental conditions further influence EPF survival. *B. bassiana* thrives optimally between 23–26 °C and can tolerate temperatures up to 45 °C (32), although conidial persistence is affected by temperature, humidity, and soil composition (33). Its survival is enhanced in temperate regions with continuous host availability (34).

The identification of both strains was supported by morphological traits consistent with previous descriptions (14; 27; 35), including synnemata formation, and was confirmed through ITS and EF1-α sequencing. Phylogenetic analyses placed HEP MS02 and HEP 32 within well-supported clades of *B. bassiana* (35; 36).

Pathogenicity assays conducted on *T. molitor* larvae demonstrated that all strains induced mortality, with HEP MS02 exhibiting the highest virulence (T_{50} = 6.7 days; T_{90} = 14 days). Conidial viability across all strains exceeded 90%, a critical parameter for field efficacy (37). Furthermore, the disinfection protocol (38; 39) ensured that observed mortality resulted from pre-mortem mycosis, thereby validating fungal pathogenicity rather than saprophytic colonization. This step is essential for confirming the onset of infection, as EPF must penetrate the insect cuticle to initiate disease (40).

This study underscores the importance of isolating native EPF strains adapted to local environmental conditions. In particular, *B. bassiana* HEP MS02 emerges as a promising candidate for incorporation into integrated pest management (IPM) strategies in yerba mate cultivation, offering a sustainable alternative to chemical pesticides and contributing to agroecological resilience.

ACKNOWLEDGMENTS

The authors express their gratitude to the National Scientific and Technical Research Council (CONICET, Argentina) for funding this research.

REFERENCES

1. Quandahor, P., L. Kim, M. Kim, K. Lee, F. Kusi, and I. H. Jeong. 2024. Effects of Agricultural Pesticides on Decline in Insect Species and Individual Numbers. Environments 11(8): 182.

2. Joop, G. and A. Vilcinskas. 2016. Coevolution of parasitic fungi and insect hosts. Zoology 119(4): 350–358.

3. Ohashi, D. V., O. De Coll, M. Mayol, N. Munaretto, R. Escalada, H. Fontana et al. 2018. Propuesta de Manejo Integrado de Plagas para el cultivo de yerba mate. Manejo integrado del cultivo. E.E.A Cerro Azul — INTA. Miscelánea N° 75/2018.

4. Gebremariama, A., Y. Chekol, and A. Fassil. 2021. Phenotypic, molecular, and virulence characterization of entomopathogenic fungi, *Beauveria bassiana* (Balsam) Vuillemin, and *Metarhizium anisopliae* (Metschn.) Sorokin from soil samples of Ethiopia for the development of mycoinsecticide. Heliyon 7. e070912.

5. Sanjuan, T., J. Tabima, S. Restrepo, T. Laessoe, J. W. Spatafora, and A. E. Franco-Molano. 2014. Entomopathogens of Amazonian stick insects and locusts are members of the *Beauveria* species complex (*Cordyceps* sensu stricto). Mycologia 106(2): 260–275.

6. Swathy, K., M. K. Parmar, and P. Vivekanandhan. 2024. Biocontrol efficacy of entomopathogenic fungi *Beauveria bassiana* conidia against agricultural insect pests. Environmental Quality Management 34(1), e22174.

7. Karabörklü, S. 2022. Biocontrol potential of *Beauveria bassiana* and *Metarhizium anisopliae* isolates from Turkey against *Hyphantria cunea* (Drury) (Lepidoptera: Arctiidae) larvae under laboratory and field conditions. Bioscience Journal 38, e38015.

8. Samal, I., T. K. Bhoi, V. Vyas, P. K. Majhi, D. K. Mahanta, J. Komal et al. 2024. Resistance to fungicides in entomopathogenic fungi: Underlying mechanisms, consequences, and opportunities for progress. Tropical Plant Pathology 49(1), 5-17.

9. Muneli, I. F. 2023. Utilización del hongo entomopatógeno *Beauveria bassiana* en tratamientos de semillas de maíz. Tesis Ingeniería Agronómica. Escuela de Ciencias Agrarias, Naturales y Ambientales. Universidad Nacional del noroeste de la Provincia de Buenos Aires, Pergamino. Pp 37.

10. González-Herrera, and M. Montero-Astúaac. 2021. Identification and phylogenetic analysis of a collection of *Beauveria* spp. Isolates from Central America and Puerto Rico. Journal of Invertebrate Pathology 184: 107642.

11. Chaudhary, R., A. Nawaz, Z. Khattak, M. A. Butt, M. Fouillaud, L. Dufossé, L. et al. 2024. Microbial bio-control agents: a comprehensive analysis on sustainable pest management in agriculture. Journal of agriculture and food research, 101421.

12. Doberski, J.W., and H. T. Tribe. 1980. Isolation of entomogenous fungi elm bark and soil with reference to the ecology of *Beauveria bassiana* and *Metarhizium anisopliae.* Transactions of the British Mycological Society 74: 95-100.

13. González, C. E., M. L. A. Encina, G. A. Bich, and M. L. Castrillo. 2021. Aislamiento, identificación y conservación de cepas entomopatogénicas del género *Beauveria* de yerbales orgánicos del Paraguay. Revista

Impacto, 1(1), 1-11.
14. Samson, R.A., H. C. Evans, and J. P. Latgé. 1988. Atlas of entomopathogenic fungi. Springer Verlag Berlin: Heidelberg.
15. Alves, S. B. 1998. Fungos entomopatogênicos. Controle microbiano de insetos. Biblioteca de Ciências Agrárias Luiz de Queiroz 4(11): 289-370.
16. Humber, R. 2012. Identification of entomopathogenic fungi. In: Lacey L, Editor. Manual of Techniques in Invertebrate Pathology. 2nd Edition. Academic Press.
17. Fonseca, M. I., Zapata, P. D., Villalba, L. L., & Castrillo, M. L. (2011). Genetic diversity of Trichoderma isolates from Misiones, Argentina. Revista Argentina de Microbiología, 43(3), 176–185.
18. White TJ, Bruns T, LeeS, Taylor. 1990. Amplification and direct sequencing of fungal ribosomal RNA genes for phylogenetics. In: Innis MA, Gelfand DH, Sninsky .IJ, White TJ, eds. PCR protocols: a guide to methods and applications. San Diego: Academic Press. P 315-322.
19. Samuels, G.J. and A. Ismaiel. 2011. Hypocrea peltata: a mycological Dr Jekyll and Mr Hyde. Mycologia, 103 (2011), pp. 616-630.
20. Ezzati-Tabrizi, R., R. Talaei-Hassanloui, and H. R. Pourian. 2009. Effect of formulating of *Beauveria bassiana* conidia on their viability and pathogenicity to the onion thrips, Thrips tabaci Lind. (Thysanoptera: Thripidae). Journal of Plant Protection Research 49: 93-103.
21. Sun, J., J. R. Fuxa and G. Henderson. 2003. Effects of virulence, sporulation, and temperature on *Metarhizium anisopliae* and *Beauveria bassiana* laboratory transmission in Coptotermes formosanus. Journal of Invertebrate Pathology 84: 38–46.
22. Dohrenwend, A. S. 2019. Socio-Environmental Impacts of Argentine Yerba Mate Cultivation: “El Problema es el Precio Bajo”. URI http://hdl.handle.net/1808/3008423 Barcenilla
23. Bich, G.A., M. L. Castrillo, F. L. Kramer, L. L. Villalba, and P. D. Zapata. 2021. Morphological and Molecular Identification of Entomopathogenic Fungi from Agricultural and Forestry Crops. Floresta Ambiente 28(2).
24. Feng, M., T. J. Poprawski, and G. G. Khachatourians. 1994. Production, formulation, and application of the entomopathogenic fungus. *Beauveria bassiana* for insect control: current status. Biocontrol Science and Technology 4, 3–34.
25. de Faria, M. R. and S. P. Wraight. 2007. Mycoinsecticides and Mycoacaricides: A comprehensive list with worldwide coverage and international classification of formulation types. Biological Control 43, 237–256.
26. Klingen, I., & S. Haukeland. 2006. The soil as a reservoir for natural enemies of pest insects and mites with emphasis on fungi and nematodes. In An ecological and societal approach to biological control (pp. 145-211). Dordrecht: Springer Netherlands.
27. Schapovaloff, M. E., L. F. Alves, U. M. Angeli and C. C. López-Lastra. 2015. Ocurrencia natural de hongos entomopatógenos en suelos cultivados con yerba mate *(Ilex paraguariensis* St. Hil.) en Misiones, Argentina. Revista Argentina de Microbiología 47(2): 138-142.
28. Bidochka, M. J., J. E. Kasperski, & G. A. Wild. 1998. Occurrence of the entomopathogenic fungi Metarhizium anisopliae and Beauveria bassiana in soils from temperate and near-northern habitats. Canadian Journal of Botany, 76(7), 1198-1204.
29. Gliessman, S. R., V. E. Méndez and V. M. Izzo. 2022. Agroecology: Leading the Transformation to a Just and Sustainable Food System (4th Ed.). New York, USA: CRC Press, Taylor & Francis.
30. Oliveira, I., J. A. Pereira, E. Quesada-Moraga, T. Lino-Neto, A. Bento & P. Baptista. 2013. Effect of soil tillage on natural occurrence of fungal entomopathogens associated to Prays oleae Bern. Scientia horticulturae, 159, 190-196.
31. Wagner, K. A., V. Pauletti, L. B. Gheno & K. M. Cavalieri-Polizeli. 2025. Growth of Yerba Mate Plants (Ilex paraguariensis A. St.-Hil.) Under Soil Compaction. Journal of Soil Science and Plant Nutrition, 1-17.
32. Quesada-Moraga, E., González-Mas, N., Yousef-Yousef, M., Garrido-Jurado, I., & Fernández-Bravo, M. (2024). Key role of environmental competence in successful use of entomopathogenic fungi in microbial pest control. Journal of Pest Science, 97(1), 1-15.
33. Lingg, A. J., & Donaldson, M. D. (1981). Biotic and abiotic factors affecting stability of Beauveria bassiana conidia in soil. Journal of Invertebrate Pathology, 38(2), 191-200.34. Vänninen
34. Ghorui, M., Chowdhury, S., Burla, S. (2024). The science behind entomopathogenic fungi: Mechanisms and applications. In Entomopathogenic Fungi: Prospects and Challenges Singapore: Springer Nature Singapore. P 3-35.
35. Barbercheck, M. E. (1992). Effect of soil physical factors on biological control agents of soil insect pests. Florida Entomologist, 539-548.
36. Solano-González, S., Castro-Vásquez, R., & Molina-Bravo, R. (2023). Genomic characterization and functional description of *Beauveria bassiana* isolates from Latin America. Journal of Fungi, 9(7), 711.
37. Liu, H., M. Skinner, M. Brownbridge and B. L. Parker. 2003. Characterization of *Beauveria bassiana* and *Metarhizium anisopliae* isolates for management of tarnished plant bug, Lygus lineolaris (Hemiptera: Miridae). Journal of Invertebrate Pathology 82(3), 139-147.

38. Porras, E. M. 2015. Evaluación de la actividad entomopatógena de diversos aislamientos de hongos y cepas de *Bacillus thuringiensis* para el potencial desarrollo de un bioformulado contra las hormigas cortadoras de hojas de la especie *Atta cephalotes*. Tesis de Ingeniería en Biotecnología. Universidad de Costa Rica. Pp 168.
39. Motholo, L. F. (2019). Endophytic establishment of Beauveria bassiana in wheat (Triticum aestivum) and its impact on Diuraphis noxia (Doctoral dissertation, North-West University (South Africa). Potchefstroom Campus).
40. Pereira, A. S. 2014. Fungos associados e ação do imunossupressor ciclosporina A sobre formigas cortadeiras. Maestría en Producción Vegetal. Universidade Federal do Tocantins, Tocantins, Brasil. Pp 81.

RECyT
Year 27 / Nº 44 / 2025 /
DOI: https://doi.org/10.36995/j.recyt.2025.44.008

In vitro evaluations of warfarin tablets available in the brazilian market

Evaluación *in vitro* de tabletas de warfarina disponible en el mercado brasileño

Isabela C. F., Barbosa[1]; Vitoria C., Crestani[1]; Nathalia S., Rodrigues[1]; Tatiana, Staudt[1]; Ana L. S., Alves[1]; Charise D., Bertol[1,*]

1- University of Passo Fundo. Passo Fundo, Brasil.
* E-mail: charise@upf.br

Received: 30/09/2024; Accepted: 27/05/2025

Abstract
The aging of the population has led to an increased use of anticoagulants such as sodium warfarin. This study evaluated the quality of 5 mg warfarin tablets by analyzing eight samples (A1–A8) in accordance with the Brazilian Pharmacopoeia, with the objective of identifying quality deviations and verifying their interchangeability with the reference medication. The samples were subjected to the following quality control tests: average weight, friability (loss <1.5%), disintegration (within 30 minutes), dosing (content between 92.5% and 107.5%), and content uniformity (acceptance value <15). However, sample A3 failed the dissolution test, releasing less than 40% of the active ingredient within 30 minutes. The equivalence assessment indicated that samples A1xA2 (69.97) and A1xA4 (54.43) were interchangeable, whereas samples A3, A5, A6, A7, and A8 were not. The comparison of dissolution profiles using the similarity factor (f_2) revealed that several samples exhibited quality deviations, potentially compromising treatment efficacy and safety, and suggesting deficiencies in Good Manufacturing Practices (GMP).

Keywords: Anticoagulants; Warfarin; Quality control; Interchangeability; Pharmacopoeia.

Resumen
El envejecimiento poblacional ha aumentado el uso de anticoagulantes como la warfarina sódica. Este estudio evaluó la calidad de comprimidos de 5 mg, analizando ocho muestras (A1-A8) según la Farmacopea Brasileña, con el objetivo de identificar desviaciones de calidad y verificar la intercambiabilidad con el medicamento de referencia. Las muestras fueron aprobadas en los ensayos de peso medio, friabilidad (pérdida menor al 1,5%), desintegración (menos de 30 min), dosificación (contenido entre 92,5% y 107,5%) y uniformidad de contenido (valor de aceptación menor a 15). Sin embargo, la muestra A3 reprobó en la prueba de disolución, liberando menos del 40% en 30 min. La evaluación de equivalencia indicó que las muestras A1xA2 (69,97) y A1xA4 (54,43) eran intercambiables, mientras que A3, A5, A6, A7 y A8 no lo eran. La comparación del perfil de disolución mediante el factor f_2 reveló que varias muestras presentaron desviaciones de calidad, comprometiendo la eficacia y seguridad del tratamiento, además de indicar fallas en las buenas prácticas de fabricación.

Palabras clave: Anticoagulantes; Warfarina; Control de calidad; Intercambiabilidad; Farmacopea.

Introduction

Human aging involves a series of physical, psychological, and social changes. Physiologically, it results in the gradual decline of organ functions, including reduced immune system capacity, loss of muscle and bone mass, and alterations in the function of vital organs. Psychologically, aging can affect cognition, memory, and the way individuals process emotions and stress (1).

This process is accompanied by an increased use of medications among older adults, as health conditions requiring pharmacological treatment become more prevalent — including the frequent use of oral anticoagulants. These drugs are essential for preventing serious conditions such as thrombosis; however, they also carry a significant risk of bleeding (1).

Warfarin is an anticoagulant widely used in the treatment and prevention of blood homeostasis disorders, including thrombosis, acute myocardial infarction, and other thromboembolic events. Its therapeutic efficacy is directly related to its mechanism of action. To achieve the desired effect, the drug must reach the recommended concentration at the site of action. However, the presence of formulations with quality deviations can compromise therapeutic outcomes (2).

Accelerated stability studies have revealed interactions affecting the solid-state characteristics of warfarin (crystalline/amorphous forms) and the particle size distribution of the active pharmaceutical ingredient (API). Commercial tablets and formulations containing crystalline or amorphous warfarin, as well as binary mixtures of warfarin with various excipients,

were evaluated. Structural changes before and after testing were monitored. The study demonstrated that certain excipients, such as calcium phosphate, can induce the conversion of sodium warfarin to its acidic form, resulting in significant alterations in dissolution behavior—particularly when combined with variations in API particle size. Therefore, the careful selection of both excipients and particle size is critical to ensure the quality and safety of generic sodium warfarin tablets (3). These findings highlight the need for rigorous regulatory oversight to guarantee the quality of pharmaceutical products available on the market (3).

Accordingly, the present study aimed to evaluate whether warfarin tablets from different brands and batches available in Brazil comply with the quality standards established by the Brazilian Pharmacopoeia.

Materials and methods

Chemical Reference Substance (CRS) and Samples

The 5 mg sodium warfarin tablet samples used in this study were obtained through donations from the municipal governments of Passo Fundo/RS, Ronda Alta/RS, Serafina Corrêa/RS, and Vanini/RS (five samples), while three additional samples were purchased from local pharmacies. In total, eight samples from different manufacturers and batches were analyzed and labeled A1–A8. Sample A1 was designated as the reference tablet. The warfarin active pharmaceutical ingredient (API), used as the Chemical Reference Substance (CRS), was commercially obtained (Manufacturer: Hangzhou Hyper Chemicals Limited; Batch: WTH-23). The API was previously characterized by Fourier Transform Infrared Spectroscopy (FTIR).

Quality control tests for the Tablets

The tests conducted followed those described in the Brazilian Pharmacopoeia (4).

Identification

Identification was carried out following the assay method described in the Brazilian Pharmacopoeia (assay section). The retention time of the principal peak in the chromatogram of the sample solution obtained in the assay was required to correspond to that of the principal peak in the standard solution.

Weight Determination

Twenty tablets from each sample were individually weighed. The mean tablet weight was calculated, along with the upper and lower specification limits. No more than two units were permitted to fall outside these limits.

Friability Test

Ten tablets from each sample were weighed and placed in a friabilator (Nova Ética, model 3001) operating at 25 revolutions per minute for 4 minutes. After the test, any powder residue on the tablet surfaces was removed, and the tablets were reweighed. None of the tablets exhibited breakage, chipping, cracking, or shattering. The tablets were considered acceptable if they showed a weight loss of ≤ 1.5%.

Hardness Test

Tablet hardness was measured using a semi-digital hardness tester (Ethiktechnology). Ten tablets from each sample were tested, and the mean, standard deviation (SD), and relative standard deviation (RSD) were calculated.

Disintegration Test

Six tablets from each sample were tested in a disintegration apparatus using water maintained at 37 ± 1 °C as the immersion medium. Each tablet was placed in a tube of the disintegration basket, with a disk added to each tube. The time required for complete disintegration was recorded, establishing the maximum disintegration time for uncoated tablets at 30 minutes.

Assay

The assay was performed by high-performance liquid chromatography (HPLC). A PerkinElmer LC Flexar chromatograph (binary pump Flexar, autosampler Flexar) equipped with a UV detector set at 280 nm and an RP-ACE octadecylsilane silica column (250 × 4.6 mm, 5 µm) was used. The mobile phase consisted of methanol, water, and glacial acetic acid (68:32:1, v/v/v), at a flow rate of 1.0 mL/min. Twenty tablets were accurately weighed and powdered. An amount of powder equivalent to 25 mg of sodium warfarin was transferred to a 25 mL volumetric flask, to which 15 mL of diluent (a mixture of pH 7.4 buffer and acetonitrile (85:15, v/v)) was added. The mixture was sonicated for 20 minutes, then the volume was completed with the same diluent, homogenized, and filtered through a 0.45 µm cellulose membrane filter. The resulting solution was further diluted with the mobile phase to obtain a final concentration of 100 µg/mL. Aliquots of 20 µL of the sample solution and the standard solution were injected separately. Chromatograms were recorded, and the areas under the peaks were measured. The content of sodium warfarin ($C_{19}H_{15}NaO_4$) in the tablets was calculated from the ratio of the responses obtained for the standard and sample solutions. A standard solution was prepared by transferring 25 mg of warfarin CRS to a 25 mL volumetric flask, adding 15 mL of pH 7.4 buffer, and sonicating for 5 minutes to obtain a 1 mg/mL solution. The volume

was then completed with the same buffer and diluted with the mobile phase to yield a final concentration of 100 µg/mL. A resolution solution was prepared by transferring 0.1 g of propylparaben CRS to a 100 mL volumetric flask, adding 50 mL of acetonitrile, and sonicating for 5 minutes. The volume was then completed with acetonitrile and homogenized. From this solution, 2.5 mL were transferred to a 25 mL volumetric flask, followed by the addition of 2.5 mL of the 1 mg/mL warfarin standard solution. The volume was completed with the mobile phase, yielding a solution containing 100 µg/mL each of propylparaben and warfarin. Replicate injections of 20 µL of the resolution solution were performed. The resolution (Rs) between the propylparaben and warfarin peaks was ≥ 2.0, and the relative standard deviation (RSD) for the peak areas of the replicates did not exceed 2.0%.

Uniformity of dosage units

Ten tablets from each batch were weighed individually and placed in 5 mL volumetric flasks. Then, 4 mL of the diluent (as described above) was added, and the mixture was allowed to stand for 20 minutes. The volume was then completed with the same diluent. A 0.5 mL aliquot was taken and transferred to a 5 mL volumetric flask, which was subsequently filled with the mobile phase (as described above). The resulting solutions were injected into the chromatograph. The content of the 10 units was determined, and the mean (X) and standard deviation were calculated to obtain the acceptance value (AV). The following equations were used to calculate AV: if the mean content (X) is between 98.5% and 101.5%, then M = X (AV = k·SD); if X < 98.5%, then M = 98.5% (AV = 98.5 − X + k·SD); if X > 101.5%, then M = 101.5% (AV = X − 101.5 + k·SD). The AV must be less than L1, where L1 = 15 for approval. In addition, no individual result should be less than (1 – L2 × 0.01) M or greater than (1 + L2 × 0.01) M, with L2 equal to 25. A retest with an additional 20 units (n = 30) may be conducted if L1 exceeds 15; however, all individual units must still comply with the individual limit criteria. The acceptance value (AV) is based on the following equation:

$AV=|M-\bar{X}|+ks$

where k is the acceptability constant (for n = 10, k = 2.4), SD is the standard deviation, X is the mean content found, and M is the value to be used when T ≤ 101.5, which is the case for warfarin, and this value will depend on X.

Dissolution Test

The dissolution test was performed using 500 mL of water as the dissolution medium and a paddle apparatus operating at 50 rpm. A total of 56 tablets were placed in the dissolution vessels. At 5, 10, 15, 20, 30, 40, and 60 minutes, 10 mL aliquots of the medium were withdrawn and filtered. After each sampling, an equal volume of fresh medium was added to maintain a constant volume. The procedure followed the same chromatographic conditions described in the Assay section. The amount of $C_{19}H_{15}NaO_4$ dissolved at each time point was calculated by comparing the obtained responses with a calibration curve prepared using the warfarin RCS solution, freshly prepared in the mobile phase on the day of analysis. According to the Brazilian Pharmacopoeia specifications, the acceptance criterion requires that not less than 80% (Q) of the declared amount of $C_{19}H_{15}NaO_4$ be dissolved within 30 minutes.
To assess the pharmaceutical equivalence between formulations, the dissolution profile data were analyzed using the similarity factor (f_2), calculated according to the model recommended by the Brazilian legislation (Resolution RDC No. 31/2010 (5), which establishes that the value must fall between 50 and 100 to be considered interchangeable.

$$f_2 = 50 \bullet \log\left\{\left[1+\left(\frac{1}{P}\right)\sum_{i=1}^{P}(R-T)^2\right]^{-1/2} \bullet 100\right\} \quad (1)$$

f_2: Similarity factor, Log: Logarithm, P: Collection Time R: Reference Medicine T: Test Medicine.

Results

The results of the quality control tests are presented below.
In the identification test, all tablet samples were confirmed as warfarin, based on the correspondence of the retention time of the main chromatographic peaks in each of the eight samples with that of the standard solution (Figure 1). The resolution between the peaks of propylparaben and warfarin was greater than 2.0.

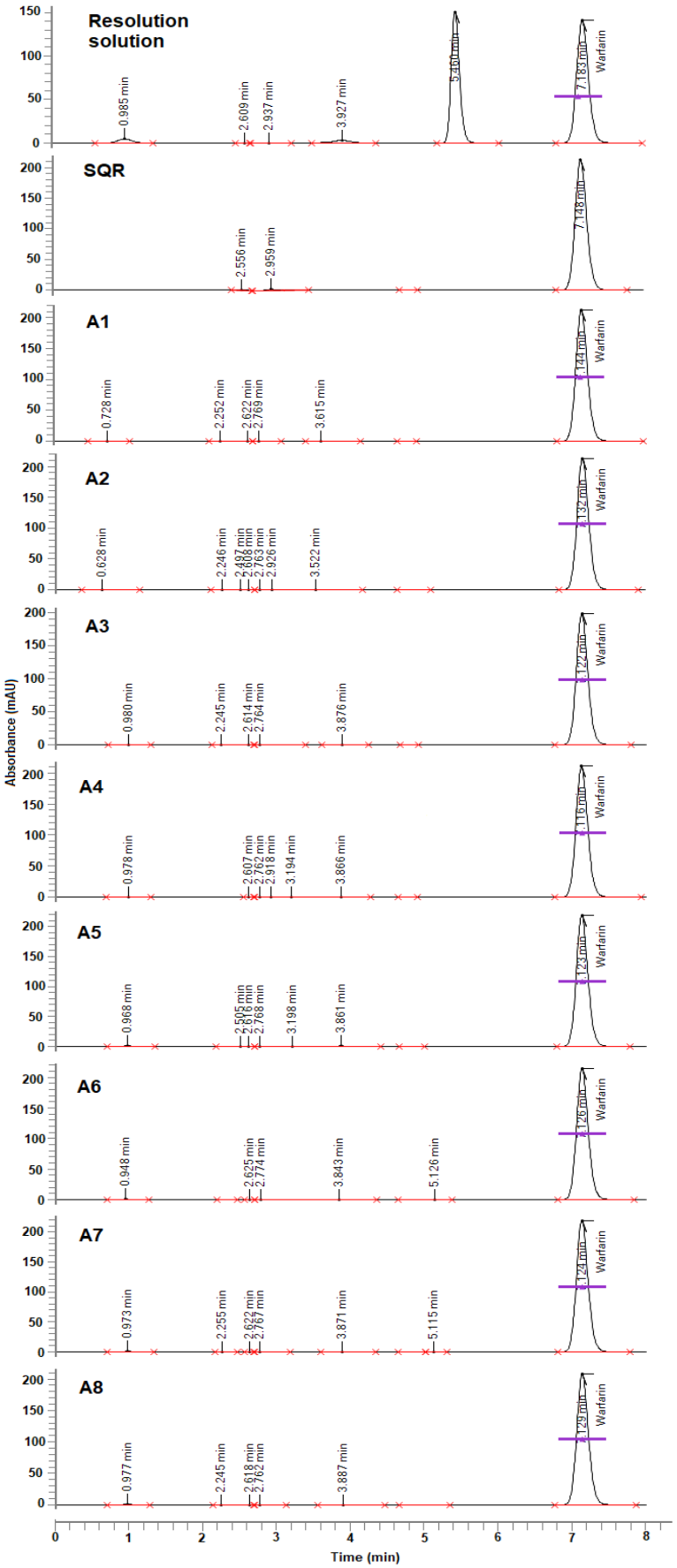

Figure 1*:* Chromatograms of warfarin tablet sample solutions, prepared at a concentration of 100 *µ*g/m.

For the average weight determination, a variation limit of 7.5% was applied, as the tablets had weights between 80 mg and 250 mg. Upon analyzing the results, it was found that one of the tablets from sample 5 exceeded the upper limit (A5, 0.155 g). Upon analysis, one tablet from sample 5 (A5, 0.155 g) exceeded the upper limit. However, the sample was still considered compliant, since the Brazilian Pharmacopoeia permits up to two units to fall outside the specified limits (4). It is important to note that no individual tablet exceeded or fell below double the specified percentage (15%). Therefore, all samples met the pharmacopoeial requirements and were approved (Table 1).

Table 1: Quality control test performed with warfarin tablets.

Control quality test	A1	A2	A3	A4	A5	A6	A7	A8
Average Weight (g)	0.1428	0.1419	0.1406	0.1414	0.1401	0.1410	0.1420	0.1408
Upper Limit (g)	0.1535	0.1525	0.1512	0.1520	0.1506	0.1516	0.1526	0.1514
Lower Limit (g)	0.1321	0.1313	0.1301	0.1308	0.1295	0.1304	0.1314	0.1302
Friability (weight loss %)	0.13%	0.03%	0.22%	0.33%	0.36%	0.30%	0.18%	0.41%
Hardness (N) (n=10)	64.65	52.4	NR	56.1	39.15	46.65	51.6	46.95
Hardness	5.62	7.36	NR	10.43	1.64	5.82	3.07	9.02
Hardness RSD (%)	8.69	14.06	NR	18.59	4.19	12.48	5.95	19.21
Disintegration Time (min:s)	08:29	09:10	07:20	06:03	04:41	03:23	03:16	03:40
Assay (%) (n=3)	101.10	100.65	92.88	100.33	100.68	102.94	104.34	97.10
Assay SD	1.55	0.23	0.09	0.36	4.00	2.67	0.08	1.61
Assay RSD	1.53	0.23	0.10	0.36	3.98	2.59	0.08	1.66

SD: Standard Deviation; RSD: Relative Standard Deviation
Sample number 3 was not conducted.

In the friability test, tablets are allowed a maximum mass loss of 1.5% (4). All analyzed samples remained within the established limits and were therefore approved (Table 1).

The hardness test is not an absolute criterion for approval or rejection but serves as an important indicator of a product's consistency and uniformity. All samples complied with the expected parameters (Table 1). Ideally, a relative standard deviation (RSD) of less than 5% is preferred, as it reflects uniformity among the measurements (4). Although sample 8 presented a higher RSD (19.21%), this variation does not entail batch rejection.

The disintegration test also yielded satisfactory results. All tablets disintegrated within the 30-minute limit defined for immediate-release formulations, confirming their suitability for this dosage form (Table 1).

For the assay, a calibration curve was constructed using five standard solutions with concentrations ranging from 80.0 µg/mL to 120.0 µg/mL, each injected in triplicate to ensure precision. The average peak areas were used to calculate the curve, which was reconstructed daily to account for possible experimental variations. For sample analysis, three aliquots from a pool of 20 crushed tablets were diluted and injected into the chromatograph. The practical concentration was determined using the equation of the calibration curve, with the chromatographic peak area being directly proportional to the analyte concentration. The theoretical concentration was defined as 100%, and the practical concentration was expressed as a percentage relative to this value. According to the Brazilian Pharmacopoeia (4), the acceptable content range for warfarin is 92.5% to 107.5%, and all analyzed samples complied with these specifications.

The uniformity of dosage units test was performed using ten tablets per batch. Ideally, the individual doses should exhibit minimal variability. The acceptance value (AV) was calculated according to pharmacopoeial requirements and must be less than 15 for approval (Table 2). The AV calculation depends on both the mean content and the standard deviation of the ten tested units. If the AV exceeds the L1 limit (15), an additional 20 units must be tested. Furthermore, each unit must not contain less than $((1 – (L2 \times 0.01)) \times M)$ or more than $((1 + (L2 \times 0.01) \times M)$, where L2 equals 25.0. Thus, no individual tablet may contain less than approximately 75% or more than approximately 125% of the declared warfarin amount (4). In this assay, all samples met the requirements, with AV values below 15 and individual results within the 75–125% range.

Table 2: Result of the Uniformity of dosage units for Warfarin Tablets (n=10).

SAMPLE	CONTENT % A1	CONTENT % A2	CONTENT % A3	CONTENT % A4	CONTENT % A5	CONTENT % A6	CONTENT % A7	CONTENT % A8
1	98.52	104.04	99.15	110.68	97.90	96.57	88.73	102.65
2	98.11	94.65	96.46	95.88	100.38	93.06	102.81	101.78
3	99.55	103.79	102.08	102.95	96.43	102.89	105.39	98.28
4	99.25	100.33	109.88	95.02	101.64	89.09	106.72	98.34
5	101.77	102.78	105.36	102.53	100.97	91.57	105.16	97.70
6	98.68	97.84	105.28	105.18	105.26	97.04	105.62	101.71
7	97.90	98.44	92.88	103.73	101.85	94.51	101.43	93.59
8	97.13	104.34	98.30	108.93	98.09	94.49	107.50	97.68
9	102.95	98.55	91.65	110.01	111.80	89.09	102.47	107.03
10	99.36	99.34	97.49	105.04	102.59	91.89	105.80	100.19
MEAN	99.33	100.41	99.85	103.99	101.69	94.02	103.17	99.30
SD	1.78	3.22	6.13	5.07	4.38	4.15	5.43	3.65
AV	4.27	7.75	14.71	14.68	10.52	14.44	14.69	8.76

Dissolution

During the dissolution test, samples were collected at 5, 15, 20, 30, 40, and 60 minutes and analyzed by HPLC. The peak areas obtained were converted into percentage of drug dissolved. According to the Brazilian Pharmacopoeia (4), at least 80% of the declared amount must be dissolved within 30 minutes. The dissolved percentage vs. time (min) data were plotted (Figure 2). All samples released more than 80% of the active ingredient within the first 30 minutes, except for sample A3, which released less than 30% at 30 minutes. Moreover, sample A3 failed to reach 40% dissolution even after 60 minutes, indicating a marked deviation from the established specification. Consequently, sample A3 was disapproved for failing to meet the minimum dissolution requirement.

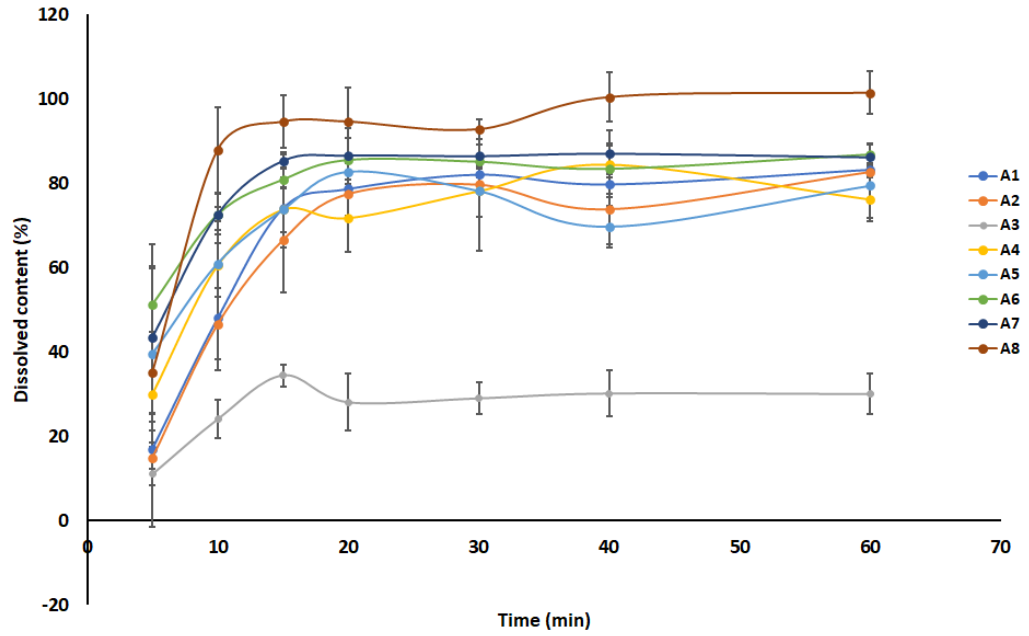

Figure 2: Dissolution Profiles of Warfarin Tablet Samples.

Pharmaceutical equivalence is assessed through physicochemical tests, and when necessary, microbiological or biological evaluations. The principal *in vitro* method used to determine equivalence between formulations is the comparative dissolution profile, where the dissolution profile of the reference drug (A1) is compared with those of the other samples using a mathematical model known as the similarity factor (f_2– equation 1). According to Resolution RDC No. 30/11, a generic or similar drug must be interchangeable with the reference product. To confirm interchangeability, the f_2 value obtained from the comparison must range between 50 and 100 (5).

In addition to the previously mentioned requirements, both the test and reference drugs must fully comply with the individual monograph. In addition to meeting these criteria, both the test and reference formulations must comply with the individual monograph requirements of the Brazilian Pharmacopoeia. In this study, all samples were compared with sample A1 (reference). The results indicated that samples A1×A2 (f_2 = 69.97) and A1×A4 (f_2 = 54.43) were interchangeable, while samples A3, A5, A6, A7,

and A8 were not, as their f_2 values fell below the required range (50–100). Similarly, A2×A3 and A3×A4 comparisons did not meet the established standard (5) (Table 3).

Table 3: Similarity Factor (f_2) calculated from the dissolution profile results. Sample 1 was used as the reference, and all other samples were compared to it.

	f_2
A1xA2	69.97
A1xA3	18.31
A1xA4	54.43
A1xA5	48.19
A1xA6	38.99
A1xA7	41.12
A1xA8	32.60
A2XA3	19.81
A3XA4	18.56

Table 4. Summary of the quality control results obtained for the analyzed samples.

Table 4: Quality Control results.

Sample/Test	A1	A2	A3	A4	A5	A6	A7	A8
Identification	A	A	A	A	A	A	A	A
Average Weight	A	A	A	A	A	A	A	A
Friability	A	A	A	A	A	A	A	A
Hardness	A	A	A	A	A	A	A	A
Disintegration	A	A	A	A	A	A	A	A
Dosage	A	A	A	A	A	A	A	A
Uniformity	A	A	A	A	A	A	A	A
Dissolution	A	A	R	A	A	A	A	A

R= rejected; A= approved

Only sample A3 failed the dissolution test. Regarding interchangeability, samples A2 and A4 were the only ones found to be interchangeable with the reference formulation.

Discussion

The study revealed that some warfarin samples did not meet quality standards, which may compromise treatment effectiveness and increase the risk of bleeding in patients. Therefore, ensuring both the interchangeability and quality of medications is essential for the safety and well-being of elderly individuals who rely on these treatments.

The main finding of this study was the detection of quality control failures in several warfarin tablet samples available on the Brazilian market. The analyzed samples were subjected to tests established by the Brazilian Pharmacopoeia. In the dissolution assays, sample A3 failed to meet the specified requirements. Moreover, the comparative dissolution profile demonstrated that many samples were not interchangeable with the reference drug—an essential criterion for a product to be considered a generic equivalent. These inconsistencies raise concerns about compliance with good manufacturing practices (GMP) and proper quality control procedures.

Although each batch is expected to undergo rigorous quality testing before marketing, the observed failures suggest that certain products may reach the market with quality deviations and deficiencies in GMP adherence.

The focus on 5 mg warfarin tablets was chosen due to the formulation's low active ingredient concentration—approximately 3% of the tablet's total mass (~150 mg). Such a small proportion of the active pharmaceutical ingredient requires a highly homogeneous blend to ensure accurate dosing and therapeutic efficacy (6). Consequently, potent drugs at low dosages are particularly susceptible to quality deviations, as achieving uniform distribution of the active compound demands a strict and precise mixing process. Another relevant factor is that patients using warfarin frequently experience challenges in stabilizing their INR levels. Before questioning *in vivo* efficacy, it is essential to first verify the *in vitro* quality of the product.

Quality control plays a crucial role in determining the potential interchangeability between reference drugs and their generic, similar, or interchangeable similar counterparts. These products contain the same active ingredient, at the same concentration, dosage form, and route of administration as the reference drug, and are considered equivalent in efficacy and safety—while generally being more affordable (7). It is important to note that generic, similar, and interchangeable similar drugs must demonstrate comparable *in vitro* dissolution profiles to the reference product, as verified by the similarity factor (f_2). In addition to *in vitro* assays, generics and interchangeable similar drugs are also subjected to *in vivo* bioavailability and bioequivalence tests during registration. In contrast, similar drugs are exempt from *in vivo* testing (8).

The equivalence test aims to provide an *in vitro* comparison of pharmaceutical equivalence. Generic, similar, and interchangeable similar drugs must exhibit *in vitro* equivalence to the reference formulation, primarily evaluated through pharmacopoeial assays, namely the dissolution profile (5).

Of the eight samples tested in this study, only two (A2 and A4) were interchangeable with the reference product (A1). The remaining samples (A3, A5, A6, A7, and A8) failed to demonstrate interchangeability. The greatest variability occurred within the first five minutes of the dissolution test, and this pronounced initial deviation was responsible for the rejection of several samples, resulting in distinct dissolution profiles. Clinically, this early-stage variation may have limited significance, as it reflects only the initial phase of drug release. Nonetheless, the similarity factor (f_2) remains an effective statistical tool for detecting and quantifying differences between dissolution profiles, as it incorporates all sampling time points.

The f_2 parameter is therefore essential for assessing dissolution similarity between formulations. It provides a robust statistical measure that considers both the mean values and standard deviations of dissolution data, enabling the reliable determination of whether a generic product can be deemed equivalent to its reference counterpart (9).

Tablet hardness can influence dissolution results. In this study, although the samples exhibited similar average hardness values, a high relative standard deviation was observed—particularly in samples A4 and A8—indicating substantial intralot variability (Table 1). Kokott et al. (10) reported unsatisfactory mechanical resistance results for orodispersible tablets in tensile and compression tests, where only one of the commercial brands analyzed met the requirements of the European Pharmacopoeia, which establishes a maximum disintegration time of three minutes. In contrast, the FDA stipulates a stricter limit of 30 seconds. Although the hardness test is not a definitive acceptance or rejection criterion, it provides important insight into potential inconsistencies in pharmaceutical formulations.

Hardness plays a key role in dissolution efficiency. Tablets with greater mechanical strength, characterized by denser and less porous structures, tend to exhibit slower dissolution rates. This occurs because the dissolution medium encounters greater resistance when penetrating the tablet matrix and releasing the active ingredient (11).

In the dissolution assay, one of the eight samples (A3) failed to meet the established parameters of the Brazilian Pharmacopoeia (4), which requires at least 80% dissolution of the declared amount within 30 minutes. Sample A3 reached only approximately 35% dissolution, indicating a failure in its quality control process (Figure 3).

A study conducted in Indonesia evaluated the quality of reference and generic formulations through physical and chemical tests. The results showed that all samples met the physical and content criteria (90%–110% of the indicated amount). The dissolution profile of branded tablets was similar to that of the innovative product, whereas generic formulations exhibited distinct profiles compared to the reference drug (12).

In the present study, which assessed the quality control of warfarin tablets, unsatisfactory results were observed in the dissolution test. It is important to highlight that, in industrial practice, companies often evaluate dissolution only at the time point specified by the Pharmacopoeia—typically 30 minutes—without conducting a complete profile analysis at multiple time intervals (5, 10, 15, 20, 30, 40, and 60 minutes). This limited approach may lead to inconsistencies across different manufacturing processes. Therefore, there is a clear need to adopt updated and more comprehensive evaluation protocols in drug manufacturing—extending beyond those currently established by pharmacopoeial standards—to prevent potential production failures and quality control issues in commercially available medications. Implementing broader quality assessment procedures could help detect deviations that remain unnoticed under conventional testing.

Many patients using warfarin experience challenges in maintaining stable INR values due to the drug's mechanism of action. However, the findings of this study indicate that dose control issues are not solely linked to *in vivo* variability but also reflect deficiencies in *in vitro* quality control tests.

Conclusion

Among the analyzed warfarin tablets, some exhibited quality deviations that may compromise both the efficacy and safety of the medications. Of the eight samples evaluated, sample A3 failed the dissolution test, and only two formulations were found to be interchangeable with the reference drug. The lack of pharmaceutical equivalence demonstrated that several generic formulations—and even one reference sample—did not meet interchangeability requirements, indicating potential differences in their *in vivo* performance. Therefore, it can be concluded that quality deviations are present among the analyzed tablets, suggesting deficiencies in good manufacturing practices. These findings raise important concerns regarding the therapeutic efficacy and safety of warfarin products available on the market.

References

(1) PAN AMERICAN HEALTH ORGANIZATION. *Decade of Healthy Aging in the Americas (2021-2030)*. Available at: https://www.paho.org/pt/decada-do-envelhecimento-saudavel-nas-americas-2021-2030. Accessed on: June 19, 2024.

(2) XUE L.,et al. Warfarin-A natural anticoagulant: **A review of research trends for precision medication. Phytomedicine**. v128, p.155-479. 2024 Jun. Disponível em: www.sciencedirect.com. Acessed on: May 22, 2024.

(3) MUSELÍK, J. et al. Structural Changes of Sodium Warfarin in Tablets Affecting the Dissolution Profiles and Potential Safety of Generic Substitution. **Pharmaceutics**, v. 13, n. 9, p. 1364, 2021. Disponível em: www.mdpi.com/1999-4923/13/9/1364. Acesso em: 05 jun. 2024.

(4) BRAZIL. Ministry of Health. National Health Surveillance Agency (ANVISA). *Brazilian*

Pharmacopoeia. 6th ed. Brasília, 2019. Available at: www.gov.br/anvisa/pt-br/assuntos/farmacopeia/farmacopeia-brasileira. Accessed on: May 5, 2024.
(5) BRAZIL. Ministry of Health. National Health Surveillance Agency. Resolution RDC No. 31, August 11, 2010. Addresses the conduct of Pharmaceutical Equivalence Studies and Comparative Dissolution Profiles. *Official Gazette of the Union*, Brasília, DF, August 12, 2010. Section 1, p. 46-47. Available at: www.in.gov.br/en/web/dou/-/resolucao-rdc-n-31-de-11-de-agosto-de-2010-1974608. Accessed on: May 6, 2024.
(6) AULTON, M.E. *Design of Pharmaceutical Forms*. 4th Edition. Rio de Janeiro: Elsevier Editora LTDA, 2016. Available at: https://www.elsevier.com/. Accessed on: June 23, 2024.
(7) BRAZIL. Ministry of Health. National Health Surveillance Agency (ANVISA). *Generic Medications*. Available at: https://www.gov.br/anvisa/pt-br/assuntos/medicamentos/genericos. Accessed on: June 23, 2024.
(8) BRAZIL. Ministry of Health. National Health Surveillance Agency. Resolution of the Collegiate Board RDC No. 58, October 10, 2014. Addresses the measures to be adopted for the registration of medications for the interchangeability of similar medications with the reference medication. *Official Gazette of the Union*, Brasília, DF, October 13, 2014. Section 1, p. 659. Available at: www.in.gov.br. Accessed on: June 23, 2024.
(9) YOSHIDA, H. et al. Comparison of Dissolution Similarity Assessment Methods for Products with Large Variations: f_2 Statistics and Model-Independent Multivariate Confidence Region Procedure for Dissolution Profiles of Multiple Oral Products. **Biological and Pharmaceutical Bulletin**, v. 40, n. 5, p. 722-725, 2017. Disponível em: www.jstage.jst.go.jp. Acessed on: June 29, 2024.
(10) KOKOTT, M., et al. Evaluation of two novel co-processed excipients for direct compression of orodispersible tablets and mini-tablets. *European Journal of Pharmaceutics and Biopharmaceutics*, v. 168, p. 122-130, 2021. Available at: www.sciencedirect.com/science/article/abs/pii/S0939641121002977. Accessed on: May 14, 2024
(11) YEKPE, Ketsia et al. Developing a quality by design approach to model tablet dissolution testing: an industrial case study. **Pharmaceutical Development and Technology**, v. 23, n. 6, p. 646-654, 2018. Disponível em: www.tandfonline.com. Acessed on: May 20, 2024.
(12) ROHMANI, Sholichah et al. Evaluation of compared dissolution profile of atorvastatin tablets in markets. **Journal of Advanced Pharmacy Education and Research**, v. 10, n. 1-2020, p. 107-115, 2020. Disponível em: www.japer.in. Acessed on: May 12, 2024.

RECyT
Year 27 / Nº 44 / 2025 /
DOI: https://doi.org/10.36995/j.recyt.2025.44.009

Study on the need for a new Technology Acceptance Model

Estudio sobre la necesidad de un nuevo Modelo de Aceptación de Tecnología

Fábio, Corrêa[1, *]; Dárlinton Barbosa Feres, Carvalho[2]; Vinícius, Figueiredo de Faria[1]; João Victor, Boechat Gomide[1]

1- Universidade FUMEC (Fundação Mineira de Educação e Cultura, FUMEC University. Minas Gerais, Belo Horizonte, Brasil.
2- Universidade Federal de São João del-Rei (UFSJ). Minas Gerais, Brasil.
* E-mail: fabiocontact@gmail.com

Received: 07/05/2024; Accepted: 13/05/2025

Abstract
This research aims to analyze the practical applications of the Technology Acceptance Model to verify whether there is a greater recurrence of the original version or its variations. It is basic exploratory research that adopts a qualitative approach for the analysis. Scientific bibliographic documents are analyzed through a systematic literature review and content analysis. As a result, firstly, the practical dominance of the Technology Acceptance Model application comes from its extensions and adaptations rather than from its original models. This does not mean that the predictors of the original versions are inadequate, but that, depending on the technology and the researcher's point of view, they are better used when adjustments are made. Secondly, given the above result, it is concluded that the Technology Acceptance Model is theoretically robust; otherwise, adaptations and extensions would not occur. The third conclusion arises from the previous ones and is based on a reflection: is an update, called Technology Acceptance Model 4, required? Therefore, we conclude that it is not necessary since 401 adaptations and 198 extensions were identified, proposing an additional structure would not eliminate the different perspectives of predictors to be included in future research.

Keywords: Technology Acceptance Model, TAM, Extension, Adaptation.

Resumen
Esta investigación tiene como objetivo analizar las aplicaciones prácticas del Modelo de Aceptación de Tecnología para verificar si existe una mayor recurrencia de la versión original o de sus variaciones. Es una investigación básica exploratoria con un enfoque cualitativo para el análisis. Los documentos bibliográficos científicos se analizan mediante una revisión sistemática de la literatura y un análisis de contenido. Como resultado, en primer lugar, el predominio práctico de la aplicación del Modelo de Aceptación de Tecnología proviene de sus ampliaciones y adaptaciones y no de sus modelos originales. No significa que los predictores de las versiones originales sean inadecuados, sino que, según la tecnología y el punto de vista del investigador, se aprovechan mejor con ajustes. En segundo lugar, dado el resultado anterior, se concluye que el Modelo de Aceptación de Tecnología es teóricamente robusto; de lo contrario, no se producirían adaptaciones y ampliaciones. La tercera conclusión surge de las anteriores y se establece a partir de una reflexión: ¿se exige una actualización, denominada Modelo 4 de Aceptación de Tecnología? En respuesta, entendemos que ¡no! Dado que se encontraron 401 adaptaciones y 198 extensiones, la propuesta de una estructura más no acabaría con las diferentes perspectivas de predictores a incluir en futuras investigaciones.

Palabras clave: Modelo de Aceptación de Tecnología, TAM, Extensión, Adaptación.

1 Introduction

Models that analyze the adoption of technological resources are positioned as a means to evaluate people's acceptance to a particular technology. These models represent the impact of scientific theory on understanding and guiding the scope of application and practical use of technology in society.

Among these models, for the purposes of this research, the Technology Acceptance Model (TAM) stands out. TAM was first proposed by Davis (1), and was later extended into the TAM2 (2) and TAM3 (3) versions. Across these versions, TAMs continue to be used in various studies, for instance, TAM in the research by Villa, Marín, and Salinas (4), Knox et al. (5); and Silva, Mendes Filho, and Marques Júnior (6); TAM2 in the study by Adji and Taufik (7); and TAM3 in Kusumastuti et al. (8). These cases may lead to the understanding that its predictors (i.e., variables) are sufficient to assess the acceptance of current technologies. However, studies by Al-Dokhny et al. (9) and Zhang et al. (10) proposed the adaptation (i.e.,

joining of models) and extension (i.e., addition and removal of predictors) of the TAM. Therefore, the aforementioned sufficiency of the predictors for evaluating today's technologies becomes questionable and inconsistent.

Through these two perspectives, this research aims to investigate the transformations (i.e., adaptations and extensions) carried out in the TAM to verify whether the original model or its variations are predominantly applied. It aims to reveal whether the theory underlying the TAM remains robust, as demarcated by Garcia et al. (11), or if the limitations presented by Marikyan and Papagiannidis (12) are compelling enough to create the need to update this model. These limitations are as follows: the lack of analysis of the impact of technology on performance; the suggestion that the greater the use of technology, the greater its performance; the limited attention given to what makes technology useful; and a specific focus on the organizational context (12).

In this sense, the following problem arises: is there a predominance in the application of the original TAM or its variations (i.e., adaptation and extension)? Based on this question, the objective is to analyze the practical application of the TAM in order to verify if the original version or its adjustments show a more prominent recurrence. Given this, we seek to understand the evolution of this theory in the context of its practical application and to assess whether a TAM4 is needed.

Furthermore, we want to foster a dialogue that contributes to the continuity of research focused on the evolution of acceptance models. For instance, the results are related to the study by Tamilmani et al. (13) that analyzed the evolution of the Unified Theory of Acceptance and Use of Technology 2 (UTAUT2) model.

2 Technology Acceptance Model-TAM

The 1980s were a milestone for technology adoption studies, as at that time, there was a growth in the use of personal computers. The aim was to understand why users adopted personal computing and information systems. For this purpose, it was necessary to apprehend the users' perception of technologies, considering aspects that predicted their adoption, which led to the formulation of models.

A model is a schematic representation of reality. It is a means by which reality is abstracted, outlining aspects that constitute the phenomenon to be investigated with the aim of understanding it. In the context of technology adoption (i.e., reality phenomenon), we seek to understand which factors (i.e., aspects) influenced this adoption. Therefore, it was necessary to establish the factors that could provide an understanding of this phenomenon. In this context, the Theory of Reasoned Action (TRA), a model proposed by Martin Fishbein and Icek Ajzen (14), is especially useful. This model (Figure 1) established that an individual's behavior was influenced by their intention, which was shaped by attitudes and norms derived from personal beliefs. It is a generic model applicable to several areas. However, regarding the field of computing, it had limitations, as it failed to consider variables specific to technology use within this field.

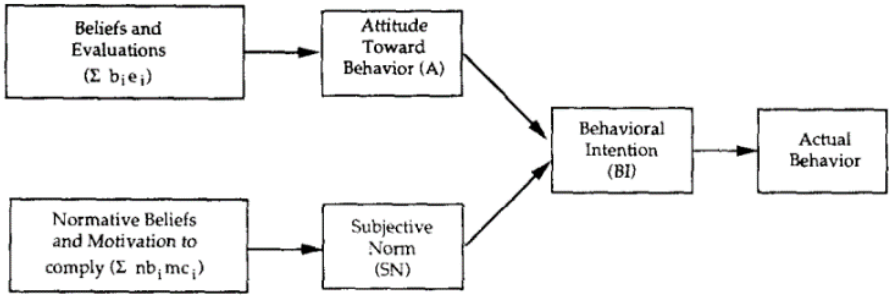

Figure 1. Theory of Reasoned Action (TRA).
Source: (15, p. 984)

Thus, the TAM (Figure 2) emerged as a model proposed by Fred D. Davis (1) for the context of digital information systems, which had the TRA as its foundation, along with the Theory of Behavioral Change (TBC) proposed by Albert Bandura (16). TBC established the concept of self-efficacy, characterized by the individual's belief in their capability to perform actions required to accomplish a task. Self-efficacy was adjusted to the perceived ease of use of the TAM, which is the degree to which the person considers (i.e., belief) that using a system is effortless. Accordingly, the individual's belief in the TRA is related to the self-efficacy in the TBC and constitutes the perceived ease of use in the TAM.

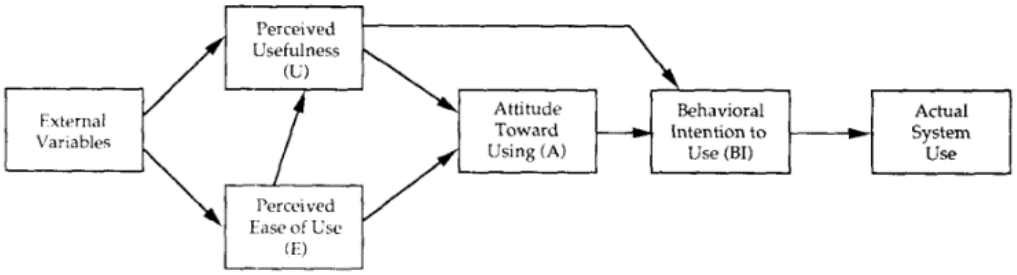

Figure 2. Technology Acceptance Model (TAM).
Source: (15, p. 985)

In the TAM, the use of the system is determined by the individual's intention to use it, which derives from perceived usefulness (i.e., performance expectation) and attitude toward using it. Attitude toward use is shaped by perceived ease of use (i.e., effort) and perceived usefulness, with the former influencing the latter. In other words:

The model implies that if an application is expected to be easy to use, users are more likely to find it useful, which increases the likelihood of technology acceptance (12, pp. 3). On average, the TAM predicted 40% of the variance in technology acceptance (2). However, the research by Davis, Bagozzi, and Warshaw (15, p. 999) identified that the subjective norm, which corresponds to the perceived utility (i.e., performance expectation), required more research to "[...] investigate the conditions and mechanisms governing the impact of social influences on usage behavior".

In 2000 – 25 years after the proposal of the TRA, and 11 years after the presentation of the TAM – Viswanath Venkatesh, together with Fred D. Davis, pointed out that the adoption and use of technology still remained a theoretical and practical concern in the field of information systems. Although technological advances were significant, the concern was that "low usage of installed systems has been identified as a major factor underlying the 'productivity paradox' surrounding lackluster returns from organizational investments in information technology" (2, pp. 186).

For them, perceived usefulness is directly linked to the individual's performance expectation through the use of technology. The utility is presented as a strong determinant of the intention of use (coefficient close to 0.6). Therefore, to address the productivity paradox established at the time, the performance expectation (i.e., perceived usefulness) should be further explored by the model, which is the central point of the TAM extension, called TAM2 (Figure 3). Thus, "a better understanding of the determinants of perceived usefulness would enable us to design organizational interventions that would increase user acceptance and usage of new systems" (2, p. 187).

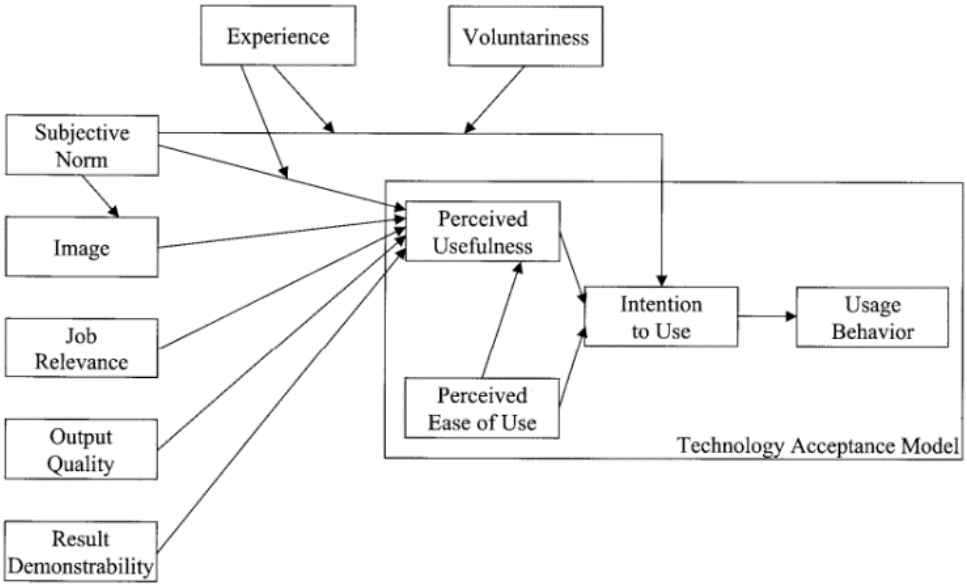

Figure 3. Technology Acceptance Model 2 (TAM2).
Source: (2, p. 188)

TAM2 introduced five additional exogenous variables (i.e., subjective norm, image, job relevance, output quality, and result demonstrability) influencing perceived usefulness as well as two moderators (i.e., experience and voluntariness) to extend the TAM. The subjective norm, image, and voluntariness represent social influence. Besides, the variables of job relevance, output quality, and result demonstrability incorporate cognitive instrumental processes into the framework.

The subjective norm, derived from the TRA, refers to the influence of people relevant to an individual regarding what he or she should or should not do (i.e., social aspect). For example, a co-worker may exert influence on an individual by expressing their opinion about the system's behavior, which in turn shapes the individual's perception. The experience moderator indicates that the subjective norm (i.e., social influence) may decrease as the system is used. Voluntariness indicates that the adoption of technology is not mandatory; in other words, it is voluntary according to the subjective norm.

Image refers to the status of an individual within a social group. Hence, belonging to a group or receiving its support may create a favorable image of the individual among its members, which may increase the probability of using the system (i.e., perceived usefulness). Job relevance establishes "[…] the individual's perception regarding the degree to which the target system is applicable to his or her job" (2, p. 191).

Output quality refers to how well the system performs tasks related to the individual's work objectives. Result demonstrability establishes that explicit results predict the perceived usefulness that the technology conveys to the individual; that is, the "[...] tangibility of the results of using the innovation" (17, p. 203).

While studies conducted with TAM showed a variation of approximately 40% in the intention to use, results based on TAM2 ranged between 37% and 52% for this factor, which is shaped by perceived usefulness. This result was verified through four field studies carried out with 48, 50, and 51 individuals from the manufacturing, financial, accounting, and banking sectors, respectively (2, 2000).

Even with the advances proposed by TAM2, Viswanath Venkatesh and Hillol Bala (3) pointed out in 2008 that the low adoption and use of technology in organizations remained a matter of concern. At that time, systems evolved to support decision-making, planning, and the management of supply chains and business resources, as well as customer relationship management. In this way, the low adoption and use of available technologies revealed a contradictory scenario regarding the promises of the technology for organizations.

The productivity paradox, presented by Venkatesh and Davis (2), expressed the divergence between investments in technology and business performance. This problem became even more pressing due to the technology failures at Nike in 2000, which cost $100 million and led to a 20% drop in stock value, and at Hewlett-Packard in 2004, which caused a financial impact of $160 million (3). The paradox became more concerning given that the global investment in technology was expected to increase by 7.7% per year from 2004 to 2008, compared to 5.1% from 2000 to 2004.

Considering the latent losses, the evolution of technological systems in the business context, and the prospect of increasing investments in technology to boost productivity, the scenario no longer seemed reasonable, as it resulted in losses. Hence, it became even more necessary to understand the factors that lead to the adoption and use of technology by "[...] identifying interventions that could influence adoption and use of new ITs, which can aid managerial decision making on successful IT implementation strategies" (3, p. 274).

TAM2 had reached successful rates of 37% to 52% in terms of intention to use. However, Venkatesh and Davis (2, p. 2000) indicated that "more broadly, future research should seek to further extend models of technology acceptance to encompass other important theoretical constructs". This statement, along with the productivity paradox, technology costs, and systems evolution, was based on the perspective that TAM2 expanded the factors predicting perceived usefulness, with no significant changes in perceived ease of use. Thus, building upon perceived ease of use, TAM3 (Figure 4) was proposed by Venkatesh and Bala (3) to increase the accuracy of the model. It is a fusion of TAM2 with the determinants of perceived ease of use, proposed by Venkatesh (18).

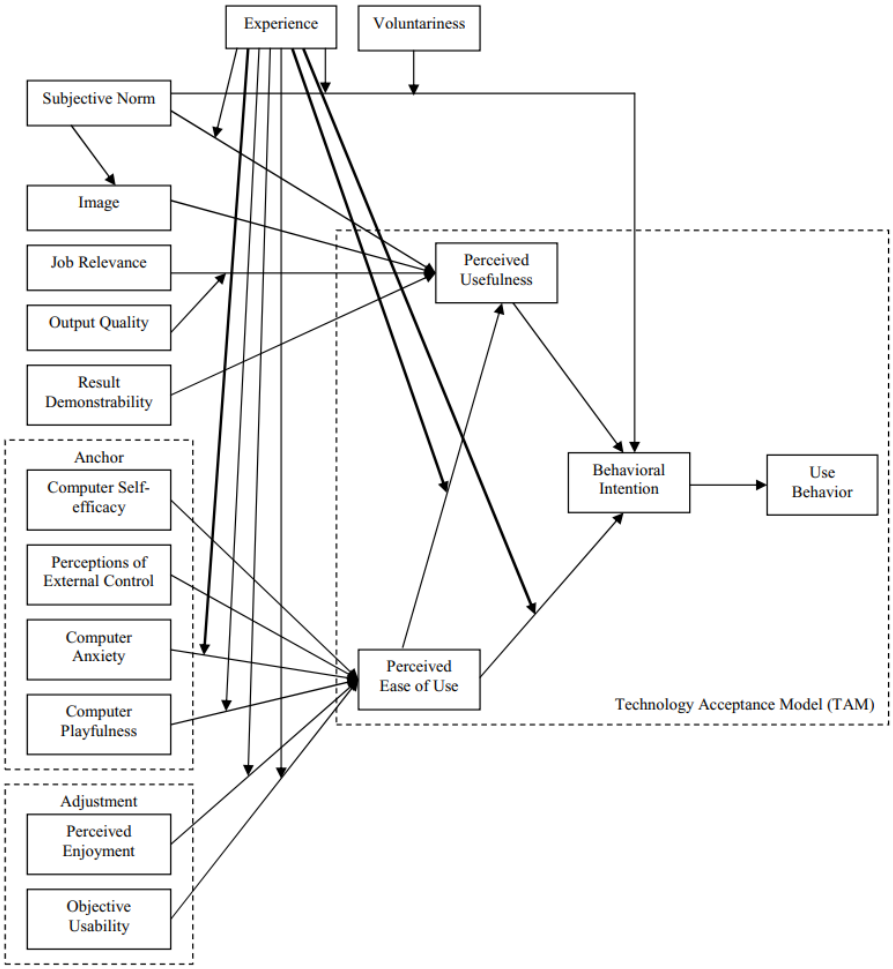

Figure 4. Technology Acceptance Model 3 (TAM3).
Source: (3, p. 280)

The determinants of the perceived ease of use construct are grouped into the anchor and adjustment groups. Regarding the anchor, Venkatesh (2000) "argued that individuals will form early perceptions of the perceived ease of use of a system based on several anchors related to individuals' general beliefs as to computers and computer use" (3, pp. 278). The anchor determinants are articulated as follows:

- Computer self-efficacy: "The degree to which an individual believes that he or she has the ability to perform a specific task/job using the computer" (3, p. 279);
- Perceptions of external control: "The degree to which an individual believes that organizational and technical resources exist to support the use of the system" (3, p. 279);
- Computer anxiety: The degree of "an individual's apprehension or even fear, when she/he is faced with the possibility of using computers" (18, p. 349); and
- Computer playfulness: "[…] 'the degree of cognitive spontaneity in microcomputer interactions'" (3, p. 279).

The pre-judgments made by the individual, based on the anchor group's computer anxiety and computer playfulness determinants, are moderated by the individual's practical experience with the new system. Practical experience also moderates the determinants of the adjustment group, theorized "[...] to play a role in determining perceived ease of use after individuals gain experience with the new system" (3, pp. 278), namely:

- Perceived enjoyment: "The extent to which 'the activity of using a specific system is perceived to be enjoyable in its own right, aside from any performance consequences resulting from system use'" (18, p. 351); and
- Objective usability: "comparison of systems based on the actual level (rather than perceptions) of effort required to complete specific tasks" (18, pp. 350–351).

In addition to the determinants of perceived ease of use, experience also began to moderate the influence of ease of use on

perceived usefulness and behavioral intention (Figure 4). TAM3 was applied in four organizations in the same segments as TAM2 – the manufacturing, financial, accounting, and banking sectors. Data were collected over five months, with samples of 38, 39, 51, and 36 respondents for the aforementioned segments, respectively, validating the model extension.

Supporting this validation, TAM3 explained between 40% and 53% of the variance in behavioral intention. This result is similar to its predecessors – TAM presented an approximate variation of 40% in this factor, while TAM2 ranged between 37% and 52% for the intention to use. However, the new determinants include broader aspects, as well as conditions and scenarios associated with facilitating technology acceptance.

Due to the evolution of technology and the high costs of implementation, TAM3 also presents, according to Venkatesh and Bala (3, p. 303), "[...] direct implications for two types of decision making in organizations—(i) employees' IT adoption decisions; and (ii) managerial decisions about managing the IT implementation process". Therefore, this model is believed to support the organization in decision-making and management.

Technology management decisions predict actions, referred to by the authors as interventions, to be carried out during the pre- and post-implementation stages of the technology adoption. For instance, for complex systems, user participation in the process, along with training and support, is an intervention that tends to favor the perception of ease of use. For voluntary systems, institutional support and system design are actions that tend to influence perceived usefulness. For organizational systems, top management support is a beneficial intervention. Thus, "[...] managers can decide on resource allocation for interventions based on the impact of interventions on different determinants of IT adoption and system types" (3, p. 304).

TAMs, in all versions, continue to be used to this day. In the field of tourism, Silva, Mendes Filho, and Marques Júnior (6) applied the TAM to assess the intention to use cryptocurrencies by managers of tourist developments. As a result, perceived usefulness influences the attitude toward use, while both perceived usefulness and perceived ease of use influence the adoption of cryptocurrencies. Therefore, they conclude that managers demonstrate a positive attitude toward using cryptocurrencies and intend to adopt them as a form of payment.

In the context of informatics applied to health, Adji and Taufik (7) evaluated the use of an application by doctors and professionals using TAM2. They concluded that this model "[...] can explain the variation of the total factor by 73.826%" (7, p. 1).

TAM3 was applied by Kusumastuti et al. (8) in the Islamic accounting sector. The intention was to evaluate the accrual-based accounting systems used in the State Budget and the Treasury System. They concluded that "[...] the accrual-based accounting system in SPAN practically does not provide convenience and tends to have a low intensity of use" (8, p. 97).

Despite the significant use of TAMs over the years, Marikyan and Papagiannidis (12) point out several limitations of these models, such as:

1. Focus on factors that make people use technology, while overlooking its impact on performance;
2. Suggest that the greater the use of technology, the better the performance, which is not valid in practice;
3. Pay little attention to what makes technology useful – namely its design and fit to the task – which are important to achieve high performance through technology use; and
4. Focus on development specifically within the organizational context.

Nevertheless, Marikyan and Papagiannidis (12) point out that these limitations cannot overshadow the contributions of TAM theory.

In this regard, the theories that support the TAM, TAM2, and TAM3 show theoretical and practical robustness, as they were developed between 1989 and 2008 —the years corresponding to TAM and TAM3 —and have been empirically applied across different contexts (6, 7, 8). The question is whether the TAM, in all its versions, remains robust, as noted by Garcia et al. (11), or whether the limitations identified by Marikyan and Papagiannidis (12) signal the need for a new version of the model. In order to provide a better understanding of the matter, a review of the literature is conducted to support the analysis of practical applications of TAM, with the aim of identifying which of the two perspectives shows greater differentiation. The methodological procedures adopted for this research are described next.

3 Methodology

This research is characterized as basic research, exploratory in nature and qualitative in its analysis. Regarding the methodological procedures, a systematic review of the

literature and content analysis (19) are employed to perform a qualitative analysis of relevant bibliographic documents (i.e., scientific research results).

Based on this characterization, the following steps are taken to conduct this research:

1. Identification of research with practical applications of TAM;
2. Selection of research to be included in the analysis corpus;
3. Analysis of the research corpus to identify the dominance of TAM applications in their original versions or transformations (i.e., adaptations and extensions).

A systematic literature review was applied to identify research with practical applications of TAM (step 1). A research protocol (Table 1) was adopted based on the one proposed by Dresch, Lacerda, and Antunes Jr. (20).

Table 1. Research Protocol.

Aspect	Description
Conceptual framework:	Practical applications of TAM.
Context:	Applied surveys that measure technology acceptance through TAM.
Time horizon:	2017-2021.
Theoretical current:	The research aims to measure the adoption of technologies through the perspective of users' acceptance.
Languages:	Portuguese and English.
The question underlying the review:	What are the practical applications of TAM?
Exclusion criteria:	1. Research that does not contain the search terms in the keywords; 2. Research other than articles from scientific journals (e.g., proceedings, abstracts, etc.), 3. Research whose abstract does not mention the TAM acceptance model.
Search terms:	"Technology acceptance model" in Keywords
Data source:	SCOPUS

The SCOPUS database was selected based on a report by Falagalas et al. (21) and Faria et al. (22), who stated that it covers research since 1966 and indexes 12,850 journals from different areas. Thus, considering the proposition of the TAM in 1989 and application of this model in several areas (6, 7, 8), this database is regarded as relevant for the purposes of this research.

Subsequently, the decision regarding which research was considered for the analysis corpus (step 2) was made by applying the exclusion criteria established in Table 1. Therefore, this research only included scientific articles available for download that applied TAM, regardless of its extensions or adaptations.

Finally, step 3 consisted of analyzing the research corpus to identify the dominance of TAM applications, whether in their original version or in modified versions (i.e., adaptations and extensions). At this stage, content analysis is applied, which consists of analyzing communications through systematic and objective procedures to describe the content of the messages in order to obtain indicators (quantitative or not) that allow knowledge to be inferred (19).

In this sense, the articles included in the corpus (step 2) were analyzed to identify which version of the TAM prevails (step 3). This is achieved through content analysis, which enables inferring whether the original version of the TAM or its adapted and extended versions are more prevalent in the corpus is applied.

4 Discussion

The search was conducted on December 18, 2021, at 08:42, according to the terms established in the research protocol (Table 1). The initial search returned 1,726 documents. Of these, 317 articles were excluded because they did not contain the search terms in the keywords (exclusion criterion 1). This occurred because SCOPUS applies its own indexing during searches, which may result in false positives. Consequently, 1,409 articles remained after applying this criterion (1,726 − 317).

At this stage, all remaining articles were from scientific journals (exclusion criterion 2). Subsequently, based on abstract analysis, 634 articles that did not mention the TAM (exclusion criterion 3) were excluded. These documents were not included because other models, such as UTAUT, match the search terms but do not align with the purposes of this research. Thus, the resulting number was 775 (1,409 - 634) documents.

After that, the articles were read in order to identify whether TAM was applied or not (exclusion criterion 4). A total of 170 studies were discarded, as they consisted of reviews and/or comparisons of acceptance models, among others, without presenting a practical application of the TAM. Thus, the final corpus of this search consists of 605 (775 – 170) scientific articles.

Only six studies, namely Estrada Villa, Marín, and Salinas (23); D'Souza, Joshi, and D'Souza (24); Knox et al. (5), Oliveira Jr., Zorzo and Neu (25); Saadatzi et al. (26) and Al-Maroof and Al-Emran (27), employed the TAM. The first four studies addressed software application technologies, while the remaining two focused on a healthcare robot and on online teaching, the latter using the Classroom platform.

The results reveal that TAM continues to be used and applied to evaluate technologies that are not in line with its inception time. When Davis (1) proposed the TAM, the intention was to understand why users adopted personal computing and information systems. The study by Saadatzi et al. (26), which applied the model to healthcare robots, suggests that the TAM continues to be suitable in contemporary contexts.

However, 401 extensions and 198 adaptations of the TAM were identified [1]. Following the inference that this model is contemporary, the number of adaptations (i.e., joining models) and extensions (i.e., addition and/or removal of predictors) leads to a reflection on why this happens. When analyzing the predictors, there are a total of 737 different articles presenting extensions and 483 unique adaptations, which allows us to infer that the aspects (i.e., factors) analyzed by the TAM are insufficient to assess the adoption of specific technologies.

As with extensions, research by Caffaro et al. (28) and Michels et al. (29) evaluated the acceptance of drone technology in Italian and German agriculture, respectively. Caffaro et al. (28) announce that using drones in agriculture can improve production, minimize costs, and conserve resources; however, adoption remains limited, thereby justifying the research. Caffaro et al. (28) extended the TAM with 18 predictors, with a total of 10 being confirmed after the application of the model (Figure 5). In this extension, the perceived ease of use (PEU) was considered but not confirmed, while the perceived usefulness (PU) remains a determining factor in the intention to adopt drone technology in agriculture.

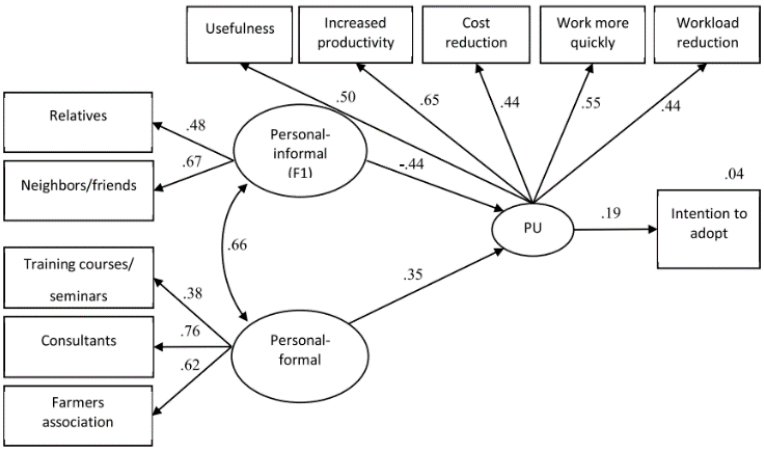

Figure 5. Extension 203 of TAM.
Source: (28, p. 6)

Likewise, Michaels et al. (2021) also identify the low adoption of drones in agriculture as the motivation for their research. Michels et al. (29) extended the TAM by incorporating the predictors of attitude of confidence in using drones in agriculture and job relevance of drone technology in agriculture (Figure 6).

[1] Access 10.5281/zenodo.11125946 (after publication) or supplementary document to the submission.

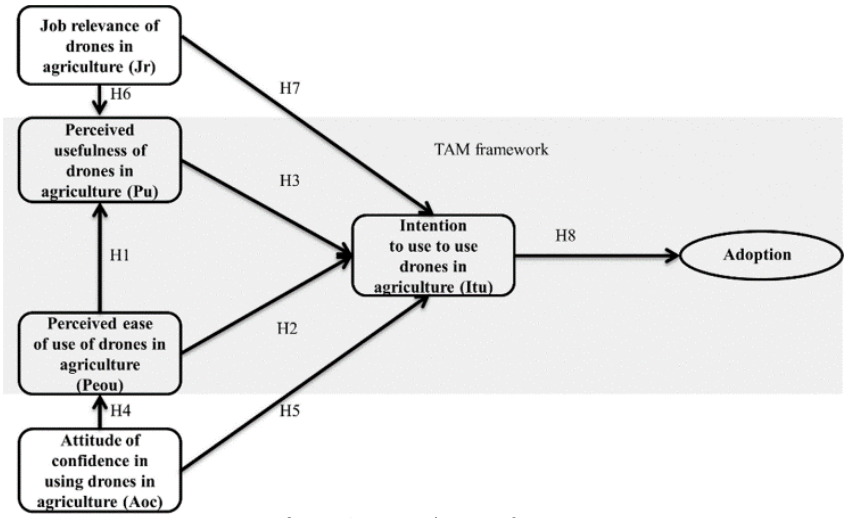

Figure 6. Extension 11 of TAM.
Source: (29, pp. 1732)

The vast amount of information required to operate drone technology justifies the inclusion of confidence in using drones in agriculture as a predictor. Therefore, producers must have confidence in the use of this technology for its adoption in precision agriculture (29). The job relevance of drones in agriculture is based on the study by Venkatesh and Davis (2), in which the job relevance predictor was added to TAM2. However, this factor was renamed in Michels et al. (29).

The hypotheses related to the predictors (H4, H5, H6, and H7) were confirmed, which led Michels et al. (29, p. 1742) to conclude that "[…] the results contribute to further empirical evidence towards the robustness of the TAM and its generality across several research disciplines". According to these researchers, despite the limitations of the explanatory and predictive power of the TAM, it continues to be the most widely applied model for predicting the intention to use technology.

In the context of the studies that conducted adaptations, the study by Bhardwaj, Garg, and Gajpal (30) investigated blockchain technology in supply chains in India, motivated by the advantages of cost optimization, effective and verified record-keeping, transparency, and route tracking. The adaptation, called TAM-TOE-DOI (Figure 7), results from the integration of TAM with the Diffusion of Innovation (DOI) and Technology-Organization-Environment (TOE) models.

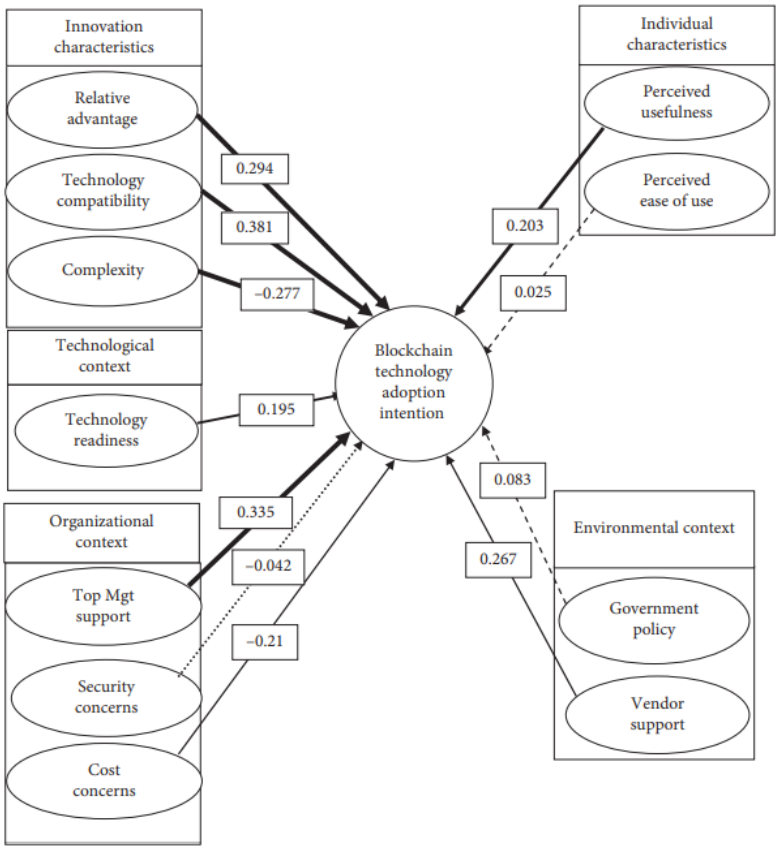

Figure 7. Adaptation 75 of TAM.
Source: (30, p. 10)

These TAM variations come from the technologies analyzed. Technologies range from physical systems, such as vehicles (31), robots (32), and wearables (33), to logical systems, such as chatbots (34), e-commerce (35), cryptocurrencies (36), and management software (37).

Thus, there is the possibility that the combination of models and the incorporation of new predictors are justified when a technology displays unique characteristics compared to other models. For example, cryptocurrencies, vehicles, and e-commerce may consider aspects related to security, while wearables, such as smartwatches, tend to consider other predictors like surface texture.

The differing perspectives observed in the practical use of TAM unveiled by this research allow us to infer that the study by Saadatzi et al. (26), which analyzed healthcare robot technology, presents TAM as a contemporary theory. However, the extensions (28, 29) and the adaptation (30) lead to the inference that the aspects (i.e., factors) analyzed by TAM are insufficient to assess the adoption of specific technologies.

5 Conclusion

Based on the analyses conducted in this research, we understood that the foreseen prospects for TAM are not dichotomous; thus, three conclusions were reached. First, the practical dominance of the application of TAM comes from its extensions and adaptations and not from its original model. This outcome does not mean that the predictors of TAM, TAM2, and TAM3 are inadequate but that, according to the technology and the researcher's perspective, they are subject to adjustments to provide a better fit between the model and reality.

Secondly, in the light of the above, it is concluded that the TAM is theoretically robust, since adaptations and extensions would not occur otherwise. Thus, despite the limitations presented by Michels et al. (29) and Marikyan and Papagiannidis (12), it is plausible to determine that the TAM theory remains robust, as defined by Garcia et al. (11) and Michels et al. (29).

The third conclusion derives from the previous considerations and involves a reflection on whether it would be appropriate to update the TAM and call it TAM4. However, given the existence of 401 adaptations and 198 extensions, the proposition of one more structure would not eliminate the different perspectives regarding potential predictors to be included in future research. It is likely that this would lead to the rise of new adaptations

and extensions. Furthermore, this would increase the variability of framework applications, as identified through this research, without addressing all technology-specific nuances regarding acceptance determinants required for a broad and robust theory.

Nevertheless, emerging technologies cannot be predicted with certainty, while the robustness of a theory depends on what has been previously and correctly theorized. This consequence means that a theory that evolves is one that provides the means for others to do so. This feature is plausibly attributed to the TAM, given the discussion above.

In the meantime, we believe this research contributes by investigating the theoretical-empirical evolution of acceptance models, specifically the TAM. The theory is thus explained through its evolutionary development and practical application over time, endorsing the science-technology-society triad and supporting broader understanding and practices.

Regarding limitations, this research relied on a single database to operationalize the systematic literature review. Although the number of analyzed documents is quantitatively representative, future research could expand this investigation by including additional scientific databases.

References

1. Davis, F.D. (1989). Perceived Usefulness, Perceived Ease of Use, and User Acceptance of Information Technology. *MIS Quarterly*, 13,3:319–340.

2. Venkatesh, V., & Davis, F.D. (2000). A Theoretical Extension of the Technology Acceptance Model: Four Longitudinal Field Studies. *Management Science*, 462:186–204.

3. Venkatesh, V. & Bala, H. (2008). Technology Acceptance Model 3 and a Research Agenda on Interventions. *Decision Sciences*, 392:273–315.

4. Villa, E.J.E., Marín, V.I., & Salinas, J. (2021). Research Skills for Information Management: Uses of Mobile Devices in Research Training. *Education Sciences*, 11:749–760.

5. Knox, L., Gemine, R., Rees, S., Bowen, S., Groom, P., Taylor, D., & Lewis, K. (2021). Using the Technology Acceptance Model to conceptualise experiences of the usability and acceptability of a self-management app (COPD. Pal®) for Chronic Obstructive Pulmonary Disease. *Health and technology*, 11,1:111–117.

6. Silva, G., Mendes Filho, L., & Marques Júnior, S. (2022). Intenção de usar criptomoedas por gestores de empreendimentos turísticos: uma abordagem utilizando o Technology Acceptance Model (TAM). *Revista Brasileira de Pesquisa em Turismo*, 16:1–15.

7. Adji, H.I., & Taufik, T.A. (2022). Analysis of the adoption and commercialization of XYZ app using TRL, CRL, TRI2 and TAM2. *In: The 5th International Conference on Management of Technology, Innovation, and Project*, 1–9.

8. Kusumastuti, R., Touriano, D., Rosita, S., & Fatricia, R. S. (2022). Effectiveness of accrual basis accounting system in state budget and treasury system in TAM 3 framework. *Journal of Islamic Accounting and Finance Research*, 4:1, 97–130.

9. Al-Dokhny, A., Drwish, A., Alyoussef, I., & Al-Abdullatif, A. (2021). Students' intentions to use distance education platforms: An investigation into expanding the technology acceptance model through social cognitive theory. *Electronics*, 10,23:2992–3015.

10. Zhang, X., Tlili, A., Shubeck, K., Hu, X., Huang, R., & Zhu, L. (2021). Teachers' adoption of an open and interactive e-book for teaching K-12 students Artificial Intelligence: a mixed methods inquiry. *Smart Learning Environments*, 8,1:1-20.

11. Garcia, S.F.A., Bottaro, H.Z., da Silva, D.D.S., & Galli, L.C.D.L.A. (2020). O impacto da facilidade de uso percebida na adoção do Instagram. *In: XXIII Seminários em Administração*, SemeAd, 1–15.

12. Marikyan, D., & Papagiannidis, S. (2022) Technology Acceptance Model: A review. In Papagiannidis, S. (Ed), *TheoryHub Book*. http://open.ncl.ac.uk

13. Tamilmani, K., Rana, N. P., Wamba, S. F., & Dwivedi, R. (2021). The extended Unified Theory of Acceptance and Use of Technology (UTAUT2): A systematic literature review and theory evaluation. *International Journal of Information Management*, 57, 102269.

14. Fishbein,M, & Ajzen, I. (1975). *Belief, Attitude, Intention and Behavior: an Introduction to Theory and Research*.

15. Davis, F.D., Bagozzi, R.P., & Warshaw, P.R. (1989). User Acceptance of Computer Technology: A Comparison of Two Theoretical Models. *Management Science*, 35,8:982–1003.

16. Bandura, A. (1977). Self-efficacy: Toward a unifying theory of behavioral change. *Psychological Review*, 84,2:191–215.

17. Moore, G.C.I., & Benbasat, I. (1991). Development of an instrument to measure the

perceptions of adopting an information technology innovation. *Inform. Systems Res*, 2:192–222.

18. Venkatesh, V. (2000). Determinants of perceived ease of use: Integrating perceived behavioral control, computer anxiety and enjoyment into the technology acceptance model. *Information Systems Research*, 11:342–365.

19. Bardin, L. (1977). *Análise de Conteúdo*.

20. Dresch, A, Lacerda, D. P., & Antunes Jr., J. A. V. (2020). *Design Science Research: Método de Pesquisa para Avanço da Ciência e Tecnologia*.

21. Falagalas, M.E., Pitsouni, E.I., Malietzis, G.A., & Pappas, G. (2008). Comparison of PubMed, Scopus, web of science, and Google scholar: strengths and weaknesses. *The FASEB journal*, 22,2:338–342.

22. Faria, V.F., Corrêa, F., Lima, P.P., Santos Jr, Z., & Dutra, F. G.C. (2022). Propósitos para mensuração do Capital Intelectual. *Fronteiras de Representação do Conhecimento*, 1:105–112.

23. Estrada Villa, E. J., Marín, V. I., & Salinas, J. (2021). Research skills for information management: Uses of mobile devices in research training. *Education Sciences*, 11(11), 749.

24. D'Souza, D.J., Joshi, H.G., & Prabhu, R. (2021). Assessment of Consumers Acceptance of E-Commerce to Purchase Geographical Indication Based Crop Using Technology Acceptance Model (TAM). *Agris On-line Papers in Economics and Informatics*, 13,3:25–33.

25. Oliveira Jr, E., Zorzo, A.F., & Neu, C.V. (2020). Towards a conceptual model for promoting digital forensics experiments. *Forensic Science International: Digital Investigation*, 35:1–15.

26. Saadatzi, M.N., Logsdon, M.C., Abubakar, S., Das, S., Jankoski, P., Mitchell, H., Chlebowy, D., & Popa, D.O. (2020). Acceptability of using a robotic nursing assistant in health care environments: experimental pilot study. *Journal of medical Internet research*, 22,11:1–7.

27. Al-Maroof, R.A.S., & Al-Emran, M. (2018). Students acceptance of google classroom: An exploratory study using PLS-SEM approach. *International Journal of Emerging Technologies in Learning*, 13,6:112–123.

28. Caffaro, F., Cremasco, M.M., Roccato, M., & Cavallo, E. (2020). Drivers of farmers' intention to adopt technological innovations in Italy: The role of information sources, perceived usefulness, and perceived ease of use. *Journal of Rural Studies*, 76:264–271.

29. Michels, M., Hobe, C.F.V., Ahlefeld, P.J.W.V., & Musshoff, O. (2021). The adoption of drones in German agriculture: a structural equation model. *Precision Agriculture*, 22,6: 1728–1748.

30. Bhardwaj, A.K., Garg, A., & Gajpal, Y. (2021). Determinants of Blockchain Technology Adoption in Supply Chains by Small and Medium Enterprises (SMEs) in India. *Mathematical Problems in Engineering*, 2021:1–14.

31. Jaiswal, D., Kaushal, V., Kant, R., & Singh, P.K. (2021). Consumer adoption intention for electric vehicles: Insights and evidence from Indian sustainable transportation. *Technological Forecasting and Social Change*, 173:1–13.

32. Martins M., & Costa, C. (2021). Are the Portuguese ready for the future of tourism? A technology acceptance model application for the use of robots in tourism. *Journal of Tourism and Development*, 36,2:39–54.

33. Al-Maroof, R.S., Alhumaid, K., Alhamad, A.Q., Aburayya, A., & Salloum, S. (2021). User acceptance of smart watch for medical purposes: an empirical study. *Future Internet*, 13,5:1–19.

34. Kim, A.J., Yang, J., Jang, Y., & Baek, J.S. (2021). Acceptance of an Informational Antituberculosis Chatbot Among Korean Adults: Mixed Methods Research. *JMIR mHealth and uHealth*, 9,11:1–17.

35. Bauerová, R., & Klepek, M. (2018). Technology acceptance as a determinant of online grocery shopping adoption. *Acta Universitatis Agriculturae et Silviculturae Mendelianae Brunensis*, 66,3:737–746.

36. Nadeem, M.A., Liu, Z., Pitafi, A.H., Younis, A., & Xu, Y. (2021). Investigating the adoption factors of cryptocurrencies—a case of bitcoin: empirical evidence from China. *SAGE open*, 11,1:1–15

37. Mohammed, A.H., Mousa, A.H., Almeyali, N.M., & Nasir, I.S. (2021). M2CIM-DSS: A Model for Measuring Continuance Intention in Decision Support Systems. *Indonesian Journal of Electrical Engineering and Informatics*, 9-3:756–765.

RECyT
Year 27 / Nº 44 / 2025 /
DOI: https://doi.org/10.36995/j.recyt.2025.44.010

Accessibility in Pure Data for visually impaired musicians: a real-time soundscape strategy

Accesibilidad en Pure Data para músicos con discapacidad visual: una estrategia de paisaje sonoro en tiempo real

Evandro J., Grisolio[1, *]; Antonio C., Penteado[1]; Vilson, Zattera[1]; Guilherme N. N., Nogueira[2]; Percy, Nohama[2]

1- Music Postgraduate Programme. Art Institute. University of Campinas (UNICAMP). SP, Brazil.
2- Postgraduate Programme in Health Technology (PPGTS). Pontifical Catholic University of Paraná. Curitiba, PR, Brazil.

* E-mail: nogueira.g@pucpr.br

Received: 28/07/2024; Accepted: 24/06/2025

Abstract
Background: Pure Data (Pd) is a predominantly visual programming language widely used by musicians in the process of composition and musical performance that involves sound synthesis. This visual characteristic implies poor accessibility for a visually impaired musician (VIM) because screen readers do not allow recognition and/or manipulation of language elements. Objectives: This work aims to present an inclusive strategy that enables VIM to interact with other musicians in real-time during performances. Methods: A sighted musician programmed a Pd script consisting of five patches. Switches and potentiometers of a MIDI controller matched elements of the script, activating and modulating parameters of sound clips. The VIM uses the screen reader to access Pd, open the programmed code, configure the MIDI controller, and enable audio output. The performance is executed by the VIM. Results: The result of the elaborate composition was a live soundscape performance that had similarity in the manipulation of the MIDI controller with that of the sighted musician. Conclusion: These strategies enabled a VIM to perform autonomously in real time using Pd patches, fostering interaction with sighted musicians and expanding accessibility.

Keywords: Accessibility; Visually impaired musicians; Pure Data; MIDI controller; Free improvisation.

Resumen
Introducción: Pure Data (Pd) es un lenguaje de programación predominantemente visual ampliamente utilizado por músicos en los procesos de composiciones e interpretaciones musicales que implican síntesis sonora. Esta característica visual implica una accesibilidad deficiente para un músico con discapacidad visual (MDV), ya que los lectores de pantalla no permiten reconocer y/o manipular los elementos del lenguaje. Objetivos: Este trabajo pretende presentar una estrategia inclusiva que permita a los MDV interactuar con otros músicos en actuaciones en directo. Métodos: Un músico vidente programó un guión de Pd compuesto por cinco parches. Los interruptores y potenciómetros de un controlador MIDI se ajustaban a los elementos del guión, activando y modulando los parámetros de los clips de sonido. El MDV utiliza el lector de pantalla para acceder a Pd, abrir el código programado, configurar el controlador MIDI y habilitar la salida de audio. El MDV ejecuta la actuación. Resultados: El resultado fue una actuación de paisaje sonoro en directo que presentaba similitudes en la manipulación del controlador MIDI con la del músico vidente. Conclusión: Estas estrategias permitieron a un MDV actuar de autónomamente en tiempo real utilizando parches de Pd, favoreciendo la interacción con músicos videntes y ampliando la accesibilidad.

Palabras clave: Accesibilidad; Músicos con discapacidad visual; Pure Data; Controlador MIDI; Libre improvisación.

Introduction

Pure Data (Pd) is an open-source, free-to-use, visual programming language [1] that focuses on the production of computational, electro-acoustic, and/or interactive music and multimedia works, thereby promoting real-time interaction among audio, MIDI, graphics, and video [2]. These characteristics confer efficiency, versatility, and robustness, making Pd a widely used tool by musicians and researchers [3-5]. A notable advantage is the active community of contributors [6], which benefits those who want to produce multimedia. Collaboration can be a crucial tool for boosting creativity in audio production, especially when a community of collaborators is available.

A recent study found that audio producers must constantly make judgments based on audio and visual evidence, using complex production tools [7]. Therefore, there is a challenge for audio producers who are either blind or have low vision. In this paper, subjects from both impairment categories are referred to as visually impaired (VI) musicians. The problem of audio equalisation was tackled by researchers who developed the HaptEQ system. It is one of the approaches to increase accessibility of digital audio production

tools for VI producers. It consists of a physical setup that uses passive tactile elements as surrogates for virtual controllers on the screen [8]. However, live digital audio synthesis remains problematic for contemporary music VI performers.

Musicians can develop Pd projects to produce audio through live presentations or live performances [9, 10]. However, despite its performance and versatility, not everything in Pd is accessible, especially for VI users. The most striking feature of this system is the systematic use of the mouse as a device that allows changing the code and providing visual feedback [9]. The creation and maintenance of source code are based on systematising small boxes (objects) that use parameters configured by numbers and letters. These objects are interconnected by virtual lines, forming a 'set of objects' (a.k.a. patch) to produce the sound result [11]. Figure 1 presents an example Pd patch. A simple analysis reveals that this fact makes it impossible for a VI musician to exploit its resources.

Assistive Technology (AT) solutions enable VI users to access digital technologies. AT is a set of resources and services that enable or enhance the functional abilities of people with disabilities and promote autonomy and inclusion [12]. Screen readers (e.g., NonVisual Desktop Access – NVDA [13]) are the primary resources used for digital inclusion. In principle, these ATs guarantee accessibility to VI users, enabling Internet browsing and the operation of various software. It expands and enhances processes related to education, communication, work, socialisation, art, entertainment, and other activities.

NVDA is one of the most widely used screen readers today, ensuring accessibility and autonomy for more than 100,000 people with visual impairment in more than 150 countries [14]. Also noteworthy is its gratuity and updates from voluntary contributions from developers, making it an attractive alternative for users and contributing to digital inclusion. However, previous studies have shown that not all graphical elements on a screen can be accessed by screen readers [15]. Relying solely on a conventional screen reader for media editing and production may not be sufficient. Lazar et al. [16] investigated its use when browsing web pages and identified many inconsistencies. The Pd use case is an excellent example of a software platform that presents difficulties to VI musicians using only a screen reader. Screen readers are ineffective at interpreting images and graphics, such as those used to manipulate Pd visual programming objects, because they do not provide adequate feedback from the interface [17].

The visual elements in the Pd canvas cannot be converted to audio feedback [15]. This limitation prevents VI musicians from fully exploiting its features and capabilities. Therefore, a VI musician cannot access Pd, which compromises the perspectives on editing, musical creation, and interaction with other musicians on this platform. Therefore, it would be of particular interest to develop an alternative mode for the operation of these elements of Pd. Thus, the objective of this work, as a preliminary study, is to promote accessibility through hardware for a visually impaired musician, allowing him to generate soundscapes in real time and autonomously, overcoming the inaccessibility of Pure Data's graphical user interface.

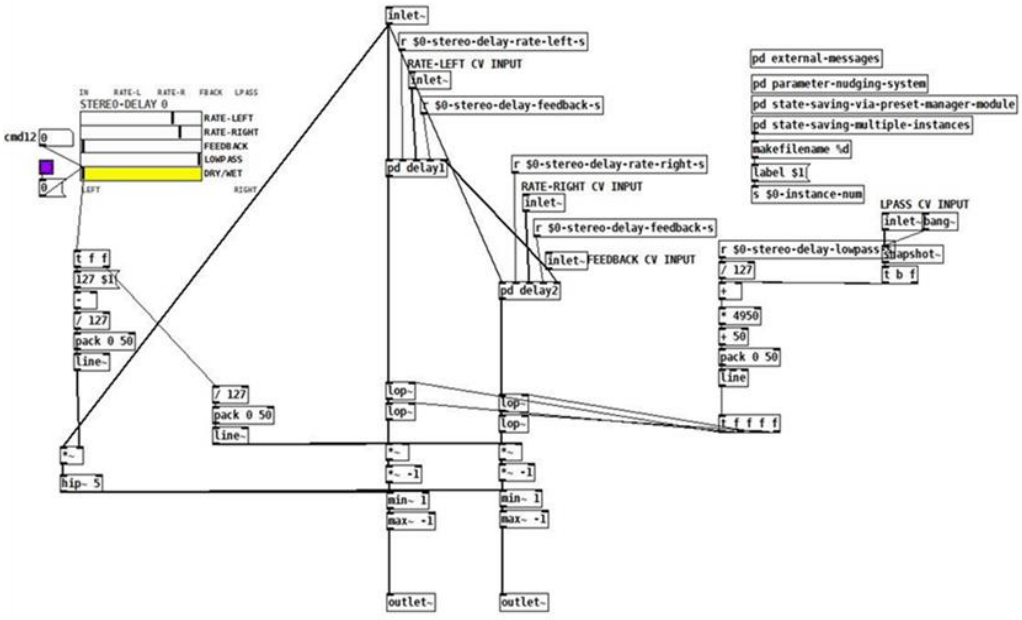

Figure 1. Example Pd patch (Source: authors).

Materials and Methods

The following subsections present the resources used by a VI musician in the approach performed and explain the method.

Computer

The solution in this work involves using a computer as the central element of the devices, with the sound synthesis software installed. The operating system (OS), hardware, and connectivity characteristics may determine the audio performance and quality. The system must have sufficient RAM space and processing power to run the patches, and the OS and screen reader must not negatively impact sound quality or synchronisation. In addition, the computer must provide internet connectivity (for remote performances) and at least one USB port.

In the present work, we used an Avel laptop (model A70 MOB) equipped with an Intel Core TM i7-11800H processor (2.3 GHz), with a 24 MB cache, 32 GB Dual Channel RAM, 1 TB SSD M.2 NVME hard drive, and GeForce RTX 3060 (6 GB GDDR6) video card running Windows 11 Server. All OS updates for November 2022 have been installed. The laptop had three USB 3.0 ports and one Realtek Audio sound card. DELL USB speakers were connected to the USB port and provided audio feedback to the VI musician.

Pure Data

In the proposed approach, Pure Data was used in its stable Vanilla 0.51.4 version. No additional external was incorporated into the installation.

MIDI Controller

This device consists of pushbuttons, knobs, and sliders, which enable the handling and control of resources, such as functions and commands in music production programs [18], replacing the computer mouse for manipulating objects in Pd. Thus, the difficulty of operating the virtual elements is minimised.

The CR-9 controller (KFX, China) was used (Figure 2), consisting of 20 pushbuttons, nine knobs (red box), nine vertical sliders (green box), and one horizontal slider (yellow box). All pushbuttons are programmable, but the ones used in this work are highlighted in the white box.

Figure 2. The CR-9 (KFX, China) MIDI controller used for the desired performance (Source: authors).

In this model, when triggered, each physical control (pushbutton, knob, or slider) sends the computer a unique number that identifies it, which can be programmed and reprogrammed, thereby modifying the original mapping of the controls. This mapping can be called a keymap. Another way to alter the keymap in real time is to use so-called banks, of which the CR-9 controller has 4. Banks are selected, and the entire keymap is modified. Only a single bank was used in the performance described in this text. However, the original keymap of the controller must be changed to match the patch objects.

Screen Reader

The screen reader used in this study was NVDA 2021.2, a free, open-source software with a large developer community. It has stable integration with the Windows OS and third-party software. An important feature is that NVDA does not use a video interception driver to avoid possible conflicts between hardware and software.

Assistive strategy

The intended strategy is divided into three stages:

a) A sighted musician

i. Creates a patch from scratch or employs other ready-made patches.
ii. Creates sound samples for use in live performances.
iii. Selects the MIDI controller.
iv. Configures keymap mapping the MIDI controller's knobs, sliders, and pushbuttons to access the objects in the new patch. It has a function that is analogous to that of the mouse.

b) Preparing to perform, a VI musician

i. Connects the MIDI controller to the computer USB port.
ii. Uses a screen reader (e.g., NVDA) to browse the OS and open the Pd patch file.
iii. Accesses the Pd menus to perform basic settings, such as enabling the MIDI controller and selecting audio inputs and outputs.

c) Free improvisation execution

i. Can be performed autonomously by a VI musician.

The Pd programming in this project consisted of five patches (Figure 3) to produce the audio in the output (dac~): two for sound oscillators, two for effects (reverb and delay), and one for controlling 17 audio samples. The configuration of the Pd

objects on the MIDI controller occurred as follows: The first oscillator (osc1) had its volume, height, time, and random note parameters set individually on the MIDI controller sliders, and a delay effect was added to the output (pd delay 2). The volume control is set up on another slider. The second oscillator (osc 2) had the same parameters as osc1, configured individually in the MIDI controller knobs. Additionally, a reverb effect was added to the output of osc2 (pd starlight), and its volume was set up in another knob.

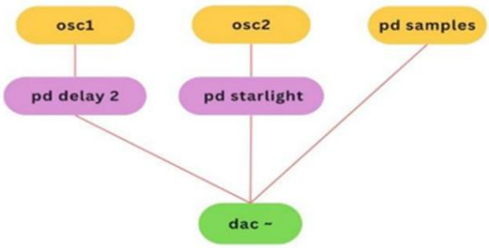

Figure 3. Block diagram exemplifying the functional links of patches (Source: authors).

The samples were programmed in the patch “pd samples” and divided into two groups. The first group (gp1) comprised samples in continuous execution (loop), and the second group (gp2) comprised short samples with durations up to 30 s. The gp1 consisted of four samples, and each sample's volume control was configured individually in sliders. The second group (gp2) consisted of 9 samples, each of which was activated separately by triggering pushbuttons. These buttons fire the samples without the volume control programmed in gp1. All channels were stereophonic. To explore the effects of sound spatialization, a sample of flying flies was configured on the MIDI controller's horizontal slider, allowing the sound to move from right to left and back again. Table 1 lists the continuous execution samples, whereas Table 2 lists short samples used in the performance.

Table 1. Description of continuous samples and mapping in the MIDI controller.

Samples	Audio description	Mapping (see Figure 2)
Pad A	Synthesiser timbre formed by overlapping several notes of A in different octaves	Slider 1
Pad B	Synthesiser timbre formed by overlapping several notes of A in different octaves	Slider 2
Didgeridoo	Australian Aboriginal musical instrument	Slider 3
Nigerian	Percussion of a cultural manifestation of a Nigerian group	Slider 4
Waters	Running water	Knob 1
Birds	Flock of birds in a forest	Knob 2
Wolf	Overlap of several howling wolves	Knob 3
Flies	Several flies flying	Horizontal slider AB

Table 2. Description of short samples and mapping in the MIDI controller.

Samples	Audio description	Mapping (see Figure 2)
Light 1	Short excerpt from the intro to the song “In the Light” by Led Zeppelin	Pushbutton 1
Light 2	Short excerpt from the intro to the song “In the Light” by Led Zeppelin	Pushbutton 2
Winds 1	Wind blowing	Pushbutton 3
Winds 2	Wind blowing and sea waves	Pushbutton 4
Whale	Song of two whales	Pushbutton 5
Ant	Sounds emitted by ants	Pushbutton 6
Frog	Various croaking frogs	Pushbutton 7
Eagle 1	Squeaks of a type of eagle	Pushbutton 8
Eagle 2	Squeaks of another type of eagle	Pushbutton V

Considerations for this Preliminary Study

Because this preliminary study is a proof-of-concept to test whether the patch-programmed system enables VI musicians to access a visual-programming sound-synthesis software, no submission to the ethics committee for research with human beings was required. One of the co-authors is a blind musician, a professor of contemporary music, and a member of research groups on accessibility for VI musicians. Even though no solid experience with sound synthesis is demanded to operate the patch, for better effectiveness and satisfaction, it is interesting that the VI musician know in advance all sounds, modulations, delays, and other effects available and which controls of the MIDI controller trigger them and are mapped by the Pd patch, as well as have knowledge of computer operation using screen readers.

The VI musician opened the Pd patch and used a standard computer input to connect to and enable the MIDI controller. Then, the VI musician selected the laptop speaker as the audio output using a screen reader to navigate the options.

The intended performance was individual and had no audience. It should be noted that the proposed methods did not include aesthetic analysis, as compositional procedures are not the focus of this study. Also, sound quality analysis was not conducted in this work.

Results

The idea of this work is to enable a VI musician to produce sounds, especially timbres, using Pure Data, within an aesthetic of “free improvisation” which, according to Derek Bailey, “… has no stylistic or idiomatic commitment. It has no prescribed idiomatic sound” [19].

The results of the first part of the method were obtained by a sighted musician with approximately one year of experience in sound synthesis using Pd. It took him about 25 days to get the finished version. Sound samples were created and added

to the patch within 5 days. Keymapping and MIDI controller selection took 11 days.

The proposed strategy requires the VI musician to connect the MIDI controller to the computer, access the OS, and open the Pd patch. This task is elementary and can be completed quickly. However, for the execution of the third part of the strategy, the VI musician took 4 days to feel safe operating all the available sound variations in this patch.

The programmed Pd patch was named “Forest Night”. This patch was used in the recorded free improvisation video, in which the initial sensation refers to a forest at night, in a ghostly and suspenseful environment that was initially created by the superposition of continuous samples (Pad sounds), a synthesiser timbre formed by the sum of several A notes of different octaves, and the sound of an Australian Aboriginal instrument. Then, the combination of different inserted sounds resembles the environment of running water in a cave and the sounds of birds, which are emphasised by the reverberation effect. Other sounds, such as those of ants, eagles, and whales, as well as percussive sounds, are added to the performance.

The “Forest Night” patch was operated and performed by a blind musician, and the video shows the hand movements on the controller and the spatial location at the performance time.

The result of the elaborate proof of concept was a free improvisation performance also entitled “Forest Night,” performed by a blind musician [20], which was not presented to an audience and was later recorded and reproduced. Figure 4 illustrates a pose of the performed dynamics, which can be followed on YouTube.

Table 3 shows the instant (in seconds) at which each sample is first committed in the recorded performance, for better description and understanding of the sounds. However, because there is no correct manner or proper sequence to activate the knobs and slides provided, the free-interpretation nature in this context means that different VI musicians could use as many effects as they want and activate all or a few of the knobs and slides available in the patch.

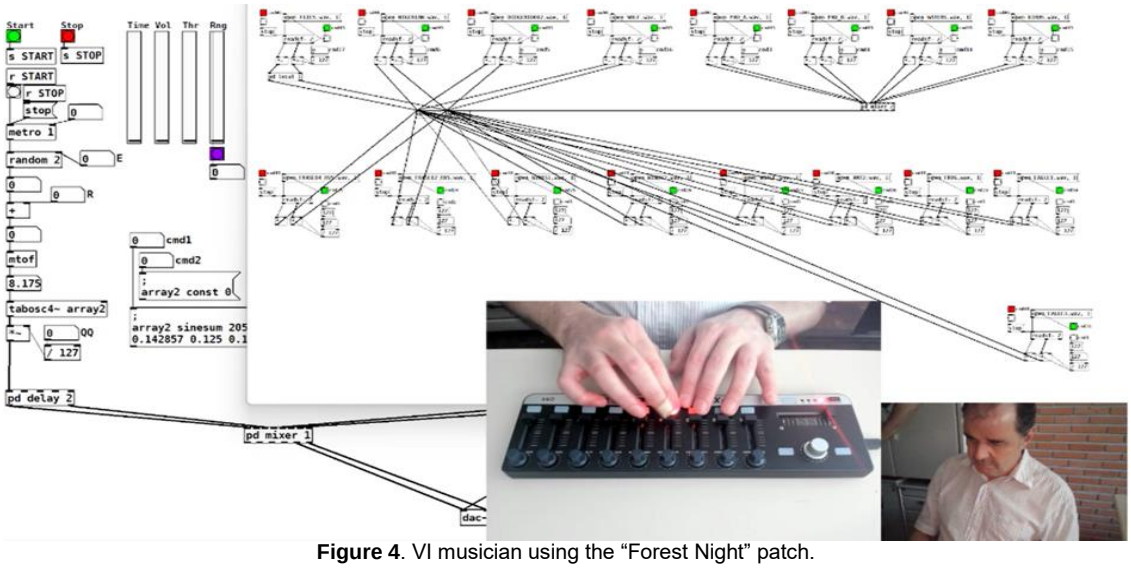

Figure 4. VI musician using the “Forest Night” patch.

Table 3. Samples and the moment of occurrence in performance.

Sample	Occurrence(s)	Control
ANT2	9	Pushbutton 6
BIRDS	60	Knob 2
DIGERIDOO2	60	Slider 3
EAGLE1	31	Pushbutton 8
EAGLE3	32	Pushbutton 9
FLIES	60	Knob 4
FRASE 2	6	Pushbutton 2
FRASE 4	6	Pushbutton 1
FROG	10	Pushbutton 7
NIGERIAN	60	Slider 4
PAD A	60	Slider 1
PAD B	63	Slider 2
WATERS	63	Knob 1
WHALE	18	Pushbutton 5
WINDS1	48	Pushbutton 3
WINGS 2	30	Pushbutton 4
WOLF	78	Knob 3

Discussion

This preliminary study aimed to overcome the inaccessibility of Pure Data's graphical user interface, enabling a VI musician to generate soundscapes in real time and autonomously. Although one could question the need for a VI musician to choose Pure Data as software for sound synthesis (since it is not the most accessible) to the detriment of other more viable alternatives, Saha and Piper [21] have already observed that the audio production industry requires an understanding that accessibility in the sound production industry is currently limited but critical for professional success. Other researchers also value strategy proposals that promote inclusive practices and preserve availability [22]. This can justify the need to develop strategies for visually impaired musicians to perform using audio synthesis software, as collaboration with other (visually impaired or sighted) musicians is compromised by the caveats posed by the software's accessibility limitations [23].

In the context of accessibility to music production software, efforts have been made to enable visually impaired musicians to access various patch features, actions, and commands that are adequately programmed by sighted musicians. HaptEQ was used as a feasible solution to increase audio production accessibility [8]. However, it focuses primarily on audio equalisation in the audio processing stages, and its applications during live performances should be tested. AirSticks focused on inclusive music improvisation and created a percussive Accessible Digital Musical Instrument (ADMI) that uses a Razer Hydra gaming controller to convert motion into sound [24]. Moving the gaming controller can adjust the sound pitch and tempo, while accounting for the need to calibrate the user's movement amplitude. This mapping was executed by Custom AirSticks MIDI Software [25]. If virtual zones are triggered, the controller can be moved to add reverb or distortion. This type of strategy could also be set to operate with multiple combinations to trigger audio samples and modulate pitch and frequency in a soundscape scenario, such as the one performed in this study. However, more work is required to change features, especially when they are not modulating together in the same virtual zone. As an advantage, strategies based on motion capture allow for various performance possibilities, as can be seen in the YouTube videos [24].

As observed in the video results, a VI musician can perform the PD patch using the controller rather than the mouse. An advantage of the proposed strategy is that the controller can be configured to the Pd without the user installing a driver. It was sufficient for the VI musician to connect it to the computer via a USB cable and enable it to access the software's MIDI input and output ports. The model was considered effective because it provided sufficient resources for free improvisation in electronic music and, for the first time, allowed this VI musician to complete the task (accessing Pd patches and producing sound synthesis) autonomously. The disadvantage could be that, compared to other alternatives, such as [24], the present strategy does not require performance in wide-body movements, which could give the interface an even more artistic aspect, although it does not reduce its functionality.

Other musicians have already been practising soundscapes [26]. Fornari *et al*. asserted the importance of broadening the notion of composition and performance using bioinspired adaptive computational systems. In this sense, the present work demonstrates a form of performance expansion for VI people. However, it should be noted that this study does not solve the issue of a VI musician building patches using Pd, given that the proposed assistive strategy does not allow or facilitate changing the interconnection of graphic elements. Such a solution is nearing completion, therefore not yet published, and it is another patch under development by the authors that explores the idea of the autonomy of blind musicians, not only in their performance but also in the construction and editing of patches by a VI musician, according to their preferences.

Another aspect of soundscape performance is that each performance is interpreted differently (free improvisation). For example, performance using the "Forest Night" patch has already been performed by a sighted musician [27]. At the time, the computer system consisted of an Easycontrol 9 (Worlde, China) MIDI controller and a Vaio notebook (model NRE4407), equipped with an Intel(R) Core i5-1035G1 CPU @ 1.00GHz, 8 GB RAM, 1 TB of storage, Windows 10 64-bit OS, version 21H1 with all updates, 3 USB ports available, a Realtek sound card model RTL8168/8111, and a Tobias Erichsen MIDI control unit model teVirtualMIDI. Empirical and observational analyses of both execution videos reveal a similarity in the manipulation of software and hardware. However, due to the free improvisation, the performance varied. This indicates that the VI musician's autonomy in interpreting the soundscape was enabled, thereby guaranteeing equality [28].

Although the performance with the "Forest Night" patch was successful, preliminary results revealed some difficulties. A problem was the Pd update stages. Version 0.51.4 was used because its most recent version (at that time, 0.52.1) presented

problems during patch execution, a problem that may be related to the computer setup.

For free improvisation performance, only one controller bank was sufficient. However, for performances that require a greater number of audio samples, effects, and oscillators that employ more than one bank, a controller with a larger number of channels than the model used in this study (CR-9, KFX, China) may be necessary.

The main disadvantage of the proposed method is related to hardware limitations. The mechanics to actuate on knobs and slides are fixed, and, mainly, the movements involve only two degrees of freedom (up/down or right/left). MIDI hardware models do not have sensors, so they do not sense changes in light, distance, movement, pressure, etc.

Even though the focus of this work is the investigation of the feasibility of employing this strategy for the free improvisation of VI musicians, the interaction with sighted musicians was not addressed in this study. However, given that the result obtained was considered effective, it is believed that interaction with other musicians using this technique is possible, and its efficiency will be investigated in future work.

Conclusion

In this paper, we have presented an accessibility strategy that enabled a visually impaired musician to perform autonomously using Pure Data. The MIDI controller enabled the functionality of a Pure Data patch, so visually impaired musicians did not experience difficulty controlling the Pure Data objects.

It is hoped that the alternative accessibility paths found with the use of the NVDA screen reader and MIDI controller can contribute positively to the community of visually impaired musicians regarding the use of Pure Data, collaborating with digital and social inclusion, knowledge, and technological improvement of people with visual impairment, resulting in an increase in the qualification of their professional curriculum.

Acknowledgments

The authors thank the National Council for Scientific and Technological Development (CNPq) for research grants (processes n. 100231/2021-7 and n. 314241/2018-3).

References

[1] M. Puckette, "Pure Data: another integrated computer music environment," presented at the 2nd Intercollege Computer Music Concerts, Tokyo, 1996. [Online]. Available: http://msp.ucsd.edu/Publications/icmc97.pdf. Accessed: 23/07/2024.

[2] J. Kreidler, Loadbang: programming electronic music in Pd. Wolke, 2009.

[3] E. Sjuve, "Prototype GO: Wireless controller for Pure Data," presented at the 8th International Conference on New Interfaces for Musical Expression (NIME08), Genova, Italy, 2008. doi: https://doi.org/10.5281/zenodo.1179629.

[4] G. Moro, A. Bin, R. H. Jack, C. Heinrichs, and A. P. McPherson, "Making high-performance embedded instruments with Bela and Pure Data," presented at the International Conference on Live Interfaces, Brighton, United Kingdom, 2016. [Online]. Available: https://qmro.qmul.ac.uk/xmlui/handle/123456789/12653. Accessed: 23/07/2024.

[5] J. Marinho and S. Venturelli, "Police, criminal, dog, dentist: An interactive audiovisual installation," DATJournal Design Art and Technology, vol. 3, no. 2, pp. 179-202, 2018, doi: https://doi.org/10.29147/dat.v3i2.90.

[6] Pure Data. "Pd community site." Available: http://puredata.info/community. Accessed: 24/08/2023.

[7] T. Deacon, P. Healey, and M. Barthet, ""It's cleaner, definitely": Collaborative process in audio production," Computer Supported Cooperative Work (CSCW), pp. 1-31, 2022, doi: http://doi.org/10.1007/s10606-022-09448-1.

[8] A. Karp and B. Pardo, "HaptEQ: A collaborative tool for visually impaired audio producers," presented at the 12th International Audio Mostly Conference on Augmented and Participatory Sound and Music Experiences, London, UK, 2017. doi: https://doi.org/10.1145/3123514.3123531.

[9] L. Princic et al. "Pure Data." Available: https://archive.flossmanuals.net/_booki/pure-data/pure-data.pdf. Accessed: 23/07/2024.

[10] A. D. Carvalho Junior, "Sensors2PD: Mobile sensors and WiFi information as input for Pure Data," presented at the International Computer Music Conference (ICMC), Greece, 2014. [Online]. Available: http://smc.afim-asso.org/smc-icmc-2014/papers/images/VOL_1/0744.pdf. Accessed: 23/07/2024.

[11] T. Hillerson, Programming sound with Pure Data: Make your apps come alive with dynamic audio. Pragmatic Programmers, 2014.

[12] M. A. Hersh and M. A. Johnson, Assistive technology for visually impaired and blind people. London: Springer, 2008.

[13] NVDA. "NV Access Download NVDA." Available: https://www.nvaccess.org/download/. Accessed: 23/07/2024.

[14] A. K. Fraser. "Contact magazine. Software by the blind, for the blind." The University of Queensland. Available : https://stories.uq.edu.au/contact-

magazine/2020/software-for-the-blind-by-the-blind/index.html. Accessed: 31/08/2023.
[15] L. H. Boyd, "The graphical user interface: Crisis, danger, and opportunity," Journal of Visual Impairment & Blindness, vol. 84, no. 10, pp. 496-502, 1990, doi: https://doi.org/10.1177/0145482X9008401002.
[16] J. Lazar, A. Allen, J. Kleinman, and C. Malarkey, "What frustrates screen reader users on the web: A study of 100 blind users," International Journal of human-computer interaction, vol. 22, no. 3, pp. 247-269, 2007, doi: https://doi.org/10.1080/10447310709336964.
[17] S. Kirboyun, "Computer aided system for users with visual impairments," presented at the 2018 IEEE/ACS 15th International Conference on Computer Systems and Applications (AICCSA), Aqaba, Jordan, 2018. doi: https://doi.org/10.1109/AICCSA.2018.8612898.
[18] R. Guérin, MIDI power!: The comprehensive guide. Course Technology PTR, 2009.
[19] WATSON, Ben. Derek Bailey and the story of free improvisation. Verso Books, 2013.
[20] Pontifícia Universidade Católica do Paraná. Performance "Forest Night". Pure Data + MIDI controller [Video]. (Nov. 25, 2022). Accessed: July 23, 2024. [Online Video]. Available: https://www.youtube.com/watch?v=N4H79qBlbxw&t=25s .
[21] A. Saha and A. M. Piper, "Understanding audio production practices of people with vision impairments," presented at the 22nd International ACM SIGACCESS Conference on Computers and Accessibility, Greece, 2020. doi: https://doi.org/10.1145/3373625.3416993.
[22] J. Harrison, A. Lucas, J. Cunningham, A. P. McPherson, and F. Schroeder, "Exploring the opportunities of haptic technology in the practice of visually impaired and blind sound creatives," Arts, vol. 12, p. 154, 2023, doi: https://doi.org/10.3390/arts12040154.
[23] W. C. Payne, A. Y. Xu, F. Ahmed, L. Ye, and A. Hurst, "How blind and visually impaired composers, producers, and songwriters leverage and adapt music technology," presented at the 22nd International ACM SIGACCESS Conference on Computers and Accessibility, Greece, 2020. doi: https://doi.org/10.1145/3373625.3417002.
[24] A. Ilsar and G. Kenning, "Inclusive improvisation through sound and movement mapping: from DMI to ADMI," presented at the 22nd International ACM SIGACCESS Conference on Computers and Accessibility, Greece, 2020. doi: https://doi.org/10.1145/3373625.3416988.
[25] NIME. "AirSticks 2.0: Instrument Design for Expressive Gestural Interaction". Accessed: 06/05/2025. Available: https://nime.pubpub.org/pub/vwbc1tlk.
[26] J. Fornari, A. Maia, and J. Manzolli, "Soundscape design through evolutionary engines," Journal of the Brazilian Computer Society, vol. 14, pp. 51-64, 2008, doi: https://doi.org/10.1007/BF03192564.
[27] Vila Jazz. Performance "Forest Night". Pure Data + MIDI controller [Video].. (Dec. 6, 2021). Accessed: 23/07/2024. [Online Video]. Available: https://www.youtube.com/watch?v=pEECxbPj8Ds
[28] J. Wolff, "Musical performance as a route to relational autonomy and social equality," in Autonomy and Equality: Relational Approaches, N. Stoljar and K. Voigt Eds. New York; Oxford: Routledge, 2021, ch. 10, pp. 220-39.

RECyT
Year 27 / Nº 44 / 2025 /
DOI: https://doi.org/10.36995/j.recyt.2025.44.011

Simulation of a phthalic anhydride production process through gaseous catalytic oxidation of o-xylene in ChemCAD® simulator

Simulación de un proceso de producción de anhídrido ftálico mediante la oxidación catalítica gaseosa del o-xileno en el simulador ChemCAD®

Amaury, Pérez Sánchez[1, *]; Elizabeth, Ranero González[1]; Eddy J., Pérez Sánchez[2]; Lizthalía, Jiménez Guerra[1]

1- Facultad de Ciencias Aplicadas, Universidad de Camagüey "Ignacio Agramonte Loynaz". Carretera Circunvalación Norte, Km. 5½, e/ Camino Viejo de Nuevitas y Ave. Ignacio Agramonte, Camagüey, Cuba.
2- Departamento comercial, Empresa de Servicios Automotores S.A. Calle C, e/ Abraham Delgado and Marcial Gómez, Ciego de Ávila, Cuba.
* E-mail: amauryps@nauta.cu

Received: 12/09/2023; Accepted: 24/06/2025

Abstract
Phthalic anhydride (PA) is a key industrial compound, particularly relevant for the large-scale production of plasticizers. This study aimed to develop the conceptual design of a proposed PA production process using the ChemCAD 7.1.2 simulation software, in which maleic anhydride (MA) was identified as the principal byproduct. Several parameters were obtained for the heat exchangers, including heat curves, heat duty, logarithmic mean temperature difference (LMTD), and overall heat transfer coefficient. Additionally, the mass flow rate and composition of the main process streams were determined through simulation, along with their temperature, pressure, and vapor fraction. Design parameters for both distillation columns were also calculated, as well as the heat duty of the catalytic reactor. Finally, the total purchase and installation costs of selected equipment were estimated. The mass flow rate of the bottom stream from the purification column was 10,921.083 kg/h, composed primarily of PA (99.19% purity) and o-xylene (0.80%), while MA was recovered in the top stream with a mass flow rate of 973.342 kg/h and a purity of 83.36%.

Keywords: ChemCAD®; Maleic anhydride; o-Xylene; Phthalic anhydride; Simulation.

Resumen
El anhídrido ftálico (AF) es un compuesto químico industrial importante, especialmente para la producción a gran escala de plastificantes. El propósito de este artículo fue el de llevar a cabo el diseño conceptual de un proceso de producción de AF en el simulador ChemCAD® 7.1.2, donde el anhídrido maleico (AM) fue el principal subproducto producido. Varios parámetros fueron obtenidos para los intercambiadores de calor, tales como las curvas de calor, carga de calor, la DMLT y el coeficiente global de transferencia de calor. También, el caudal másico y composición de las corrientes principales fueron determinadas, incluyendo su temperatura, presión y fracción de vapor. Además, algunos parámetros de diseño fueron calculados para ambas columnas de destilación, así como también el calor intercambiado del reactor catalítico. Finalmente, los costos totales de compra e instalación fueron determinados considerando algunos equipos específicos. El caudal másico de la corriente del fondo de la columna de purificación fue 10 921,083 kg/h, la cual está compuesta principalmente por AF (99,19% de pureza) y o-xileno (0,80%), mientras que el AM es obtenido en al corriente del tope de esta columna con un caudal másico de 973,342 kg/h y una pureza de 83,36%.

Palabras claves: ChemCAD®; Anhídrido maleico; o-Xileno; Anhídrido ftálico; Simulación.

Introduction

Phthalic anhydride (PA) is an organic compound that can be synthesized from precursors such as o-xylene or naphthalene via oxidation in the presence of a catalyst, typically vanadium/titanium oxide. However, some authors [1] have proposed the conceptual design of a PA production process using corn stover, incorporating energy integration strategies, water consumption analysis, and life cycle greenhouse gas emissions assessment.

PA is a crucial chemical intermediate with major applications in the manufacture of plasticizers for PVC, unsaturated polyesters, and alkyd resins used in surface coatings. Its minor applications include polyester polyols, pigments, dyes, sweeteners, and flame retardants [2].

In 1872, BASF developed the naphthalene oxidation process for PA production, marking the beginning of its continuous commercial synthesis. PA was the first commercially used anhydride of a dicarboxylic acid, and its industrial relevance is comparable to that of acetic acid [3].

PA is produced through oxidation reactions occurring at approximately 360–390 ºC from:

- o-xylene, with a reaction enthalpy ranging from 1300 to 1800 kJ/mol and expected yields of 110–112 kg PA per 100 kg o-xylene.
- naphthalene, with a reaction enthalpy between 2100 and 2500 kJ/mol and yields typically not exceeding 98 kg PA per 100 kg naphthalene; carbon dioxide is a co-product.

Until the late 1950s, coal-tar-derived naphthalene remained the preferred feedstock in the United States and Germany. However, a shortage of naphthalene and the growing availability of xylenes from the expanding petrochemical industry led to a shift toward o-xylene. The air oxidation of 90% pure o-xylene to PA was commercialized in 1946. One advantage of o-xylene is its theoretical yield of 1.395 kg PA per kg of feedstock, whereas naphthalene yields a maximum of 1.157 kg/kg due to carbon dioxide losses. Although both feedstocks are viable, o-xylene is predominantly favored. Coal-tar naphthalene is still used in specific contexts, such as when readily available from coke production in steel mills [4].

Over 90% of PA is produced via vapor-phase oxidation of o-xylene over a fixed-bed catalyst. In the 1960s, two types of fixed-bed processes were employed: low-temperature/low space velocity and high-temperature/high space velocity. Advances in catalyst technology enabled higher space velocities under low-temperature conditions while maintaining high yields. Consequently, the low-temperature process, operating below 400 ºC, became the industry standard. A commercially viable plant must achieve a selectivity of at least 75 mol% with an o-xylene feed concentration of 60 g/m³, which exceeds the lower explosion limit of 43 g/m³ [4].

The preference for o-xylene in PA manufacturing is driven by its superior yields, availability, and cost-effectiveness. However, this dependence exposes the process economics to fluctuations in feedstock prices and the volatility of mixed xylenes in global markets. To mitigate this risk, some facilities incorporate o-xylene/naphthalene switching capabilities or xylene separation units [1].

The fixed-bed process utilizes a catalyst composed of vanadium oxide and titanium dioxide, coated onto an inert, non-porous carrier in layers ranging from 0.02 to 2.0 mm in thickness. Ring-shaped supports are preferred over spherical ones to extend catalyst life, reduce reactor pressure drop, and enhance yields [4].

Numerous studies have simulated PA production plants using commercial software. For instance, [5] developed a simulation model of PA production from o-xylene using Aspen Plus, incorporating heat integration and separation processes. Similarly, [6] employed Aspen Plus for steady-state simulation and exported the model to Aspen Dynamics for dynamic simulation and hazard and operability (HAZOP) analysis. In another study, [7] designed and simulated a simplified PA production process using corn stover as feedstock to evaluate scalability. The plant was configured to process 104,167 kg/h of milled corn stover with 20% moisture content. The vapor-liquid equilibrium was modeled using the NRTL method, with gases such as O_2, N_2, CO_2, CH_4, and H_2 treated under Henry's Law. Additionally, [8] assessed the techno-economic feasibility of establishing a PA production facility in Argentina via partial oxidation of o-xylene, identifying an optimal production capacity of 9,000 tons/year.

Other researchers have focused on reactor design and optimization. For example, [9] analyzed thermowell systems for temperature monitoring in fixed-bed catalytic reactors used in the highly exothermic partial oxidation of o-xylene to PA. Particle-resolved computational fluid dynamics (CFD) simulations were conducted for randomly packed spheres in cylindrical tubes with varying tube-to-particle diameter ratios. The presence of thermowells influenced mass and heat transfer, particularly at the reactor core. Likewise, [3] conducted a kinetic study of o-xylene oxidation over a V_2O_5/TiO_2 catalyst in a fluidized bed reactor, enabling accurate kinetic data collection despite the reaction's exothermic nature. In another study, [10] evaluated the performance of highly conductive structured metallic monoliths for PA production, concluding that their use significantly enhances plant productivity. [11] investigated the effect of inlet gas temperature on fixed-bed reactor performance for o-xylene oxidation, using a two-dimensional heterogeneous model across a temperature range of 120 to 450 ºC. [12] demonstrated that PA selectivity can be improved by adjusting operating conditions such as temperature and oxygen partial pressure, based on reactor-scale simulations of industrial units. [13] mathematically analyzed the performance of a fixed-bed tubular reactor for PA production, comparing conversion rates and temperature profiles with data from a petrochemical unit in Iran and pilot plant literature, yielding satisfactory correlations. Finally, [14] proposed a framework integrating ANSYS Fluent with other computing platforms via lock synchronization to extend CFD solvers' applications from modeling and design to control and optimization, selecting PA synthesis due to its industrial relevance and pronounced exothermicity.

Rising energy and feedstock costs have intensified the demand for efficient chemical process design and optimization. Advances in

computational capabilities have facilitated the application of mathematical methods to address these challenges. The development of new processes increasingly relies on high-efficiency synthesis methodologies that prioritize sustainability and performance [15].

Process flow sheet design and optimization are supported by commercial simulation software known as process simulators [16]. Among the most widely used simulators by researchers and engineers for modeling real-world systems are Aspen Plus, SuperPro Designer, UniSim, ProSim Plus, EMSO, ChemCAD, gPROMS, and PRO/II [17].

ChemCAD [18] is an integrated suite developed by Chemstations to enhance productivity and solve complex chemical process models [19]. Its versatility lies in its broad range of thermodynamic models, compatibility with diverse operating conditions, extensive component databases, and user-friendly interface. The simulator is widely adopted in industry due to its comprehensive library of predefined unit operations—including pumps, distillation columns, tanks, heat exchangers, reactors, and compressors—which can be interconnected to model complete chemical facilities. Substances are introduced into the system via feed streams [20].

A chemical company has outlined concrete plans to produce PA via catalytic gaseous oxidation of o-xylene, leveraging the availability of raw materials, budgetary resources, and market demand. To support this initiative, the company requires detailed information on the temperature, pressure, composition, and flow rates of the main process streams, as well as the operating parameters of the equipment involved. Additionally, data on plant yield and throughput are essential. In this context, the present study presents the conceptual design of the proposed PA production process using ChemCAD 7.1.2, aiming to determine the mass and energy balances of the principal streams and assess plant productivity and final PA purity. Key parameters of the heat exchangers, distillation columns, and catalytic reactor were calculated, along with the total purchase and installation costs of selected equipment. The throughput and purity of the byproduct MA were also determined.

Materials and Methods

Physicochemical Properties of Phthalic Anhydride

As reported by [4], the principal physicochemical properties of phthalic anhydride (PA) are summarized in Table 1.

Table 1. Principal physicochemical properties of PA.

Property	Value	Units
Melting point	131	ºC
Boiling point	284.5	ºC
Triple point	131	ºC
Heat of vaporization at 131 ºC	65.3	kJ/mol
Specific gravity at 4 ºC	1.527	-
Specific heat at 90 ºC	422	J/kg.K
Heat of combustion at 25 ºC	- 3,259	kJ/mol
Heat of formation at 25 ºC	- 460	kJ/mol
Heat of sublimation at 131 ºC	88.70	kJ/mol
Heat of fusion at 131 ºC	22.93	kJ/mol

Description of the Proposed Phthalic Anhydride Production Process through Catalytic Oxidation of Gaseous o-Xylene

A stream of dried air, with a total flowrate of approximately 317,240 kg/h and composed of 76.7% nitrogen (243,320 kg/h) and 23.3% oxygen (73,920 kg/h), is compressed from atmospheric pressure (101.325 kPa) to 220 kPa using a centrifugal polytropic compressor. This compressed stream is subsequently heated to 245 ºC in a shell-and-tube heat exchanger (Pre-heater 1) using high-pressure steam available at 254 ºC.

In a separate section of the plant, a liquid stream of pure o-xylene with a flowrate of 11,678 kg/h is pumped through a shell-and-tube heat exchanger (Vaporizer), where its temperature is raised to 245 ºC using the same high-pressure steam, resulting in complete vaporization. The vaporized air and o-xylene streams are then mixed and fed into a fixed-bed catalytic reactor at an inlet temperature of 245 ºC and a pressure of 200 kPa. For safety purposes, the o-xylene concentration is maintained at or below the lower explosive limit of 1 mol%, with the air-to-o-xylene ratio controlled via a ratio controller positioned between the compressor and the pump's control valve.

Within the reactor, o-xylene undergoes oxidation, yielding the target product phthalic anhydride (PA), the byproduct maleic anhydride (MA), and various combustion products. These reactions are highly exothermic, necessitating temperature regulation via a concurrent flow of Dowtherm A through the shell side of the reactor. A pressure drop of 70 kPa is observed inside the reactor due to the passage of reactant gases through catalyst-packed tubes.

The reaction mixture exits the reactor at 353 ºC and 130 kPa and is directed to a shell-and-tube heat exchanger (Cooler 1), where it is cooled to 260 ºC using boiler feed water at 110 ºC. This cooling step generates high-pressure steam at 254 ºC. The mixture is then further cooled to 165 ºC in a second shell-and-tube heat exchanger (Cooler 2), also using boiler feed water at 110 ºC, producing low-pressure steam at 159 ºC. Finally, the stream is cooled to 45 ºC in a third shell-and-

tube heat exchanger (Cooler 3) using cooling water at 30 ºC.

At this stage, the cooled reaction stream is a two-phase mixture and is sent to a set of switch condensers for PA recovery. PA is desublimated as a solid in one condenser using chilled oil, then melted in a second condenser using hot oil, while a third condenser remains on standby. As noted by [21], due to the low partial pressure of PA in the stream, it desublimates rather than condenses. The process stream is cooled using low-temperature oil in tubes to promote desublimation. Once solid PA accumulates on the heat transfer surface, gas flow to the condenser is halted and higher-temperature oil is circulated to melt the solid. This cycle is repeated across three units: one in desublimation mode, one in melting mode, and one on standby. The result is a liquid stream containing condensable components and a vapor stream comprising MA, PA, o-xylene, water, and non-condensables. It is assumed that all light gases remain uncondensed and undissolved, and that 99% of the organics are desublimated and melted. In ChemCAD, the switch condensers are simulated using a component separator, as recommended by [21].

The liquid stream from the switch condensers is depressurized to 70 kPa via a pressure-reducing valve and then heated to 230 ºC in a shell-and-tube heat exchanger (Pre-heater 2) using high-pressure steam. This heated stream is fed into a sieve tray distillation column (Water Column), where a top stream primarily composed of water is separated, and a bottom stream containing mostly PA and MA is collected. The bottom stream is subsequently fed into a second sieve tray distillation column (Purification Column), where PA is recovered at the bottom with a purity of 99.19 wt%, and MA is obtained at the top with a purity of 83.36 wt%. Finally, the bottom stream of the purification column is cooled to 30 ºC in a shell-and-tube heat exchanger (Cooler 4) using chilled water at 5 ºC.

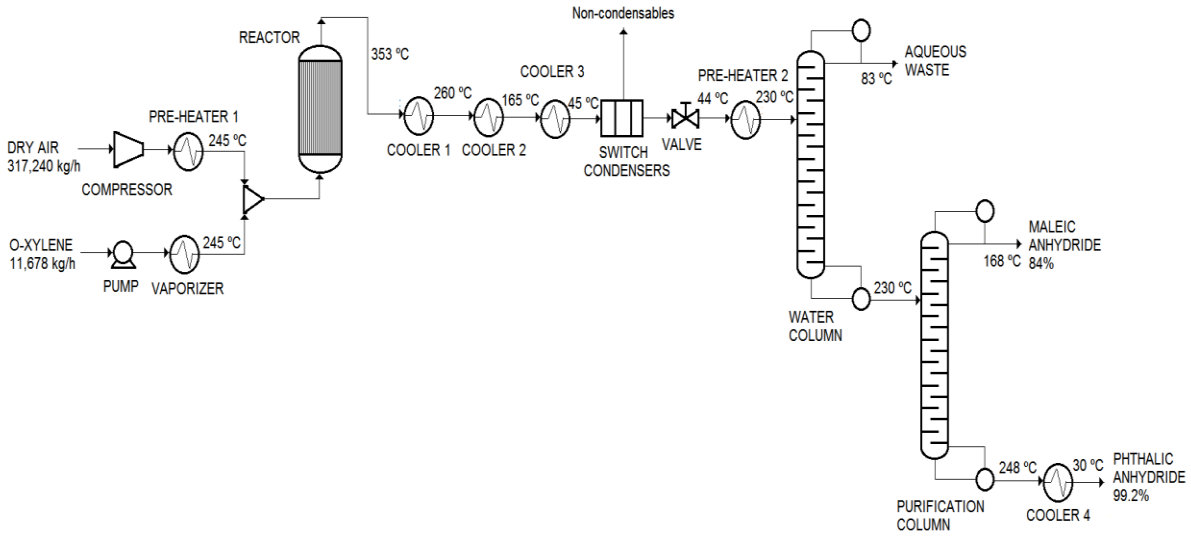

Figure 1. Process flow diagram of the PA production process from the catalytic oxidation of o-xylene.

Reactions

Table 2 presents the stoichiometry and selectivity of the principal reactions occurring within the catalytic reactor, as considered in this study. Table 3 outlines the corresponding reaction kinetics [21].

Table 2. Stoichiometry and selectivity of the reactions occurring in the catalytic reactor.

Number	Reaction	Selectivity
1	Formation of phthalic anhydride: $C_6H_4(CH_3)_2 + 3O_2 \rightarrow C_6H_4(CO)_2O + 3H_2O$	0.70
2	Combustion of phthalic anhydride: $C_6H_4(CO)_2O + \frac{15}{2}O_2 \rightarrow 8CO_2 + 2H_2O$	0.10
3	Complete combustion of o-xylene: $C_6H_4(CH_3)_2 + \frac{21}{2}O_2 \rightarrow 8CO_2 + 5H_2O$	0.15
4	Formation of maleic anhydride: $C_6H_4(CH_3)_2 + \frac{15}{2}O_2 \rightarrow C_2H_2(CO)_2O + 4CO_2 + 4H_2O$	0.10
5	Combustion of maleic anhydride: $C_2H_2(CO)_2O + 3O_2 \rightarrow 4CO_2 + H_2O$	0.08

Table 3. Reaction kinetics of the reactions occurring in the reactor.

Number	Reaction kinetics
1	$r_1 = -\frac{27{,}000}{RT} + 19.837$
2	$r_2 = -\frac{31{,}000}{RT} + 20.86$
3	$r_3 = -\frac{28{,}600}{RT} + 18.97$
4	$r_4 = -\frac{27{,}900}{RT} + 19.23$
5	$r_5 = -\frac{30{,}400}{RT} + 20.47$

Where: R = 1.987 cal·K^{-1}·mol^{-1} T = Temperature in Kelvin

Catalyst

The catalyst employed in this study was vanadium pentoxide (V_2O_5, vanadia) supported on titanium dioxide (TiO_2, anatase) [3][22], with the following physical parameters [21]:

- Catalyst particle diameter: 3 mm
- Catalyst particle density: 1,600 kg/m³
- Void fraction: 0.50

V_2O_5/TiO_2 is a widely used catalyst in various industrial reactions, including the selective oxidation of o-xylene to phthalic anhydride, selective catalytic reduction of NO_x, and selective oxidation of alkanes. The partial oxidation of o-xylene to synthesize phthalic anhydride is a highly exothermic reaction, which leads to the formation of hot spots on the catalyst surface. The yield of phthalic anhydride is strongly influenced by the activity and stability of the catalyst [23].

According to [24], vanadia-anatase supported catalysts used for the oxidation of o-xylene to phthalic anhydride undergo significant deactivation over time. Consequently, the catalyst must be replaced after approximately five years of operation, with the most pronounced decline in activity occurring in the hot spot region. This trend has been observed in catalysts used for 24, 34, 45, and 55 months. During the first 45 months, the catalyst maintains relatively stable activity in the front section of the bed (0–30 cm), whereas the markedly reduced activity observed in catalysts aged 60.5 months beyond the 100 cm region of the bed is likely attributable to reversible deactivation caused by product accumulation on active sites.

Design Parameters of the Equipment

Table 4 presents the design specifications of the shell-and-tube heat exchangers, catalytic reactor, and distillation columns used in the simulation of the phthalic anhydride (PA) production process. These parameters were selected based on recommendations and design criteria reported in [21], [25], [26], [27], and [28].

Table 4. Principal design parameters of the equipment employed in the simulated PA production process.

Equipment	Design parameters
Pre-heater 1	Area: 3,300 m^2 1-2 shell and tube heat exchanger, floating head, and carbon steel. Process stream in tubes.
Vaporizer	Area: 450 m^2 1-2 shell and tube heat exchanger, floating head, and carbon steel. Process stream in shell.
Cooler 1	Area: 2,600 m^2 1-2 shell and tube heat exchanger, floating head, and carbon steel. Process stream in tubes.
Cooler 2	Area: 3,200 m^2 1-2 shell and tube heat exchanger, floating head, and carbon steel. Process stream in tubes.
Cooler 3	Area: 2,800 m^2 1-2 shell and tube heat exchanger, floating head, and carbon steel. Process stream in shell.
Pre-heater 2	Area: 300 m^2 1-2 shell and tube heat exchanger, floating head, and carbon steel. Process stream in tubes.
Cooler 4	Area: 700 m^2 1-2 shell and tube heat exchanger, floating head, and carbon steel. Process stream in shell.
Reactor	Carbon steel construction, 18,000 2-inch diameter tubes each 6 m long. Triangular arrangement, 2-inch pitch. Overall reactor diameter: 7 m. Overall reactor length: 10 m. Co-current flow, process stream in tubes, Dowtherm A in shell.
Water column	Carbon steel, Diameter: 0.95 m, Height 14.5 m, Tray type: Sieve. Trays spacing: 1 ft. (0.3048 m).
Purification column	Carbon steel, Diameter: 0.85 m, Height 8 m, Tray type: Sieve. Trays spacing: 1 ft. (0.3048 m).

Selection of the thermodynamic model

Based on the minimum and maximum temperature and pressure values handled throughout the production process, and using the "Thermodynamics Wizard" feature, the ChemCAD simulator recommended the UNIFAC model for the Global K-Value calculation, incorporating vapor phase association via the Hayden–O'Connell method. For enthalpy calculations, the Peng–Robinson model was selected as the Global Enthalpy Model.

This selection differs from the thermodynamic package proposed by [21] for simulating processes of this nature, which suggested the Soave–Redlich–Kwong (SRK) model for both vapor–liquid equilibrium and enthalpy calculations across all unit operations.

Equipment purchase and installation cost

The purchase and installation costs of selected equipment involved in the proposed production process were estimated using the "Costing" module of the ChemCAD simulator. The Chemical Engineering Plant Cost Index (CEPCI) embedded in the simulator's costing database was updated to March 2023, based on the data reported by [29]. According to the simulator, both purchase and installation costs are calculated using methodologies and reference data published in [30].

It is important to note that the simulator does not provide cost estimation options for the reactor and distillation columns; therefore, their purchase and installation costs were not determined within the scope of this simulation.

Results and discussion

Figure 2 illustrates the process flow diagram obtained from the simulation of the phthalic anhydride (PA) production process using the ChemCAD simulator.

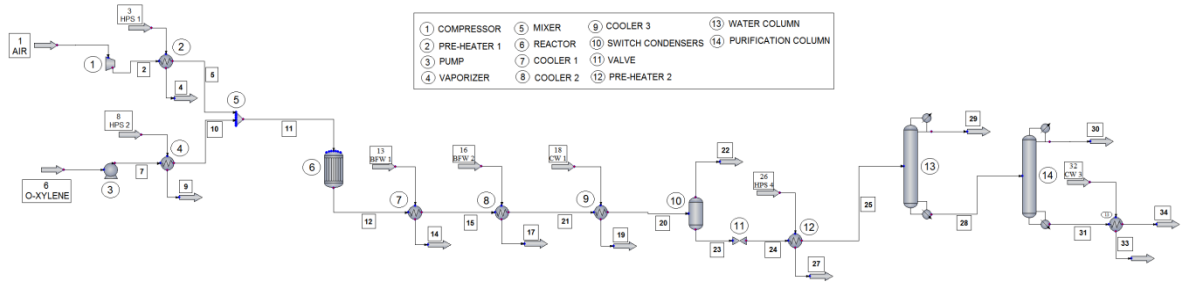

Figure 2. Process flow diagram of the phthalic anhydride (PA) production process via catalytic oxidation of o-xylene, as simulated using ChemCAD®.

Parameters and mass flowrates of the process streams

As a result of the simulation conducted using the ChemCAD® software, the principal parameters of the process streams involved in the phthalic anhydride (PA) production process were determined. These parameters are detailed in Table 5.

Table 5. Main parameters of the process streams involved in the PA production process (refer to Figure 2).

Parameter	Stream number (refer to Figure 2)					
	1	5	6	10	11	12
Temperature (ºC)	25	245	25	245	244.82	353
Pressure (kPa)	101	218	101	290	200	130
Vapor fraction	1	1	0	1	1	1
Component	Mass flowrate (kg/h)					
PA	-	-	-	-	-	11,404.720
MA	-	-	-	-	-	1,078.604
Carbon dioxide	-	-	-	-	-	7,745.515
Nitrogen	243,320	243,320	-	-	243,320	243,320
Oxygen	73,920	73,920	-	-	73,920	58,345
Water	-	-	-	-	-	6,440.158
o-Xylene	-	-	11,678	11,678	11,678	583.900
TOTAL	317,240	317,240	11,678	11,678	328,918	328,917.897

Table 5. Main parameters of the process streams involved in the PA production process (Cont.…)

Parameter	Stream number (refer to Figure 2)				
	15	21	20	22	23
Temperature (ºC)	260	165	45	45	45
Pressure (kPa)	120	110	100	100	100
Vapor fraction	1	1	0.986	0.999	0
Component	Mass flowrate (kg/h)				
PA	11,404.720	11,404.720	11,404.720	570.236	10,834.484
MA	1,078.604	1,078.604	1,078.604	53.930	1,024.674
Carbon dioxide	7,745.515	7,745.515	7,745.515	7,744.740	0.775
Nitrogen	243,320	243,320	243,320	243,295.600	24.40
Oxygen	58,345	58,345	58,345	58,339.150	5.850
Water	6,440.158	6,440.158	6,440.158	2,576.063	3,864.095
o-Xylene	583.900	583.900	583.900	496.315	87.585
TOTAL	328,917.897	328,917.897	328,917.897	313,076.034	15,841.863

Table 5. Main parameters of the process streams involved in the PA production process (Final)

Parameter	Stream number (refer to Figure 2)				
	25	28	29	30	34
Temperature (ºC)	230	230	83.39	168.275	30
Pressure (kPa)	60	52	50	40	42
Vapor fraction	1	0	1	1	0
Component	Mass flowrate (kg/h)				
PA	10,834.484	10,834.484	-	1.083	10,833.401
MA	1,024.674	973.439	51.235	973.342	0.097
Carbon dioxide	0.775	-	0.775	-	-
Nitrogen	24.40	-	24.40	-	-
Oxygen	5.850	-	5.850	-	-
Water	3,864.095	193.205	3,670.890	193.205	-
o-Xylene	87.585	87.585	-	-	87.585
TOTAL	15,841.863	12,088.713	3,753.150	1,167.630	10,921.083

The amounts of oxygen and o-xylene that reacted to generate the various products were 15,575 kg and 11,094.1 kg, respectively, corresponding to 21.07% and 95% of the total quantities fed into the process for each compound. The outlet stream from the tubular catalytic reactor was composed primarily of nitrogen (73.97%), phthalic anhydride (3.47%), and carbon dioxide (2.35%).

In the switch condenser stage, both PA and MA were recovered at a rate of 95%. However, approximately 570 kg/h of PA and 54 kg/h of MA were lost due to venting during this stage, a figure that is considered unacceptable. At this point in the process, carbon dioxide (99.99% removal), nitrogen (99.99%), oxygen (99.99%), water (39.99%), and o-xylene (85%) were separated from the liquid stream and released in gaseous form. The resulting liquid stream was composed mainly of PA (68.39%), water (24.39%), and MA (6.47%). It is therefore recommended to evaluate, design, and implement appropriate recovery systems to reclaim the 496.315 kg/h of o-xylene and the vented PA. These could be recycled into the main process—o-xylene as a high-purity feedstock and PA as a valuable product—thus increasing the overall throughput of the plant.

The most efficient emission control system (96%) for o-xylene-based production involves the combined use of a water scrubber and a thermal incinerator. A thermal incinerator alone achieves approximately 95% efficiency in the combustion of pollutants. Emissions from pretreatment and distillation—such as particulates and hydrocarbons—are typically treated using the same scrubber and/or incinerator systems employed for the main process streams (reactor and condenser), or with scrubbers alone, with comparable efficiency levels [31].

In the water column, the top stream consisted primarily of water (97.81%), while the bottom stream contained mostly PA (89.62%) and MA (8.05%). This bottom stream was subsequently fed into the purification column, where the top stream had a total flowrate of 1,167.63 kg/h and was composed mainly of MA (973.342 kg/h) with a purity of 83.36%, water being the principal impurity (16.55%). Likewise, the bottom stream of the purification column yielded 10,921.083 kg/h, primarily composed of PA (10,833.401 kg/h) with a purity of 99.2%, with o-xylene as the main impurity (0.80%).

Finally, the production yields obtained in this study were 0.927 kg of PA and 0.083 kg of MA per kg of o-xylene. The PA yield is below the value reported by [4], which is 1.395 kg PA/kg o-xylene, and also below the range reported by [1], which is 110–112 kg PA per 100 kg o-xylene. Considering the recovery of the 570 kg/h of PA vented in the switch condensers—through scrubbers or other recovery methods—the PA yield increases to 0.976 kg/kg of o-xylene, which nonetheless remains below the values reported in the consulted literature.

Parameters of the reactor and distillation columns

The design specifications for the two distillation columns employed in the production process are presented in Table 6. These parameters were determined using the ChemCAD® simulator.

Table 6. Design parameters of the two distillation columns calculated by the ChemCAD® simulator.

Parameter	Distillation column 1 (Water column)	Distillation column 2 (Purification column)	Units
Condenser duty	- 22,936.5	- 1,128.37	MJ/h
Reboiler duty	16,134.3	2,236.18	MJ/h
Minimum stages	25	10	-
Feed stage	10	6	-
Reflux ratio, minimum	3.67	0.51	-

The heat duty required to maintain the reactor temperature at 353 ºC was calculated at –153,938 MJ/h, a value that reflects the highly exothermic nature of the catalytic gaseous oxidation of o-xylene to phthalic anhydride and associated byproducts. This substantial energy demand is consistent with findings reported in [3], [11], and [14].

For the water column, the condenser and reboiler duties were –22,936.5 MJ/h and 16,134.3 MJ/h, respectively. In the purification column, these values were –1,128.37 MJ/h and 2,236.18 MJ/h, respectively. The water column required 25 theoretical stages, with the feed introduced at stage 10, while the purification column operated with 10 stages and a feed point at stage 6. The minimum reflux ratios were 3.67 for the water column and 0.51 for the purification column, indicating the relative separation difficulty and energy requirements of each unit.

Heat curves of the heat exchangers

Figure 3 displays the heat curves corresponding to each of the seven shell-and-tube heat exchangers utilized in the phthalic anhydride (PA) production process. These curves were generated using the ChemCAD® simulator.

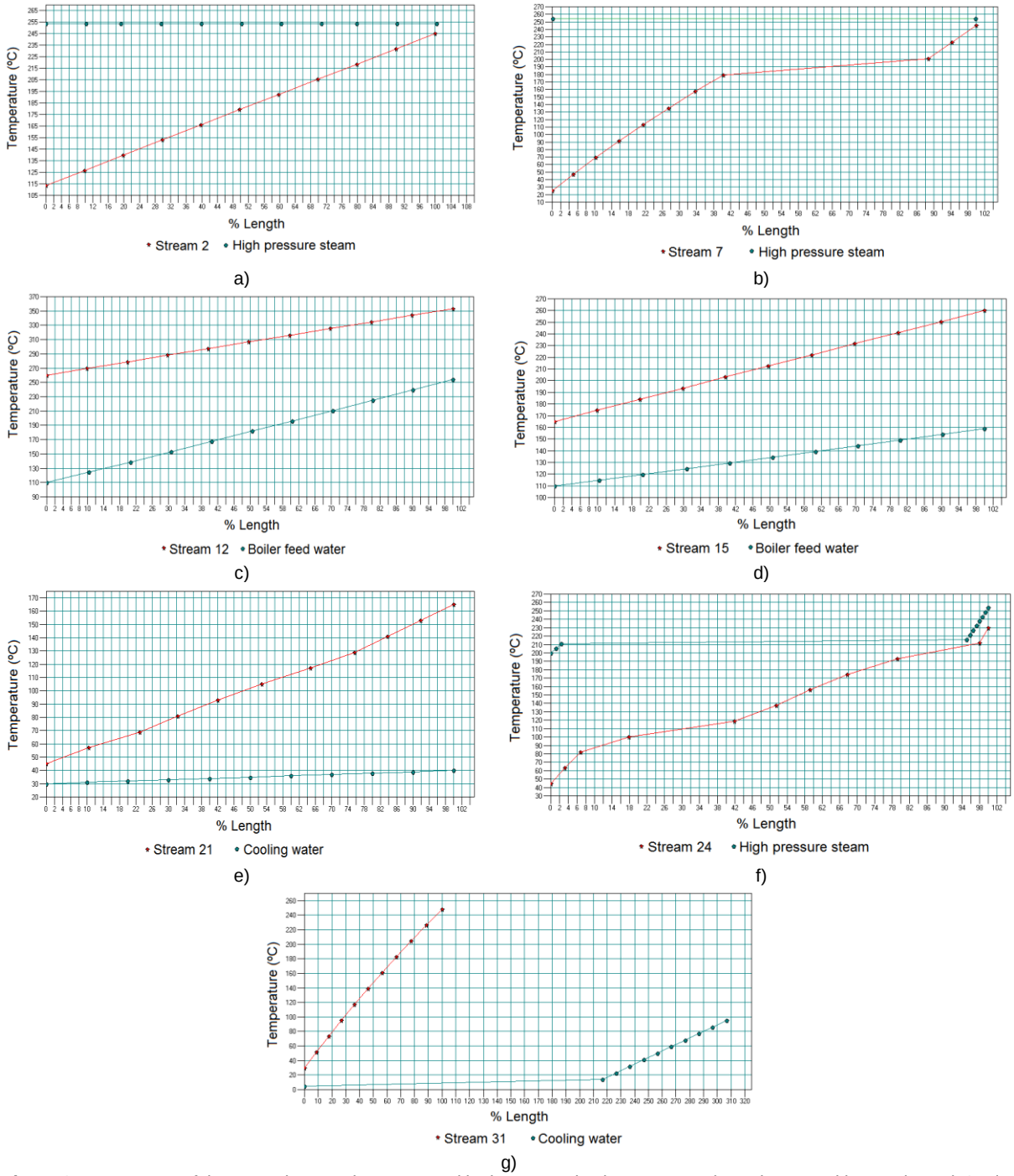

Figure 3. Heat curves of the seven heat exchangers used in the PA production process. a) Pre-heater 1; b) Vaporizer; c) Cooler 1; d) Cooler 2; e) Cooler 3; f) Pre-heater 2; g) Cooler 4.

The heat curve of Pre-heater 1 (Figure 3a) exhibits a linear profile for the high-pressure steam, indicating that the temperature of this auxiliary stream remains constant throughout the entire length of the heat exchanger at 254 °C. In contrast, Stream 2 (compressed air) displays a steadily increasing temperature pattern, evidencing continuous heating until it reaches the target temperature of 245 °C.

Regarding the heat curve of the Vaporizer (Figure 3b), it similarly shows a constant linear profile for the high-pressure steam, maintaining a uniform temperature of 254 °C along the entire exchanger length. Stream 7 (liquid o-xylene) presents an initial linear temperature increase up to approximately 40% of the exchanger length (from 25 °C to 180 °C), followed by a characteristic phase change behavior between 40% and 89% of the equipment length (vaporization). Subsequently, the stream resumes a linear temperature increase from 200 °C to 245 °C between 89% and 100% of the exchanger length, indicating sensible heating

without phase change until the desired temperature is achieved.
In the case of Cooler 1 (Figure 3c), the boiler feed water stream exhibits a linear temperature increase from 110 °C to approximately 254 °C along the entire exchanger length, indicating heating without phase change (sensible heat). Meanwhile, Stream 12 (gaseous outlet from the tubular reactor) shows a linear temperature decrease from 353 °C to 260 °C, confirming cooling without phase transition.
The heat curve of Cooler 2 (Figure 3d) reveals a linear temperature increase for the boiler feed water from 110 °C to approximately 150 °C, indicating sensible heating. Simultaneously, Stream 15 (cooled outlet from Cooler 1) undergoes a linear temperature decrease from 260 °C to 165 °C, reflecting cooling without phase change.
In Cooler 3 (Figure 3e), the cooling water stream displays a linear temperature increase from 30 °C to 40 °C, while Stream 21 (outlet from Cooler 2) shows a linear temperature decrease from 165 °C to 45 °C, both indicative of sensible heat exchange without phase change.
With respect to the heat curve of Pre-heater 2 (Figure 3f), the high-pressure steam exhibits a linear temperature decrease between 100% and 95% of the exchanger length, indicating cooling without phase change. This is followed by a curved temperature profile between 95% and 2% of the exchanger length, suggesting the occurrence of a phase change (condensation). Finally, the steam resumes a linear temperature decrease until reaching approximately 200 °C. In total, this stream cools from 255 °C to around 200 °C, undergoing condensation. The heat curve of Stream 24 (liquid stream from the switch condensers) shows a linear temperature increase up to 7% of the exchanger length (from approximately 45 °C to 82 °C), followed by a non-linear temperature rise between 7% and 98% of the length (from 82 °C to approximately 212 °C), indicative of a phase change (vaporization). The final segment, from 98% to 100% of the exchanger length, presents a linear temperature increase until reaching the target temperature of 230 °C.
Lastly, the heat curve of Cooler 4 (Figure 3g) is not discussed due to an anomalous behavior observed in the cooling water stream, which displays a range of exchanger length from 0% to 310%. This inconsistency is both contradictory and physically implausible, rendering the data invalid for analysis.

Parameters of the heat exchangers

Figure 4 presents the calculated values of heat duty, logarithmic mean temperature difference (LMTD), and overall heat transfer coefficient for each shell-and-tube heat exchanger employed in the phthalic anhydride (PA) production process. These parameters were obtained using the ChemCAD® simulation software.

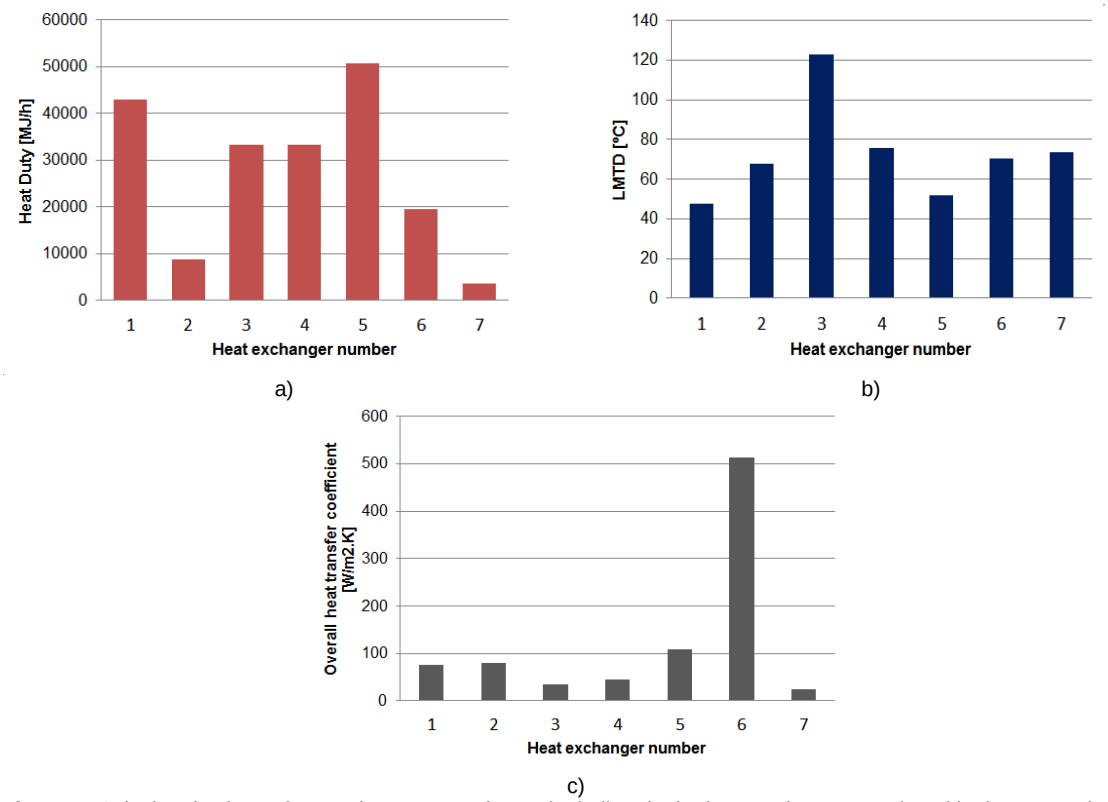

Figure 4. Calculated values of several parameters for each shell and tube heat exchanger employed in the PA production process: a) Heat duty, b) LMTD and c) Overall heat transfer coefficient.

The results presented in Figure 4 indicate that the heat exchanger with the highest heat duty is unit number 5 (Cooler 3), with a value of 50,590.4 MJ/h. This is attributed to the cooling operation performed on the outlet gaseous stream from Cooler 2, which undergoes a temperature reduction from 165 ºC to 45 ºC. The substantial temperature drop of 120 ºC results in the release of a significant amount of thermal energy during the cooling process. Additionally, the volume of gas to be cooled and the specific heat capacities of the stream components likely contribute to the elevated heat duty observed in this unit.

With respect to the logarithmic mean temperature difference (LMTD), the highest value was recorded in heat exchanger number 3 (Cooler 1), at 122.74 ºC. This is primarily due to the fact that this unit is responsible for cooling the gaseous stream exiting the tubular reactor, which reaches the highest temperature in the entire production process (353 ºC). The cooling is achieved using boiler feed water at 110 ºC, resulting in a pronounced temperature gradient across the exchanger.

Finally, the heat exchanger exhibiting the highest overall heat transfer coefficient was unit number 6 (Pre-heater 2), with a value of 513.48 W/m²·K. This unit facilitates both the preheating and vaporization of the outlet stream from the switch condensers, elevating its temperature to a maximum of 230 ºC prior to its introduction into the first distillation column. Consequently, this exchanger demonstrates optimal utilization of the thermal energy provided by the auxiliary service (high-pressure steam at 254 ºC), rendering it the most efficient in terms of heat transfer performance.

Equipment purchase and installation cost

Table 7 presents the estimated purchase and installation costs for the compressor, pump, and all shell-and-tube heat exchangers incorporated into the proposed phthalic anhydride production process. These values were calculated using the ChemCAD® simulator, based on updated data from the Chemical Engineering Plant Cost Index (CEPCI) corresponding to March 2023.

Table 7. Total purchase and installation cost for selected equipment.

Equipment	Purchase cost (USD $)	Installation cost (USD $)
Compressor + Motor + Driver	752,366	978,075
Pre-heater 1	122,543	245,087
Pump	6,695	18,747
Vaporizer	133,347	266,694
Cooler 1	91,368	182,737
Cooler 2	117,936	235,873
Cooler 3	100,016	200,032
Pre-heater 2	90,647	181,294
Cooler 4	378,246	756,492
TOTAL	1,793,164 ~ 1,794,000	3,065,031 ~ 3,066,000

The data presented in Table 7 reveal that the total costs associated with equipment procurement and installation amounted to approximately USD 1,794,000 and USD 3,066,000, respectively.

Conclusions

A conceptual design of a proposed phthalic anhydride (PA) production process via the gaseous catalytic oxidation of o-xylene was developed using the ChemCAD® 7.1.2 simulator, with the objective of determining the temperature, pressure, vapor fraction, mass flow rate, and composition of the main process streams. The principal design parameters of the equipment included in the process flowsheet were presented, along with the stoichiometry and kinetics of the reactions involved. The thermodynamic model employed in this simulation study was UNIFAC with vapor-phase association according to Hayden–O'Connell, while the Peng–Robinson model was selected as the Global Enthalpy Model. Several parameters were determined for the heat exchangers, including heat curves, heat duty, logarithmic mean temperature difference (LMTD), and overall heat transfer coefficient, as well as the heat duty of the catalytic reactor and specific design parameters of both distillation columns. The total purchase and installation costs associated with the specific equipment incorporated into the proposed production process were also estimated. The bottom stream of the purification column exhibits a mass flow rate of 10,921.083 kg/h, with PA as the predominant component, achieving a purity of 99.19%, while maleic anhydride (MA) is recovered in the top stream of the column with a mass flow rate of 973.342 kg/h and a purity of 83.36%. It is recommended to recover, purify, and recycle the gaseous PA and o-xylene vented through the switch condensers in order to enhance plant productivity. The simulation model developed in this study may serve as a basis for further optimization analyses, as well as for evaluating additional process improvements aimed at increasing throughput and enhancing production efficiency.

References

1. Giarola, S., Romain, C., Williams, C. K., Hallett, J. P., & Shah, N. (2016). Techno-economic assessment of the production of phthalic anhydride from corn stover. *Chemical Engineering Research and Design, 107*, 181-194. https://doi.org/10.1016/j.cherd.2015.10.034

2. Speight, J. G. (2002). *Chemical and Process Design Handbook*. New York, USA: The McGraw-Hill Companies, Inc.

3. Gimeno, M. P., Gascón, J., Téllez, C., Herguido, J., & Menéndez, M. (2008). Selective

oxidation of o-xylene to phthalic anhydride over V_2O_5/TiO_2: Kinetic study in a fluidized bed reactor. *Chemical Engineering and Processing, 47*, 1844–1852. https://doi.org/10.1016/j.cep.2007.10.010

4. Kirk, R. E., Othmer, D. F., Grayson, M., & Eckroth, D. (2004). *Kirk-Othmer Encyclopedia of Chemical Technology* (4th ed. Vol. 18). Hoboken, New Jersey: John Wiley & Sons.

5. Jara, J. A., Garea, A., & Irabien, J. A. (2005). *Simulation of o-Xylene Oxidation into Phthalic Anhydride: Rigorous Multitubular Catalytic Reactor Modelling and Exportation into the Process Flowsheet*. Paper presented at the European Symposium on Computer Aided Process Engineering - 15.

6. García, A. F. (2009). *Estudios de peligro y operabilidad (HAZOP) para una planta de anhídrido ftálico usando una herramienta de simulación dinámica.* (Bachelor Degree Thesis), Universidad de Los Andes, Bogotá, Colombia.

7. Giarola, S., Romain, C., Williams, C. K., Hallett, J. P., & Shah, N. (2015). *Production of phthalic anhydride from biorenewables: process design*. Paper presented at the 12th International Symposium on Process Systems Engineering and 25th European Symposium on Computer Aided Process Engineering, Copenhagen, Denmark.

8. Berrino, P. B., & Tavella, F. B. (2020). *Producción de anhídrido ftálico por oxidación parcial de o-xileno.* (Bachelor Degree Thesis), Universidad Tecnológica Nacional, Córdoba, Argentina.

9. Dixon, A. G., & Wu, Y. (2020). Partial oxidation of o-xylene to phthalic anhydridein a fixed bed reactor with axial thermowells. *Chemical Engineering Research and Design, 159*, 125-137. https://doi.org/10.1016/j.cherd.2020.03.027

10. Nandi, S. (2012). Modeling and simulation of phthalic anhydride production in a structured metallic monolith reactor. *Procedia Engineering, 38*, 1286-1290. https://doi.org/10.1016/j.proeng.2012.06.158

11. Nikolov, V. A., & Anastasov, A. I. (1992). Influence of the inlet temperature on the performance of a fixed-bed reactor for oxidation of o-xylene into phthalic anhydride. *Chico1 Engineering Science, 47*(5), 1291-1298.

12. Papageorgiou, J. N., & Froment, G. F. (1996). Phthalic anhydride synthesis. Reactor optimization aspects. *Chemical Engineering Science, 51*(10), 2091-2098.

13. Rahimi, A., & Hamidi, S. (2011). Modeling of a Fixed–Bed Reactor for the Production of Phthalic Anhydride. *Chemical Product and Process Modeling, 6*(1), 1-17. https://doi.org/10.2202/1934-2659.1626

14. Whu, Z., Tran, A., Ren, Y. M., Barnes, C. S., Chen, S., & Christofides, P. D. (2019). Model predictive control of phthalic anhydridesynthesis in a fixed-bed catalytic reactor viamachine learning modeling. *Chemical Engineering Research and Design, 145*, 173-183. https://doi.org/10.1016/j.cherd.2019.02.016

15. Otte, D., Lorenz, H.-M., & Repke, J.-U. (2016). A toolbox using the stochastic optimization algorithm MIPT and ChemCAD for the systematic process retrofit of complex chemical processes. *Computers and Chemical Engineering, 84*, 371-381. http://dx.doi.org/10.1016/j.compchemeng.2015.08.023

16. Cséfalvay, E., Szitkai, Z., Mizsey, P., & Fonyó, Z. (2008). Experimental data based modelling and simulation of isopropanol dehydration by pervaporation. *Desalination, 229*, 94-108. https://doi.org/10.1016/j.desal.2007.07.029

17. Ferdous, J., Bensebaa, F., & Pelletier, N. (2023). Integration of LCA, TEA, Process Simulation and Optimization: A systematic review of current practices and scope to propose a framework for pulse processing pathways. *Journal of Cleaner Production, 402*, 136804. https://doi.org/10.1016/j.jclepro.2023.136804

18. Chemstations. (2017). ChemCAD® (Version 7.1.2). Houston, USA: Chemstations, Inc.

19. Kancherla, R., Nazia, S., Kalyani, S., & Sridhar, S. (2021). Modeling and simulation for design and analysis of membrane-based separation processes. *Computers and Chemical Engineering, 148*, 107258. https://doi.org/10.1016/j.compchemeng.2021.107258

20. Denz, N., Ausberg, L., Bruns, M., & Viere, T. (2014). Supporting resource efficiency in chemical industries - IT-based integration of flow sheet simulation and material flow analysis. *Procedia CIRP, 15*, 537-542. https://doi.org/10.1016/j.procir.2014.06.060

21. Turton, R., Shaeiwitz, J. A., Bhattacharyya, D., & Whiting, W. B. (2018). *Analysis, Synthesis, and Design of Chemical Processes* (5th ed.). New York, USA: Pearson Education, Inc. [35]

22. Dias, C. R., Portela, M. F., & Bond, G. C. (1997). Synthesis of Phthalic Anhydride: Catalysts, Kinetics, and Reaction Modeling. *Catalysis Reviews, 39*(3), 169-207. http://dx.doi.org/10.1080/01614949709353776

23. Sarosh, A., Hussain, A., Pervaiz, E., & Ahsan, M. (2018). Computational Fluid Dynamics (CFD) Analysis of Phthalic Anhydride's Yield Using Lab Synthesized and Commercially Available (V_2O_5/TiO_2) Catalyst. *Engineering,*

Technology & Applied Science Research, 8(2), 2821-2826.
24. Anastasov, A. I. (2003). Deactivation of an industrial V_2O_5/TiO_2 catalyst for oxidation of oxylene into phthalic anhydride. *Chemical Engineering and Processing, 42*, 449-460.
25. Sinnott, R., & Towler, G. (2020). *Chemical Engineering Design* (6th ed.). Oxford, United Kingdom: Butterworth-Heinemann.
26. Green, D. W., & Southard, M. Z. (2019). *Perry's Chemical Engineers' Handbook* (9th ed.). New York, USA: McGraw-Hill Education.
27. Peters, M. S., Timmerhaus, K. D., & West, R. E. (2003). *Plant Design and Economics for Chemical Engineers* (5th ed.). New York, USA: McGraw-Hill.
28. Couper, J. R., Penney, W. R., Fair, J. R., & Walas, S. M. (2012). *Chemical Process Equipment Selection and Design* (3rd ed.). Oxford, United Kingdom: Butterworth-Heinemann.
29. Jenkins, S. (2023). Economic Indicators. *Chemical Engineering, 130,* 48.
30. Walas, S. M. (1990). *Chemical Process Equipment Selection and Design.* Oxford, UK: Butterworth-Heinemann.
31. Schwartz, W. A., Higgins, F. B., Lee, J. A., Morris, R. B., Newirth, R., & Pervier, J. W. (1975). *Engineering and Cost Study of Air Pollution Control For the Petrochemical Industry, Vol. 7: Phthalic Anhydride Manufacture From Ortho-Xylene*. (EPA-450/3-73-006g). North Carolina, USA.

RECyT
Year 27 / Nº 44 / 2025 /
DOI: https://doi.org/10.36995/j.recyt.2025.44.012

Fuel interchangeability: a comparative study of propane and methane in an industrial furnace burner

Intercambiabilidad de combustible: un estudio comparativo de propano y metano en un quemador de horno industrial

Alexandre Tiago, Martins[1, *]; Aldo, Ramos Santos[1]

1- Universidade Santa Cecília (UNISANTA). Santos, Brasil.
* E-mail: alexandre.engenharia@yahoo.com

Received: 3/09/2024; Accepted: 23/09/2025

Abstract
The need for studies on interchangeability prediction arose when street gas, generated from mineral coal, began to be replaced by natural gas or petroleum-derived gases. This need emerged mainly from the fact that burners have limited flexibility in responding to variations in the composition of their fuel. Subsequently, it was necessary to evaluate the performance of burners with different natural gas compositions. The current study assessed the feasibility of substituting fuel gas used in the furnace.

Keywords: Wobbe index, *Weaver index*, *gas interchangeability*.

Resumen
La necesidad de estudios de predicción de intercambiabilidad surgió cuando comenzó el reemplazo del gas de la calle, generado a partir de carbón mineral, por gas natural o gases derivados del petróleo. Esta necesidad provino principalmente del hecho de que los quemadores tienen una pequeña flexibilidad ante la variación de la composición de su combustible. Posteriormente, fue necesario evaluar el rendimiento de los quemadores con diferentes composiciones de gas natural. El estudio actual evaluó la viabilidad de sustituir el gas combustible utilizado en el horno.

Palabras clave: índice de Wobbe, *índice de Weaver*, *Intercambiabilidad de gas*.

Introduction
The concept of fuel interchangeability refers to the assessment of whether a gas or a mixture of combustible gases can be substituted with another without causing significant operational difficulties in the same burner or burner system [1, 2, 3]. Gases are considered interchangeable if they can be burned in each equipment without requiring mechanical modifications to the original burners, while maintaining operational safety and adequate energy performance. A thorough assessment of parameters that integrate the consequences of compositional deviations during combustion is imperative for this analysis [1,3].

Objective
The objective of this study was to demonstrate the occurrence of gas interchangeability in the case study, enabling a fuel gas substitution without requiring mechanical modifications to the combustion equipment (industrial furnace). Propane (C_3H_8) was used in this process, and due to strategic reasons, it was intended to replace this gas which had natural gas (CH_4). For stoichiometric calculations, propane and natural gas were both considered to be of high purity under standard temperature and pressure (STP) conditions.

Materials and methods
The academic research, grounded in classical literature, provided a technical foundation for application to contemporary needs through the comparison of established industry indices, specifically the Wobbe Index (WI) and, among the several Weaver indices, the Flame Front Speed Factor (SI) [3, 4, 5].
One of the main parameters of gas interchangeability is the WI, which depends on the volumetric Lower Heating Value (LHV) of the gas and its relative density, i.e., on the heating value and molecular weight characteristic of each gas assessed [1, 6, 7, 8, 9, 10].
This index is a parameter for verifying the thermal performance of different gases in each burner or pilot, and it expresses the ability of a given fuel to maintain a relationship between the amount of energy released and the pressure drop in the burner. This means that gases with similar WI values (5%) do not require adjustments to operating pressure nor physical alterations to the equipment in order to provide the same energy

release, as their resulting thermal performance curves are equivalent (Equation 1).

Wobbe Index (WI);

$$WI = \frac{LHV}{\sqrt{\rho}} \quad (1)$$

Being:
WI: Wobbe Index;
LHV: Lower Heating Value;
ρ: Relative density.

However, the Weaver Index (SI) is another crucial parameter to be considered, as it compares the flame propagation speeds of the gases being assessed. This index is calculated as a ratio of the combustible components in the gas, weighted by their respective characteristic flame speeds (using hydrogen (H_2) as a reference due to its high velocity), and the proportion of inert components (since a higher inert content results in lower flame speeds). The amount of air in the combustion (stoichiometric air-fuel ratio) also influences this calculation.
Higher SI values compared to the original ones indicate a faster flame propagation speed, meaning a greater tendency for the flame to lift off the burner or even flashback.
Conversely, a lower SI values suggest a slower flame propagation speed, potentially causing the flame to liftoff.
This method was developed by testing mixtures of methane, hydrogen, carbon monoxide, ethane, propane, butane, ethene, propene, acetylene, benzene, nitrogen, and carbon dioxide to simulate manufactured and natural gases (Equation 2).
Flame Propagation Speed Factor (SI);

$$SI = \frac{\sum xiFi}{A+5Z-18{,}8Q+1} \quad (2)$$

Being:
SI = Weaver flame speed factor;
xi = Volumetric fraction of component i;
Fi = Weaver flame speed coefficient for component i;
A = Air required for stoichiometric combustion, vol. of air/ vol. of gas;
Z = Volumetric fraction of inert components (N_2, CO_2) in the mixture;
Q = Volumetric fraction of oxygen in the mixture;
Table 1 shows the Weaver flame speed coefficients for the evaluated gases [1].

Table 1 – Flame speed coefficient for some gases (%).

Gas	Chemical formula	*Fi*
Propane	C_3H_8	398
Methane	CH_4	148

Source: Garcia, R. (2013)

Results and Discussion

Stoichiometric calculations were first performed to determine the air required for combustion, according to equations 3 and 4.

$C_3H_8 + 5O_2 \rightarrow 3\ CO_2 + 4H_2O$ (3)
O_{2Est} = 5 mol
O_{2Fuel} = 0
O_{2Teo} = 5 mol
O_{2Rea} = 5 mol
N_2 = 5 × 79/21 = 18,8
Air = 23,8 mol
Air = 23,8 × (22,4 L/mol) = 533,1 L
$C_3H_{8\ (fuel)}$ = 5 mol × (22,4 L/mol) = 112,0 L
Air/ fuel ratio = 533,1 L/112,0 L = 4,76 L

$CH_4 + 2\ O_2 \rightarrow CO_2 + 2H_2O$ (4)
O_{2Est} = 2 mol
O_{2Fuel} = 0
O_{2Teo} = 2 mol
O_{2Rea} = 2 mol
N_2 = 2 × 79/21 = 7,5
Air = 9,5 mol
Air = 9,5 × (22,4 L/mol) = 212,8 L
$CH_{4\ (Fuel)}$ = 2 × (22,4 L/mol) = 44,8 L
Air/ fuel ratio = 212,8L/44,8L = 4,7 L

Subsequently, both the Wobbe Index (WI) and the Weaver Index (SI) were calculated and graphically represented on a scatter plot (see Figure 1), where each evaluated gas was plotted relative to the original gas. In the literature, gases with WI varying up to ±5% and SI varying up to ±10% are considered equivalent. From equations 1, 2, 3, and 4, the results expressed in equations 5, 6, 7, and 8 were obtained.

$$WI_{(C_3H_8)} = \frac{22389}{\sqrt{1{,}55}} = 17983\ \frac{kcal}{m^3} \quad (5)$$

$$WI_{(CH_4)} = \frac{9430}{\sqrt{0{,}60}} = 7300\ \frac{kcal}{m^3} \quad (6)$$

$$SI_{(C_3H_8)} = \frac{3\times398}{4{,}76+0-0+1} = 207{,}29 \quad (7)$$

$$SI_{(CH_4)} = \frac{1\times148}{4{,}76+0-0+1} = 25{,}96 \quad (8)$$

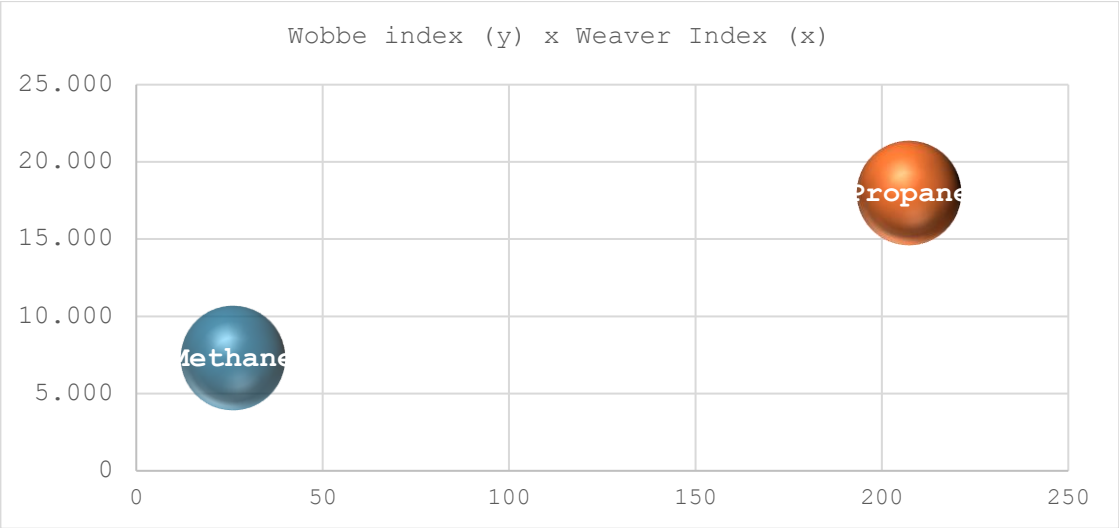

Figure 1 – Gas interchangeability map**.**

The abscissa (x-axis) was scaled in %mol, while the ordinate (y-axis) was scaled in kcal/m³ at standard temperature and pressure (STP).

Conclusions

This evaluation aimed to verify the feasibility of using Methane gas as an alternative to Propane gas in a specific industrial furnace. To this end, potential effects, such as flame lift-off and flashback in the burners, were analysed. The findings revealed that the gases are not interchangeable, and the existing equipment cannot operate safely with the new fuel without mechanical adjustments.

References

1. Garcia R. Combustíveis e combustão industrial. Interciência, 2002.
2. Szklo AS. Fundamentos do refino de petróleo. Interciência, 2005.
3. Weaver ER. Fuel gases interchangeability formulas and graphs. J Res Natl Bur Stand, 1951;46(3):213–45.
4. Baukal CEJ. The John Zink Hamworthy Combustion Handbook. CRC Press, 2013.
5. Harmen DV et al. Natural gas/hydrogen mixtures: Interchangeability analysis for domestic appliances. Appl Energy, 2017;208:1007–19.
6. Abeysekera M et al. Gas network steady state analysis with alternative gas injection. Appl Energy, 2016;164:991–1002.
7. Pellegrino S et al. Modelling distributed alternative fuels in gas networks. Renew Sustain Energy Rev, 2017;70:266–86.
8. Engineering Science. Exhaust gases from combustion and industrial processes. EPA, 1971. Contract EHSD 71-36.
9. Perry JH. Chemical Engineers Handbook. McGraw-Hill, 1963.
10. Massara V et al. Optimizing natural gas distribution networks using biomethane and hydrogen. Lat Am J Energy Res, 2025.